

Entanglement and geometry

Per Øyvind Sollid



Thesis submitted for the degree of
Philosophiae Doctor

Department of Physics
University of Oslo

December 2010

© Per Øyvind Sollid, 2011

*Series of dissertations submitted to the
Faculty of Mathematics and Natural Sciences, University of Oslo
No. 1054*

ISSN 1501-7710

All rights reserved. No part of this publication may be
reproduced or transmitted, in any form or by any means, without permission.

Cover: Inger Sandved Anfinsen.
Printed in Norway: AIT Oslo AS.

Produced in co-operation with Unipub.
The thesis is produced by Unipub merely in connection with the
thesis defence. Kindly direct all inquiries regarding the thesis to the copyright
holder or the unit which grants the doctorate.

Preface

The work presented in this thesis has been focused on understanding entanglement and entangled states in quantum physics. Entanglement is a fundamental property of quantum mechanics which leads to many difficult interpretational and philosophical problems. It appears counterintuitive to our everyday understanding of how things work and is therefore highly interesting in and of itself.

Although conceptually challenging and philosophically interesting, there are also several motivating factors for the study of entanglement in applications of quantum theory. Entanglement is considered a resource in quantum information theory, and is used in quantum computers which may be used to outperform classical computers in various applications of interest, and for secure communication by ways of quantum cryptography. The problem however, is that entanglement is a fragile resource still. Despite our best efforts, it is difficult to remove the danger of losing the entanglement in practical implementations. If not kept completely isolated, quantum systems will interact with the environment around them, which leads to loss of entanglement in the total system itself.

In order to deal with loss of entanglement in practice, methods such as entanglement distillation have been invented in order to distill the less entangled states to more entangled ones, but with one caveat. The existence of the qualitatively different types of entanglement called free and bound entanglement. The type referred to as bound entanglement has been shown to be impossible to distill [1]. This means that states that initially contained free entanglement, but who evolved in time through interactions with the environment in such a way that the entanglement in the state became bound, are useless at that point as a resource. This is another aspect that motivates the study of bound entangled states.

For a general overview of the current state of affairs regarding the study of entanglement, see for instance [2]. In 1996 a criterion for determining whether or not a state was entangled, based on the partial transposition map, was presented [3]. It appeared to clearly distinguish separable and

entangled states in the sense that it formulated an easily testable condition which separable states satisfied, but which entangled states did not. However, in 1997 there was provided an example of an entangled state that that satisfied this condition [4].

The study of bipartite bound entanglement has since been focused somewhat on generating examples of states or classes of states with special symmetries in addition to being bound entangled [5, 6, 7, 8, 9, 10, 11]. Some of these examples have been constructed directly, while others have come by way of studying entanglement witnesses that detect certain states. This is also true today, though the activity has shifted a bit from bipartite to multipartite systems.

One particular approach to the study of entanglement is through geometry [12, 13, 14, 15]. The geometrical aspects of entanglement is interesting in itself, and it might lead to new insight. A geometric approach to the study of entanglement was developed in [14], on which the work presented in this thesis is built upon. The idea was that while developing explicit examples has been both important and fruitful, it becomes necessary to try to obtain a larger picture by studying the entire set of states, as well as subsets of states with special properties. The approach is concerned with the convex nature of various sets of matrices in quantum mechanics, called density matrices, and exploiting the fact that convex sets are described entirely by their extreme points.

Analytic studies regarding the geometry of entanglement is in general quite hard, especially since the dimensions of the systems grow so rapidly. In hopes of gaining new information and analytical starting points, we have therefore developed and used numerical tools to aid in the study of entanglement.

The work in this thesis builds on the work in [14, 16, 17]. It is there that many of the concepts and tools we have used in this work were discussed for the first time, and really my work has to be seen in context with the work presented there. In [14] many of the underlying ideas were explored, and in [16] an operational criterion for detecting a particular type of bound entangled states, extremal positive partial transpose states, was given together with numerically obtained examples. These results motivated the work presented here.

Thesis structure

The thesis is organized in two parts. The first part consists of an introduction to the main topics that are the underpinnings of the work presented in the four papers that constitute the second part of the thesis. The first part is

organized as follows.

In chapter 1 we give a short historical overview of some important aspects of the development of quantum mechanics and the role played by entanglement. It showcases some reasons why entanglement is both unintuitive and interesting. It also gives a short description of entanglement as a resource in areas of quantum information theory.

In chapter 2 we give a short introduction to the formal description of quantum systems and present concepts vital to the work in this thesis such as partial transposition and special linear product transformations on quantum systems.

In chapter 3 we give an introduction to the geometrical aspects of density matrices and entanglement.

In chapter 4 we present four of the numerical methods that have been developed and used in the work presented in this thesis.

In chapter 5 we give short summaries of the papers and end with some conclusions and remarks.

Acknowledgements

There are many people who deserve thanks for their support in various ways during the last few years. In no particular order, well, apart from my supervisors, here they are.

First and foremost I would like to thank my supervisor Jon Magne Leinaas for a very rewarding collaboration and excellent supervision. I thank you for the support and patience you have shown me and for always being available whenever there was a problem to discuss. Your understanding of and skills in communicating physics are truly inspiring and I hope to take some of that with me in the future.

I also wish to thank my co-supervisor Jan Myrheim of whom I have learned a lot. I want to thank you for excellent collaboration and for the hospitality shown me whenever I visited in Trondheim. On that same note I want to thank Leif Ove Hansen and Andreas Hauge.

Special thanks go out to my current and former colleagues at the Theory Group. I want to thank Eirik Ovrum for helping me when I first started this PhD, and Mats Horsdal for your help with classical mechanics. I also want to thank both you guys for sharing the office at Ø469. In the last couple of years I have shared this office with Jaakko Nissinen, who, in addition to having an amazing sense of Finnish humor, has been extremely helpful with many discussions and careful proof reading of parts of this thesis. I also wish to thank Juha Suorsa for many great conversations. And I want to thank Jan Olav Eeg for a great collaboration on the course in classical mechanics. In particular I want to thank Marius Lysebo for many rewarding conversations, sometimes about physics, but mostly not, and your invaluable help in proof reading this thesis.

I have a bunch of friends that I wish to thank. I thank Morten Munthe for being an amazing friend I know I always can count on to help take my mind off of work, and Gunhild for letting us play videogames all the time. I thank Lars Erlend Leganger for providing countless hours of entertainment, and for listening and giving helpful advice. I also have to thank you and Maria for giving me a place to stay and hang out when I am in Trondheim.

I thank Øyvind Nordang, Mads Stormo Nilsson, Bernt Jørgen Nordbotten and Jostein Henrik Bakke for contributing to my social life.

Last but not least, I want to thank my family. Without your support this thesis would not have been possible. In particular I want to thank Marion for your amazing love, support and patience.

List of papers

- Paper I:** Jon Magne Leinaas, Jan Myrheim and Per Øyvind Sollid,
Numerical studies of entangled positive-partial-transpose states in composite quantum systems,
Phys. Rev. A **81**, 062329 (2010)
- Paper II:** Jon Magne Leinaas, Jan Myrheim and Per Øyvind Sollid,
Low-rank extremal positive-partial-transpose states and unextendible product bases,
Phys. Rev. A **81**, 062330 (2010)
- Paper III:** Per Øyvind Sollid and Jon Magne Leinaas,
Unextendible product bases and extremal density matrices with positive partial transpose,
Preprint (2010)
- Paper IV:** Leif Ove Hansen, Andreas Hauge, Jan Myrheim and Per Øyvind Sollid,
Low rank positive partial transpose states and their relation to product vectors,
Preprint (2010)

Contents

I	Introduction	1
1	Introduction	3
1.1	Quantum mechanics and entanglement	4
1.1.1	The EPR paradox	6
1.1.2	The Bell inequality	8
1.2	Entanglement as a resource	11
1.2.1	Quantum computing	12
1.2.2	Quantum communication	13
1.2.3	Decoherence	16
2	Describing quantum systems	17
2.1	Composite systems and entanglement	21
2.2	Partial trace, entanglement and decoherence	25
2.3	Partial transposition and positive maps	29
2.4	$SL \otimes SL$ transformations and SLOCC equivalence	33
3	Geometrical aspects of entanglement	39
3.1	The geometry of density matrices	39
3.1.1	The real vector space of Hermitian matrices	40
3.1.2	Inner product	41
3.2	Convex sets	44
3.2.1	Extreme points of convex sets	45
3.2.2	\mathcal{D} , the convex set of density matrices	47
3.2.3	\mathcal{S} , the convex set of separable density matrices	48
3.2.4	\mathcal{P} , the convex set of PPT density matrices	48
3.2.5	The positive convex cone	50
3.3	Simplexes and unitary transformations	51
3.4	Two-dimensional cross sections	55
3.5	Flat faces and extremality in \mathcal{D}	62
3.6	Flat faces and extremality in \mathcal{P}	67
3.7	Surfaces of density matrices with specified ranks	72

4	Numerical methods	77
4.1	Obtaining density matrices with specified rank	78
4.2	$SL \otimes SL$ equivalence to projectors	82
4.3	SL equivalence between sets of vectors	86
4.4	Obtaining product vectors in a given subspace	88
5	Summary and outlook	93
5.1	Paper I	93
5.2	Paper II	95
5.3	Paper III	96
5.4	Paper IV	97
5.5	Concluding remarks	98
	Bibliography	107
II	Papers	109

Part I
Introduction

Chapter 1

Introduction

Quantum mechanics is a framework or set of laws that we use to describe some of the smallest systems in Nature. It was developed in a burst of activity in the beginning of the twentieth century as a series of attempts to describe several experimental observations that should have been impossible according to the physics at the time. Quantum mechanics has since been able to give predictions that are in amazing agreement with later experiments and led to discovery of a whole plethora of particles and effects which form our understanding of Nature today.

Classical physics is mostly concerned with the macroscopic world, where we are used to deterministic properties of Nature. If we perform a measurement on a large object, check the color of a ball, say, and find that the ball is red, then our intuition tells us that the ball was also red before we looked at it. This is a philosophical question, regarding the nature of reality, and something that quantum mechanics seemed to challenge our understanding of. The tradeoff that quantum mechanics makes is that it describes outcomes of measurements by probabilities. Say that we have a quantum version of the ball, and we know before we check that the ball could be either blue or red, but once we check we find that the ball is red. Classically we said that well then the ball was also red before we checked, but quantum mechanics says that before we checked, the ball was blue with a certain probability p and red with probability $1 - p$. By looking at the ball we apparently somehow collapse the state of the ball to be a red ball.

This counterintuitive way of describing things has led to many philosophical debates on what is considered to be real, discussions about whether or not quantum mechanics can be considered a complete theory and how one is supposed to understand this apparent collapse of the state of the system during a measurement. At the heart of many of these problems and arguably the defining property of quantum mechanics is the concept of entanglement.

Entanglement manifests itself as correlations between results of measurements on different systems that cannot be explained classically. When such correlations are observed, the systems measured are said to be entangled.

The philosophical aspects and counterintuitive nature of quantum mechanics has been and is still a large part of the motivation for studying entanglement and its properties. Another central motivation is found in the field of quantum information theory, which is a collective term that encompasses such things as quantum computation and quantum cryptography. As quantum mechanics developed, it became apparent that entanglement is a fundamental property of the theory, and that it could be used as a resource. Information was understood to be a physical quantity, and the particular kind of information stored in entanglement could possibly be harnessed for tasks where it can be shown to theoretically outperform classical analogues significantly. This has led to theories of quantum computers and other quantum systems where a key aspect is to be able to control quantum systems. This is a very hard thing to do, because entanglement is very sensitive to interactions between the quantum system and the environment.

1.1 Quantum mechanics and entanglement

In the late 1800s physicists made several observations that seemed at odds with the predictions at the time. Even worse, with new insight from groundbreaking experiments the physical laws predicted absurdities. An idealized black body at thermal equilibrium was for instance predicted to apparently emit radiation with infinite power. This was clearly unphysical and was never observed.

Another set of strange predictions of the time involved the atom, and specifically the structure of the atom. Rutherford had proposed his model of the atom analogous to the solar system model with the nucleus in the center and electrons as orbiting the nucleus. According to the Rutherford model, each electron could follow any one of an infinite number of different orbits around the nucleus, and the orbit could be at any distance from the nucleus. A big problem with this was that classical physics predicted that since the electrons constantly change direction or momentum or both, they should constantly emit radiation. By emitting radiation they would lose energy, and when losing energy they would have to spiral towards the nucleus and be absorbed in the end. Thus, all atoms would have to be unstable, and we should not exist. This, clearly, was wrong.

The third and final problem we will mention might be the one that lead to some of the most counterintuitive and imaginative explanations of the

three, the problem with the photoelectric effect and the nature of light. The photoelectric effect concerns the fact that shining light on metals causes electrons to be ejected. According to classical physics electrons should be ejected at any frequency of the light, but this was not observed. Instead, the frequency had to be raised above a specific point at which electrons suddenly were ejected. This frequency gap was impossible to reconcile with classical electromagnetic theory.

All of the problems mentioned above were resolved with the introduction of quanta in physics. In order to explain the black body radiation problem, Planck proposed in 1900 that the radiated energy E of the black body could only be emitted in quantized form, $E_n = nh\nu$, proportional to the frequency ν of the radiation with n the number of quanta. The proportionality constant h was dubbed Planck's constant and was obtained through experiments. Bohr introduced the concept of quanta in relation to the orbits of electrons around the nucleus, by proposing that the orbits themselves should be treated as quantized. Hence, the electrons could not continuously move from one orbit to another, the only possibility were for them to spontaneously jump from one orbit to another. This explained both the never observed instability of all atoms and also the already experimentally observed frequency bands of emitted light from atoms.

Albert Einstein explained the photoelectric effect when he proposed the novel idea that light may be mathematically treated as quanta. These quanta would later be called photons. The idea that light was somehow consisting of light particles seemed very counterintuitive at the time, but was a nice explanation for the observed properties of the photoelectric effect. Even though he later presented his well known special and general theories of relativity, it was the photoelectric effect that garnered him the Nobel Prize in physics in 1921. Some three years later Louis de Broglie proposed, based on the theory that light could be viewed as particles, that particles also could be described as waves. The theory was built on special relativity and initially concerned only a single particle.

The explanations involving quanta in physics were at first very phenomenological, in the sense that they explained the phenomena but there was no framework, no set of tools, to use in describing the physical implications of the theories. In 1925, building on de Broglie's work, Erwin Schrödinger invented wave mechanics while Werner Heisenberg and Max Born invented matrix mechanics, two seemingly different approaches to quantum mechanics. Later Schrödinger showed that the two approaches actually are equivalent. Now equipped with a formalized framework for quantum mechanics, the field has only continued to grow since.

1.1.1 The EPR paradox

Although the explanatory power of quantum mechanics was strong, some of the questions it raised were rather eye popping. Some of the initial criticism towards quantum mechanics was formulated as a famous thought experiment by Albert Einstein, Boris Podolsky and Nathan Rosen in their paper titled "Can Quantum-Mechanical Description of Physical Reality Be Considered Complete?" from 1935 [18]. In the paper they point to counterintuitive properties of quantum mechanics such as the act of one system instantaneously affecting another system infinitely far away and the completeness of the information content in quantum mechanics. Does a quantum mechanical description contain all the information in a system, or is it lacking something?

Completeness in the sense of EPR means that in a complete theory of Nature, there exists an element in the theory corresponding to every element of reality. They argued that a sufficient condition for a quantity to be an element of reality is that it is possible to predict the value of the quantity with absolute certainty without disturbing the system in any way. This is known as the principle of reality. In addition they argued that a physical theory should respect the principle of locality, which says that if two systems are sufficiently separated no action on one of the systems can influence the other in any physical way.

The paradox arises from the fact that it appears as though arguing that quantum mechanics is a complete theory leads to consequences that are in strict contradiction with the theory itself. In order to illustrate the paradox, we will look at an example concerning the spin of two spin-1/2 particles in the form of an electron and a positron created from the decay of a pion. The pion was initially at rest so the electron and positron shoot off in opposite directions. The pion has spin zero, so conservation of angular momentum requires that the electron and the positron are in what is known as the singlet configuration where their spins are anti-correlated. If the spin of the electron is measured to point upwards along a chosen axis, the spin of the positron will point downwards along the same axis, and vice versa. Both of the particles are in a state which is a superposition of their state pointing up or down, with equal probability for measuring either on any one of the particles by themselves. The situation is illustrated in figure 1.1.

We want to measure the spin of the electron along the z -axis. In accordance with the locality principle we assume that the electron and positron are separated by a large enough distance before performing the measurement such that the act of measuring the electron cannot affect the positron in any real sense.

If performing the measurement of the spin of the electron yields the re-

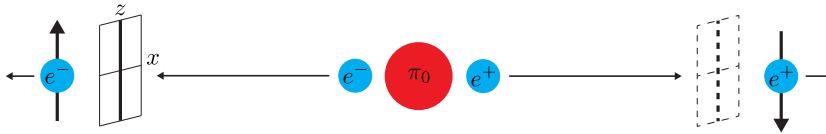


Figure 1.1: Illustration of the EPR thought experiment. A pion π_0 decays into an electron e^- and a positron e^+ . Since the pion has spin zero, the spin of the electron and the spin of the positron will be anti-correlated. The two particles shoot off in opposite directions before the electron passes through a spin measuring device represented by the solid frame. We are assuming here that the particles are sufficiently far apart when the measurement occurs that the measurement cannot affect the positron in any physical way. After the measurement the spin of the electron is known to be pointing up along the measuring axis (the thick line in the frame), and since the two particles are entangled we know that the spin of the positron along the same axis points downward. The act of measuring the spin of the electron can then be seen as an effective measurement of the spin of the positron, represented by the dashed frame.

sult that it points up, because the spins are anti-correlated we now know with certainty that the spin of the positron points down along the z -axis. In this sense, measuring the electron is effectively equivalent to measuring the positron. But we have assumed locality, which means that the electron measurement cannot influence the positron in a physical way. Thus, according to the principle of reality the z -component of the positron spin must be an element of reality and must therefore have been pointing down all along.

But we can consider having chosen to measure along the x -axis rather than the z -axis, and then we would know with certainty the component of the spin of the positron in the x -direction without disturbing it in any way. But then by the same argument, the spin of the positron along the x -axis is also an element of reality and must have had a fixed value all along as well.

The paradox now arises when realizing that this means that if quantum mechanics is complete, it must be able to predict with absolute certainty the value of the spin of the positron along both the x - and z -axis simultaneously, and quantum mechanics states that this is not possible. The two components of the spin of the positron are represented by non-commuting operators in quantum mechanics, which means that they are incompatible observables and cannot be known with certainty simultaneously. Therein lies the paradox.

According to EPR quantum mechanics cannot be complete, because if it is

then it is inconsistent. The alternative is that one or both of the assumptions that any physical theory must respect locality and reality is false. This seems to imply that there exists no objective reality other than that revealed through experiments.

The crux of the problem seems to lie with the fact that the electron and positron are entangled. In other words, entanglement is responsible for the paradox. Before the measurement of the electron, both particles were in states that were superpositions of having spin up and spin down. When we measure the electron it seems as if there is an instantaneous action affecting the positron as well, since we suddenly know with certainty what the outcome of a measurement of its spin will be.

However, there is no way to detect the correlation of the positron measurement with the electron measurement without consulting the results from the electron measurement. If someone measures the spin of the positron right after the electron measurement is performed by someone else far away, they will have to assume that they have a fifty percent chance of getting spin up and fifty percent chance of spin down. Therefore the change produced in the total system of the electron plus positron is not detectable at the positron measurement, and thus there is no violation of causality for instance. A change has occurred, but it is undetectable.

1.1.2 The Bell inequality

The claim was that quantum mechanics was, at best, incomplete. In order to fix this, several theories were created where hidden variables were introduced that were supposed to carry the extra information quantum mechanics did not. They were called hidden variables because nobody knew how to measure them if they existed. In 1964 though, John S. Bell proved that there were no local hidden variable theories that were compatible with quantum mechanics.

Bell proposed studying correlations between measurements of the spin components on both the positron and the electron where the measurement axes for the electron and the positron were independently oriented. We will in the following examine such a situation and see that hidden variable theories and quantum mechanics are in fact incompatible. The description of the Bell inequality given here is based on [19].

Suppose we have a source that prepares pairs of anti-correlated electrons and positrons that shoot off in opposite directions before they pass through detectors, and that the detector for the electrons is oriented along an axis defined by the unit vector \vec{a} while the detector for the positrons is oriented along the unit vector \vec{b} . This situation is illustrated in figure 1.2.

We introduce the locality principle when we assume that the detectors

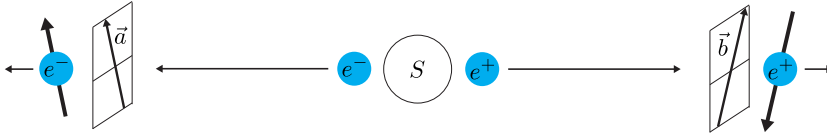


Figure 1.2: Illustration of the setup in a Bell type experiment. A source S produces anti-correlated pairs of electrons e^- and positrons e^+ which fly off in opposite directions before they pass through a measurement device indicated by the frames. The measurement device that the electrons pass through measure their spin along an axis represented by the vector \vec{a} , while the positron detector measures the spin of the positrons along an axis \vec{b} . The orientations of \vec{a} and \vec{b} are assumed to be independent of each other.

are sufficiently separated so that the outcome of the electron measurement cannot influence the orientation \vec{b} of the positron measurement.

The average value of the product of the spins will depend on the detector orientations, and we will denote it by $P(\vec{a}, \vec{b})$. When the detectors are aligned in parallel, $\vec{a} = \vec{b}$, we recover the EPR setup discussed previously, where the spin of one of the particles points down and the other points up. Let us for simplicity denote the spins as $+1$ for up and -1 for down, then the product in the EPR setup is always -1 , and so then is the average

$$P(\vec{a}, \vec{a}) = -1 \quad (1.1)$$

In the case the detectors are oppositely aligned, $\vec{a} = -\vec{b}$, we would get $P(\vec{a}, -\vec{a}) = +1$. For arbitrary detector directions quantum mechanics predicts

$$P(\vec{a}, \vec{b}) = -\vec{a} \cdot \vec{b} \quad (1.2)$$

We assume now that there exists a hidden variable λ that together with standard quantum mechanics gives the complete description of an electron/positron pair. Since we have assumed locality, there must exist a function $F_e(\vec{a}, \lambda)$ that with certainty tells us the result of the electron measurement even before the measurement takes place. Similarly, there should exist such a function $F_p(\vec{b}, \lambda)$ for the positron measurement.

In accordance with the known results of quantum mechanics we will further assume that the above mentioned functions can only take values between -1 and $+1$, i.e.

$$F_e(\vec{a}, \lambda) = \pm 1 \quad \text{and} \quad F_p(\vec{b}, \lambda) = \pm 1 \quad (1.3)$$

We also know then that when the detectors are aligned, we have anti-correlation between the functions in the sense that

$$F_e(\vec{a}, \lambda) = -F_p(\vec{a}, \lambda) \quad (1.4)$$

which must be true for any value of λ .

We then introduce a probability distribution $\rho(\lambda)$ for the hidden variable λ which satisfies

$$\int \rho(\lambda) d\lambda = 1 \quad (1.5)$$

and make no assumptions about it other than as any probability density it is positive. The correlation between the electron and positron spin can then be written as

$$P(\vec{a}, \vec{b}) = \int \rho(\lambda) F_e(\vec{a}, \lambda) F_p(\vec{b}, \lambda) d\lambda \quad (1.6)$$

From eq. (1.4) we can get rid of $F_p(\vec{b}, \lambda)$ in order to write the above expression as

$$P(\vec{a}, \vec{b}) = - \int \rho(\lambda) F_e(\vec{a}, \lambda) F_e(\vec{b}, \lambda) d\lambda \quad (1.7)$$

We can then compare correlation functions in the following way:

$$P(\vec{a}, \vec{b}) - P(\vec{a}, \vec{c}) = - \int \rho(\lambda) \left[F_e(\vec{a}, \lambda) F_e(\vec{b}, \lambda) - F_e(\vec{a}, \lambda) F_e(\vec{c}, \lambda) \right] d\lambda \quad (1.8)$$

From eq. (1.3) it follows that $F_e^2(\vec{b}, \lambda) = 1$ which we insert in the second term above to get

$$P(\vec{a}, \vec{b}) - P(\vec{a}, \vec{c}) = - \int \rho(\lambda) F_e(\vec{a}, \lambda) F_e(\vec{b}, \lambda) \left[1 - F_e(\vec{b}, \lambda) F_e(\vec{c}, \lambda) \right] d\lambda \quad (1.9)$$

Then from eq. (1.4) we find that this can be written as

$$\begin{aligned} P(\vec{a}, \vec{b}) - P(\vec{a}, \vec{c}) &= - \int \rho(\lambda) F_e(\vec{a}, \lambda) F_p(\vec{b}, \lambda) \\ &\quad \times \left[1 + F_e(\vec{b}, \lambda) F_p(\vec{c}, \lambda) \right] d\lambda \end{aligned} \quad (1.10)$$

From eq. (1.3) we have $F_e(\vec{a}, \lambda) F_p(\vec{b}, \lambda) = \pm 1$, and since

$$\rho(\lambda) \left[1 - F_e(\vec{b}, \lambda) F_e(\vec{c}, \lambda) \right] \geq 0 \quad (1.11)$$

it follows that

$$\left| P(\vec{a}, \vec{b}) - P(\vec{a}, \vec{c}) \right| \leq \int \rho(\lambda) \left[1 - F_e(\vec{b}, \lambda) F_e(\vec{c}, \lambda) \right] d\lambda = 1 + P(\vec{b}, \vec{c}) \quad (1.12)$$

And thus we arrive at one version of the Bell inequality:

$$\left| P(\vec{a}, \vec{b}) - P(\vec{a}, \vec{c}) \right| \leq 1 + P(\vec{b}, \vec{c}) \quad (1.13)$$

which must hold for any hidden variable theory and for arbitrary directions \vec{a} , \vec{b} and \vec{c} . The only assumptions we made were the ones in eqs. (1.3) and (1.4).

Quantum mechanics strictly breaks this inequality. This is best observed by choosing a particular value for the measurement axes. Assume that all three vectors lie in a two-dimensional plane, that \vec{a} and \vec{b} are orthogonal and that \vec{c} points in a 45° angle between them. Using eq. (1.2) we then have

$$P(\vec{a}, \vec{b}) = 0 \quad \text{and} \quad P(\vec{a}, \vec{c}) = P(\vec{b}, \vec{c}) = -\frac{1}{\sqrt{2}} \quad (1.14)$$

which gives

$$\frac{1}{\sqrt{2}} \not\leq 1 - \frac{1}{\sqrt{2}} \quad (1.15)$$

clearly in violation of the inequality in eq. (1.13).

This is a very important result, because it shows that quantum mechanics and hidden variable theories are incompatible. It is not possible to extend quantum mechanics by hidden variables. The natural next step was to do experiments testing these inequalities, in order to find out once and for all which was the correct description of physical reality.

In the early 1980s Aspect, Grangier and Roger succeeded, and their results were in excellent agreement with quantum mechanics [20, 21, 22]. Since then though, there have been pointed out several loopholes in the experiments of Aspect et al., particularly with regards to faults in the experimental setup, procedure or behavior of the equipment. Groups around the world have been working hard at constructing and performing experiments that close these loopholes [23, 24, 25, 26, 27, 28], and so far all results seem to favor quantum mechanics as the correct description of reality. There are still loopholes to be filled and proposals for loophole-free experiments are currently being presented [29, 30, 31].

1.2 Entanglement as a resource

Clearly entanglement represents some information content that we can't access directly, but could there be any way of exploiting it nonetheless? Such

questions have led to the development of quantum information theory and quantum computation, scientific areas where entanglement is used as a resource in order to perform tasks that would not be possible with classical systems.

1.2.1 Quantum computing

Classical computing is based on using classical bits. A bit is a unit of information, and characterizes the total information content in a system that can be in one of two distinct states. Bits are usually defined as variables that can take two distinct values, for instance 0 or 1. Bits can be implemented in many ways, for instance as electrical switches that can be either on or off, or electrical circuits that permit two distinct levels of a current or voltage.

In quantum computing one uses quantum bits. Quantum bits, or qubits, are units of quantum information, and characterize the total information content in a quantum system that can be in a superposition of two distinct states. The superposition aspect is very important, and it means that if we denote the two distinct states of the quantum system as 0 and 1, the qubit is a superposition of these values when represented as a variable. This variable is the state vector of a two-level system.

Qubits contain more information than a classical bit, as it takes more information to characterize a superposition or two states rather than an either/or situation such as for the classical bits.

Entanglement between systems represent a type of extra information that is contained in the total system. Since the two-level quantum systems representing the qubits can be entangled, a set of qubits can contain even more information than already discussed relative to a classical set of bits. This extra information is entirely nonclassical and a very important feature in quantum computing.

In order to make use of the qubits we need to be able to manipulate quantum systems in a controlled way, a difficult task indeed. In addition to accessing each qubit individually, we have to be able to do two-particle operations. It has been shown that in order to reproduce the abilities of a classical computer, which is a reasonable first criterion for a quantum computer, one must be able to perform a set of one-particle operations on each single qubit that together can approximate unitary operations. Taken together with two-qubit operations on any two qubits, this is enough to reproduce classical computational abilities, and in addition we have the possibilities in exploiting the quantum properties such as entanglement.

These days such finely-tuned control over quantum systems is possible through various methods. Atomic force microscopy for instance can be used

to identify, image and manipulate individual atoms. Shining lasers on atoms can be used to trap the atoms in a very small space and then one can use other lasers to manipulate these trapped atoms in various ways. Such control over quantum systems can then be used as the machinery in a quantum computer. An example of a realized quantum computer is the NMR quantum computer, based on nuclear magnetic resonance [32]. The qubits in such a computer are the spin states of molecules. These can be manipulated by varying a magnetic field which interacts with the spins of the molecules. It has been used to factor the number 15 into 3 and 5 using 7 qubits, an experimental demonstration of the principle of the quantum algorithm known as Shor's algorithm, which exploits quantum systems to factor numbers a lot faster than classical computers could.

The motivation behind quantum computers can among other places be found in these quantum algorithms that have been developed over the years. A quantum computer will not be able to outperform a classical computer in all imaginable computations, but in some areas it may outperform its classical counterparts significantly. The benefit is in most cases due to an exponential speed up in computational time and/or reduction in the amount of storage needed. A simulation of N two-level systems on a classical computer requires 2^N bits, while a quantum computer requires only N qubits. As N increases this becomes a substantial gain in required storage, which means that a quantum computer can simulate a substantially larger system than a classical computer.

1.2.2 Quantum communication

The realization that information is physical has tremendous consequences when considering the information content in physical systems that are described by quantum mechanics. Entanglement becomes an important information theoretical resource that can be used to perform tasks in quantum information theory that is impossible in classical information theory. In order to illustrate some of the power of entanglement in communication tasks, we will look at some examples. The first example is encoding two bits in a single qubit, the second is what is known as quantum teleportation and the third is quantum key distribution.

In classical communication, if we want to send two bits of information, we can accomplish this by sending two physical bits to the receiver. Because of entanglement we can accomplish sending the same amount of information by only sending one quantum particle between the parties. That is, we can communicate two bits of information by physically transporting only one quantum two-level system between the two parties in the communication.

This is what is known as dense coding and was first treated in [33].

Two physical bits can be used to communicate one of four different messages. Each bit can have the value 0 or 1, so the four possible messages with two physical bits available are 00, 01, 10 and 11.

Dense coding is entirely reliant on entanglement. We will illustrate the concept by considering an entangled pair of spin-1/2 particles, like an electron and a positron as in the EPR setup. To each of the particles is associated a qubit. Two parties, Alice and Bob, want to communicate a message consisting of two bits by physically sending only one qubit. They each have one of the particles in the pair, Alice has the electron and Bob the positron.

Alice then performs one of four specific unitary transformations on the electron before sending it to Bob. The four operations are equivalent to doing nothing, or rotating the spin about the x -, y - or z -axis by 180° . Quantum mechanics tells us that this local transformation that Alice performs on the electron affects the entire system in a way that is not detectable by measuring any of the particles by themselves, but by measuring the particles jointly, Bob can determine which of the four operations Alice performed.

Since Bob has received one of four possible messages, he has obtained two bits of information. But here only one physical object, the electron, was transmitted between the parties. In this way two bits of information has been encoded in one qubit, but it would not have worked unless the particles were entangled.

The advantage in quantum dense coding lies in that some of the exchanged physical objects can be exchanged ahead of time of the actual communication. The scheme is no more efficient than encoding the two bits of information in one particle each and sending the two particles with respect to the number of particles used and the number of exchanges of particles necessary. But it enables Alice and Bob to perform some of the exchange of particles whenever they want, irrespective of when they choose to send a message at a later time, which might be very convenient.

The second example we will look at in terms of illustrating the power of entanglement is quantum teleportation. Classical teleportation schemes in science fiction seems to present no problems. It could be considered working in the following way. We just measure the state of every atom in the object that is to be teleported, transmit that information and then the receiver can reconstruct the object as many times as he wants based on that information. Quantum mechanics, however, puts severe limits on the accuracy of any such operation.

The reason is that one cannot experimentally determine an unknown state. The best one can do experimentally is distinguish between a set of N orthogonal states, if one knows what they are. When measuring the un-

known particle we change the state of the particle to one of those N states and so we can know nothing about the unknown state before the measurement. Exactly copying, or cloning, an unknown quantum state is therefore impossible. It would require being able to exactly measure all the properties of the unknown state simultaneously, including the non-commuting ones, which quantum mechanics expressly forbids because of the uncertainty principle.

What we can do however, is transfer an unknown quantum state from one particle to another, which is what is known as quantum teleportation and was originally described in [34]. It works as follows. Assume as before that Alice and Bob share an entangled pair of spin-1/2 particles with Alice having the electron and Bob the positron. In addition, Alice has another particle in an unknown state ψ which is the state that she wants to teleport to Bob.

Alice then proceeds to bring this particle and the electron together and performs a specific joint measurement on those two particles. This is the same measurement that Bob performed in the final stage of the two-bit communication scheme discussed above. There are four outcomes of this measurement, but by performing this measurement Alice destroys the entanglement between her electron and Bob's positron.

Alice then proceeds to send Bob this information in a classical way, for instance by calling him up on the phone. Based on the information he receives, Bob can perform one of the four unitary operations mentioned in the dense coding scheme on his particle, with the end result being that the state of his positron is identical to the state ψ of Alice's original particle. Note that the state is still unknown for both Alice and Bob, but now Bob is in possession of a particle with the unknown state while Alice is not.

A third application of quantum communication is found in quantum cryptography, a form of communication where the signal is encrypted using quantum techniques in such a way that it is secure against eavesdropping. An application of quantum cryptography that is already commercially available today is quantum key distribution [35, 36, 37, 38].

The idea is the following. Assume that Alice and Bob share a key. A key in this sense is a list that relates measurement outcomes to numbers and/or letters. Using the key, Alice encodes a message in a set of qubits by preparing her particles in such a way that when Bob performs measurements on them he can compare his results with the key/list and translate the message.

Alice then sends her particles to Bob. Eavesdropping on this communication would imply performing measurements on the particles being sent to Bob. If some third party, Eve, is eavesdropping, Bob should be able to detect this because quantum mechanics says that any measurement will disturb the

system. Bob can then just discard the key and inform Alice that someone is eavesdropping. Despite this, a group at NTNU has shown that a certain type of attack called intercept-resend attack can be performed undetectably in some implementations of quantum key distribution [39].

1.2.3 Decoherence

An important property of any full-fledged quantum computer that we have yet to mention is scalability. The number of quantum bits, two-level systems or particles in a quantum computer will have to be of a significant size. The problem with this is that entanglement is a rather unstable resource at present, because quantum states are highly susceptible to what is known as decoherence.

Decoherence is basically the loss of entanglement in a state. It is a result of the quantum state interacting with the environment. In most applications in quantum computation, the states used are pure, entangled states, but as they interact with the environment they will become more and more mixed. In practice this leads to severe problems. If we start with a batch of entangled pure states and start using them for whatever purpose we have in mind, after a while they will decohere and the resource, entanglement, has been diminished. All is not lost, since there exists several ways of dealing with the problem after it has occurred, such as entanglement distillation and quantum error correcting [40]. Quantum distillation is a process where a number of mixed entangled states can be converted into a smaller number of pure entangled states. This helps in order to be able to use more of the entanglement, but ideally we would want to keep the entangled states from interacting with the environment.

Even though we have become increasingly good at controlling quantum systems, being able to isolate them over a long period of time is incredibly hard. This puts limits on the implementations of quantum computers and quantum communication. For instance, it makes it difficult to send quantum signals over long distances with high fidelity. Using fibreoptic cables and entangled photons communication distances of 147.8 km have been demonstrated [41]. Fibreoptics are fine for joining local computers together, but in order to perform worldwide quantum communication it would be nice to be able to use satellites. Thus we would have need of free-space quantum communication in order to send the signal to a satellite relay and back down to the receiver. The current distance record for free-space quantum communication is 144 km, sending entangled photons from La Palma to Tenerife [42, 43]. Recently the possibility of extending the distance to 300 km was proposed and deemed feasible [44].

Chapter 2

Describing quantum systems

In quantum mechanics a state is represented by a state vector ψ in a complex vector space \mathcal{H} called the Hilbert space. One of the properties of a vector space is that adding two vectors produces another vector, which is the formal representation of the superposition principle. Given two states ψ_1 and ψ_2 of some system, the system may also be in the state $\psi = \alpha\psi_1 + \beta\psi_2$ with α and β as complex numbers.

We can also multiply a state vector ψ by a complex number c to produce $c\psi$. One of the postulates of quantum mechanics is that ψ and $c\psi$ represent the same physical state as long as $c \neq 0$. In this sense only the direction in the vector space is of real significance, and so the space of physical states is actually a projective space consisting of lines in the Hilbert space.

A system that has N distinct states is called an N -level system. The state vectors describing the states of the system are then N -component complex vectors, that is, vectors in \mathbb{C}^N . Operators acting on an N -level system are represented as $N \times N$ complex matrices.

Observables are the common name for the quantities that one can measure. Energy is an observable, angular momentum is another. To every observable in quantum mechanics there is associated a Hermitian, linear operator which acts on the state space of the system. A Hermitian matrix A is a matrix for which $A^\dagger = (A^T)^* = A$. It follows that a Hermitian matrix has real eigenvalues. To each Hermitian operator F corresponds a set of eigenvectors ϕ_k with associated real eigenvalues λ_k with the property that when F acts on ϕ_k it returns $\lambda_k\phi_k$ such as

$$F\phi_k = \lambda_k\phi_k \quad (2.1)$$

In a given basis $\{e_k\}$ the components of F are given by

$$F_{kl} = e_k^\dagger F e_l \quad (2.2)$$

Assume that the system is in some state ψ . A postulate in quantum mechanics says that when measuring an observable F , the result will be one of the eigenvalues λ_k of F with the probability of getting that specific eigenvalue given by the overlap $|\phi_k^\dagger \psi|^2$. After the measurement, the system will be in the state described by ϕ_k . This is the effect dubbed as the collapse of the state. Before the measurement the system was in the state ψ , but the measurement collapsed it into the state ϕ_k . This is an idealized situation and the type of measurement performed is a special kind of measurement called a projective measurement.

The average value of the measurement is given by the expectation value of the observable F in the state ψ of the system

$$\langle F \rangle = \psi^\dagger F \psi \quad (2.3)$$

A matrix F is said to be *normal* if it commutes with its adjoint, that is, if $FF^\dagger = F^\dagger F$. There is a remarkable result regarding the representation of normal matrices called the spectral theorem [40]. Clearly, Hermitian matrices are also normal. As the observables are represented by Hermitian matrices, the spectral theorem tells us that any observable operator can be written in terms of its eigenvalues and eigenvectors as

$$F = \sum_k \lambda_k \phi_k \phi_k^\dagger \quad (2.4)$$

and thus we get

$$\langle F \rangle = \psi^\dagger F \psi = \sum_k \left| \phi_k^\dagger \psi \right|^2 \lambda_k \quad (2.5)$$

which is the weighted sum of possible outcomes λ with the weight being the probability of that particular outcome.

For a system in a state described by a single state vector, the uncertainty about the outcome of any particular measurement on the system is not attributed to a lack of information of the system. A state described by a single state vector is referred to as a pure state, and in the standard interpretation of quantum mechanics it represents a system for which we have maximal knowledge. In order to know more about the system, we must perform measurements on the system which will irrevocably change the state of the system.

In general we may have less than maximal knowledge of a system. For instance it could be that a system is prepared in one of several states in an ensemble $\{\psi_k\}$ with a probability distribution $\{p_k\}$ describing the probability

for the final state to be ψ_k . The average value of a measurement on an observable F in an ensemble such as this is

$$\langle F \rangle = \sum_k p_k \psi_k^\dagger F \psi_k = \sum_k p_k \langle F \rangle_k \quad (2.6)$$

which is a weighted sum of each possible average value weighted by the probability of the system being in the given state.

This motivates the introduction of density operators ρ defined as a probability distribution of projections onto the possible state vectors ψ_k

$$\rho = \sum_k p_k \psi_k \psi_k^\dagger, \quad p_k \geq 0, \quad \sum_k p_k = 1 \quad (2.7)$$

The coefficients p_k are all real and sum up to one, as they define a probability distribution. Even though there is a formal difference between the operator and its matrix representation, it is common in physics to use the terms interchangeably.

It follows from the above definition of a density matrix that it is a Hermitian positive semidefinite matrix. The Hermiticity is evident from the definition since all the coefficients p_k are real. The positivity follows from the fact that all the coefficients p_k are greater than or equal to one. If we take the expectation value of a density matrix in any vector ψ we find

$$\psi^\dagger \rho \psi = \sum_k p_k |\psi^\dagger \psi_k|^2 \geq 0 \quad (2.8)$$

which proves the positive semidefiniteness of density matrices. This implies that all the eigenvalues λ_k of ρ are positive or equal to zero which we write as

$$\rho \geq 0 \Leftrightarrow \lambda_k \geq 0 \quad (2.9)$$

Taking the trace of the density matrix we get

$$\text{Tr}(\rho) = \sum_k p_k \text{Tr}(\psi_k \psi_k^\dagger) = \sum_k p_k (\psi_k^\dagger \psi_k) = \sum_k p_k = 1 \quad (2.10)$$

where we have assumed that the state vectors ψ_k are normalized to unit length. Thus, all density matrices have trace equal to one.

The average value of a measurement on F can now be expressed in terms of the density matrix ρ as

$$\langle F \rangle = \text{Tr}(F\rho) = \sum_k p_k \psi_k^\dagger F \psi_k = \sum_k p_k \langle F \rangle_k \quad (2.11)$$

Density matrices are referred to as being either mixed or pure. If the number of terms in the decomposition (2.7) is one we say that we have a pure state, since the ensemble consists of only a single state vector. If the number of terms is larger than one we say we have a mixed state, and the ensemble consists of two or more state vectors. For a general density matrix we have

$$\rho^2 = \sum_k p_k^2 \psi_k \psi_k^\dagger \quad \rightarrow \quad \text{Tr}(\rho^2) = \sum_k p_k^2 > 0 \quad (2.12)$$

Only for a pure state is $\rho^2 = \rho$ since then ρ is a projection onto a single pure state, and then the trace of the square of ρ is equal to one. If ρ is mixed, we see from the above equation that the trace of the square of ρ is less than one. Thus, the trace of the square of the density matrix is a measure of how mixed it is in the sense that

$$0 < \text{Tr}(\rho^2) \leq 1 \quad (2.13)$$

which is equal to one only if ρ represents a pure state. This is called the degree of mixing.

The standard description of the degree of mixing of a quantum state is given by the von Neumann entropy S , defined as

$$S = -\text{Tr}(\rho \log \rho) \quad (2.14)$$

In the eigenbasis of ρ where it is diagonal, the von Neumann entropy is expressed as

$$S = -\sum_k \lambda_k \log \lambda_k \quad (2.15)$$

Since all eigenvalues λ_k have values between 0 and 1, it follows that the von Neumann entropy is positive or zero. It is equal to zero when ρ is a pure state and increases as the probability is distributed among more and more states, that is it increases the more mixed the state is.

The trace of the square of the density matrix is equal to the sum of the square of its eigenvalues, therefore the lower bound of eq. (2.13) is found when all the eigenvalues are nonzero and equal. If ρ is represented by an $N \times N$ matrix, the minimum is found when all the eigenvalues are equal to $1/N$. This yields the degree of mixing equal to $1/N$, and corresponds to us having minimal knowledge of the system, since all states are equally probable. The density matrix corresponding to this,

$$\rho = \frac{\mathbb{1}}{N} \quad (2.16)$$

is referred to as the maximally mixed state. Here $\mathbb{1}$ is the identity operator, represented as the $N \times N$ identity matrix. In conclusion, for any density matrix ρ acting on a Hilbert space of dimension N we have

$$\frac{1}{N} \leq \text{Tr}(\rho^2) \leq 1 \quad (2.17)$$

This is also the state that maximizes the von Neumann entropy, since the probabilities are equally distributed among all states.

It is important to note that the expansion of a density matrix in terms of state vectors in eq. (2.7) is not unique. There are several ensembles $\{\psi_k\}$ of state vectors that give rise to the same density matrix. So even though we consider the density matrix to contain all the information available in the system in the sense that it gives the correct expectation value in eq. (2.11), there may be additional information required to specify the specific physical ensemble for the particular system under consideration.

It is tempting to consider the probability distribution $\{p_k\}$ has as having a purely classical origin, as in the case where the system is prepared in a state in an ensemble with certain probabilities. But the distribution $\{p_k\}$ can also arise from a purely quantum mechanical effect, when the system under consideration is entangled with another system. We will see in the next sections how entanglement can give rise to mixed states when we consider composite systems.

2.1 Composite systems and entanglement

When we have a system composed of two or more subsystems, we have a composite system. An example of such a system could be a system of two particles, as in the EPR case with an electron, a positron and their respective spins. We will mostly be considering systems involving two subsystems, and we call such composite systems bipartite.

As we have seen, entanglement is a property that manifests itself as correlations between measurements. In other words, studying entanglement is equivalent to studying correlations between measurements. Such correlations can be expressed in terms of correlation functions. Given two systems A and B and two observables F_A and F_B each acting independently on their respective systems, the correlation function $C(F_A, F_B)$ describing the correlations between measurements on F_A and F_B can be expressed as

$$C(F_A, F_B) = \langle F_A \otimes F_B \rangle - \langle F_A \rangle \langle F_B \rangle \quad (2.18)$$

If the correlation function is equal to zero, there are no correlations between the systems. In the following we will look at how these correlations can be described in composite quantum systems.

To each subsystem we associate a Hilbert space \mathcal{H}_A and \mathcal{H}_B , and the Hilbert space of the composite system is described as the tensor product of the two subspaces, $\mathcal{H} = \mathcal{H}_A \otimes \mathcal{H}_B$. Let the dimensions of the two subsystems be N_A and N_B respectively. The dimension of the full Hilbert space is then $N = N_A N_B$. We will at times refer to such a system as a system of dimension $N_A \times N_B$ in order to make it clear what type of system we are considering.

Any vector ψ in \mathcal{H} can be expressed using a complete set of product vectors, in the sense that the set of product vectors span the entire Hilbert space \mathcal{H} . Let $\{e_i\}$ be a basis for \mathcal{H}_A and $\{f_j\}$ a basis for \mathcal{H}_B , then a complete set of basis vectors for \mathcal{H} can be found by taking tensor products of vectors from the two sets. We then express the vector ψ as

$$\psi = \sum_{ij} \psi_{ij} e_i \otimes f_j \quad (2.19)$$

with the components obtained by multiplication with the basis vectors:

$$\psi_{ij} = (e_i \otimes f_j)^\dagger \psi \quad (2.20)$$

The full Hilbert space will contain state vectors ψ which are tensor products of state vectors from each of two subsystems. If the coefficients in eq. (2.20) factor as $\psi_{ij} = \phi_i \chi_j$ we get

$$\psi = \sum_{ij} \phi_i \chi_j e_i \otimes f_j = \left(\sum_i \phi_i e_i \right) \otimes \left(\sum_j \chi_j e_j \right) = \phi \otimes \chi \quad (2.21)$$

which is a product vector in \mathcal{H} .

The components of ψ are then

$$\psi_k = \phi_i \chi_j = \psi_{ij}, \quad \begin{array}{l} i = 1, \dots, N_A \\ j = 1, \dots, N_B \\ k = 1, \dots, N \end{array} \quad (2.22)$$

On the left hand side ψ is indexed as a vector in \mathcal{H} while using the double index on the right hand side explicitly implies the product structure of \mathcal{H} . As an example, consider two 2-level systems. Then we have two components for ϕ and two for χ and we get

$$\psi = \begin{pmatrix} \psi_1 \\ \psi_2 \\ \psi_3 \\ \psi_4 \end{pmatrix} = \phi \otimes \chi = \begin{pmatrix} \phi_1 \\ \phi_2 \end{pmatrix} \otimes \begin{pmatrix} \chi_1 \\ \chi_2 \end{pmatrix} = \begin{pmatrix} \phi_1 \chi_1 \\ \phi_1 \chi_2 \\ \phi_2 \chi_1 \\ \phi_2 \chi_2 \end{pmatrix} \quad (2.23)$$

The product structure extends to operators on \mathcal{H} as well. If F_A is an operator on \mathcal{H}_A and F_B an operator on \mathcal{H}_B , a product operator on \mathcal{H} will be $F = F_A \otimes F_B$. The elements of matrices representing operators acting on bipartite Hilbert spaces can be expressed in terms of four indices with two referring to subsystem A and the other two to subsystem B . Let any operator F act on the total system $\mathcal{H}_A \otimes \mathcal{H}_B$. In the product basis $\{e_i \otimes f_j\}$ we define the components of F as

$$F_{ijkl} = (e_i \otimes f_j)^\dagger F (e_k \otimes f_l) \quad (2.24)$$

The expectation value of an operator F in a product vector $\psi = \phi \otimes \chi$ is then

$$(\phi \otimes \chi)^\dagger F (\phi \otimes \chi) = \sum_{ijkl} \phi_i^* \chi_j^* F_{ijkl} \phi_k \chi_l \quad (2.25)$$

The expectation value of such a product operator in a product state $\psi = \phi \otimes \chi$ gives

$$\begin{aligned} \langle F_A \otimes F_B \rangle &= (\phi^\dagger \otimes \chi^\dagger) (F_A \otimes F_B) (\phi \otimes \chi) \\ &= (\phi^\dagger F_A \phi) \otimes (\chi^\dagger F_B \chi) \\ &= \langle F_A \rangle \langle F_B \rangle \end{aligned} \quad (2.26)$$

From eq. (2.18) we observe that then $C(F_A, F_B) = 0$ which means that there are no correlations present. For product vectors this is always the case, and thus we say that they are separable.

An ensemble of product vectors gives rise to a type of density matrix which we refer to as a separable state. Consider an ensemble $\{\psi_{kl} = \phi_k \otimes \chi_l\}$ together with a probability distribution $\{p_{kl}\}$. This gives rise to a density matrix

$$\rho = \sum_{kl} p_{kl} \psi_{kl} \psi_{kl}^\dagger = \sum_{kl} p_{kl} \rho_k^A \otimes \rho_l^B \quad (2.27)$$

where

$$\rho_k^A = \phi_k \phi_k^\dagger \quad \text{and} \quad \rho_l^B = \chi_l \chi_l^\dagger \quad (2.28)$$

A separable density matrix can also be expressed as a convex combination of projections onto vectors that are not product states. For example, the eigenvectors of a separable density matrix are not necessarily product vectors. The defining property of a separable density matrix is that it is possible to find an ensemble of product states such that it can be expressed as in eq. (2.27).

A system described by a separable density matrix will in general contain correlations. This can be seen as follows. The expectation value of a product operator in a separable density matrix is

$$\langle F_A \otimes F_B \rangle = \text{Tr}(\rho(F_A \otimes F_B)) = \sum_{kl} p_{kl} \langle F_A \rangle_k \langle F_B \rangle_l \quad (2.29)$$

with

$$\langle F_A \rangle_k = \text{Tr}(\rho_k^A F_A) \quad \text{and} \quad \langle F_B \rangle_l = \text{Tr}(\rho_l^B F_B) \quad (2.30)$$

With the local probability distributions $\{p_k^A\}$ and $\{p_l^B\}$ obtained by $p_k^A = \sum_l p_{kl}$ and $p_l^B = \sum_k p_{kl}$ we find that the product of the expectation values of the operators separately is

$$\begin{aligned} \langle F_A \rangle \langle F_B \rangle &= \left(\sum_k p_k^A \text{Tr}(\rho_k^A F_A) \right) \left(\sum_l p_l^B \text{Tr}(\rho_l^B F_B) \right) \\ &= \sum_{kl} p_k^A p_l^B \langle F_A \rangle_k \langle F_B \rangle_l \end{aligned} \quad (2.31)$$

Comparing this with eq. (2.29) we see that only in the special case that the probabilities factor as $p_{kl} = p_k^A p_l^B$ do we have no correlations between the systems A and B for separable systems.

There are in a sense three levels of correlations in a bipartite quantum system. The first is when we have no correlations. In that case the system can be described by a separable density matrix as in eq. (2.27) but with factoring probabilities. The second level is when the system is described by a separable density matrix with non-factoring probabilities. These kinds of correlations are referred to as classical correlations.

The third and final level is when the system cannot be described by a separable density matrix. In this case it is not possible to find an ensemble of product vectors such that the density matrix can be expressed as in eq. (2.27). Instead the system is described by an ensemble of state vectors $\{\psi_k\}$ and probabilities $\{p_k\}$ so that the density matrix for the full system can be written as

$$\rho = \sum_k p_k \psi_k \psi_k^\dagger \quad (2.32)$$

where not all the vectors ψ_k can be product vectors. Such density matrices are referred to as entangled, as opposed to separable. The correlations in systems described in this way can be considered purely quantum mechanical,

or they may have both classical and quantum mechanical origin, as we will see in the next section.

A particular feature of separable density matrices is that there must exist a set of product vectors that span their image. This can be seen as follows. Any separable density matrix can be written as

$$\rho = \sum_k p_k \rho_k^A \otimes \rho_k^B = \sum_k p_k (\phi_k \otimes \chi_k) (\phi_k \otimes \chi_k)^\dagger = \sum_k p_k \psi_k \psi_k^\dagger \quad (2.33)$$

simply by taking eq. (2.27) and defining $p_1 \equiv p_{11}, p_2 \equiv p_{12}, \dots$ and renaming the product vectors. Note that this sum runs over more terms than the sums in eq. (2.27). If i and j take m and n different values respectively, k in eq. (2.33) runs over at most mn terms. The image is defined as $Img(\rho) = \{\psi \in \mathcal{H} \mid \psi = \rho\theta \text{ for some } \theta \in \mathcal{H}\}$ while the kernel is defined as $Ker(\rho) = \{\psi \in \mathcal{H} \mid \rho\psi = 0\}$. For a vector ψ in $Ker(\rho)$ it follows that $\psi^\dagger \rho \psi = 0$. Let ψ be any vector in $Ker(\rho)$ and we get

$$\psi^\dagger \rho \psi = \sum_k p_k \left| \psi_k^\dagger \psi \right|^2 = 0 \quad (2.34)$$

Since the sum only contains positive terms, it follows that $\psi_k^\dagger \psi$ must be equal to zero for every ψ_k . Since this must hold for any ψ in the kernel of ρ , it follows that all ψ_k lie in the image of ρ .

The fact that the image, also known as the range, of a separable density matrix is spanned by a set of product vectors is known as the range criterion. It was first developed in [4], and we have used it to check the separability of various density matrices in Paper I. Note that the implication only works one way, in the sense that if a density matrix is separable its image is spanned by product vectors, while the converse is not necessarily true.

2.2 Partial trace, entanglement and decoherence

For composite systems the partial trace is a trace operation with respect to a subset of the systems. That is, it is the contraction of a subset of indices for the matrix representation of a composite operator. Consider a bipartite system $\mathcal{H} = \mathcal{H}_A \otimes \mathcal{H}_B$ and let ρ be a density matrix acting on \mathcal{H} . The partial trace with respect to subsystem B is defined as

$$\rho_{ik}^A = \sum_j \rho_{ijkj} \quad (2.35)$$

where we sum over the indices of subsystem B . The result is a reduced density matrix ρ^A that acts on \mathcal{H}_A ,

$$\rho^A = \text{Tr}_B(\rho) \quad (2.36)$$

Equivalently one may obtain the reduced density matrix acting on \mathcal{H}_B by taking the partial trace with respect to subsystem A as

$$\rho^B = \text{Tr}_A(\rho) \quad (2.37)$$

The ranks r_A and r_B of the reduced density matrices $\rho_A = \text{Tr}_B(\rho)$ and $\rho_B = \text{Tr}_A(\rho)$ respectively, we call the local ranks of ρ . They are important, among other things because if ρ appears to belong to a system of dimension $N_A \times N_B$ and $r_A < N_A$ or $r_B < N_B$, then ρ can be viewed as belonging to a composite system of smaller dimension.

Consider a situation where we have a system A which interacts with another system that we label system B . Performing measurements of observables F_A acting on system A means we need to know the density matrix ρ^A which describes system A in order to find the expectation values $\langle F_A \rangle = \text{Tr}(F_A \rho^A)$. The total state of the system is ρ , and in order to get the density matrix ρ^A we have to take the partial trace of ρ with respect to system B .

Assume that the state of system A is prepared in a pure state described by a state vector ψ_A and let system B be modeled at time of preparation by some density matrix ρ^B . Then initially the state of our system is

$$\rho_0 = (\psi_A \psi_A^\dagger) \otimes \rho^B \quad (2.38)$$

After a while the system has changed according to some unitary time evolution operator on the whole system

$$\rho = U \rho_0 U^\dagger \quad (2.39)$$

If the two systems evolve independently of each other, the unitary evolution would be a product operator $U = U_1 \otimes U_2$ and then we would have a final state that is still a product state

$$\rho = (U_1 \psi_A \psi_A^\dagger U_1^\dagger) \otimes (U_2 \rho^B U_2^\dagger) \quad (2.40)$$

Tracing out the system B we would get a density matrix for system A that is still a pure state

$$\rho^A = \text{Tr}_B(\rho) = U_1 \psi_A \psi_A^\dagger U_1^\dagger \equiv \hat{\psi}_A \hat{\psi}_A^\dagger \quad (2.41)$$

On the other hand, if the two systems interact with each other, the time evolution of the system will be described by a non-product operator U , and then the reduced operator ρ^A will in general not be a pure state. This is a formal description of entanglement. Even if we know exactly the state of the full system AB after the time evolution, that is the full state ρ is described by a non-product vector ψ , the reduced density matrix

$$\rho^A = \text{Tr}_B (\psi\psi^\dagger) \quad (2.42)$$

will be a mixed state.

We can see this by using eq. (2.19) and expanding the above expression as

$$\begin{aligned} \rho^A &= \text{Tr}_B \left(\sum_{ijkl} \psi_{ij} \psi_{kl}^* (e_i \otimes f_j) (e_k \otimes f_l)^\dagger \right) \\ &= \sum_{ijkl} \psi_{ij} \psi_{kl}^* (f_l^\dagger f_j) (e_i e_k^\dagger) = \sum_{ijk} \psi_{ij} \psi_{kj}^\dagger e_i e_k^\dagger \end{aligned} \quad (2.43)$$

where $\{e_i\}$ and $\{f_i\}$ are orthonormal bases in subsystem A and B respectively. Define a new set of vectors $\{\phi_j\}$ in \mathcal{H}_A as

$$n_j \phi_j = \sum_i \psi_{ij} e_i \quad (2.44)$$

where n_j are normalization coefficients so that the ϕ_j are unit vectors. Then we can write eq. (2.43) as

$$\rho^A = \sum_j n_j^2 \phi_j \phi_j^\dagger \quad (2.45)$$

which shows that ρ^A is a mixed state. Only in the case that A and B evolve independently will we end up with a pure state.

The partial trace allows us to shed some further light on the origin of the uncertainty in a quantum state. In the most general case the total system is described by an ensemble $\{\psi_k\}$ and probabilities $\{p_k\}$ so that the density matrix ρ is

$$\rho = \sum_k p_k \psi_k \psi_k^\dagger \quad (2.46)$$

Following the example of the pure state description, we end up with a reduced density matrix for system A given by

$$\rho^A = \sum_{kj} p_k n_j^2 \phi_{kj} \phi_{kj}^\dagger \quad (2.47)$$

where the index k refers to the original ensemble while the index j refers to the chosen basis for the environment. But this we can rewrite as

$$\rho^A = \sum_i \tilde{p}_i \tilde{\phi}_i \tilde{\phi}_i^\dagger \quad (2.48)$$

by a simple reordering and renaming the terms in the sum. Now we see that the probabilities \tilde{p}_k in general can have contributions from both the ensemble probabilities p_j of the total system and the probabilities n_j^2 . The latter arise from the entanglement between the systems, and in this sense are of quantum origin. Thus, it is not in general clear whether the ensemble probabilities for a given system can be regarded as purely classical or purely quantum mechanical.

If system B is completely inaccessible to us, the evolution of the state of system A from a pure state to a mixed state is called decoherence. The most common way to think about this is that system B is a model of the environment, with an infinite number of degrees of freedom. Since we have no control over the environment, we cannot invert the effect of time evolution on the total system in order to regain a pure state description of system A .

If system A is itself a composite system consisting of system C and D , $A = CD$, and system B is a model of the environment, the decoherence leads to loss of entanglement in system A . This is the crucial problem in practical implementation of quantum systems. The interactions between system A and the environment B will in general destroy correlations between subsystems C and D that make up system A , and will in this sense lead to leakage of entanglement in system A to the environment. Since we cannot control the environment, the entanglement is lost to us.

In the above discussion we assumed at a point that we knew everything there was to know about the total system, but showed that we still may have uncertainties related to the subsystems. This is a fascinating quantum mechanical feature. A striking example of this is the case two spin-1/2 particles with spin pointing up or down, as in the EPR example. The Bell states are maximally entangled states of two qubits. Let ψ_+ and ψ_- be single-particle vectors describing whether the spin points up or down. The four Bell states

are then written as

$$\begin{aligned}
\psi_1 &= \frac{1}{\sqrt{2}} (\psi_+ \otimes \psi_+ + \psi_- \otimes \psi_-) \\
\psi_2 &= \frac{1}{\sqrt{2}} (\psi_+ \otimes \psi_+ - \psi_- \otimes \psi_-) \\
\psi_3 &= \frac{1}{\sqrt{2}} (\psi_+ \otimes \psi_- + \psi_- \otimes \psi_+) \\
\psi_4 &= \frac{1}{\sqrt{2}} (\psi_+ \otimes \psi_- - \psi_- \otimes \psi_+)
\end{aligned} \tag{2.49}$$

Assume that the spins are anti-correlated and that the spin of the total system is zero. Then the state of the system is described by the Bell state ψ_4 , called the singlet. Taking the partial trace with respect to the second subsystem we find then

$$\rho^A = \text{Tr}_B (\psi_4 \psi_4^\dagger) = \frac{1}{2} (\psi_+ \psi_+^\dagger + \psi_- \psi_-^\dagger) = \frac{1}{2} \mathbb{1}_2 \tag{2.50}$$

which is the maximally mixed state in subsystem A . Taking the partial trace with respect to system A leads to the maximally mixed state in subsystem B . In fact, this is true for all the Bell states. This tells us that even though we have maximal knowledge of the full state (it is a pure state), we have minimal knowledge of each of the particles by themselves. The spin of a single particle has 50% chance of pointing up and 50% of pointing down.

2.3 Partial transposition and positive maps

To determine whether a given density matrix is separable or entangled is in general a very difficult problem. Although the definition of separability gives a necessary and sufficient condition, it is in general hard to test. On the other hand, some easily testable necessary conditions have been found. One particularly important one is the positive-partial-transpose criterion [3, 45]. It is related to positive maps between matrices, and we will present it in the following.

A positive map is a map Φ which maps positive semidefinite complex $n \times n$ matrices to positive semidefinite complex $m \times m$ matrices, $\Phi : \mathbb{C}^{n \times n} \rightarrow \mathbb{C}^{m \times m}$. An example of such a map is the transposition map τ which maps a $n \times n$ positive matrix B to a $n \times n$ positive matrix $\tau(B) = B^T$. Positive maps in bipartite systems are classified according to k -positivity. Let I_k be the identity map $I_k(B) = B$ on $k \times k$ matrices, then the map

$$I_k \otimes \Phi : \mathbb{C}^{k \times k} \otimes \mathbb{C}^{n \times n} \rightarrow \mathbb{C}^{k \times k} \otimes \mathbb{C}^{m \times m} \tag{2.51}$$

is a natural map on the product space in the sense that

$$(I_k \otimes \Phi)(B \otimes A) = B \otimes \Phi(A) \quad (2.52)$$

A positive map Φ for which $I_k \otimes \Phi$ is also positive is called a k -positive map. If $I_k \otimes \Phi$ is positive for any k , then the map Φ is said to be completely positive.

An example of a positive map that fails to be 2-positive is the transposition map τ . In a composite system of dimension 2×2 the matrix

$$\begin{pmatrix} 1 & 0 & 0 & 1 \\ 0 & 0 & 0 & 0 \\ 0 & 0 & 0 & 0 \\ 1 & 0 & 0 & 1 \end{pmatrix} \quad (2.53)$$

is positive semidefinite. After acting on it with $I_2 \otimes \tau$ and thus transposing each 2×2 block we get

$$\begin{pmatrix} 1 & 0 & 0 & 0 \\ 0 & 0 & 1 & 0 \\ 0 & 1 & 0 & 0 \\ 0 & 0 & 0 & 1 \end{pmatrix} \quad (2.54)$$

which is clearly not positive. The action of the composite operator $I_k \otimes \tau$ is known as partial transposition.

For any matrix F acting on a bipartite space, the elements of the partial transpose F^P is given by

$$(F^P)_{ijkl} = F_{ilkj} \quad (2.55)$$

which is simply interchanging the indices referring to the subsystem we take the transpose of in the partial transposition, in this case subsystem B .

All separable density matrices remain positive semidefinite under partial transposition. This can be seen by taking a separable density matrix ρ and applying the partial transpose to get.

$$(I \otimes \tau)(\rho) \equiv \rho^P = (I \otimes \tau) \left(\sum_k p_k \rho_k^A \otimes \rho_k^B \right) = \sum_k p_k \rho_k^A \otimes \tau(\rho_k^B) \quad (2.56)$$

and the transposition on the density matrices in the second subsystem preserves their positivity so that the partial transpose of a separable density matrix is another separable density matrix. States that are positive under partial transposition we refer to as PPT for short.

Partial transposition is very important, since any state that is not PPT is necessarily entangled. This follows from the above discussion in that separable density matrices are always PPT. This can be phrased as a condition for separability and we refer to it as the PPT criterion. It was developed in [3, 45] and it was shown that the criterion is both necessary and sufficient to determine separability in systems of dimension 2×2 and 2×3 . The implication in the PPT criterion only works one way, however. If a state is separable it must be PPT, but the converse is not true in general. The first example of entangled PPT states (PPTES) was given in [4].

Another important aspect of partial transposition is that it marks a separation of entanglement into two qualitatively different types. It was shown in [1] that states from which entanglement can be distilled cannot be PPT. Thus, the entanglement contained in PPTES is impossible to access in a sense. Because of this, entanglement contained in PPTES is usually referred to as bound, while non-PPT states contain free entanglement. Later it has been shown that bound entangled states can be used as catalysts in distillation protocols in multipartite settings [46, 47, 48, 49, 50, 51, 52, 53]. This is often referred to as either activation or superactivation of bound entanglement, depending on the protocol.

The study of positive maps is intrinsically linked with the study of entanglement witnesses. An entanglement witness is an operator A which satisfies

$$\text{Tr}(A\rho_S) \geq 0 \quad (2.57)$$

for all separable states ρ_S , while for some entangled state or set of entangled states we would get $\text{Tr}(A\rho) < 0$. In this way, the operator A identifies, or witnesses, the state as entangled.

By the Choi-Jamiolkowski isomorphism [54, 55] every positive map $\Phi : \mathbb{C}^{n \times n} \rightarrow \mathbb{C}^{m \times m}$ has a representation as an operator on $\mathbb{C}^{m \times m} \otimes \mathbb{C}^{n \times n}$. Assume that we have two matrices A and B in $\mathbb{C}^{m \times m}$ and $\mathbb{C}^{n \times n}$ respectively, and that they are related by a linear map, $A = \Phi(B)$. For some complete set of basis matrices $\{E_{jl}\}$ in $\mathbb{C}^{n \times n}$ and b_{jl} as the components of B in this basis, we can write this as

$$A = \Phi(B) = \Phi\left(\sum_{jl} b_{jl} E_{jl}\right) = \sum_{jl} b_{jl} \Phi(E_{jl}) \quad (2.58)$$

Now $\Phi(E_{jl})$ is a matrix in $\mathbb{C}^{m \times m}$, so any component of A can be written as

$$A_{ik} = \sum_{jl} b_{jl} \Phi(E_{jl})_{ik} \equiv \sum_{jl} P_{ikjl} b_{jl} \quad (2.59)$$

The matrix P can be represented as a $mn \times mn$ matrix in $\mathbb{C}^{m \times m} \otimes \mathbb{C}^{n \times n}$ with indices P_{ijkl} obtained by expectation values in a product vector basis as in eq. (2.24).

Because of the product structure we can think of the matrix representation of F as a block matrix, $F_{ijkl} \equiv (G_{jl})_{ik}$, that is an $N_B \times N_B$ matrix where each element G_{ik} is an $N_A \times N_A$ matrix. For example, let $N_A = 2$ and $N_B = 3$, then we could represent F as the block matrix

$$F = \begin{pmatrix} G_{11} & G_{12} & G_{13} \\ G_{21} & G_{22} & G_{23} \\ G_{31} & G_{32} & G_{33} \end{pmatrix} \quad (2.60)$$

where each element G_{jl} is a 2×2 matrix, so that the above matrix is a 6×6 matrix.

The block representation of P will look like

$$P = \begin{pmatrix} \Phi(E_{11}) & \dots & \Phi(E_{1n}) \\ \vdots & \ddots & \vdots \\ \Phi(E_{n1}) & \dots & \Phi(E_{nn}) \end{pmatrix} \quad (2.61)$$

where each element $\Phi(E_{jl})$ is an $m \times m$ matrix, similar to the case in eq. (2.60). The matrix P in this form is often referred to as the Choi-matrix of the map Φ .

The entanglement witnesses are the matrix representations of positive maps, and the reason why they fulfill eq. (2.57) for all separable states is the following. All positive $n \times n$ matrices can be written as convex combinations of rank one projectors. Thus, consider a rank one projector

$$B = yy^\dagger, \quad B_{jl} = y_j y_l^* \quad (2.62)$$

Inserting this into eq. (2.59) we get

$$A_{ik} = \sum_{jl} P_{ijkl} y_j y_l^* \quad (2.63)$$

The expectation value of A in some vector x can then be written as

$$x^\dagger A x = \sum_{ik} x_i^* A_{ik} x_k = \sum_{ijkl} x_i^* y_j P_{ijkl} x_k y_l^* \quad (2.64)$$

Introduce the vector \bar{y} whose elements are the complex conjugated of the elements of y in the basis we are working in, $\bar{y}_i = y_i^*$, then we also have $\bar{y}_i^* = y_i$ and can rewrite the above expression as

$$x^\dagger A x = \sum_{ijkl} x_i^* \bar{y}_j^* P_{ijkl} x_k \bar{y}_l \quad (2.65)$$

Comparing with eq. (2.25) we see that this is in fact equal to the expectation value of P in the product vector $z \equiv x \otimes \bar{y}$. Since we are assuming that P represents a positive map and B is positive, we know that A is as well and therefore the expectation value of A in any vector is positive. In particular $x^\dagger Ax \geq 0$, and therefore

$$x^\dagger Ax = (x \otimes \bar{y})^\dagger P(x \otimes \bar{y}) = z^\dagger Pz = \text{Tr}(Pzz^\dagger) \geq 0 \quad (2.66)$$

Expanding a separable state ρ_S in terms of a set of product vectors z_k we get

$$\text{Tr}(P\rho_S) = \text{Tr}\left(P \sum_k p_k z_k z_k^\dagger\right) = \sum_k p_k \text{Tr}(Pz_k z_k^\dagger) \geq 0 \quad (2.67)$$

because the trace is linear. In this sense, the entanglement witnesses P are said to be dual to the separable states.

2.4 SL \otimes SL transformations and SLOCC equivalence

In the work presented in this thesis we have made extensive use of the properties of linear transformations and their actions on state vectors and density matrices. The reason for this is that it greatly simplifies our efforts in characterizing density matrices since it allows us to focus on properties of density matrices that are invariant with respect to a particular type of linear transformations. We will in the following review such transformations and their properties.

In quantum information theory a situation of particular interest is when several spatially separate parties share a composite system in an entangled state. They can then perform local operations on the particle they possess and communicate classical information to each other. This will in general lead to modifications in the entanglement properties of the state, and in particular they can try to transform one entangled state into another. Transformations using local operations and classical communication is known as LOCC transformations.

One can then define equivalence relations between states. Two states ψ and $\tilde{\psi}$ are said to be equivalent under LOCC if they can be transformed into each other with certainty using only local operations and classical communication. This is a desirable property, for instance because then the parties can regard the two states as indistinguishable and use them for exactly the same task, and we say that they contain the same entanglement.

But this also means that we are restricting the class of transformations from all LOCC transformations to those that are invertible. Thus, in the following, when we write LOCC transformations, it is always implied that we are talking about invertible product transformations.

It turns out that two states are LOCC equivalent if and only if they are related by local unitary operators [56, 57]. Specifying in the following to a bipartite system $\mathcal{H} = \mathcal{H}_A \otimes \mathcal{H}_B$, and with ψ and $\tilde{\psi}$ in \mathcal{H} , this means that ψ and $\tilde{\psi}$ are LOCC equivalent if and only if

$$\psi = U\tilde{\psi} \quad \text{with} \quad U = U_A \otimes U_B \quad \text{and} \quad U_{A/B}^\dagger = U_{A/B}^{-1} \quad (2.68)$$

so U_A and U_B are elements in the groups $U(N_A)$ and $U(N_B)$ respectively. For an ensemble of states $\{\psi_k\}$ we may then consider it to be LOCC equivalent to an ensemble $\{\tilde{\psi}_k\}$ if and only if there exists a unitary product operator $U = U_A \otimes U_B$ such that

$$\rho = \sum_k p_k \psi_k \psi_k^\dagger = \sum_k p_k U \tilde{\psi}_k \tilde{\psi}_k^\dagger U^\dagger = U \tilde{\rho} U^\dagger \quad (2.69)$$

for some associated probability distribution $\{p_k\}$.

We may extend the equivalence class by allowing the transformations between the two states ψ and $\tilde{\psi}$ to succeed with some nonzero probability. This is a broader class of transformations known as stochastic LOCC, or SLOCC for short. They are interesting because states equivalent under SLOCC may still be used for the same task, it just means that the probability of success for the task depends on which state one uses.

Mathematically, ψ and $\tilde{\psi}$ are considered SLOCC equivalent if and only if there exists linear invertible local operators V_A and V_B such that

$$\psi = V\tilde{\psi} \quad \text{with} \quad V = V_A \otimes V_B \quad (2.70)$$

We no longer require that V is a unitary product matrix, only that V_A and V_B are elements in the groups $GL(N_A)$ and $GL(N_B)$ of nonsingular linear operators respectively. In the following, as with LOCC transformations, when we write SLOCC transformations, it is implied that we are talking about invertible product transformations.

Analogously to the LOCC case, we may consider two ensembles $\{\psi_k\}$ and $\{\tilde{\psi}_k\}$ to be SLOCC equivalent if and only if there exists local invertible operators V_A and V_B such that

$$\rho = \sum_k p_k \psi_k \psi_k^\dagger = \sum_k p_k V \tilde{\psi}_k \tilde{\psi}_k^\dagger V^\dagger = V \tilde{\rho} V^\dagger \quad \text{with} \quad V = V_A \otimes V_B \quad (2.71)$$

for some associated probability distribution $\{p_k\}$.

Without loss of generality we may write the SLOCC transformations on state vectors ψ and density matrices ρ on the following form:

$$\tilde{\psi} \mapsto \psi = cV\tilde{\psi}, \quad c \in \mathbb{C} \quad (2.72)$$

$$\tilde{\rho} \mapsto \rho = aV\tilde{\rho}V^\dagger, \quad a \in \mathbb{R} \quad (2.73)$$

Here c and a are positive normalization factors and $V = V_A \otimes V_B$, with V_A and V_B elements of the special linear groups $\text{SL}(N_A, \mathbb{C})$ and $\text{SL}(N_B, \mathbb{C})$ respectively. That is, they are linear nonsingular $N_A \times N_A$ and $N_B \times N_B$ complex matrices respectively, with determinants equal to 1.

In our work we refer to such transformations as SL \otimes SL transformations, and we say that states that can be transformed into each other by such transformations are SL \otimes SL equivalent, or just SL equivalent for short when it is clear from the context that we are considering product transformations.

Our interest in SL \otimes SL transformations stems from the fact that such transformations conserve several key properties of density matrices, including the rank, positivity and separability. The rank is conserved because we are only considering invertible transformations. To see that the positivity is conserved, let $\tilde{\rho}$ be expanded in a suitable ensemble of state vectors as

$$\tilde{\rho} = \sum_k p_k \tilde{\psi}_k \tilde{\psi}_k^\dagger \quad (2.74)$$

Then take the expectation value of the transformed density matrix in any vector ψ to get

$$\begin{aligned} \psi^\dagger \rho \psi &= \psi^\dagger (aV\tilde{\rho}V^\dagger) \psi \\ &= a \sum_k p_k \left(\psi^\dagger V \tilde{\psi}_k \right) \left(\tilde{\psi}_k^\dagger V^\dagger \psi \right) = a \sum_k p_k \left| \psi^\dagger V \tilde{\psi}_k \right|^2 \geq 0 \end{aligned} \quad (2.75)$$

which is true since $a > 0$ and $p_k \geq 0$, and since ψ is arbitrary it follows that the transformed density matrix is also positive semidefinite.

To see that SL \otimes SL transformations preserve separability, observe that if we transform a separable state vector $\tilde{\psi} = \tilde{\phi} \otimes \tilde{\chi}$ we get

$$\tilde{\psi} \mapsto \psi = cV\tilde{\psi} = c(V_A \otimes V_B) (\tilde{\phi} \otimes \tilde{\chi}) = c(V_A \tilde{\phi}) \otimes (V_B \tilde{\chi}) = c\phi \otimes \chi \quad (2.76)$$

which is also a product vector. This means in particular that SLOCC transformations preserve the number of product vectors in any subspace of \mathcal{H} , like the image and kernel of a density matrix for instance. Then note that a separable density matrix can be written as in eq. (2.74) but with all $\tilde{\psi}_k$

as product vectors. Then it follows that the transformed state is a convex sum of projections on transformed vectors $V\psi_k$ which themselves are product vectors, and hence the transformed density matrix is also separable.

$\text{SL} \otimes \text{SL}$ transformations also preserve the positivity of the partial transpose, regardless of whether the state is separable or entangled. To see this, let $\tilde{\rho}$ be a PPT state and consider the components of the transformed state ρ :

$$\rho_{ijkl} = a \sum_{mnr s} (V_A)_{im} (V_B)_{jn} \tilde{\rho}_{mnr s} (V_A)_{kr}^* (V_B)_{ls}^* \quad (2.77)$$

The components of the partial transpose are given by $\rho_{ijkl}^P = \rho_{ilkj}$, so we get

$$\begin{aligned} \rho_{ijkl}^P &= a \sum_{mnr s} (V_A)_{im} (V_B)_{ln} \tilde{\rho}_{mnr s} (V_A)_{kr}^* (V_B)_{js}^* \\ &= a \sum_{mnr s} (V_A)_{im} (V_B)_{ln} \tilde{\rho}_{msrn}^P (V_A)_{kr}^* (V_B)_{js}^* \\ &= a \sum_{mnr s} (V_A)_{im} (V_B)_{js}^* \tilde{\rho}_{msrn}^P (V_A)_{kr}^* (V_B)_{ln} \end{aligned} \quad (2.78)$$

Now introduce a new matrix \bar{V}_B with coefficients $(\bar{V}_B)_{jl} = (V_B)_{jl}^*$ and rewrite the above expression as

$$\rho_{ijkl}^P = a \sum_{mnr s} (V_A)_{im} (\bar{V}_B)_{js} \tilde{\rho}_{msrn}^P (V_A)_{kr}^* (\bar{V}_B)_{ln}^* \quad (2.79)$$

Comparing with eq. (2.77) it follows that we get

$$\rho^P = a \hat{V} \tilde{\rho}^P \hat{V}^\dagger \quad \text{with} \quad \hat{V} = V_A \otimes \bar{V}_B \quad (2.80)$$

Since $\text{SL} \otimes \text{SL}$ transformations preserve positivity, it follows that if $\tilde{\rho}^P$ is positive semidefinite, so is ρ^P .

The study of equivalence under deterministic transformations (LOCC) between pure states was initiated in [58], and the extension to SLOCC equivalence was proposed in [59]. The study of equivalence under LOCC and SLOCC has been largely focused on means of classifying the entanglement contained in both pure and mixed states. The classifications are based on identifying entanglement monotones, that is, quantities $E(\rho)$ that do not increase under LOCC or SLOCC. For an overview of various entanglement monotones see [2].

SLOCC transformations have been studied also in relation to representations of states, mixed and pure. That is, efforts directed at identifying

particularly useful representations of density matrices obtainable through SLOCC transformations. For multipartite states one such representation is the normal form introduced in [60] where it is shown that any state ρ can be transformed using SLOCC transformations to a form where all but one of the reduced density matrices computable from ρ is proportional to the identity operator on the reduced system.

For bipartite systems of dimension 2×2 it was shown in [14] that any state ρ can be transformed by $SL \otimes SL$ transformations to a standard form which enables a particularly nice, simple and geometric proof of the necessity and sufficiency of the PPT criterion in 2×2 . In other words, it is shown that all PPT states in 2×2 are SLOCC equivalent to separable states with a particular representation.

In Paper II and III we have extensively studied entangled PPT states of rank 4 with respect to a standard form for such states. In Paper II we present a standard form parametrized by $SL \otimes SL$ invariants for such rank 4 entangled PPT states. This standard form enables an explicit analytical construction of all states equivalent to this representation. We also present numerical evidence supporting our claim that all rank 4 entangled PPT states can be transformed by $SL \otimes SL$ transformations to this standard form, which we base on the fact that it is true for all known explicit examples of such states found in the literature and all numerical examples we have obtained. In Paper III we discuss a possible generalization of the standard form to states of higher rank in higher dimensional systems.

Chapter 3

Geometrical aspects of entanglement

The set of density matrices, which we denote \mathcal{D} , consists of all positive semidefinite Hermitian matrices with trace equal to one. When referring to the set we usually have density matrices representing systems of a specific size in mind, which should be clear from the context. For instance, we could be considering the set of density matrices that describe any bipartite system consisting of two two-level systems. In that case the set \mathcal{D} consists of all 4×4 positive semidefinite Hermitian matrices with trace equal to one.

The set of density matrices is convex. This follows from the positivity of the density matrices, and we will show this later. As we will see, the PPT and separable density matrices form convex subsets, \mathcal{P} and \mathcal{S} respectively, of \mathcal{D} as well.

The set of Hermitian matrices has a natural structure as a real vector space. This leads to a representation of the density matrices as real vectors instead of Hermitian matrices, and this is a very useful tool when studying the sets. This is one of the key concepts that we have used in our work.

The material in this chapter is based on [14, 16, 17]. The ideas and concepts presented in the following lays the foundation for the work presented in this thesis.

3.1 The geometry of density matrices

The geometry of sets of density matrices is important. The study of the geometry of density matrices is interesting in itself, but it is particularly motivated by the study of entanglement. Determining whether a given density matrix is separable can be rephrased as determining where in the set \mathcal{D} the

density matrix lies. Specifically, it is separable if it lies in the set of separable states. But there is in general no easy way of checking this. Thus, studying the geometry of the set \mathcal{D} and its subsets is both interesting and important.

3.1.1 The real vector space of Hermitian matrices

An unspecified Hermitian $N \times N$ -matrix contains N^2 real parameters in total. This can be seen by observing that since the matrix is Hermitian, the elements on the upper half of the matrix are repeated on the lower half (excluding the diagonal) and, counting from the lower right, there are $1 + 2 + \dots + (N - 1) = N(N - 1)/2$ complex elements on the upper half of the matrix which equals $N(N - 1)$ real elements. Add to this the N real elements on the diagonal, and we get $N^2 - N + N = N^2$. This tells us that the set of Hermitian $N \times N$ -matrices is of dimension N^2 , and we can expand such a matrix in a set of N^2 Hermitian basis matrices as

$$A = \sum_{k=1}^{N^2} a_k D_k \quad (3.1)$$

with N^2 real parameters a_k .

We can think of the a_k as the elements of an N^2 -dimensional real vector $\mathbf{A} = \sum_{k=1}^{N^2} a_k \mathbf{e}_k$ and in this sense the $N \times N$ Hermitian matrices define a real N^2 -dimensional vector space \mathbb{R}^{N^2} . In particular, we can take two Hermitian matrices A and B , represent them as vectors \mathbf{A} and \mathbf{B} in \mathbb{R}^{N^2} and add them to obtain a new vector $\mathbf{C} = \mathbf{A} + \mathbf{B}$. This vector can then be represented as a Hermitian matrix C .

The set \mathcal{D} of density matrices does not form a real vector space. This can most easily be seen by the fact that the addition of two density matrices does not produce a new density matrix. This follows from the requirement that the trace of a density matrix is equal to one. Let ρ_1 and ρ_2 be two density matrices, then

$$\rho = \rho_1 + \rho_2 \quad \text{has} \quad \text{Tr}(\rho) = \text{Tr}(\rho_1) + \text{Tr}(\rho_2) = 2 \quad (3.2)$$

It is a required property for a vector space that the addition of two vectors produces a new vector in the set. The above matrix is not a density matrix, even though it is a sum of two density matrices. Thus, \mathcal{D} cannot directly be regarded as a vector space.

It turns out however, that \mathcal{D} can still be described entirely by an associated vector space together with the requirement on the positivity of the density matrices. The trace requirement on the density matrices is an additional real constraint that they must satisfy, which means that the number

of free parameters in an unspecified $N \times N$ density matrix is $N^2 - 1$. We can use this freedom to specify one of the coefficients in eq. (3.1). This allows us to represent any density matrix as

$$\rho = \frac{\mathbb{1}}{N} + \sum_{k=1}^{N^2-1} x_k D_k \equiv \frac{\mathbb{1}}{N} + \sigma(x) \quad (3.3)$$

where $\{D_k\}$ is a set of traceless Hermitian matrices and forms a basis for all traceless $N \times N$ Hermitian matrices. The coefficients x_k are not entirely free, in the sense that they must be chosen so that ρ is positive semidefinite.

The set of traceless $N \times N$ Hermitian matrices forms a real vector space of dimension $N^2 - 1$ and entirely describes the set \mathcal{D} when the positivity of the density matrices is taken into account. The latter follows from eq. (3.3) since all the variation sits in the traceless part of ρ . To see the former, observe that the traceless Hermitian matrices can be represented as real vectors in \mathbb{R}^{N^2} . Given any two traceless Hermitian matrices σ_1 and σ_2 we have

$$\sigma = \sigma_1 + \sigma_2 \quad \text{and} \quad \text{Tr}(\sigma) = \text{Tr}(\sigma_1) + \text{Tr}(\sigma_2) = 0 \quad (3.4)$$

so that σ is also a traceless Hermitian matrix. Thus, the set of traceless Hermitian matrices also forms a vector space. In fact, this is just \mathbb{R}^{N^2-1} , since there are $N^2 - 1$ linearly independent D_k in eq. (3.3) and we can choose them such that they are orthonormal with respect to the Hilbert-Schmidt-metric described below.

3.1.2 Inner product

In the matrix representation the Euclidean inner product in \mathbb{R}^{N^2} is recognized as the Hilbert-Schmidt inner product. It is defined for complex matrices as

$$\langle A, B \rangle \equiv \text{Tr}(A^\dagger B) \quad (3.5)$$

Let A and B be Hermitian. Then the Hilbert-Schmidt inner product can be written as

$$\langle A, B \rangle = \text{Tr}(AB) \quad (3.6)$$

To see the equivalence between the Euclidean inner product in \mathbb{R}^{N^2} and the Hilbert-Schmidt inner product we employ the representation in eq. (3.1)

for the matrices A and B to get

$$\begin{aligned}\langle A, B \rangle &= \text{Tr}(AB) = \text{Tr}\left(\left(\sum_{k=1}^{N^2} a_k D_k\right)\left(\sum_{l=1}^{N^2} b_l D_l\right)\right) \\ &= \sum_{k,l=1}^{N^2} a_k b_l \text{Tr}(D_k D_l)\end{aligned}\quad (3.7)$$

If we choose the basis in such a way that the matrices D_k are orthogonal in the sense $\text{Tr}(D_k D_l) = \delta_{kl}$ we get

$$\langle A, B \rangle = \sum_{k=1}^{N^2} a_k b_k \quad (3.8)$$

which we recognize as the Euclidean inner product in \mathbb{R}^{N^2} .

We now immediately have access in the matrix space to familiar concepts in the vector space such as angles and distances. Analogous to the vector space we get the angles from

$$\cos \theta = \frac{\text{Tr}(AB)}{\sqrt{\text{Tr}(AA)}\sqrt{\text{Tr}(BB)}} \quad (3.9)$$

and the distances from

$$|A - B|^2 = \text{Tr}((A - B)^2) \quad (3.10)$$

For density matrices there is a natural choice of origin in the set \mathcal{D} . From eq. (3.1) we immediately see that setting all the parameters x_k to zero gives

$$\rho(\mathbf{x} = \mathbf{0}) = \frac{\mathbb{1}}{N} \quad (3.11)$$

which makes the maximally mixed state on the right hand side the natural choice of origin in \mathcal{D} . All the information in the density matrix is now encoded in the traceless matrix $\sigma(x)$. For instance, given two density matrices ρ_A and ρ_B we see that

$$|\rho_A - \rho_B|^2 = \text{Tr}((\rho_A - \rho_B)^2) = \text{Tr}((\sigma_A - \sigma_B)^2) = |\sigma_A - \sigma_B|^2 \quad (3.12)$$

The distance to the maximally mixed state can be expressed as

$$\left|\rho - \frac{\mathbb{1}}{N}\right|^2 = \text{Tr}(\sigma^2) = \sum_{k=1}^{N^2-1} x_k^2 \quad (3.13)$$

There is a close connection between the degree of mixing of a state ρ and its distance to the maximally mixed state. One expression for the degree of mixing was given in eq. (2.13) as the trace of the square of ρ . We can express the distance to the maximally mixed state for any ρ as

$$\left| \rho - \frac{\mathbb{1}}{N} \right|^2 = \text{Tr}(\rho^2) - \frac{1}{N} \quad (3.14)$$

This shows the connection to the degree of mixing. The larger the distance to the origin, the less mixed the state. The pure states $\rho = \psi\psi^\dagger$ have maximal distance to the origin, since for the pure states $\rho^2 = \rho$. In this case the distance is therefore always equal to

$$\left| \psi\psi^\dagger - \frac{\mathbb{1}}{N} \right| = \sqrt{\frac{N-1}{N}} \quad (3.15)$$

The inner product can be used to calculate the components of the matrix representation of a map Φ obtained by the Choi-Jamiolkowski isomorphism [54, 55]. We mentioned the Choi-Jamiolkowski isomorphism in section 2.3 as a map that allows us to take any map Φ that maps $m \times m$ complex matrices to $n \times n$ complex matrices and represent it as an $mn \times mn$ matrix P_Φ . In the following, assume that $m = n = N$, and that we have two Hermitian matrices A and B both in \mathcal{H} . We can then represent them as in eq. (3.1) in the following way

$$A = \sum_k^{N^2} a_k D_k, \quad B = \sum_l^{N^2} b_l D_l \quad (3.16)$$

Assume further that there is a map Φ that maps B to A , that is $A = \Phi(B)$. We can write this in the following way

$$A = \sum_k a_k D_k = \Phi(B) = \sum_l b_l \Phi(D_l) \quad (3.17)$$

where the last equality follows because we only consider linear maps. Using the inner product to find the component a_r of A we get the following

$$a_r = \text{Tr}(D_r A) = \sum_l b_l \text{Tr}(D_r \Phi(D_l)) \quad (3.18)$$

Now define a matrix \mathbf{P}_Φ with components

$$(\mathbf{P}_\Phi)_{rl} \equiv \text{Tr}(D_r \Phi(D_l)) \quad (3.19)$$

Inserting this into eq. (3.18) we get

$$a_r = \sum_l (\mathbf{P}_\Phi)_{rl} b_l \quad \Rightarrow \quad \mathbf{a} = \mathbf{P}_\Phi \mathbf{b} \quad (3.20)$$

which is a vector equation in \mathbb{R}^{N^2} . The matrix \mathbf{P}_Φ is real and symmetric.

3.2 Convex sets

In the following we will be considering sets with underlying structure of a vector space, such that we have access to properties such as addition, multiplication by scalars and so on. A set of points is convex if every point on a line between two points in the set, also is contained in the set. That is to say, if a and b are two points in our set, then all points $c = \lambda a + (1 - \lambda)b$ for $\lambda \in [0, 1]$ are also in the set. This is illustrated in figure 3.1a. There are many

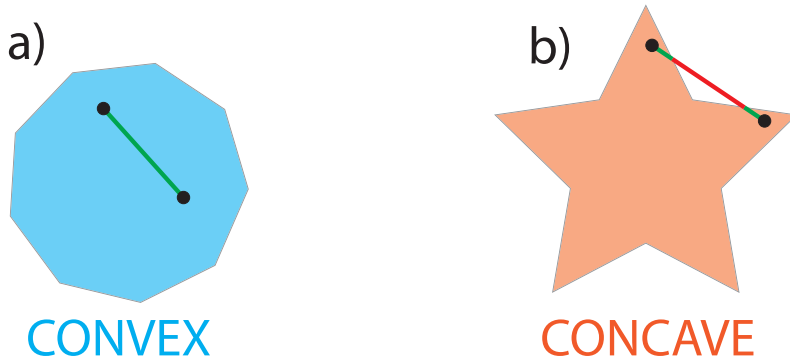


Figure 3.1: Illustration of a convex set in a) and a concave set in b). In a convex set all points along a line between two points in the set are also contained in set (green line), while in a concave set it is possible to choose a line between two points in the set such that some of the points on the line lie outside the set (red line).

examples of convex sets, such as a circle, a triangle, a rectangle, a pyramid and so on. These examples are all easy for us to visualize of course, since they are three-dimensional or lower, but the general concept extends to any dimension. If a set is not convex, it is said to be concave. An example of a concave set is shown in figure 3.1b. For a convex set S , n points a_1, a_2, \dots, a_n in S and nonnegative coefficients $\lambda_1, \lambda_2, \dots, \lambda_n$ such that $\sum_{k=1}^n \lambda_k = 1$, the point b defined as

$$b = \sum_{k=1}^n \lambda_k a_k \quad (3.21)$$

is also contained in the set S .

The convex hull of a set X is the smallest convex set that contains X . A nice analogy can be made in two dimensions. Imagine having a planar object, and the set X is the set of points that this object consists of. Take a rubber band, expand it and place it such that the object is clearly inside of the rubber band, and then let go. The rubber band will snap into place around the object, and the set Y of points inside the rubber band will constitute the convex hull of X . If X itself is convex we will have $Y = X$ and the rubber band hugging the object at all points along the circumference. Should X be concave then the rubber band will now define a convex set of points Y that is larger than the set X . In higher dimensions this analogy is not necessarily valid. The rubber band assumes the shape that minimizes its potential energy. In two dimensions this is the same shape that minimizes the length of the rubber band and corresponds to the convex hull. But in three dimensions it assumes the shape that minimizes its surface, which is not necessarily equivalent to the convex hull.

3.2.1 Extreme points of convex sets

So why is convexity such a useful property? Probably the nicest feature of convex sets has to do with its extreme points. An extreme point of a convex set is a point that does not lie on a line between two other points in the set. Think of the triangle. The extreme points of the triangle are its corner points. More formally, a point $c = \lambda a + (1 - \lambda)b$ is extremal if the only solution for λ is either $\lambda = 1$ in which case $c = a$ and a is an extreme point, or $\lambda = 0$ and $c = b$ and b is an extreme point.

There is a nice way of visualizing how to obtain an extreme point of a set. Imagine starting from a point inside a pyramid, then choose a random direction and start moving in that direction. After a while we will most likely reach one of the sides of the pyramid, unless we just so happened to walk in one of the very specific directions that would take us to one of the corners. If we now restrict ourselves to only move along the side of the pyramid, we can again choose a random direction along the side and start moving. Then we will end up in a corner, from which we cannot move anywhere except out into one of the sides or the interior of the pyramid. This is illustrated in figure 3.2. In a sense, it is the inverse of this process that makes the extreme points so useful. Simply speaking, once we know them we can reconstruct the entire set of points, since all we have to do is draw lines between them to obtain the sides, and then draw lines between the sides to obtain the interior points, effectively constructing the convex hull of the set. Therefore, if we can identify the extreme points of a convex set, we know the entire set.

There is an alternative way of defining convex sets rather than using

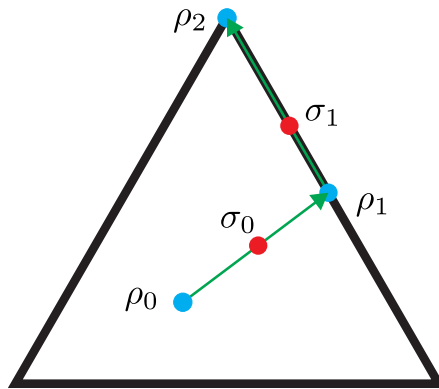


Figure 3.2: Illustration of the usefulness of the convexity of a set in obtaining extreme points of the set exemplified using a triangle. Start at a point ρ_0 and choose a random point σ_0 which defines a line between ρ_0 and itself. Move along the line until the edge is reached at the point ρ_1 , and choose another random point σ_1 on the edge which again defines a direction from ρ_1 . Follow this line until the corner is reached at the extreme point ρ_2 .

extreme points. This is by use of inequalities defining the interior points of the set, with equality at the boundary. Whether one uses extreme points or inequalities can often depend on what appears easiest for the given set one is studying. For instance, it turns out to be rather easy to define both extreme points and inequalities for the full set of density matrices, while for the set of separable states it is still easy to determine the extreme points while inequalities appear difficult to obtain.

3.2.2 \mathcal{D} , the convex set of density matrices

That the set \mathcal{D} of density matrices is convex, follows from eq. (2.7). We repeat here for convenience that any density matrix can be expressed as

$$\rho = \sum_k p_k \psi_k \psi_k^\dagger, \quad p_k \geq 0 \quad \forall k \quad (3.22)$$

Since the coefficients p_k are all positive or zero, it follows that the above is a convex sum of pure states. Thus, it also follows that the extreme points of \mathcal{D} are the pure states $\psi\psi^\dagger$. As we saw in eq. (3.15) the pure states also have maximal distance to the origin, another indication that they are extreme points in the set.

The dimension of the full set \mathcal{D} is larger than the dimension of the set of pure states. If the dimension of \mathcal{H} is N , a pure state is a one dimensional projection in the Hilbert space \mathcal{H} onto a normalized vector in \mathbb{C}^N which has N complex components. When we normalize the vector we get one real constraint, so we are left with $2N - 1$ real free parameters in a normalized vector in \mathbb{C}^N . In addition we can multiply the vector ψ_k with a phase factor, $\psi_k \rightarrow e^{i\alpha_k} \psi_k$, and the pure state $\psi_k \psi_k^\dagger$ would remain unchanged. Removing the phase factor gives one more real constraint, so that the total number of free parameters in a pure state is $2(N - 1)$. The dimension of the full set of density matrices is $N^2 - 1$, larger than the set of pure states for all $N > 1$.

For any convex set, the dimension of its boundary is always one less than the dimension of the interior. In particular this means that the boundary of \mathcal{D} has dimension $N^2 - 2$. For $N = 2$ the dimension of the set of density matrices is 3, while the dimension of the boundary exactly coincides with the dimension of the pure states, which is 2. This is why the entire boundary of \mathcal{D} consists of the pure states in this case, as can be seen in the Bloch sphere representation of density matrices in systems of dimension 2×2 (also shown in fig. 3.8).

Complementary to the extreme points, we can identify the boundary of \mathcal{D} by inequalities for the interior points. Remember that the density matrices are positive semidefinite, meaning that their eigenvalues are nonnegative.

Thus, for any $N \times N$ density matrix in the interior of \mathcal{D} we have N inequalities $\lambda_k \geq 0$ for the eigenvalues λ_k . On the boundary, at least one of these equations are satisfied with equality. This means that on the boundary, the determinant of ρ is equal to zero. Thus, the N th-degree characteristic polynomial in the eigenvalues identifies the boundary.

3.2.3 \mathcal{S} , the convex set of separable density matrices

Just as the full set of density matrices is a convex set, so is the set \mathcal{S} of separable density matrices in a bipartite system, as evident from equation (2.33). \mathcal{S} is a proper subset of \mathcal{D} , and the extreme points of \mathcal{S} are the pure product states $\psi\psi^\dagger$, $\psi = \phi \otimes \chi$. Again we can count the number of free parameters in a pure product state in order to determine the dimension of the set of such states. The pure product state is a projection in $\mathcal{H} = \mathcal{H}_A \otimes \mathcal{H}_B$ onto a normalized product vector in $\mathbb{C}^{N_A} \otimes \mathbb{C}^{N_B}$. For a general product vector $\psi = \phi \otimes \chi$, the vector ϕ has $2N_A$ real elements while χ has $2N_B$ real elements, where N_A and N_B are the dimensions of the two subsystems respectively. In total we therefore have $2(N_A + N_B)$ real parameters before we apply any restrictions. For the product vector to be normalized we require both ϕ and χ to be normalized, therefore the normalization condition leads to two real equations which together reduces the number of real parameters by two. In addition we may remove the phase from both ϕ and χ , subtracting another two real parameters. In the end we are left with $2(N_A + N_B - 2)$ real parameters for the set of pure product states. The set \mathcal{S} has the same dimension as \mathcal{D} , since any state close enough to the maximally mixed state is separable.

It is unfortunately much more difficult to obtain inequalities defining the boundary for \mathcal{S} than for \mathcal{D} . This is in a sense one of the main reasons that the separability problem is so difficult. Had we been able to obtain such inequalities, one could simply check whether a given density matrix violated any of them in order to determine whether it is separable or not.

3.2.4 \mathcal{P} , the convex set of PPT density matrices

The set of partially transposed density matrices, which we will call \mathcal{D}^P , can be obtained by taking the partial transpose of every point in the set \mathcal{D} of density matrices. Since the partial transposition map is reversible and linear, it maps extreme points to extreme points.

If the map is reversible and linear, it maps line segments to line segments. This is because any point c on a line segment can be written as a sum of other points, i.e. $c = xb + (1-x)a$, and when the linear map acts on c it

gives $c' = xb' + (1-x)a'$ with c' , b' and a' as mapped points, which again is a line segment. In this way the extreme points a and b of a line segment is mapped to extreme points a' and b' of a new line segment. This is illustrated in figure 3.3.

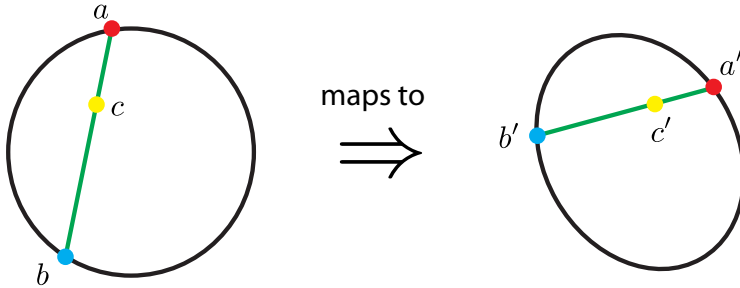


Figure 3.3: Illustration of the action of a reversible linear map on a line section in a convex set. The line segment is defined by the extreme points a and b and gets mapped to a new line segment defined by new extreme points a' and b' .

Thus the extreme points of \mathcal{D}^P must be the partially transposed extreme points of \mathcal{D} . From eq. (2.56) we see that the partially transposed density matrix is just a convex combination of partially transposed pure states, $\rho^P = \sum_k p_k \left(\psi_k \psi_k^\dagger \right)^P$. This shows that \mathcal{D}^P is also a convex set.

In order to get the set \mathcal{P} of states that are positive under partial transposition (the PPT states), we need now only take the intersection between the sets \mathcal{D} and \mathcal{D}^P , that is to say we have $\mathcal{P} = \mathcal{D} \cap \mathcal{D}^P$. In general, the intersection between two convex sets is itself a convex set, so that the set \mathcal{P} is also a convex set, as illustrated in figure 3.4. In section 2.3 we mentioned that the partial transposition map is a very useful tool to distinguish between separable and entangled states in systems of dimension 2×2 and 2×3 since there the states that remain positive under partial transposition are known to be separable. In higher dimensions there were found examples of states that were PPT but still entangled [4]. This means that in 2×2 and 2×3 we have $\mathcal{S} = \mathcal{P} \subset \mathcal{D}$, while in general the set \mathcal{P} is larger than \mathcal{S} so that we

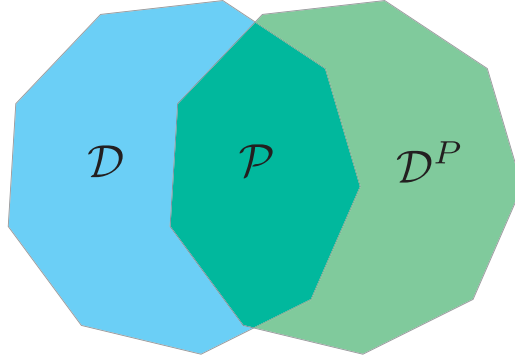


Figure 3.4: In general the intersection of two convex sets is another convex set. The set \mathcal{D} of density matrices and the set \mathcal{D}^P are both convex, and thus the Peres set $\mathcal{P} = \mathcal{D} \cap \mathcal{D}^P$ of states positive under partial transposition is also a convex set.

have $\mathcal{S} \subset \mathcal{P} \subset \mathcal{D}$. This is illustrated in figure 3.5.

For the set \mathcal{D} we know both the extreme points, namely the pure states, and the inequalities identifying the boundary, $\rho \geq 0$. For the separable states \mathcal{S} we know the extreme points, the pure product states, but we do not know of any inequalities identifying the boundary. For the PPT states the situation lies somewhere in between these cases. We know some of the extreme points, namely the pure product states that are shared with \mathcal{S} , but we also know that there has to be other ones. On the other hand, we do know the inequalities identifying the boundary of \mathcal{P} . They are the intersection of the inequalities $\rho \geq 0$ and $\rho^P \geq 0$.

3.2.5 The positive convex cone

If we ignore the normalization condition, that is, we allow matrices which are simply density matrices multiplied by a positive scalar, $a\rho$, the visual representation changes from a planar convex set to a positive convex cone as shown in figure 3.6. The points in the set of density matrices now become rays in the convex cone, with the ray in the center of the cone corresponding to the scaled maximally mixed state. The set of density matrices will then be the intersection of the positive cone and the hyperplane of Hermitian matrices with trace equal to one.

The convex cone is also useful as a visual representation of the density

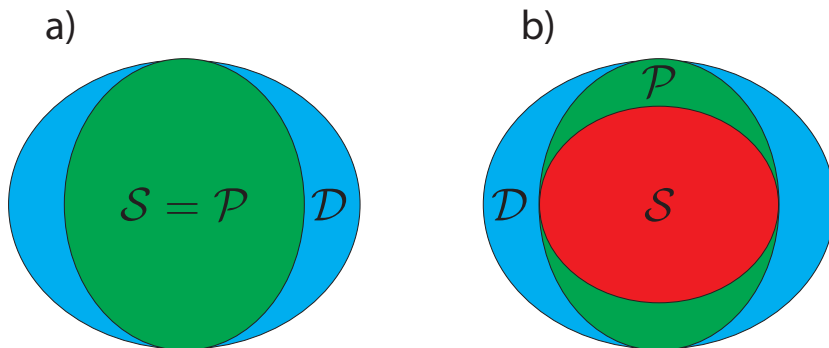


Figure 3.5: a) For the 2×2 and 2×3 systems the set \mathcal{S} of separable states is equal to the set \mathcal{P} of states positive under partial transposition, and contained in the set \mathcal{D} of all states. b) In systems of larger dimension the set \mathcal{P} is strictly larger than \mathcal{S} and we have the inclusions $\mathcal{S} \subset \mathcal{P} \subset \mathcal{D}$.

matrix decomposition in eq. (3.3). We observe that all the information in the density matrix can be encoded in the projection of \mathcal{D} onto the floor of the cone, where $a = 0$. In this projected set, the traceless matrices $\sigma(x)$ form the points of the set, and in order to obtain the density matrix one just adds the maximally mixed state, as illustrated in figure 3.6. The projection of \mathcal{D} onto the floor of the cone is then the underlying vector space that completely describes \mathcal{D} , as previously discussed.

As we in general have the inclusions $\mathcal{S} \subset \mathcal{P} \subset \mathcal{D}$, the set of separable states and the set of PPT states will form nested cones within the full cone of density matrices, as illustrated in figure 3.7.

3.3 Simplexes and unitary transformations

A density matrix acting on a Hilbert space \mathcal{H} of dimension N is characterized by $N^2 - 1$ free parameters. Since all Hermitian matrices are diagonalizable by unitary matrices, a general density matrix can be described by an $N \times N$ diagonal matrix D and a special unitary transformation U in $SU(N)$. The number of free parameters in the diagonal matrix D is $N - 1$ since the sum of the diagonal elements must equal 1. The dimension of $SU(N)$ is $N^2 - 1$, but there are $N - 1$ of these that give rise to a unitary transformation that

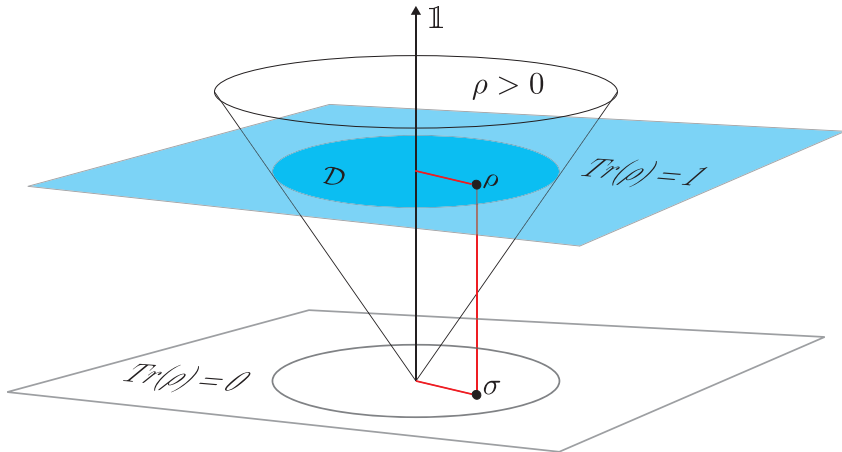


Figure 3.6: Illustration of the convex cone of density matrices obtained when ignoring the trace equal to one restriction on the density matrices. The set \mathcal{D} of true density matrices, with trace equal to one, is found in the intersection of the cone and the plane defined by the trace condition. The inside of the cone consists of all Hermitian matrices of full rank with positive eigenvalues, while on the edge of the cone we have the Hermitian matrices of less than full rank and with nonnegative eigenvalues. In the center lies the maximally mixed state $\mathbb{1}$, which in the set \mathcal{D} is a point, but in the cone defines a ray in the middle. The set \mathcal{D} can be projected down onto the plane where the trace equals zero, in the following referred to as the floor of the convex cone. Here all the information in the density matrices is contained in the traceless matrices σ , as indicated.

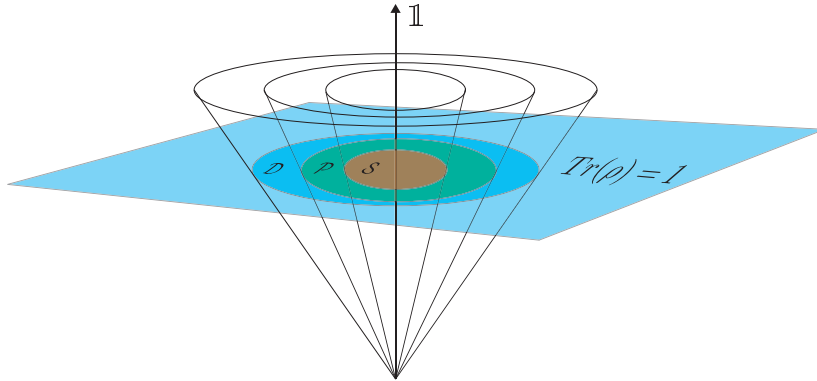


Figure 3.7: Illustration of the nested convex cones of the full set \mathcal{D} of density matrices, the set \mathcal{P} of PPT density matrices and the set \mathcal{S} of separable density matrices. Since we have the set inclusions $\mathcal{S} \subset \mathcal{P} \subset \mathcal{D}$ we get a similar inclusion for the cones as represented here.

commutes with diagonal matrices, hence they do not change the D . In terms of the extreme points of \mathcal{D} , the diagonal matrix D is a convex combination of the orthogonal projections onto the N basis vectors of \mathcal{H} . In the case $N = 2$, we get

$$D = x \begin{pmatrix} 1 & 0 \\ 0 & 0 \end{pmatrix} + (1-x) \begin{pmatrix} 0 & 0 \\ 0 & 1 \end{pmatrix} \quad (3.23)$$

where we have used the projections onto the vectors $(1,0)^T$ and $(0,1)^T$. The eigenvalues are completely determined by x , and any unitarily equivalent density matrix can be obtained by a suitable unitary transformation on D . We can visualize the diagonal matrix as a point on a line between the two pure states, as in figure 3.8a. We can then use the unitary transformations to rotate this line in the two remaining dimensions into the full set of density matrices in two dimensions as shown in figure 3.8b and c, visualized as a three-dimensional ball known as the Bloch sphere. The pure states are then the points on the surface of the sphere, while the points in the interior of the ball are mixed states and in the centre we find the maximally mixed state.

In three dimensions, $N = 3$, the diagonal matrix D can be represented by two parameters x and y , and the pure states that project onto the three basis states. D can then be visually represented as a triangle, which will be rotated into six other dimensions to represent the entire eight dimensional

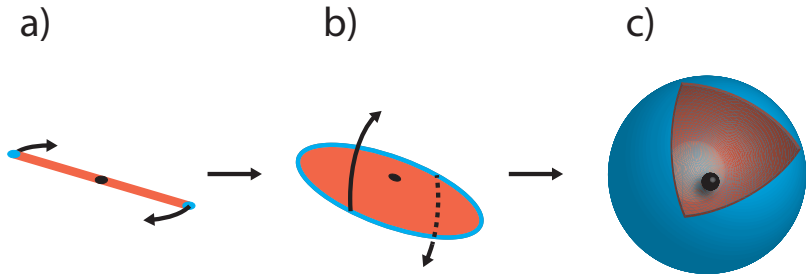


Figure 3.8: Illustration of the Bloch sphere for a two-dimensional system. In a) we have the two extreme points (cyan), all diagonal states as convex combinations of these (red line) and the maximally mixed state in the center (black). In b) we have rotated the figure in a) into a second dimension. We get a filled circle with extreme points (cyan) as the circumference, the interior (red) as mixed states and the maximally mixed state in the center (black). In c) we have rotated the figure in b) into the third dimension. We then get a ball with the extreme points as the surface (cyan), the interior ball as mixed states and the center of the ball as the maximally mixed state. This Bloch sphere contains all states in a two-dimensional system. Note that the sizes of points are enlarged for illustrative purposes, for instance the maximally mixed state is a point and not an actual ball in the center of the Bloch sphere.

set of density matrices. Generalizing to dimension N , the diagonal matrix D can be represented by an N -simplex, which is a generalized triangle with N vertices in $N - 1$ dimensions. As we have seen, in two and three dimensions the simplex is a line and a triangle respectively, while a 4-simplex is a pyramid and so on, as shown in figure 3.9.

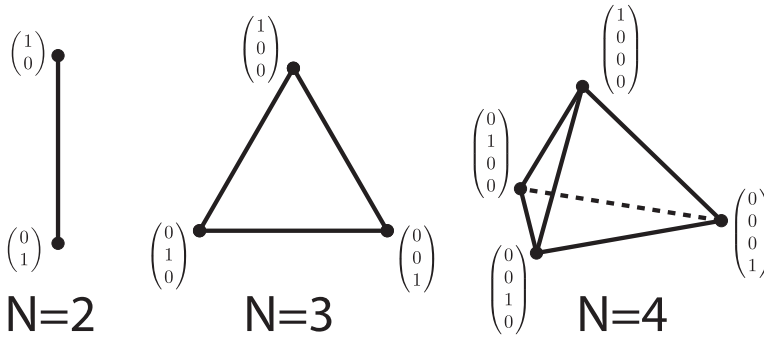


Figure 3.9: Graphical representation of the diagonal states in a Hilbert space of dimension N as simplexes for $N = 2, 3, 4$. The corners correspond to the pure projections onto the vectors indicated in the figure, while all interior points of the simplex are convex combinations of these.

3.4 Two-dimensional cross sections

Because of the rapid increase in dimension as N grows, the set of density matrices is in general difficult to visualize. Restricting to the diagonal states helps a little, and we can visualize them up to $N = 4$, but for larger systems that also becomes difficult. What we can do however, is find ways of taking low dimensional slices through the different sets. Such visualizations may be helpful in illustrating various properties of the set.

For any set of points, once we have three points in the set, we can define a two-dimensional plane. In the case of density matrices, this means that if we have three of them, they define a two-dimensional plane through \mathcal{D} . Let one of the three density matrices be the maximally mixed state $\rho_0 = \mathbb{1}/N$, and denote the other two by ρ_1 and ρ_2 respectively. Immediately we see that

a combination like

$$\hat{\rho} = \rho_0 + x\rho_1 + y\rho_2 \quad (3.24)$$

is not a density matrix, since it fails the unit trace requirement unless $x = -y$. We have seen however, that all the information content in a density matrix can be stored in a traceless matrix by the expansion (3.3). Using this we find that the proper density matrix in the two-dimensional plane is given by

$$\rho = \rho_0 + x\sigma_1 + y\sigma_2 = \frac{\mathbb{1}}{N} + \sigma(x, y) \quad (3.25)$$

where we have defined $\sigma(x, y) \equiv x\sigma_1 + y\sigma_2$. If we want, we may introduce orthogonal unit matrices in the cross section analogous to unit vectors. Let the x -axis be defined by ρ_1 , then we may take

$$\sigma_x = \frac{\sigma_1}{\sqrt{\text{Tr}(\sigma_1^2)}} \quad (3.26)$$

so that $\text{Tr}(\sigma_x^2) = 1$. We then take the component of ρ_2 orthogonal to ρ_1 as defining the y -axis

$$\sigma_y = \frac{\tilde{\sigma}_y}{\sqrt{\text{Tr}(\tilde{\sigma}_y^2)}} \quad (3.27)$$

where

$$\tilde{\sigma}_y = \sigma_2 - \text{Tr}(\sigma_x\sigma_2)\sigma_x \quad (3.28)$$

Thus, using these as unit directions and switching to polar coordinates we can write any density matrix ρ in the cross section as

$$\rho = \frac{\mathbb{1}}{N} + r(\cos\theta\sigma_x + \sin\theta\sigma_y) = \frac{\mathbb{1}}{N} + r\sigma(\theta) \quad (3.29)$$

where we have defined $\sigma(\theta) \equiv \cos\theta\sigma_x + \sin\theta\sigma_y$. In this way the traceless matrix σ (suppressing the angle in the notation) defines a direction, while the distance r will be limited by the boundary.

The inequalities that identify the boundary of \mathcal{D} are $\rho \geq 0$, meaning that the eigenvalues λ_k of ρ satisfy $\lambda_k \geq 0 \forall k$. Since the determinant is just the product of the eigenvalues, $\det\rho = \prod_k\lambda_k$, the inequalities imply that $\det\rho \geq 0$ for all interior points and in particular that $\det\rho = 0$ on the

boundary. Let ρ be a point on the boundary of \mathcal{D} in a two-dimensional cross section, then the determinant can be written

$$\begin{aligned}\det \rho &= \det \left(\frac{\mathbb{1}}{N} + r\sigma \right) = r \det \left(\sigma - \left(-\frac{1}{Nr} \right) \mathbb{1} \right) \\ &\equiv r \det (\sigma - \lambda \mathbb{1}) = 0\end{aligned}\quad (3.30)$$

which we recognize as the eigenvalue equation for σ with the eigenvalues λ related to the distance r by

$$r \equiv -\frac{1}{N\lambda}\quad (3.31)$$

The eigenvalues λ of σ thus determine at which points along a line in the two-dimensional cross section the determinant equals zero. When we move away from the maximally mixed state towards the boundary of \mathcal{D} , we know that as soon as we cross the boundary one or more of the eigenvalues will become negative. As we continue past this point we may get to a point at which another eigenvalue becomes zero while the first one is still negative. This is also a valid solution to $\det \rho = 0$, but lies outside the set \mathcal{D} . This means that we are really only interested in the smallest r for any given angle, since this is a point on the actual boundary of \mathcal{D} . This corresponds to the largest eigenvalue of σ . The boundary of \mathcal{D} is shown in fig. 3.10a in a two-dimensional cross section between two orthogonal Bell states and in 3.10b between two random states on the boundary in the 2×2 system.

If the two states that we use in addition to the maximally mixed states commute with each other, we will get straight lines when plotting the boundary in the cross section. This is because when they commute, they can be diagonalized simultaneously. Take an example with two 2×2 matrices. When adding two matrices which can be diagonalized simultaneously we would get something like

$$\begin{aligned}Ax + By &= \begin{pmatrix} 0.46 & 0 \\ 0 & 0.54 \end{pmatrix} x + \begin{pmatrix} 0.25 & 0 \\ 0 & 0.75 \end{pmatrix} y \\ &= \begin{pmatrix} 0.46x + 0.25y & 0 \\ 0 & 0.54x + 0.75y \end{pmatrix}\end{aligned}\quad (3.32)$$

Taking the determinant and requiring it to be equal to zero, we find that it factors to

$$(0.46x + 0.25y)(0.54x + 0.75y) = 0\quad (3.33)$$

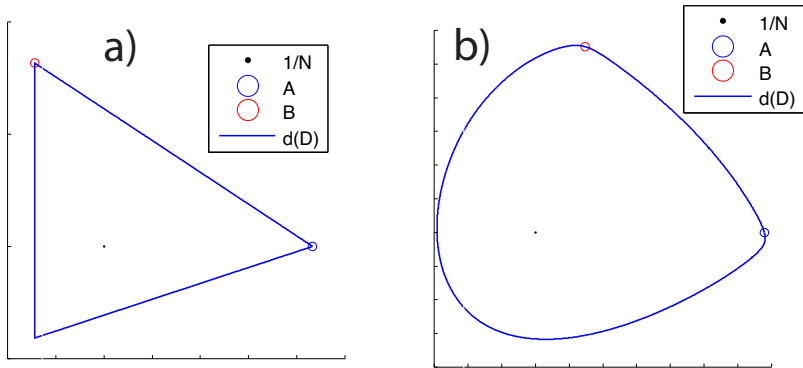


Figure 3.10: Two-dimensional cross sections with the maximally mixed state $\mathbb{1}/N$ in the middle in the 2×2 system ($N = 4$). The blue line is the boundary $\partial\mathcal{D}$ of the set \mathcal{D} of density matrices. a) The cross section is defined by two orthogonal Bell states. Since they are orthogonal they commute, which is why the lines are all straight. b) The cross section is defined by two randomly chosen states on the boundary which both are of rank 3. They do not commute, which is why the lines are all curved.

which means that one or both of the two factors are zero independently, and those are equations for straight lines.

When adding non-commuting matrices we will instead get curved lines. This is readily observed from the fact that when taking the determinant we in general get a polynomial of degree equal to the rank of the matrix. In the above example, if A and B did not commute, we would get a polynomial in x and y of second order which would not factor. Thus the lines would be curved.

We can identify the boundary of \mathcal{D}^P , the set of states which are the partial transposes of the states in \mathcal{D} , in the two-dimensional cross section in the same way as for \mathcal{D} . The boundary of \mathcal{D}^P is identified by $\rho^P \geq 0$, and on the boundary we have $\det \rho^P = 0$. The identity $\mathbb{1}$ is invariant under partial transposition, so analogous to eq. (3.30) we get

$$r^P \det (\sigma^P - \lambda^P \mathbb{1}) = 0 \quad (3.34)$$

with the distance r^P to the boundary of \mathcal{D}^P related to the eigenvalues λ^P of σ^P , the partially transposed of σ , by

$$r^P \equiv -\frac{1}{N\lambda^P} \quad (3.35)$$

Again we are interested in the smallest r^P , and thus the largest eigenvalue λ^P of σ^P .

If we now wanted to identify the boundary of \mathcal{P} , the density matrices that remain positive under partial transposition, we will find them in the cross section between \mathcal{D} and \mathcal{D}^P . In fig. 3.11 we have plotted the same two-dimensional cross sections as in fig. 3.10, but now with both the boundary of \mathcal{D} and the boundary of \mathcal{D}^P . The boundary of \mathcal{P} is the intersection of these, which, since we are in the 2×2 system, is equal to \mathcal{S} . In fig. 3.11a both the matrices themselves as well as their partial transposes commute, thus we get straight lines for both boundaries. We also see in fig. 3.11b that the two randomly chosen rank 3 states happen to lie outside the boundary of \mathcal{D}^P , which means that they are not positive under partial transposition. In addition, neither the states themselves nor their partial transposed counterparts commute, therefore the lines are all curved. We can also have situations where for example the matrices commute, while their partial transposes do not. A nice example of this is the cross section with a Bell state and a pure product state, as shown in fig. 3.12. The Bell state is a pure state and as such maximally entangled, and we observe from the figure that it also has the largest distance to the separable states.

If we consider a PPT state with ranks lower than N for both the state and its partial transpose, it will satisfy both $\det \rho = 0$ and $\det \rho^P = 0$ at

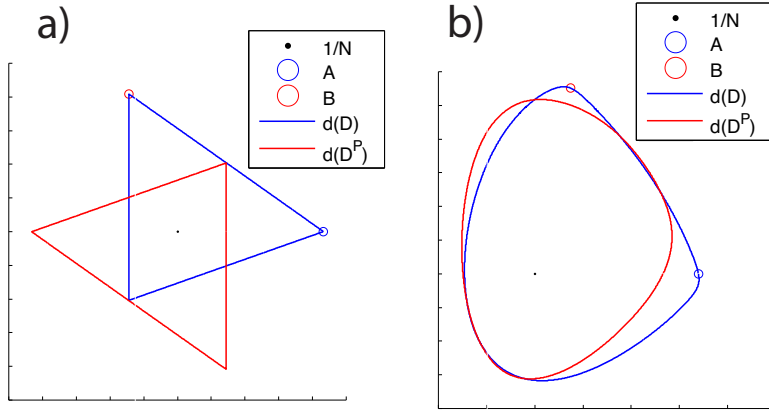


Figure 3.11: Plot of the same cross sections as in figure 3.10, but now including the boundary of \mathcal{D}^P . a) The cross section is defined by two orthogonal Bell states A and B . Since they are orthogonal they commute, which is why the lines are all straight. The points inside the blue and red parallelogram in the middle are the states which are positive under partial transposition, that is the set \mathcal{P} , and also separable since we are in the 2×2 system. The two Bell states are both pure nonproduct states, so they lie outside $\mathcal{P} = \mathcal{S}$ and have equal distance to the separable states. b) The cross section is defined by two randomly chosen states A and B on the boundary of \mathcal{D} which both are of rank 3. They do not commute, which is why the lines are all curved. They lie outside the boundary of \mathcal{D}^P , so neither of them are positive under partial transposition.

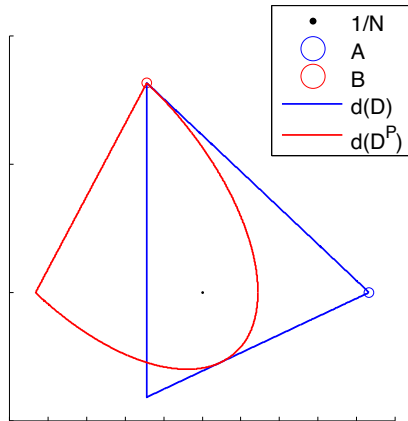


Figure 3.12: Two-dimensional cross section defined by a Bell state A and a pure product state B with the maximally mixed state $\mathbb{1}/N$ in the middle in the 2×2 system ($N = 4$). The blue line is the boundary $\partial\mathcal{D}$ of the set \mathcal{D} of density matrices, while the red line is the boundary $\partial\mathcal{D}^P$ of the set \mathcal{D}^P of partially transposed states. The Bell state and the pure state commute, which is why the blue lines are all straight, while their partially transposed counterparts do not, which is why the red line is curved.

the same time, and therefore lie on an intersection of the two boundaries. In figure 3.13 is shown a two-dimensional cross section between two rank $(8,8)$ states in the 3×3 system. Note that even though points may appear as

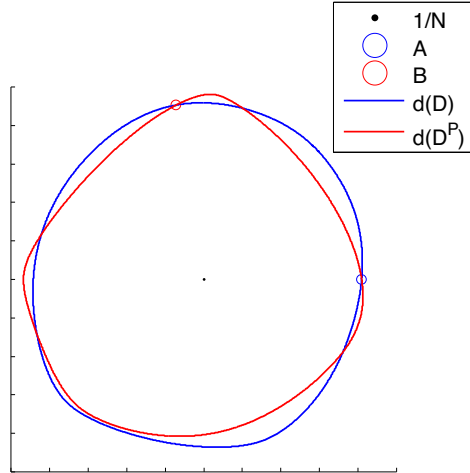


Figure 3.13: Two-dimensional cross section defined by two $(8,8)$ states A and B with the maximally mixed state $\mathbb{1}/N$ in the middle in the 3×3 system ($N = 9$). Since both states have two eigenvalues equal to zero, one for the state itself and one for its partial transpose, each of them lie on the boundary of both \mathcal{D} and \mathcal{D}^P , and as shown here will lie on intersections between the two boundaries.

extreme points in the two-dimensional cross sections, they might not be. It is just that the directions in which the points are not extreme lie outside of the cross section. Much the same as taking a plane and cutting a pyramid in the middle, where the midpoints on the sides would seem like extreme points in the triangle of intersection points in the plane.

3.5 Flat faces and extremality in \mathcal{D}

Up to unitary transformations, the boundary of \mathcal{D} consists of faces, analogous to the faces of a pyramid or a cube. We will here define the faces, and in the end show that we regain the entire boundary when we include unitary transformations that rotate the faces in the full space.

Given any density matrix ρ , we define a face $\mathcal{F}_{\mathcal{D}}(\rho)$ on \mathcal{D} as the set of density matrices with the same image as ρ . The face $\mathcal{F}_{\mathcal{D}}(\rho)$ will in particular contain ρ as an interior point. This is illustrated in fig. 3.14. Note that the boundary of set \mathcal{D} consists of both flat and curved surfaces, because of the unitary transformations that must be included in addition to the faces in order to describe \mathcal{D} . The faces are flat in the sense that they can be

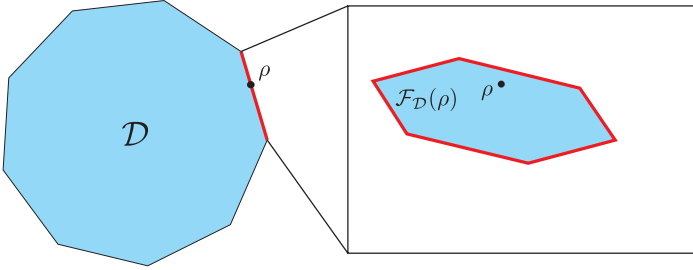


Figure 3.14: Illustration of the face $\mathcal{F}_{\mathcal{D}}(\rho)$ on \mathcal{D} . The face is defined by the set of density matrices with the same image as ρ .

associated with real vector spaces, as we will see in the following.

Let ρ be a given density matrix which defines the face $\mathcal{F}_{\mathcal{D}}(\rho)$ on \mathcal{D} and let P be the projection on the image of ρ . The condition for any Hermitian matrix $\tilde{\sigma}$ to have the same image as ρ can be expressed as

$$P\tilde{\sigma}P = \tilde{\sigma} \quad (3.36)$$

But this is a map Φ_P between matrices

$$\Phi_P : \tilde{\sigma} \mapsto P\tilde{\sigma}P \quad (3.37)$$

and as such has a representation as a matrix \mathbf{P} acting on \mathbb{R}^{N^2} by the Choi-Jamiolkowski isomorphism. In \mathbb{R}^{N^2} eq. (3.36) is expressed as

$$\mathbf{P}\tilde{\sigma} = \tilde{\sigma} \quad (3.38)$$

which shows that the condition that $\tilde{\sigma}$ has the same image as ρ can be recast as that the vector representation $\tilde{\sigma}$ is an eigenvector of \mathbf{P} with corresponding eigenvalue equal to one. The matrix \mathbf{P} is real and symmetric. It is also a projection operator since

$$\Phi_P(\Phi_P(\tilde{\sigma})) = \Phi_P(P\tilde{\sigma}P) = P^2\tilde{\sigma}P^2 = P\tilde{\sigma}P = \Phi_P(\tilde{\sigma}) \quad \Rightarrow \quad \mathbf{P}^2 = \mathbf{P} \quad (3.39)$$

Thus, the number of linearly independent solutions to eq. (3.36) is just the rank of \mathbf{P} .

The rank of \mathbf{P} will depend on the rank of ρ . Assume that ρ has rank $m \leq N$. Then we can find a basis where the representation of ρ in block form is

$$\begin{pmatrix} \hat{\rho} & 0 \\ 0 & 0 \end{pmatrix} \quad (3.40)$$

where $\hat{\rho}$ is an $m \times m$ Hermitian matrix. But then we know that $\hat{\rho}$ can be represented as an $m^2 \times 1$ vector in \mathbb{R}^{m^2} , an m^2 -dimensional subspace of \mathbb{R}^{N^2} . Since \mathbf{P} is a projection operator which projects onto this subspace, it follows that it has rank m^2 .

Let $\{\tilde{\sigma}_k\}$ be the set of m^2 eigenvectors of \mathbf{P} . We may then represent the set as a set of Hermitian matrices $\{\tilde{\sigma}_k\}$ and define a set $\{\sigma_k\}$ of traceless Hermitian matrices as

$$\sigma_k \equiv \tilde{\sigma}_k - \text{Tr}(\tilde{\sigma}_k) \rho \quad (3.41)$$

Since ρ is obviously a solution to eq. (3.36) it is eliminated in the set $\{\sigma_k\}$. The latter therefore consists of $m^2 - 1$ traceless matrices which, together with ρ , form a basis for the face $\mathcal{F}_{\mathcal{D}}(\rho)$. We may then represent any density matrix ρ' in $\mathcal{F}_{\mathcal{D}}(\rho)$ as

$$\rho' = \rho + \sum_{k=1}^{m^2-1} x_k \sigma_k \quad (3.42)$$

implying that the dimension of $\mathcal{F}_{\mathcal{D}}(\rho)$ is $m^2 - 1$. A two-dimensional cross section through \mathcal{D} showing two density matrices lying in the same face on \mathcal{D} is given in fig. 3.15.

The face $\mathcal{F}_{\mathcal{D}}(\rho)$ does not form a vector space itself. However, analogous to the case with \mathcal{D} , $\mathcal{F}_{\mathcal{D}}(\rho)$ is entirely described by a vector space together with the positivity condition on the density matrices. The vector space in question is the one spanned by the set $\{\sigma_k\}$ which, together with ρ , form a basis for \mathbb{R}^{m^2} . Since this is a vector space, we say that $\mathcal{F}_{\mathcal{D}}(\rho)$ is a flat face. Another way of looking at it is to say that the face has a traceless projection on the floor of the convex cone.

Let $\hat{\rho}'$ be the $m \times m$ Hermitian matrix in a block representation of ρ' similar to eq. (3.40). Then the boundary of $\mathcal{F}_{\mathcal{D}}(\rho)$ is found by the condition

$$\det \hat{\rho}' = 0 \quad (3.43)$$

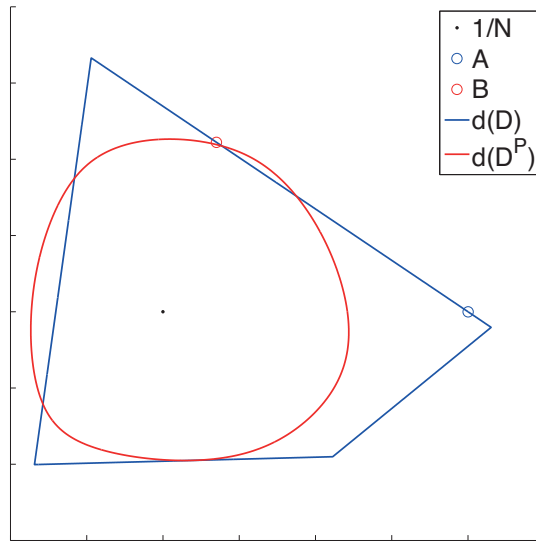


Figure 3.15: Two-dimensional cross section through \mathcal{D} in the 3×3 system showing two density matrices A and B , both of rank 7, lying in the same face on \mathcal{D} . Neither A nor B are PPT, hence they lie outside the boundary of \mathcal{D}^P .

and identified by the m th-degree characteristic polynomial. Note the similarity between the description of the faces and the full set \mathcal{D} . This is no coincidence. Starting with a density matrix of full rank ($m = N$) we find that eqs. (3.3) and (3.42) are equivalent, only differing by the choice of basis. In that case the face is identical to the full set itself.

When a face has dimension zero it corresponds to a single point, and this point is an extreme point of \mathcal{D} . This is completely analogous to the intuitive case with a three-dimensional pyramid. It has two-dimensional faces as sides, each of which has one-dimensional lines as boundaries. Each of the lines end up in zero-dimensional corner points. From the fact that the extreme points of a convex set defines zero-dimensional faces, we recover that the extreme points of \mathcal{D} are the pure states. We have $m^2 - 1 = 0$ for $m = 1$, which means that the corresponding density matrix is a rank one projection operator, also known as a pure state.

To recover the boundary of \mathcal{D} from the faces, we must include unitary transformations. A density matrix ρ on the boundary of \mathcal{D} with rank m defines a face of dimension $m^2 - 1$. We can then perform $U(N)$ -transformations on all the density matrices in the face to rotate the face in the full space. However, the subgroups $U(m)$ and $U(N - m)$ that act on the image and kernel of the density matrices respectively do not change the orientation of the face. They just rotate within the image and kernel separately. Thus, the transformations that actually change the orientation of the face are the ones belonging to $U(N)/U(m) \times U(N - m)$, the number of which are

$$N^2 - m^2 - (N - m)^2 = 2Nm - 2m^2 \quad (3.44)$$

Combining the dimension of the face with the number of unitary transformations that change the face, we get

$$m^2 - 1 + 2Nm - 2m^2 = 2Nm - m^2 - 1 \quad (3.45)$$

which is equal to the dimension of the surface of density matrices of rank m .

The boundary of \mathcal{D} is reached when the rank of the density matrix is reduced from N to $N - 1$. Thus, the dimension of the boundary should be equal to the dimension of the surface of density matrices with rank $m = N - 1$. Inserting this into eq. (3.45) we find that the dimension of the surface of such states is

$$2N(N - 1) - (N - 1)^2 - 1 = N^2 - 2 \quad (3.46)$$

which is exactly the dimension of the boundary of \mathcal{D} . Notice also that if we set $m = 1$ in eq. (3.45) we find that the dimension of the surface of pure states is $2N - 2$, agreeing with the previous parameter counting of pure states.

3.6 Flat faces and extremality in \mathcal{P}

A density matrix which has a positive partial transpose defines a flat face on \mathcal{P} which is an intersection of two hypersurfaces, as we will see in the following. Recall that we defined the set \mathcal{P} of density matrices with positive partial transpose as the intersection of the set \mathcal{D} of density matrices and the set \mathcal{D}^P of partially transposed density matrices.

A given PPT state ρ by itself defines a flat face $\mathcal{F}_{\mathcal{D}}(\rho)$ on \mathcal{D} . Similarly, the partial transpose ρ^P defines a flat face $\mathcal{F}_{\mathcal{D}^P}(\rho^P)$ also on \mathcal{D} . Let $\mathcal{F}_{\mathcal{D}^P}(\rho)$ be the hyperplane obtained by taking the partial transpose of all of the points in $\mathcal{F}_{\mathcal{D}}(\rho^P)$. It is then a face on \mathcal{D}^P . Since we know that ρ^P is an interior point in $\mathcal{F}_{\mathcal{D}}(\rho^P)$, it follows that ρ is an interior point in $\mathcal{F}_{\mathcal{D}^P}(\rho)$. But then $\mathcal{F}_{\mathcal{D}}(\rho)$ and $\mathcal{F}_{\mathcal{D}^P}(\rho)$ share a point, and so they must intersect. This is illustrated in figure 3.16. The intersection of the two hyperplanes defines a new hyperplane

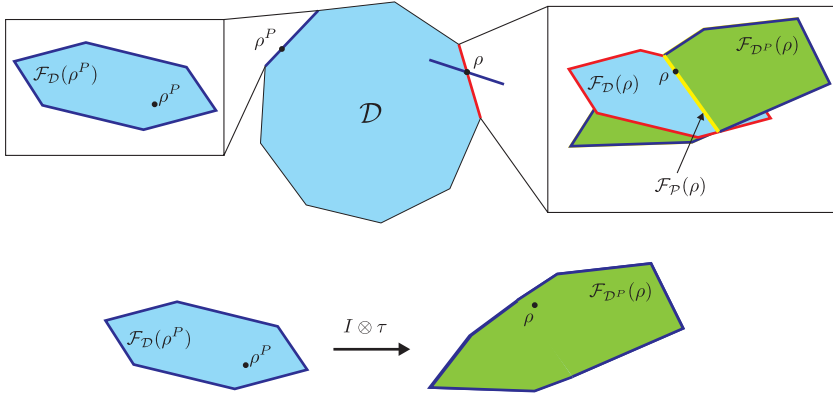


Figure 3.16: Illustration of the relation between faces on \mathcal{D} and \mathcal{P} . A PPT density matrix ρ defines a face $\mathcal{F}_{\mathcal{D}}(\rho)$ on \mathcal{D} while the partial transpose ρ^P defines a face $\mathcal{F}_{\mathcal{D}^P}(\rho^P)$. Taking the partial transpose $I \otimes \tau$ of all points in the latter, we get a face $\mathcal{F}_{\mathcal{D}^P}(\rho)$ on \mathcal{D}^P that intersects $\mathcal{F}_{\mathcal{D}}(\rho)$. The intersection of the faces defines a face $\mathcal{F}_{\mathcal{P}}(\rho) = \mathcal{F}_{\mathcal{D}}(\rho) \cap \mathcal{F}_{\mathcal{D}^P}(\rho)$ on \mathcal{P} with ρ as an interior point.

$\mathcal{F}_{\mathcal{P}}(\rho) = \mathcal{F}_{\mathcal{D}}(\rho) \cap \mathcal{F}_{\mathcal{D}^P}(\rho)$, which we will see is a flat face of \mathcal{P} .

As before we can express the conditions for a Hermitian matrix $\tilde{\sigma}$ to lie in a face $\mathcal{F}_{\mathcal{D}}(\rho)$ as vector equations in \mathbb{R}^{N^2} . Let P be the projection on the image of ρ . Then the conditions on σ can be expressed as in eq. (3.38). If ρ

is a PPT state, we can perform exactly the same analysis for ρ^P and obtain expressions for states in the face defined by ρ^P similar to eq. (3.38) for ρ . Let \tilde{P} be the projection on the image of ρ^P . Then the condition for a given Hermitian matrix $\tilde{\sigma}^P$ to lie in the face $\mathcal{F}_{\mathcal{D}}(\rho^P)$ can be expressed as

$$\tilde{P}\tilde{\sigma}^P = \tilde{\sigma}^P \quad (3.47)$$

with $\tilde{\sigma}^P$ as the vector representation of σ^P in \mathbb{R}^{N^2} .

A matrix σ which lies in the face defined by ρ , and whose partial transpose σ^P lies in the face defined by ρ^P , must fulfill both sets of equations in eq. (3.38) and eq. (3.47). By the Choi-Jamiolkowski isomorphism the partial transpose map $I \otimes \tau$ can be represented as an operator $\mathbf{\Pi}$ acting on \mathbb{R}^{N^2} , in the sense that applying $\mathbf{\Pi}$ to the vector representation of $\tilde{\sigma}$ returns the vector representation of $\tilde{\sigma}^P$ as follows

$$\mathbf{\Pi}\tilde{\sigma} = \tilde{\sigma}^P \quad (3.48)$$

The matrix $\mathbf{\Pi}$ is its own inverse in the sense that $\mathbf{\Pi}^2 = \mathbb{1}$ where $\mathbb{1}$ is the identity on \mathbb{R}^{N^2} because taking the partial transposition twice reproduces the original matrix, $(\tilde{\sigma}^P)^P = \tilde{\sigma}$. Defining a new projection operator

$$\hat{P} \equiv \mathbf{\Pi}\tilde{P}\mathbf{\Pi}, \quad \hat{P}^2 = \mathbf{\Pi}\tilde{P}\mathbf{\Pi}^2\tilde{P}\mathbf{\Pi} = \mathbf{\Pi}\tilde{P}^2\mathbf{\Pi} = \mathbf{\Pi}\tilde{P}\mathbf{\Pi} = \hat{P} \quad (3.49)$$

allows us to express eqs. (3.38) and (3.47) as a single vector equation

$$P\hat{P}P\tilde{\sigma} = \tilde{\sigma} \quad (3.50)$$

In detail, what happens when we let the operator $P\hat{P}P$ act on some vector \mathbf{w} is the following. First \mathbf{w} is projected onto the hyperplane defined by P with the result being the projected vector $\mathbf{x} = P\mathbf{w}$. Then \hat{P} first maps \mathbf{x} to \mathcal{D}^P by $\mathbf{\Pi}\mathbf{x} = \mathbf{x}^P$, before projecting \mathbf{x}^P onto hyperplane defined by \tilde{P} with the result $\mathbf{y}^P = Q\mathbf{x}^P$. This vector is then mapped back to \mathcal{D} by $\mathbf{y} = \mathbf{\Pi}\mathbf{y}^P$, where finally the resulting vector is projected back down to the hyperplane defined by P by $\mathbf{z} = P\mathbf{y}$. This would correspond to

$$P\hat{P}P\mathbf{w} = \mathbf{z} \quad (3.51)$$

Any vector \mathbf{w} for which $\mathbf{z} = \mathbf{w}$ in the above equation and that represents a density matrix, represents a density matrix which lies in $\mathcal{F}_{\mathcal{D}}(\rho)$ and whose partial transpose lies in $\mathcal{F}_{\mathcal{D}}(\rho^P)$.

The number of eigenvalues of $P\hat{P}P$ equal to one is not the same as the rank of the matrix, since it is not a projection operator. This can easily be verified by applying the operator twice

$$(P\hat{P}P)^2 = P\hat{P}P^2\hat{P}P \quad (3.52)$$

which in general is not equal to $P\hat{P}P$. However, we can take the eigenvectors of $P\hat{P}P$ that correspond to eigenvalues equal to one, and form a projection operator B that projects onto the subspace spanned by these eigenvectors. The conditions in eq. (3.50) can then be written as

$$B\sigma = \sigma \quad (3.53)$$

and the rank r of B is then the number of linearly independent solutions.

Let $\{\tilde{\sigma}_k\}$ be the set of r linearly independent solutions to the above equation. Then as before we can construct a traceless set of Hermitian matrices by

$$\sigma_k = \tilde{\sigma}_k - \text{Tr}(\sigma_k)\rho \quad (3.54)$$

Since ρ is one of the solutions to eq. (3.53) it is not included in the new set $\{\sigma_k\}$.

Any density matrix in the face $\mathcal{F}_{\mathcal{P}}(\rho)$ can be expressed in terms of the new set as

$$\rho' = \rho + \sum_{k=1}^{r-1} x_k \sigma_k \quad (3.55)$$

The set $\{\sigma_k\}$ thus forms an $(r-1)$ -dimensional vector space that together with the condition on the positivity of density matrices completely describes the face $\mathcal{F}_{\mathcal{P}}(\rho)$. It follows that the dimension of $\mathcal{F}_{\mathcal{P}}(\rho)$ is $r-1$. A two-dimensional cross section through \mathcal{D} showing two density matrices on the same face of \mathcal{P} is given in fig. 3.17.

The rank r of B depends on more than just the rank of ρ and is in general hard to predict. But we can derive a lower limit on r in the following way. Equation (3.38) implies that the matrix $\tilde{\sigma}$ must satisfy $N^2 - m^2$ real constraints. Similarly, eq. (3.47) implies that the partial transpose $\tilde{\sigma}^P$ must satisfy $N^2 - n^2$ real constraints. If all the constraints are linearly independent we have a maximum of $2N^2 - m^2 - n^2$ real constraints in total. The rank r of B is the number of free parameters left after subtracting the number of constraints from the total of N^2 free parameters. It thus follows that

$$r \geq N^2 - (2N^2 - m^2 - n^2) = m^2 + n^2 - N^2 \quad (3.56)$$

This also implies that the dimension $d = r - 1$ of the face $\mathcal{F}_{\mathcal{P}}(\rho)$ has a lower bound given by

$$d \geq m^2 + n^2 - N^2 - 1 \quad (3.57)$$

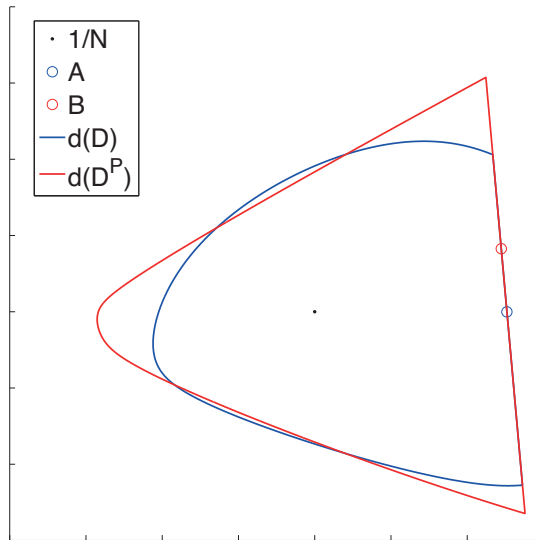


Figure 3.17: Two-dimensional cross section through \mathcal{D} showing two density matrices A and B , both of rank $(7, 7)$, lying in the same face on \mathcal{P} .

The lower bound on the dimension of $\mathcal{F}_{\mathcal{P}}(\rho)$ implies an upper bound on the ranks (m, n) of ρ for ρ to be an extreme point of \mathcal{P} . As discussed previously, the dimension of the face defined by an extreme point is zero. Thus, by eq. (3.57), we get

$$d = 0 \geq m^2 + n^2 - N^2 - 1 \quad (3.58)$$

implying that for an extreme point we have

$$m^2 + n^2 \leq N^2 + 1 \quad (3.59)$$

The lower bound on the rank of \mathbf{B} implies that generic PPT states with ranks (m, n) that satisfy eq. (3.59) are extremal in \mathcal{P} . For sufficiently generic PPT states ρ we would expect a minimal intersection of the faces $\mathcal{F}_{\mathcal{D}}(\rho)$ and $\mathcal{F}_{\mathcal{D}^P}(\rho)$. This corresponds to the maximum number of constraints on $\tilde{\sigma}$ or equivalently the lower bound on the rank of \mathbf{B} . Then we see from eq. (3.57) that we get a series of negative values for the rank of \mathbf{B} as m and n become smaller. But since we know that ρ lies in the intersection, we know that the rank of \mathbf{B} is at least one. Thus, if we know that ρ is a sufficiently generic PPT state with ranks that satisfy eq. (3.59), we expect that the rank of \mathbf{B} is one and that ρ is extremal in \mathcal{P} .

Take a system of dimension 3×3 as an example. The upper limit is then given by

$$m^2 + n^2 \leq 82 \quad (3.60)$$

For a PPT state of rank $(4, 4)$ we get $m^2 + n^2 = 32$, so in the generic case, where we can expect the constraints on ρ and ρ^P to be independent, we expect that the $(4, 4)$ states are extremal. For a PPT state of rank $(7, 6)$ we find that the relevant numbers are $m^2 + n^2 = 85$ and the lower limit on the rank of \mathbf{B} is four. Such states can then not be extremal PPT states.

The fact that low rank PPT states are typically expected to be extremal in \mathcal{P} implies that low rank PPT states typically are entangled. This follows from the fact that any extremal PPT state that is not a pure product state must be entangled. If it were separable it could be written as a convex combination of projections on pure product states and thus would not be extremal. In fact we can use the lower bound in eq. (3.57) on the face $\mathcal{F}_{\mathcal{P}}(\rho)$ to say something about the separability of sufficiently generic states.

Combining the lower limit on the dimension of a face on \mathcal{P} with the range criterion yields an upper bound on the ranks (m, n) of PPT states that can be separable, providing they are sufficiently generic. Let ρ be a separable density matrix of rank (m, n) and without loss of generality assume that

$m \geq n$. The range criterion states that a separable density matrix ρ of rank m must have at least m linearly independent product vectors in its image. Consider a separable state that can be expressed as

$$\rho = \sum_{k=1}^m p_k \psi_k \psi_k^\dagger = \sum_{k=1}^m p_k \rho_k, \quad \psi_k = \phi_k \otimes \chi_k \quad (3.61)$$

Then each $\rho_k = \psi_k \psi_k^\dagger$ lies in the face $\mathcal{F}_\rho(\rho)$ which means that the face must at least be m -dimensional. In other words, if the face has dimension lower than m , it cannot contain the necessary number of pure product states to express ρ as a separable state. In that case ρ must be entangled.

Thus it follows that a sufficiently generic PPT state with ranks (m, n) that satisfy

$$d < m \quad \Rightarrow \quad m(m-1) + n^2 < N^2 + 1 \quad (3.62)$$

is entangled. Either the lower bound on d is negative and ρ is extremal, or the lower bound is positive but less than m and ρ cannot be expressed as a convex combination of the minimum required number of separable pure states.

A class of entangled PPT states closely related to the extremal PPT states are the so-called edge states. The concept of edge states was introduced and further studied in [61, 62, 63, 64, 65, 66]. As stated in [11], an edge state ρ is an entangled PPT state such that for all $\epsilon \geq 0$ and any product vector $\psi = \phi \otimes \chi$, the matrix

$$\rho' = \rho - \epsilon \psi \psi^\dagger \quad (3.63)$$

is not positive or does not have a positive partial transpose. In light of this, we see that the extremal PPT states are also edge states. The set of edge state constitutes a set which is larger than the set of extremal PPT states. For example, a convex combination of two low rank extremal PPT states can be a higher rank edge state. If a PPT state is an edge state and not extremal, then it must be a convex combination of extremal PPT states.

3.7 Surfaces of density matrices with specified ranks

In the above discussion we have seen that when keeping the images of ρ and ρ^P fixed, the resulting set of density matrices with the same images form faces

on \mathcal{D} and \mathcal{P} . The structure of \mathcal{S} in terms of faces has also been investigated [67].

A natural next step is to study surfaces of density matrices with specific ranks (m, n) embedded in \mathbb{R}^{N^2} . It is reasonable to assume that these surfaces may be curved and twisted in the embedding space. What we can do, however, is to study the tangent space of a surface at given points. This will in particular allow us to calculate the local dimension of the surface. If we choose sufficiently generic points on the surface, the local dimension should correspond to the dimension of the whole surface.

Let ρ be a PPT state of rank m acting on a Hilbert space of dimension N . In the following we will work in a basis for \mathcal{H} where the matrix representation of ρ is as in eq. (3.1). For a general Hermitian matrix A , we can then represent it as

$$\begin{pmatrix} B & C^\dagger \\ C & D \end{pmatrix} \quad (3.64)$$

With P and Q projecting on the image and kernel of ρ respectively, we have

$$PAP = B \quad (3.65)$$

$$QAQ = D \quad (3.66)$$

$$QAP = (QAP)^\dagger = C \quad (3.67)$$

Consider a perturbation $\tilde{\sigma}$ which perturbs the state ρ as

$$\rho' = \rho + \epsilon \tilde{\sigma}, \quad |\epsilon| \ll 1 \quad (3.68)$$

We want to ensure that the rank of ρ' is the same as the rank of ρ in order to stay on the surface of rank- m density matrices. If $m < N$ the zero-eigenvalues of ρ are degenerate, so we need degenerate perturbation theory. To first order in ϵ the zero-eigenvalues of ρ are perturbed into ϵ times the eigenvalues of $Q\tilde{\sigma}Q$. In order to not increase the rank of ρ' beyond m to first order in ϵ , it follows that $\tilde{\sigma}$ must satisfy

$$Q\tilde{\sigma}Q = 0 \quad (3.69)$$

Thus $\tilde{\sigma}$ will have the matrix representation

$$\begin{pmatrix} B & C \\ C^\dagger & 0 \end{pmatrix} \quad (3.70)$$

The number of independent columns in this matrix is the same as for ρ , which means that the rank of ρ and ρ' are equal for small perturbations.

We can perform the same analysis with respect to the partially transposed matrices ρ^P and $\tilde{\sigma}^P$ and arrive at similar conditions for $\tilde{\sigma}^P$. Let \tilde{P} and \tilde{Q} be the projections on the image and kernel of ρ^P respectively. In order for $\tilde{\sigma}^P$, to not increase the rank of $\rho'^P = \rho^P + \epsilon\sigma^P$ to first order in ϵ , it must obey

$$\tilde{Q}\tilde{\sigma}^P\tilde{Q} = 0 \quad (3.71)$$

Since $Q = I - P$ and $\tilde{Q} = I - \tilde{P}$, we can rewrite eqs. (3.70) and (3.71) as

$$\tilde{\sigma} = P\tilde{\sigma} + \tilde{\sigma}P - P\tilde{\sigma}P \equiv \Theta_P(\tilde{\sigma}) \quad (3.72)$$

$$\tilde{\sigma}^P = \tilde{P}\tilde{\sigma}^P + \tilde{\sigma}^P\tilde{P} - \tilde{P}\tilde{\sigma}^P\tilde{P} \equiv \Theta_{\tilde{P}}(\tilde{\sigma}^P) \quad (3.73)$$

By using the Choi-Jamiolkowski isomorphism we can represent the maps Θ_P and $\Theta_{\tilde{P}}$ as matrices \mathbf{R} and $\tilde{\mathbf{R}}$ in \mathbb{R}^{N^2} and rewrite the above expressions as vector equations

$$\mathbf{R}\tilde{\sigma} = \tilde{\sigma} \quad (3.74)$$

$$\tilde{\mathbf{R}}\tilde{\sigma}^P = \tilde{\sigma}^P \quad (3.75)$$

It follows from applying the maps twice that both \mathbf{R} and $\tilde{\mathbf{R}}$ are projection operators. We can now define a new matrix $\hat{\mathbf{R}} \equiv \mathbf{R}\tilde{\mathbf{R}}\mathbf{R}$ and combine the two sets of equations into a single vector equation

$$\mathbf{R}\hat{\mathbf{R}}\tilde{\sigma} = \tilde{\sigma} \quad (3.76)$$

where $\mathbf{R}\hat{\mathbf{R}}\mathbf{R}$ is not a projection operator. As before we can define a projection operator \mathbf{K} as the sum of projections on the eigenvectors of $\mathbf{R}\hat{\mathbf{R}}\mathbf{R}$ with corresponding eigenvalue equal to one. The vector equation can then be expressed as

$$\mathbf{K}\tilde{\sigma} = \tilde{\sigma} \quad (3.77)$$

Let $\{\tilde{\sigma}_k\}$ be the set of s solutions to the above equation where s is the rank of \mathbf{K} . We can then define a set $\{\sigma_k\}$ of $s-1$ traceless Hermitian matrices given by

$$\sigma = \tilde{\sigma} - \text{Tr}(\tilde{\sigma})\rho \quad (3.78)$$

Since ρ is contained in $\{\tilde{\sigma}_k\}$ it follows that it is not included in $\{\sigma_k\}$ and thus we have reduced the number of elements in the set from s to $s-1$. The set $\{\sigma_k\}$ then spans the local tangent space at ρ which implies that the local dimension of the surface of density matrices with rank (m, n) at ρ is equal to $s-1$.

By themselves, eqs. (3.74) and (3.75) define the tangent space to the surface of rank- m density matrices at ρ and rank- n density matrices at ρ^P respectively. Equation (3.77) represents the local intersection of these two spaces at ρ . This intersection is thus the tangent space to the surface of PPT density matrices with rank (m, n) on which ρ sits.

We can derive a lower bound for the number of solutions to eq. (3.76) in the following way. Equations (3.69) and (3.70) imply that a $(N-m) \times (N-m)$ Hermitian submatrix of σ is equal to zero. This means that the number of constraints from eq. (3.69) is equal to $(N-m)^2$. Similarly we get $(N-n)^2$ constraints from eq. (3.71). If all the constraints are independent we have a total of $(N-m)^2 + (N-n)^2$ constraints. The rank s of \mathbf{K} is the number of free parameters left after subtracting the actual number of constraints from the total of N^2 free parameters. It follows that the dimension d of the tangent space to the surface of PPT density matrices with rank (m, n) at ρ is

$$d = s - 1 \geq 2N(m+n) - N^2 - m^2 - n^2 - 1 \quad (3.79)$$

We find numerically that the lower bound is satisfied with equality for generic PPT states ρ in systems of dimension 3×3 , 3×4 , 3×5 , 3×6 , 4×4 and 4×5 when the rank (m, n) satisfies

$$m, n > N_A + N_B - 2 \quad (3.80)$$

while for generic states with

$$m = n = N_A + N_B - 2 \quad (3.81)$$

the dimension appears to be larger.

Chapter 4

Numerical methods

In this chapter we will review the most important numerical methods developed and used by us during the work with this thesis. There are mainly four tools we have used, and in the next chapter we will elaborate in more detail how and why they were implemented, and the results obtained.

The first is a method for obtaining density matrices of a specific rank with or without specific restrictions on the nonzero eigenvalues, and with the option of demanding similar conditions on the partial transpose. This method lies at the heart of all of the work in this thesis, as it has allowed us to obtain a large amount of density matrices of various ranks that we have studied. This method is presented in Paper I.

The second is a method used for examining possible $SL \otimes SL$ equivalence between a given density matrix and a projector. This method has been instrumental in our extension of the results in Paper II to the results in Paper III, and is presented in Paper III.

The third is a method used for checking for possible SL equivalence between two sets of vectors, and by extension, $SL \otimes SL$ equivalence between two sets of product vectors. This method is presented in Paper II, and is the basis for the results there.

The fourth and final is a method used for obtaining product vectors in a given subspace. The method has been instrumental in the work presented in this thesis, as we in Paper II, III and IV have focused in particular on the relationship between low rank PPT states and product vectors.

To fix the context, assume in the following that we are studying the set of density matrices that act on a bipartite Hilbert space $\mathcal{H} = \mathcal{H}_A \otimes \mathcal{H}_B$ with total dimension $N = N_A N_B$ with N_A and N_B the dimensions of the respective subsystems.

4.1 Obtaining density matrices with specified rank

We will here present an iterative method for obtaining density matrices with specific rank based on expanding the eigenvalues in a set of variables, restricting to first order in the expansion and show that each iteration reduces to solving a set of linear equations.

The eigenvalues λ_k of a density matrix ρ are functions of a set of variables. The variables are the coefficients x_i in eq. (3.3) which we restate here for convenience

$$\rho = \frac{\mathbb{1}}{N} + \sum_{i=1}^{N^2-1} x_i D_i \quad (4.1)$$

The eigenvalues λ_k must thus be functions of the x_i , $\lambda_k = \lambda_k(\mathbf{x})$, where \mathbf{x} is an $(N^2 - 1)$ -component vector with the x_i as components. Since the partial transpose, ρ^P is uniquely defined by ρ , and thus by the x_i , the eigenvalues λ_k^P of ρ^P are also functions of the same variables, $\lambda_k^P = \lambda_k^P(\mathbf{x})$.

Demanding a specific rank of ρ and ρ^P introduces conditions on some of their eigenvalues. Assume that we want ρ to have rank m and ρ^P to have rank n , that is, we want ρ to be a rank (m, n) state. Then $\tilde{m} = N - m$ of the eigenvalues of ρ and $\tilde{n} = N - n$ of the eigenvalues of ρ^P must be equal to zero. Ordering the eigenvalues such that the \tilde{m} first of ρ and the \tilde{n} first of ρ^P are zero, we can write this as

$$\begin{aligned} \lambda_k &= 0, & k &= 1, \dots, \tilde{m} \\ \lambda_k^P &= 0, & k &= 1, \dots, \tilde{n} \end{aligned} \quad (4.2)$$

We are also free to put conditions on the nonzero eigenvalues of ρ and ρ^P . We could specify exactly what we would like all or some of the nonzero eigenvalues to be by equations like

$$\begin{aligned} \lambda_k &= \eta_k & k &\in \{\tilde{m} + 1, \dots, N\} \\ \lambda_k^P &= \eta_k^P & k &\in \{\tilde{n} + 1, \dots, N\} \end{aligned} \quad (4.3)$$

where the η_k are explicitly chosen by us. In particular we could choose $\eta_k = 1/m$ for all nonzero eigenvalues λ_k in order to obtain a density matrix proportional to a rank m projection operator. Simultaneously choosing all $\eta_k^P = 1/n$ for all nonzero eigenvalues λ_k^P would lead to the final density matrix being proportional to a rank m density matrix while its partial transpose would be proportional to a rank n projection operator.

We can collect all the conditions from eqs. (4.2) and (4.3) on the eigenvalues of ρ and ρ^P in a single vector relation

$$\boldsymbol{\mu}(\mathbf{x}) = \boldsymbol{\nu} \quad (4.4)$$

where the components of the vector $\boldsymbol{\mu}(\mathbf{x})$ are the eigenvalues $\lambda_k(\mathbf{x})$ and $\lambda_k^P(\mathbf{x})$ on which we are putting restrictions, and the components in $\boldsymbol{\nu}$ are the chosen conditions. As an example, if we only want to restrict the rank, the vectors $\boldsymbol{\mu}$ and $\boldsymbol{\nu}$ would be $(\tilde{m} + \tilde{n})$ -components vectors

$$\begin{aligned} \boldsymbol{\mu} &= [\lambda_1, \dots, \lambda_{\tilde{m}}, \lambda_1^P, \dots, \lambda_{\tilde{n}}^P]^T \\ \boldsymbol{\nu} &= [0, \dots, 0, 0, \dots, 0]^T \end{aligned} \quad (4.5)$$

where we have suppressed the \mathbf{x} -dependence of $\boldsymbol{\mu}$ in the notation.

Assume that we start with a value of \mathbf{x} that does not satisfy our conditions. We write the deviation from the exact solution \mathbf{x}' as $\Delta\mathbf{x} = \mathbf{x}' - \mathbf{x}$ and treat this as a perturbation. Expanding to first order in $\Delta\mathbf{x}$ we obtain the following on component form

$$\nu_k = \mu_k(\mathbf{x} + \Delta\mathbf{x}) \approx \mu_k + \sum_i \Delta x_i \frac{\partial \mu_k}{\partial x_i} \quad (4.6)$$

with the terms in the approximation being evaluated at the starting point \mathbf{x} .

The previous equation can be rewritten as a set of linear equations

$$A\Delta\mathbf{x} = \mathbf{b} \quad (4.7)$$

with A a square, positive and real matrix. To see this, note first that the second term in the approximation in eq. (4.6) is exactly the expression for a matrix B with components $B_{ki} = \partial\mu_k/\partial x_i$ acting on a vector $\Delta\mathbf{x}$ with components Δx_i . We can then write eq. (4.6) as

$$\sum_i B_{ki} \Delta x_i = \nu_k - \mu_k \quad (4.8)$$

Since the components of B are derivatives of the eigenvalues of ρ and ρ^P which are all real, B is a real matrix. The components can be obtained via ordinary first order perturbation theory, which says that if ψ_k is the eigenvector of ρ associated with eigenvalue λ_k , then the change in λ_k to first order can be computed as

$$\frac{\partial \lambda_k}{\partial x_i} = \psi_k^\dagger \frac{\partial \rho}{\partial x_i} \psi_k \quad (4.9)$$

From eq. (4.1) we get a nice and easy expression for the right hand side of the above equation. Since ρ is linear in the x_i , we get the following easily evaluated expression for the change in the eigenvalues

$$B_{ki} = \frac{\partial \lambda_k}{\partial x_i} = \psi_k^\dagger D_i \psi_k \quad (4.10)$$

In order to obtain a square, positive and real matrix, multiply eq. (4.6) with B^T from the left and define

$$\begin{aligned} A &\equiv B^T B \\ \mathbf{b} &\equiv B\boldsymbol{\nu} - B\boldsymbol{\mu} \end{aligned} \quad (4.11)$$

Thus we obtain the expression in eq. (4.7). This equation is suitable to solve with the conjugate gradient method, and we obtain a vector $\Delta\mathbf{x}$ with which to update our original vector \mathbf{x} .

Since the expansion of eq. (4.4) to first order in general will not be a good approximation unless we are really close to the true solution, the updated vector $\mathbf{x} + \Delta\mathbf{x}$ will typically not be a solution either. But it should be closer than \mathbf{x} , and thus we may iterate the procedure to obtain better and better solutions until the method converges.

It is important to note that the above procedure does not by itself secure that the density matrix we obtain in the end is positive semidefinite, nor that it is positive under partial transposition. It is however, possible to implement these conditions when constructing the vectors $\boldsymbol{\mu}$ and $\boldsymbol{\nu}$.

The way to do this is to manually insert one dummy eigenvalue equal to zero in each of the sets of eigenvalues of ρ and ρ^P in each iteration, and then order the two sets independently from the largest negative to the largest positive number before constructing the vectors $\boldsymbol{\mu}$ and $\boldsymbol{\nu}$. To illustrate the point, assume for simplicity that we only want to constrain the ranks of ρ and ρ^P in the end so that they are m and n respectively. The vector $\boldsymbol{\nu}$ is then constructed as an $(\tilde{m} + \tilde{n} + 2)$ -component vector consisting entirely of zeros. The additional two zeros we have added compared to eq. (4.5) are inserted as component 1 and $\tilde{m} + 2$.

Assume further that the eigenvalues of ρ and ρ^P at the beginning of an iteration are

$$\{\lambda_1, \dots, \lambda_N\} \quad \text{and} \quad \{\lambda_1^P, \dots, \lambda_N^P\}$$

where they are sorted so that $\lambda_1 \leq \lambda_2 \leq \dots \leq \lambda_N$ and similarly for λ_k^P . Then insert one zero in both of the sets to obtain

$$\{0, \lambda_1, \dots, \lambda_N\} \quad \text{and} \quad \{0, \lambda_1^P, \dots, \lambda_N^P\} \quad (4.12)$$

Assume that the only negative eigenvalues are λ_1 and λ_1^P . When we reorder the sets now we would then get

$$\{\lambda_1, 0, \lambda_2, \dots, \lambda_N\} \quad \text{and} \quad \{\lambda_1^P, 0, \lambda_2^P, \dots, \lambda_N^P\} \quad (4.13)$$

When we now construct the vector $\boldsymbol{\mu}$ it would look like

$$\boldsymbol{\mu} = [\lambda_1, 0, \lambda_2, \dots, \lambda_{\tilde{m}}, \lambda_1^P, 0, \lambda_2^P, \dots, \lambda_{\tilde{n}}^P] \quad (4.14)$$

and have $\tilde{m} + \tilde{n} + 2$ components. In this way, the largest negative eigenvalue of ρ in each iteration will be placed as element 1 in $\boldsymbol{\mu}$ and thus by $\boldsymbol{\nu}$ be required to be zero. Similarly, the largest negative eigenvalue of ρ^P will be placed as element $\tilde{m} + 2$ in $\boldsymbol{\mu}$, and by $\boldsymbol{\nu}$ be required to be equal to zero. This will force the procedure to search for a solution where neither ρ nor ρ^P contain any negative eigenvalues.

Since the zeros we have added are only dummy eigenvalues, they should not contribute to the solution and therefore the dummy eigenvectors associated with them are simply the N-component zero-vector. Then they do not contribute to the matrix B in eq. (4.10).

The introduction of the dummy eigenvalues ensures that regardless of the rank we choose, even if we choose full rank for ρ and/or ρ^P , that is $\tilde{m} = 0$ and/or $\tilde{n} = 0$, they will always be positive semidefinite. In practice this could be implemented in such a way that we may choose whether to restrict ρ and/or ρ^P to be positive semidefinite in the end by inserting a dummy eigenvalue for ρ and/or ρ^P , but we have in the work presented in this thesis always required positive semidefiniteness of both ρ and ρ^P .

In short the method looks like the following:

- Construct the constraint vector $\boldsymbol{\nu}$ and choose a random starting point \boldsymbol{x}_0 .
- Use the current \boldsymbol{x}_0 to calculate ρ, ρ^P , their eigenvalues and corresponding eigenvectors.
- Insert dummy eigenvalues and order the eigenvalues independently from the largest negative to the largest positive and construct the vector $\boldsymbol{\mu}$.
- Use $\boldsymbol{\mu}$ and the corresponding eigenvectors to calculate the components of B according to eq. (4.10), then use $B, \boldsymbol{\mu}$ and $\boldsymbol{\nu}$ to calculate A and \boldsymbol{b} according to eq. (4.11), and solve eq. (4.7) to obtain an update $\Delta\boldsymbol{x}$.

- Update the original vector to obtain $\mathbf{x}_1 = \mathbf{x}_0 + \Delta\mathbf{x}_1$. If \mathbf{x}_1 is not a true solution to eq. (4.4), iterate the procedure with the updated vector in order to obtain a better approximation. Continue to iterate until the method converges.

Note that the method does not ensure that the target ranks (m, n) are the ranks the final density matrix will have, since the method does not detect whether or not the rank is smaller than m or n respectively. Both when the ranks are equal to (m, n) and when one or both of them are smaller, the density matrix satisfies the conditions that $N - m$ and $N - n$ of the eigenvalues are equal to zero. Thus, in practice, one may end up with a final density matrix with smaller ranks than intended. This turns out to be especially true if the ranks are highly asymmetric, for example rank $(9, 5)$ in systems of dimension 3×3 . The common result when looking for density matrices with this rank using the method outlined here is a density matrix with rank $(7, 5)$ or $(6, 5)$.

The performance of the method is good for $N \leq 20$ and passable up to $N = 25$ with results obtained in seconds in the simplest cases and a couple of days for the most difficult cases in the largest dimensions.

4.2 SL \otimes SL equivalence to projectors

Here we present an iterative method to search for a linear product transformation of the form SL \otimes SL that transforms a chosen density matrix into a projection operator. This was useful in Paper II and III where we investigated the relationship between projection operators and density matrices in the context of obtaining methods for constructing low rank PPT states.

Assume that we have a density matrix ρ_0 and that it is SL \otimes SL equivalent to a projection operator P , that is, there exists a complex product matrix $S = S_1 \otimes S_2$ such that

$$S\rho_0S^\dagger = P \quad (4.15)$$

Since P is a projection operator we have

$$S\rho_0S^\dagger S\rho_0S^\dagger = P^2 = P = S\rho_0S^\dagger \quad (4.16)$$

We are only considering nonsingular product transformations, therefore the above equation implies

$$\rho_0S^\dagger S\rho_0 = \rho_0 \quad (4.17)$$

Assume that the rank of ρ_0 is m , then we can write the above equation as a vector equation

$$\mathbf{F} = \boldsymbol{\rho}_0 \quad (4.18)$$

where \mathbf{F} and $\boldsymbol{\rho}_0$ are m^2 -component vectors in the real vector space of Hermitian $m \times m$ -matrices that have the same image as ρ_0 . This is so, because whatever matrix A we have on the left hand side of eq. (4.17) is projected down by ρ_0 so that the matrix on the left hand side has the same image as ρ_0 . Additionally, since ρ_0 has rank m , the projected matrix on the left hand side in eq. (4.17) has at most rank m . They can then both be represented as Hermitian $m \times m$ -matrices, and thus also as m^2 real vectors.

A particular choice of basis matrices for all $m \times m$ -matrices that share image with ρ_0 is given by the eigenvectors ψ_k of ρ_0 corresponding to the m nonzero eigenvalues. The orthogonal basis matrices can be chosen as

$$D_k = \left(1 - \frac{1}{2}\delta_{ij}\right) (\psi_i\psi_j^\dagger + \psi_j\psi_i^\dagger), \quad i, j = 1, \dots, m \quad (4.19)$$

$$D_k = \frac{i}{\sqrt{2}} (\psi_i\psi_j^\dagger - \psi_j\psi_i^\dagger), \quad j > i, i = 1, \dots, m \quad (4.20)$$

There are $m(m+1)/2$ matrices of the type in eq. (4.19) and $m(m+1)/2 - m$ of the type in eq. (4.20), so altogether m^2 matrices. It is straight forward to check that they constitute an orthogonal basis under the trace product, $\text{Tr}(D_k D_l) = \delta_{kl}$. In this basis the matrix ρ_0 would be expressed as

$$\rho_0 = \sum_{k=1}^{m^2} d_k D_k \quad (4.21)$$

with d_k being the components of the vector $\boldsymbol{\rho}_0$. The components of \mathbf{F} are then given by

$$F_k = \text{Tr}(D_k \rho_0 S^\dagger S \rho_0) \quad (4.22)$$

We can restrict the transformations S_1 and S_2 to be Hermitian. This is because any unitary product transformation on P will give another projection operator, and since we have not specified P other than that it is a projection operator, the unitary part of the transformations S_1 and S_2 are uninteresting here. We allow here S_2 to be an element in $GL(\mathbb{C}, N_B)$ for convenience. We may fix the trace of S_1 rather than the determinant, the choice of normalization does not matter because of the relationship between the determinant and trace. Thus, in the following we fix the trace of S_1 to be 1.

Considering S_1 and S_2 as full rank $N_A \times N_A$ and $N_B \times N_B$ Hermitian matrices respectively, they can now be represented as

$$S_1 = \frac{\mathbb{1}}{N_A} + \sum_{k=1}^{N_A^2-1} x_k D_k^A \quad \text{and} \quad S_2 = \sum_{k=1}^{N_B^2} y_k D_k^B \quad (4.23)$$

where $\{D_k^A\}$ is a complete set of orthonormal basis matrices for $N_A \times N_A$ traceless Hermitian matrices, and $\{D_k^B\}$ is a complete set of orthonormal basis matrices for $N_B \times N_B$ Hermitian matrices. In other words, $\{D_k^A\}$ and $\{D_k^B\}$ are the generators of $SU(N_A)$ and $U(N_B)$ respectively. We can then define a vector

$$\mathbf{z} = \left[x_1, \dots, x_{N_A^2-1}, y_1, \dots, y_{N_B^2} \right]^T \quad (4.24)$$

which contains all the variables in the product matrix S . The vector \mathbf{F} on the left hand side of eq. (4.18) is then a function of these variables, and we have

$$\mathbf{F}(\mathbf{z}) = \boldsymbol{\rho}_0 \quad (4.25)$$

Assume that \mathbf{z} is not an exact solution. Then we treat the deviation from the true solution \mathbf{z}' as a perturbation which we write as $\Delta\mathbf{z} = \mathbf{z}' - \mathbf{z}$. To first order in $\Delta\mathbf{z}$ we get on component form

$$F_k + \sum_i \Delta z_i \frac{\partial F_k}{\partial z_i} = d_k \quad (4.26)$$

with the terms on the left hand side evaluated at \mathbf{z} . This we can rewrite as a set of equations

$$A\Delta\mathbf{z} = \mathbf{b} \quad (4.27)$$

with

$$A \equiv B^T B \quad \text{and} \quad \mathbf{b} = B^T \boldsymbol{\rho}_0 - B^T \mathbf{F} \quad (4.28)$$

and where the components of the matrix B are given by

$$B_{ki} = \frac{\partial F_k}{\partial z_i} \quad (4.29)$$

The calculation of the components of B can be a bit further elaborated. From eqs. (4.17) and (4.18) we have that

$$F_k = (\boldsymbol{\rho}_0 S^\dagger S \boldsymbol{\rho}_0)_k \quad (4.30)$$

Since ρ_0 is fixed, when taking the derivative in order to find the components of B we see that this means that we get

$$B_{ki} = \frac{\partial F_k}{\partial z_i} = \left(\rho_0 \frac{\partial(S^\dagger S)}{\partial z_i} \rho_0 \right)_k = \left(\rho_0 \left[\frac{\partial S^\dagger}{\partial z_i} S + h.c. \right] \rho_0 \right)_k \quad (4.31)$$

From eq. (4.23) we see that the derivative of S is easily computed as

$$\frac{\partial S}{\partial z_i} = \begin{cases} D_j^A \otimes S_2 & \text{if } z_i = x_j \\ S_1 \otimes D_j^B & \text{if } z_i = y_j \end{cases} \quad (4.32)$$

This allows us to calculate the components of B .

We can then solve eq. (4.27) in order to obtain a better approximation to the true solution \mathbf{z}' . If the updated vector $\mathbf{z} + \Delta\mathbf{z}$ is not equal to \mathbf{z}' , then we iterate the procedure finding better and better approximations to the solution until the method converges. In short the procedure is the following:

- Choose a density matrix ρ_0 and a random initial starting vector \mathbf{z} and use ρ_0 to define the basis according to eqs. (4.19) and (4.20).
- Use \mathbf{z} to calculate S_1 , S_2 and $S = S_1 \otimes S_2$ according to eq. (4.23).
- Calculate \mathbf{F} and B according to eqs. (4.22), (4.31) and (4.32), then compute A and \mathbf{b} according to eq. (4.28).
- Solve eq. (4.27) in order to obtain an update $\Delta\mathbf{z}$ to \mathbf{z} , and check whether or not $\mathbf{z}' = \mathbf{z} + \Delta\mathbf{z}$ is a true solution to the original problem in eq. (4.15).
- If it is not, use \mathbf{z}' as the new starting vector and iterate the procedure until the method converges.

The method appears to work well in cases where we know or expect that there exists solutions, and the solutions are typically found within seconds. Consider the number of free parameters in S and constraints from eq. (4.17). From eq. (4.23) it follows that the number of free parameters in S is $N_A^2 + N_B^2 - 1$. Equation (4.17) specifies m^2 independent second order constraint equations. Thus, we at least expect to find solutions if $N_A^2 + N_B^2 - 1 \geq m^2$. In Paper III we present numerical evidence that we always find solutions for generic states of rank $m = 4$ in systems of dimension 3×3 . In this case we indeed have

$$3^2 + 3^2 - 1 = 17 > 4^2 = 16 \quad (4.33)$$

so we might expect that there is in fact a one-dimensional continuous set of solutions. This is discussed in detail in Paper III.

4.3 SL equivalence between sets of vectors

This method can be used to determine whether or not two sets of product vectors are equivalent in the sense that one set can be transformed into the other by SL transformations. In particular, for two sets of product vectors, it can be used to determine such equivalence for the two sets of vectors in each subsystem separately. This would allow us to determine whether the two sets of product vectors could be transformed into each other by $SL \otimes SL$ transformations. We have used it in Paper I to check such equivalence between sets of product vectors in the kernel of $(4, 4)$ states in systems of dimension 3×3 and sets of real orthogonal product vectors parametrized in a special way.

Consider two sets, $\{\phi_k\}$ and $\{u_k\}$, of vectors ϕ_k and u_k in \mathbb{C}^N and let each set contain d vectors. We may ask whether the sets are related by a linear transformation in the following way:

$$u_k = \alpha_k A \phi_k \quad (4.34)$$

where A is a nonsingular complex matrix and α_k is some normalization factor. We include this factor to allow for different normalizations between the vectors and so we can consider $A \in SL(N, \mathbb{C})$. We will show here that this can be formulated as an eigenvalue equation where A can be represented as an eigenvector of a matrix C with corresponding eigenvalue equal to zero.

Let \mathbf{A} be the complex $N^2 \times 1$ vector obtained by stacking the columns of A such that

$$\mathbf{A} = [A_{11}, \dots, A_{1N}, A_{21}, \dots, A_{NN}]^T \quad (4.35)$$

Define a new set of vectors as the result of letting A act on ϕ_k as

$$v_k = A \phi_k \quad (4.36)$$

We then let \mathbf{v} and \mathbf{u} be the $dN \times 1$ vectors obtained by stacking the d vectors v_k and u_k respectively, such that

$$\mathbf{v} = [v_{11}, \dots, v_{1N}, v_{21}, \dots, v_{dN}]^T \quad (4.37)$$

$$\mathbf{u} = [u_{11}, \dots, u_{1N}, u_{21}, \dots, u_{dN}]^T \quad (4.38)$$

Now introduce a $dN \times N^2$ matrix C_T that transforms \mathbf{A} to \mathbf{v} as

$$\mathbf{v} = C_T \mathbf{A} \quad (4.39)$$

It has the following matrix representation:

$$\mathbf{C}_T = \begin{pmatrix} D_{11} & \dots & D_{1N} \\ \vdots & \ddots & \vdots \\ D_{d1} & \dots & D_{dN} \end{pmatrix} \quad (4.40)$$

where $D_{ki} = \phi_{ki} \mathbb{1}_N$ and $\mathbb{1}_N$ is the $N \times N$ identity matrix.

We want to find an \mathbf{A} such that v_k and u_k are proportional for each k . If the two vectors are proportional, it follows that their exterior product will be zero:

$$v_k \wedge u_k = 0 \Leftrightarrow v_k = \alpha_k u_k \quad (4.41)$$

The dimension of the resulting vector obtained by the exterior product in this case is $N(N-1)/2$. We now introduce a matrix \mathbf{C}_\wedge which acts on \mathbf{v} in the following way:

$$\mathbf{C}_\wedge \mathbf{v} = [v_1 \wedge u_1, v_2 \wedge u_2, \dots, v_d \wedge u_d]^T \quad (4.42)$$

The matrix \mathbf{C}_\wedge is then a $p \times dN$ matrix with $p = dN(N-1)/2$. It can be viewed as a $d \times d$ block matrix where each element is an $N(N-1) \times N$ matrix. In block form it is a diagonal matrix with diagonal elements

$$\text{diag}(\mathbf{C}_\wedge) = [E_1, E_2, \dots, E_d] \quad (4.43)$$

Let $\{e_i\}$ be a basis for \mathbb{C}^N so that $\{e_i \wedge e_j \mid i < j\}$ is a basis for $\mathbb{C}^N \wedge \mathbb{C}^N$. Then the matrices E_k can be constructed from

$$(e_i \wedge e_j)^\dagger (E_k v_k) = v_{ki} u_{kj} - v_{kj} u_{ki} \quad (4.44)$$

If $v_k = \alpha_k u_k$ for all k it follows that

$$\mathbf{C}_\wedge \mathbf{v} = \mathbf{C}_\wedge \mathbf{C}_T \mathbf{A} = 0 \quad (4.45)$$

We may multiply from the left by $\mathbf{C}_T^\dagger \mathbf{C}_\wedge^\dagger$ and define

$$\mathbf{C}_T^\dagger \mathbf{C}_\wedge^\dagger \mathbf{C}_\wedge \mathbf{C}_T \equiv \mathbf{C} \quad (4.46)$$

in order to obtain

$$\mathbf{C} \mathbf{A} = 0 \quad (4.47)$$

where \mathbf{C} is an $N^2 \times N^2$ positive, possibly semidefinite, Hermitian matrix. If it has any eigenvalues equal to zero, the corresponding eigenvectors are

vector representations of different matrices A that satisfy eq. (4.34). However, the solutions may be singular, in which case we are not interested in them. Therefore, one must always check whether the solutions are nonsingular.

The rectangular matrix $\mathbf{C}_\wedge \mathbf{C}_T$ has $dN(N-1)/2 \equiv r$ rows and $N^2 \equiv c$ columns. It follows that the rank of \mathbf{C} is

$$\text{rank}(\mathbf{C}) \leq \min\left(\frac{dN(N-1)}{2}, N^2\right) = \min(r, c) \quad (4.48)$$

To see this, observe that the maximal rank is N^2 , and if $r < c$ the rank is at most r . In the case that $r < c$ it follows that \mathbf{C} has at least one zero-eigenvalue and thus there exists at least one solution to eq. (4.47). Thus, for $r < c$ there exists at least one A which satisfies eq. (4.34).

If we choose $d \leq N$ we immediately see that $r < c$, thus we always have at least one solution. This is not surprising, as this means that $\{\phi_k\}$ and $\{u_k\}$ are both sets of d (nonorthogonal) basis vectors of \mathbb{C}^N , and we can always perform a change of basis in order to go from one set to the other, which is a linear transformation.

For $d > N$ we in general expect no solution, and indeed we also then see from eq. (4.48) that $r > c$ which also indicates that there might not be a solution in the generic case. If the two sets of vectors we have chosen are somehow special in the sense that there does exist at least one solution, the method outlined in this section should identify all possible solutions.

4.4 Obtaining product vectors in a given subspace

We present here a method to numerically obtain product vectors in a given subspace, or equivalently, orthogonal to a given subspace. It is highly useful as a tool in determining whether or not a state satisfies the range criterion for instance. We have also used it in Paper I in order to check separability for states with ranks within a given interval. Here we will present the method in the context of obtaining product vectors that have zero expectation value on a density matrix.

To this end, let ρ be a density matrix for which we want to find a product vector $\psi = \phi \otimes \chi$ such that

$$\psi^\dagger \rho \psi = 0 \quad (4.49)$$

with the additional constraint that ψ , and therefore ϕ and χ are normalized to one. In order to include these constraints, we introduce real Lagrange

multipliers λ and μ , and define a function f as

$$f = \sum_{ijkl} \phi_i^* \chi_j^* \rho_{ijkl} \phi_k \chi_l - \lambda \left(\sum_k \phi_k^* \phi_k - 1 \right) - \mu \left(\sum_k \chi_k^* \chi_k - 1 \right) \quad (4.50)$$

with $f = f(\phi, \chi)$. We now want to find local minima of the first term in f under the two constraints implemented through the Lagrange multipliers in the other two terms. Thus, we need to extremalize f .

Taking the derivative with respect to the components of ϕ and χ and demanding that the resulting equations are equal to zero, we get the equations that ϕ and χ must satisfy in order to extremalize f . The vectors are both complex, which means that their components are complex. Normally we would have to take the derivative with respect to both ϕ_k and ϕ_k^* , but in this case they are satisfied simultaneously. Since f is real valued it follows that $\partial f / \partial \phi_k = (\partial f / \partial \phi_k^*)^*$, and so when one of them is equal to zero it follows that the other one is too.

The two equations that must be satisfied in order to extremalize f are then

$$\frac{\partial f}{\partial \phi_i^*} = \sum_{jkl} \chi_j^* \rho_{ijkl} \chi_l \phi_k - \lambda \phi_i = 0 \quad (4.51)$$

$$\frac{\partial f}{\partial \chi_j^*} = \sum_{ikl} \phi_i^* \rho_{ijkl} \phi_k \chi_l - \mu \chi_j = 0 \quad (4.52)$$

From the first one we see that if we multiply from the left by ϕ_i^* and sum over i , we get

$$\sum_i \phi_i^* \frac{\partial f}{\partial \phi_i^*} = \sum_{ijkl} \phi_i^* \chi_j^* \rho_{ijkl} \phi_k \chi_l - \lambda \sum_i \phi_i^* \phi_i = \psi^\dagger \rho \psi - \lambda \phi^\dagger \phi \quad (4.53)$$

Under the assumption that ϕ and χ are normalized to one, and performing a similar analysis of eq. (4.52) with χ_j^* , we find that the values of the Lagrange multipliers at an extremum are

$$\lambda = \psi^\dagger \rho \psi = \mu \quad (4.54)$$

Introducing the matrices B and C with components

$$B_{ik} = \sum_{jl} \chi_j^* \rho_{ijkl} \chi_l \quad \text{and} \quad C_{jl} = \sum_{ik} \phi_i^* \rho_{ijkl} \phi_k \quad (4.55)$$

we write eqs. (4.51) and (4.52) as vector equations

$$B\phi - \lambda\phi = 0 \quad (4.56)$$

$$C\chi - \mu\chi = 0 \quad (4.57)$$

Consider having a product vector $\psi = \phi \otimes \chi$ that does not satisfy the above equations. If we are somewhat close to a minimum, we can calculate the gradients of ϕ and χ , add a bit of them to ϕ and χ respectively and get a better approximation $\psi' = \phi' \otimes \chi'$ to a true solution.

The gradients are given by

$$x \equiv B\phi - \lambda\phi \quad (4.58)$$

$$y \equiv C\chi - \lambda\chi \quad (4.59)$$

with λ given by eq. (4.54) using the starting vector ψ . Then we define new vectors ϕ' and χ' as

$$\phi' = \phi + \epsilon x \quad \text{and} \quad \chi' = \chi + \epsilon y \quad (4.60)$$

and we need to find the optimal step size ϵ along the gradients. To first order in ϵ we then have

$$\psi' = \phi' \otimes \chi' \approx \psi + \epsilon w \equiv s(\epsilon) \quad (4.61)$$

with

$$w \equiv \phi \otimes y + x \otimes \chi \quad (4.62)$$

The step size ϵ we move along the gradients can be found by minimizing

$$g(\epsilon) = \frac{s^\dagger \rho s}{s^\dagger s} \quad (4.63)$$

Taking the derivative of g with respect to ϵ and demanding that it is zero, we get the following second order equation for ϵ :

$$\epsilon^2 + b\epsilon + c = 0 \quad (4.64)$$

with

$$b \equiv 2 \frac{(w^\dagger w)(\psi^\dagger \rho \psi) - (w^\dagger \rho w)}{(w^\dagger w)(\psi^\dagger \rho w + w^\dagger \rho \psi)} \quad \text{and} \quad c \equiv -\frac{1}{w^\dagger w} \quad (4.65)$$

In theory we would calculate the second order derivatives and figure out which one of the two solutions to eq. (4.64) is the minimum, but in practice we just calculate both solutions and choose the one that is the minimum.

The new vector ψ' should be a better approximation to a true solution of eq. (4.49), and if it is not a true solution, we can use the new vector as input and iterate the procedure in order to get better and better approximations. In short, the procedure is the following:

- Given a density matrix ρ choose a random initial product vector $\psi = \phi \otimes \chi$.
- Calculate the gradients x and y according to eqs. (4.55), (4.58) and (4.59).
- Solve eq. (4.64) with the help of eqs. (4.62) and (4.65) and choose the solution that minimizes eq. (4.63).
- Update the product vector ψ according to eq. (4.60).
- If the new product vector ψ' does not satisfy eq. (4.49), set $\psi = \psi'$ and iterate the procedure until the method converges.

The method outlined above allows us to search for all product vectors in a given subspace that are different in the sense that no one product vector is proportional to any other. Since the method searches for local minima, we can expect to find all the different minima by sufficiently varying the initial product vector. Then it is just a matter of checking whether each new product vector is proportional to the ones already obtained.

Since the density matrix ρ is a positive semidefinite matrix, it follows that ψ lies in the kernel of ρ when it satisfies eq. (4.49). In fact, we may replace ρ with any positive semidefinite matrix A in the above procedure, and obtain product vectors in the kernel of A . In particular, we could use the projections P and Q on the image and kernel of ρ respectively. Replacing ρ with P accomplishes nothing new, the method will still be looking for product vectors in the kernel of ρ . However, replacing ρ with Q allows us to look for product vectors in the image of ρ instead of its kernel. Let \tilde{Q} project on the kernel of ρ^P . Then we can search for product vectors that are candidates in a separable decomposition of ρ by replacing ρ in the above procedure with $Q + \tilde{Q}^P$. The details of why this works is discussed in Paper I.

Chapter 5

Summary and outlook

In this chapter we will present short summaries of each paper included in this thesis. The motivations behind the papers and the main results will be discussed and related to the topics in the previous chapters. We end with some conclusions and comments on possibilities for further research.

5.1 Paper I

In this paper we study states with positive partial transpose (PPT states) in bipartite systems of low dimension. The work is a continuation of the effort to characterize entanglement, with a particular focus on the geometry of the sets of density matrices, started in [16]. As discussed in section 3.2 the set \mathcal{D} of density matrices is convex and contains convex subsets \mathcal{P} and \mathcal{S} of PPT and separable states respectively, with $\mathcal{S} \subset \mathcal{P} \subset \mathcal{D}$. Since states that are not PPT are entangled, it follows that identifying the entangled PPT states is of particular interest.

The set \mathcal{P} is convex and thus defined by its extreme points. In [16] the criterion for identifying extremal states of \mathcal{P} discussed in section 3.6 was presented. In the same paper, by a numerical implementation of the criterion, several examples of extremal PPT states were obtained, classified by the ranks (m, n) of the state and its partial transpose.

In this paper we take a slightly different approach. We develop and use the numerical method in section 4.1 to obtain PPT states of various ranks in systems of dimension 2×2 , 2×3 , 2×4 , 2×5 , 3×3 , 3×4 , 3×5 , 4×4 and 4×5 . Since we only impose constraints on the ranks of these PPT states, we consider them to be generic. We further calculate the dimension of the face on \mathcal{P} for each state and compare with the lower bound (section 3.6). We also develop the method described in section 4.4 and use it to identify the

number of product vectors in the image and kernel of each state respectively.

The main result is the information contained in the tables in Appendix B of the paper, where we list the states we have obtained numerically in the systems mentioned previously and their properties. As an alternative to specific examples, the paper thus provides an overview of the properties of generic PPT states of nearly every rank in several low dimensional systems. In particular it shows that PPT states exist for almost all ranks. The results are also diagrammatically represented in figures in section III in the paper.

The results show several regularities. In particular, PPT states with ranks below the upper bound in eq. (3.59) are observed to be extremal, and hence entangled, until the ranks reach a certain lower threshold. Using the method described in section 4.4 we were also able to check the separability of some PPT states with ranks above the limit in eq. (3.59), and find that also they are typically entangled.

The lowest rank for which we find extremal PPT states is especially interesting. We find generic PPT states to be extremal for ranks between the upper limit in eq. (3.59) and the lower limit

$$N_A + N_B - 2 \tag{5.1}$$

for all the systems we have examined. For states with rank lower than this we typically find the generic states to be separable.

There is a known lower bound on the ranks of PPT states that can be entangled given in [64]. There it was shown that PPT states in systems of dimension $N_A \times N_B$ with ranks lower than

$$\max(N_A, N_B) + 1 \tag{5.2}$$

will be separable, which is mirrored in our results. Only for systems of dimension 3×3 do eqs. (5.1) and (5.2) coincide, and for systems of larger dimension eq. (5.1) is larger than eq. (5.2).

As an example, the limit set by eq. (5.2) implies that rank 4 PPT states in systems of dimension 4×4 are separable, but PPT states of rank 5 could in principle typically be entangled. Our results show that generic rank 5 PPT states are separable, while in some cases they may be entangled. When we find them to be entangled, they are always convex combinations of extremal states with less than full local ranks (section 2.2). Generic PPT states of rank 6 and above however, are typically extremal and thus entangled. The rank 6 is exactly the one given by eq. (5.1).

Thus, based on the structure and regularity observed in our numerical results, we therefore conjecture that the lower limit on the rank of extremal PPT states is given by eq. (5.1). We have unfortunately not been able to

prove the conjecture analytically. Neither can we by our numerical methods exclude that there exist special cases where PPT states with ranks between the limits in eqs. (5.1) and (5.2) are extremal, but we do not know of any examples.

5.2 Paper II

In this paper we study the PPT states of rank $(4, 4)$ in systems of dimension 3×3 . The results of Paper I indicated that the lowest rank of extremal PPT states is given by eq. (5.1), and that such states always contain a finite set of (nonorthogonal) product vectors in their kernel. Additionally, in [68] a construction of specific examples of entangled PPT states of rank $(4, 4)$ in systems of dimension 3×3 was given using a set of orthogonal product vectors that end up sitting in the kernel of the state. The state itself is proportional to a projection operator.

The product vectors used in [68] are special in the sense that they are orthogonal and that there does not exist any product vector orthogonal to all members of the set. The set is therefore referred to as unextendible and called an unextendible product basis (UPB). The idea in [68] is to create a real and separable projection operator that projects on the space spanned by the product vectors and consider the density matrix that is proportional to the projection on the subspace orthogonal to the product vectors. Because of the UPB requirement, the image of the density matrix cannot contain any product vectors, hence the state is entangled. Since the projection operator on the kernel of the state is real and separable it is invariant under partial transposition, hence so too is the density matrix, and thus it is a PPT state.

In this paper we generalize this construction by parametrizing all possible UPBs using four real parameters and show that these are $SL \otimes SL$ invariants (see section 2.4). Since such transformations preserve separability, the entire set of rank $(4, 4)$ entangled PPT states obtainable through this construction is divided into classes parametrized by the $SL \otimes SL$ invariants.

The main result of the paper is that all entangled PPT states of rank $(4, 4)$ that we have tested are $SL \otimes SL$ equivalent to states constructed by the UPB method. This includes all entangled PPT states of rank $(4, 4)$ states obtained by us using the method described in section 4.1, but also all examples of such states found in the literature. It is a highly nontrivial result that all known entangled PPT states of rank $(4, 4)$ are $SL \otimes SL$ equivalent to the states constructed by the UPB method.

We arrive at the result in the following way. For each state we use the method described in section 4.4 to obtain the product vectors in the kernel

of the state. By use of special functions defined by determinants, which are explained in the paper, we obtain the four real parameters that describe the product vectors on the special UPB form. The fact that we find these real parameters is the first nontrivial indication that the state is equivalent to a state constructed by a UPB. We use the real parameters to construct the corresponding UPB. We then use the method described in section 4.3 check for $SL \otimes SL$ equivalence between the set of product vectors in the kernel of the state and the UPB. By this we also obtain the product transformation and can check that it actually transforms the original state to a state with the UPB in question in its kernel. The fact that this works for all entangled PPT states of rank $(4, 4)$ that we have tested is highly nontrivial.

5.3 Paper III

In this paper we focus on a generalization of the construction in Paper II of entangled PPT states of rank $(4, 4)$ and a possible extension to entangled PPT states with ranks given by eq. (5.1) in systems of higher dimensions. The results from Paper I indicate strong similarities between the lowest rank extremal states in the systems studied. In particular, they all contain a finite number of product vectors in their kernel. However, the construction presented in Paper II does not lend itself to a straight forward generalization because of the orthogonality requirement on the UPB.

Instead, we focus on a generalization of the UPB construction where we still consider unextendible sets of product vectors, but allow the product vectors to be nonorthogonal and thus we extend the term UPB to cover also these types of sets. The constructed density matrix will still be proportional to a projection operator, however it will not necessarily be a real matrix since we do not require the product vectors to be real. The projection operator on the kernel of the state is considered as a linear combination of projections onto the product vectors in the UPB and as such does not necessarily represent a separable state.

We present the construction in the context of an explicit example in systems of dimension 3×3 where the UPB forms a regular icosahedron, and show that there is a continuous one-parameter family of states on the same form that correspond to a linear deformation of the icosahedron. As a special case of this example, we obtain the state constructed in [68] for a particular deformation of the icosahedron.

The main result of the paper is that all entangled PPT states of rank $(4, 4)$ in systems of dimension 3×3 that we have tested are $SL \otimes SL$ equivalent to states constructed by the generalized UPB construction. We arrive at

this result by taking generic states produced by the method described in section 4.1 and applying the method described in section 4.2 to search for the most general product transformation that transforms the state to projection form. This is also done for all entangled PPT states of rank $(4, 4)$ found in the literature. We always find transformations that do not correspond to those considered in Paper II, and we present numerical evidence indicating that there is a continuous one-parameter family of such transformations for a given state.

For generic states of the lowest rank in higher dimensional systems we are not able to confirm whether it is possible to transform them to a projection form using $SL \otimes SL$ transformations. Instead, we use the method described in section 4.1 to search for PPT states on projection form with this same lowest rank. We are always able to find such states, and obtaining them appears to be no more difficult than to obtain generic PPT states of the same rank. We also check to see whether these states fit into the generalized UPB construction scheme, which they always seem to do. The fact that these states exist, are easy to find and can be described by the generalized UPB construction shows that there is at least the possibility of constructing a subset of entangled PPT states with rank given by eq. (5.1) also in higher dimensional systems.

5.4 Paper IV

In this paper we study the entangled PPT states of rank $(5, 5)$ in systems of dimension 3×3 . We also consider an alternative approach to the construction of entangled PPT states with ranks given by eq. (5.1). The study of the $(5, 5)$ states is a natural progression from the $(4, 4)$ states, and in particular we make use of our knowledge of the entangled PPT states of rank $(4, 4)$ in studying the $(5, 5)$ states. The alternative approach to the construction of entangled PPT states is motivated by the regularities discovered in Paper I that also motivated Paper III, namely that the generic entangled PPT states with ranks given by eq. (5.1) contain a finite set of product vectors in their kernel.

The main results of this paper are twofold. The first is that we show how to construct entangled PPT states of rank $(5, 5)$ from the entangled PPT states of rank $(4, 4)$. We accomplish this by use of perturbation theory and ideas similar to those described in section 3.7. Thus, we obtain entangled PPT states of rank $(5, 5)$ infinitesimally close to the $(4, 4)$ states, which means that they lie infinitesimally close to the boundary of the surface of $(5, 5)$ states.

We calculate the dimension of the surface of PPT states of rank $(5, 5)$ by use of the ideas discussed in section 3.7, and find that this is the same as the number of parameters involved in the perturbation scheme. In order to find generic PPT states of rank $(5, 5)$ that are not infinitesimally close to $(4, 4)$ states we present a method for doing numerical integration along curves on the surface of $(5, 5)$ states.

The second main result is that the number of product vectors in the kernel of a PPT state needed to specify it is in general smaller than the dimension of the kernel. We show for instance that while generic PPT states of rank $(6, 6)$ in systems of dimension 4×4 have 20 different product vectors in their 10 dimensional kernel (so only 10 of them are linearly independent), the number of product vectors needed to specify such a state is 7. And even then, the 7 product vectors are not completely generic.

5.5 Concluding remarks

The work presented in this thesis has been focused on understanding entanglement and entangled states in quantum physics. Entanglement is an important and interesting theme both in itself and in the context of quantum information theory. As a resource entanglement is quite fragile, in the sense that interactions with the environment has a tendency to destroy the entanglement contained in a composite system.

Both from a practical point of view and as part of the theoretical framework of quantum mechanics, it is important to ask how one can determine whether a given state is entangled or separable. A powerful tool in low dimensional bipartite systems for determining separability is given by the PPT criterion, and while it is both necessary and sufficient in systems of dimension 2×2 and 2×3 , it is no longer sufficient in higher dimensional systems. Still, identifying the set of all PPT states is a worthwhile objective, as the states that are not PPT are necessarily entangled.

Our approach has been of a geometric nature, where we exploit the convex nature of the sets of density matrices. Since the set \mathcal{P} of all PPT states is convex, it is completely described by its extreme points, and so it becomes important to identify the entangled extreme points of \mathcal{P} .

As a complimentary approach to the construction of specific examples we tried in Paper I to map out the properties of generic PPT states of nearly every rank in several low dimensional bipartite systems. This should be of interest to anyone working in the same field, as it presents a bigger picture of the properties and geometric structure of generic PPT states.

In particular the regularities concerning the lowest rank extremal and

entangled PPT states stands out in our results. We investigated these states in systems of dimension 3×3 , where they are of rank $(4, 4)$ in Paper II and III and also for higher dimensional systems in Paper III. In Paper IV we exploited our knowledge of the states of rank $(4, 4)$ to construct states of rank $(5, 5)$, and investigated the connection between lowest rank extremal PPT states and product vectors in their kernel. From the results of the work presented in Paper I through IV there emerges several interesting subjects for further study.

One such subject is an analytical proof or disproof of our conjecture in Paper I, that the lower bound on the rank of extremal PPT states is given by $N_A + N_B - 2$. Although all our numerical results are consistent with this conjecture, and there exists no counterexamples as far as we know, a formal proof is obviously desirable.

In addition, a formal proof of $SL \otimes SL$ equivalence between any extremal PPT state of rank $(4, 4)$ in systems of dimension 3×3 and a PPT state obtained by the construction presented in Paper II is needed. Again all our numerical results suggest that this is the case. Parameter counting indicates that any state of rank 4 can be transformed by such transformations to a form where it is proportional to a projection operator, but as we show in Paper III, this does not necessarily imply that the transformed state is of the form obtained through the UPB construction from Paper II.

However, as discussed, the UPB construction in Paper II is too limiting in higher dimensional systems, and so an explicit construction is needed for the lowest rank extremal PPT states in systems of higher dimension. In Paper III we explored one possible generalization of the construction from Paper II, but were unable to confirm $SL \otimes SL$ equivalence between generic lowest rank extremal PPT states and states obtained through the generalized construction. In addition, we were not able to give an explicit recipe for constructing the states.

We were, however, able to numerically obtain generic lowest rank extremal PPT states that are proportional to projection operators in higher dimensional systems and show that they fit into the generalized UPB construction. Parameter counting in higher dimensional systems seems to indicate that generic lowest rank extremal PPT states are not $SL \otimes SL$ equivalent to projection operators, however we cannot exclude it. Whether or not such an equivalence exists in general, and if it does, whether or not the states proportional to projection operators fit into the generalized UPB construction, might be further illuminated if analytical proofs for the case of systems of dimension 3×3 .

Another subject for further study is the relationship between PPT states and product vectors in the kernel of such states. This is interesting because

a feature of generic lowest rank extremal PPT states seems to be that they contain a finite number of product vectors in their kernel. We examined the constraints product vectors place on the density matrix to which they are orthogonal in the case of systems of dimension 3×3 and 4×4 in Paper IV, but only in the 3×3 case are we able to explicitly identify the constraints on the product vectors such that the density matrix is PPT.

With further analysis of product vectors in the kernel of PPT states we might be able to solve some of the aforementioned problems. For instance, PPT states of rank less than $N_A + N_B - 2$ will typically have an infinite set of different product vectors in their kernel, and one can wonder whether this is incompatible with extremality. At least so far as our results are concerned, we have never observed an extremal PPT state with an infinite number of different product vectors in their kernel except for the rank 1 states, but these are separable.

Another topic for further research is the study of surfaces of PPT states under various conditions. For instance, it gives us new means of studying the properties of generic density matrices. By numerical integration we can move along surfaces of PPT states with either specified ranks or specified ranks and fixed image for the density matrix, as shown in Paper IV. The rank $(5, 5)$ states in systems of dimension 3×3 obtained through perturbations of states of rank $(4, 4)$ can be taken as starting points from which we might be able to access all PPT states of rank $(5, 5)$ by integrating along the surface of states with this rank. Controlled perturbations such as these could possibly also be used to extract more information about the constraints imposed on the lowest rank extremal PPT states by product vectors in their kernel in higher dimensional systems.

Lastly, it would be interesting to try to further optimize the numerical tools we have already developed, in order to map out properties of generic states in even more higher dimensional systems. This would for instance allow us to further study numerically the increasing difference between the lower bounds in eqs. (5.1) and (5.2). Optimization of the tools could imply both optimization of the code in particular, but also recoding in C or C++. Further analytical study might also reveal better algorithms that could be used.

Describing physics in geometric terms is a time honored tradition and has proven to be very useful, such as Einstein's general theory of relativity and gauge theories of particle physics. A geometrical approach to the study of entanglement is a natural road to take, and will surely play a vital role in improving our understanding of entanglement and entangled states.

Bibliography

- [1] Michał Horodecki, Paweł Horodecki, and Ryszard Horodecki. Mixed-state entanglement and distillation: Is there a “bound” entanglement in nature? *Phys. Rev. Lett.*, 80(24):5239–5242, Jun 1998.
- [2] Ryszard Horodecki, Paweł Horodecki, Michał Horodecki, and Karol Horodecki. Quantum entanglement. *Rev. Mod. Phys.*, 81(2):865–942, Jun 2009.
- [3] Asher Peres. Separability criterion for density matrices. *Phys. Rev. Lett.*, 77(8):1413–1415, Aug 1996.
- [4] Paweł Horodecki. Separability criterion and inseparable mixed states with positive partial transposition. *Phys. Lett. A*, 232(5):333 – 339, 1997.
- [5] Dagmar Bruß and Asher Peres. Construction of quantum states with bound entanglement. *Phys. Rev. A*, 61(3):030301, Feb 2000.
- [6] Dariusz Chruściński and Andrzej Kossakowski. Circulant states with positive partial transpose. *Phys. Rev. A*, 76(3):032308, Sep 2007.
- [7] Marco Piani. Class of bound entangled states of $n + n$ qubits revealed by nondecomposable maps. *Phys. Rev. A*, 73(1):012345, Jan 2006.
- [8] Géza Tóth and Otfried Gühne. Entanglement and permutational symmetry. *Phys. Rev. Lett.*, 102(17):170503, May 2009.
- [9] Heinz-Peter Breuer. Optimal entanglement criterion for mixed quantum states. *Phys. Rev. Lett.*, 97(8):080501, Aug 2006.
- [10] Kil-Chan Ha, Seung-Hyeok Kye, and Young Sung Park. Entangled states with positive partial transposes arising from indecomposable positive linear maps. *Phys. Lett. A*, 313(3):163 – 174, 2003.

-
- [11] Lieven Clarisse. Construction of bound entangled edge states with special ranks. *Phys. Lett. A*, 359(6):603 – 607, 2006.
- [12] Marek Kuś and Karol Życzkowski. Geometry of entangled states. *Phys. Rev. A*, 63(3):032307, Feb 2001.
- [13] Arthur O. Pittenger and Morton H. Rubin. Geometry of entanglement witnesses and local detection of entanglement. *Phys. Rev. A*, 67(1):012327, Jan 2003.
- [14] Jon Magne Leinaas, Jan Myrheim, and Eirik Ovrum. Geometrical aspects of entanglement. *Phys. Rev. A*, 74(1):012313, Jul 2006.
- [15] I. Bengtsson and K. Życzkowski. *Geometry of quantum states: an introduction to quantum entanglement*. Cambridge Univ Pr, 2006.
- [16] J. M. Leinaas, J. Myrheim, and E. Ovrum. Extreme points of the set of density matrices with positive partial transpose. *Phys. Rev. A*, 76(3):034304, Sep 2007.
- [17] Eirik Ovrum. *Geometry of entanglement and quantum simulators*. PhD thesis, University of Oslo, 2007.
- [18] A. Einstein, B. Podolsky, and N. Rosen. Can quantum-mechanical description of physical reality be considered complete? *Phys. Rev.*, 47(10):777–780, May 1935.
- [19] D.J. Griffiths. *Introduction to quantum mechanics*. Prentice Hall, 2005.
- [20] Alain Aspect, Philippe Grangier, and Gérard Roger. Experimental tests of realistic local theories via bell’s theorem. *Phys. Rev. Lett.*, 47(7):460–463, Aug 1981.
- [21] Alain Aspect, Philippe Grangier, and Gérard Roger. Experimental realization of einstein-podolsky-rosen-bohm gedankenexperiment: A new violation of bell’s inequalities. *Phys. Rev. Lett.*, 49(2):91–94, Jul 1982.
- [22] Alain Aspect, Jean Dalibard, and Gérard Roger. Experimental test of bell’s inequalities using time-varying analyzers. *Phys. Rev. Lett.*, 49(25):1804–1807, Dec 1982.
- [23] W. Tittel, J. Brendel, B. Gisin, T. Herzog, H. Zbinden, and N. Gisin. Experimental demonstration of quantum correlations over more than 10 km. *Phys. Rev. A*, 57(5):3229–3232, May 1998.

- [24] W. Tittel, J. Brendel, H. Zbinden, and N. Gisin. Violation of bell inequalities by photons more than 10 km apart. *Phys. Rev. Lett.*, 81(17):3563–3566, Oct 1998.
- [25] Gregor Weihs, Thomas Jennewein, Christoph Simon, Harald Weinfurter, and Anton Zeilinger. Violation of bell’s inequality under strict einstein locality conditions. *Phys. Rev. Lett.*, 81(23):5039–5043, Dec 1998.
- [26] T.P. Simon Gr
”oblacher, C. Rainer Kaltenbaek, et al. An experimental test of non-local realism. *Nature*, 446(7138):871–875, 2007.
- [27] D. Salart, A. Baas, J. A. W. van Houwelingen, N. Gisin, and H. Zbinden. Spacelike separation in a bell test assuming gravitationally induced collapses. *Phys. Rev. Lett.*, 100(22):220404, Jun 2008.
- [28] M. Ansmann, H. Wang, R.C. Bialczak, M. Hofheinz, E. Lucero, M. Neeley, AD O’Connell, D. Sank, M. Weides, J. Wenner, et al. Violation of Bell’s inequality in Josephson phase qubits. *Nature*, 461(7263):504–506, 2009.
- [29] R. García-Patrón, J. Fiurásek, N. J. Cerf, J. Wenger, R. Tualle-Brouri, and Ph. Grangier. Proposal for a loophole-free bell test using homodyne detection. *Phys. Rev. Lett.*, 93(13):130409, Sep 2004.
- [30] M. Stobinska, P. Horodecki, R. Chhajlany, and R. Horodecki. Loophole-free Bell inequality test via preselected macro-qubit entanglement. In *Conference on Lasers and Electro-Optics*. Optical Society of America, 2010.
- [31] Se-Wan Ji, Jaewan Kim, Hai-Woong Lee, M. S. Zubairy, and Hyunchul Nha. Loophole-free bell test for continuous variables via wave and particle correlations. *Phys. Rev. Lett.*, 105(17):170404, Oct 2010.
- [32] L.M.K. Vandersypen, M. Steffen, G. Breyta, C.S. Yannoni, M.H. Sherwood, and I.L. Chuang. Experimental realization of Shor’s quantum factoring algorithm using nuclear magnetic resonance. *Nature*, 414(6866):883–887, 2001.
- [33] Charles H. Bennett and Stephen J. Wiesner. Communication via one- and two-particle operators on einstein-podolsky-rosen states. *Phys. Rev. Lett.*, 69(20):2881–2884, Nov 1992.

- [34] Charles H. Bennett, Gilles Brassard, Claude Crépeau, Richard Jozsa, Asher Peres, and William K. Wootters. Teleporting an unknown quantum state via dual classical and einstein-podolsky-rosen channels. *Phys. Rev. Lett.*, 70(13):1895–1899, Mar 1993.
- [35] Dominic Mayers. Quantum key distribution and string oblivious transfer in noisy channels. In Neal Koblitz, editor, *Advances in Cryptology ? CRYPTO ?96*, volume 1109 of *Lecture Notes in Computer Science*, pages 343–357. Springer Berlin / Heidelberg.
- [36] Hoi-Kwong Lo and H. F. Chau. Unconditional Security of Quantum Key Distribution over Arbitrarily Long Distances. *Science*, 283(5410):2050–2056, 1999.
- [37] Peter W. Shor and John Preskill. Simple proof of security of the bb84 quantum key distribution protocol. *Phys. Rev. Lett.*, 85(2):441–444, Jul 2000.
- [38] C. H. Bennett and G. Brassard. Quantum cryptography: Public-key distribution and coin tossing. In *Proceedings of IEEE International Conference on Computers, Systems and Signal Processing*, pages 175–179, 1984.
- [39] L. Lydersen, C. Wiechers, C. Wittmann, D. Elser, J. Skaar, and V. Makarov. Hacking commercial quantum cryptography systems by tailored bright illumination. *Nature Photonics*, 2010.
- [40] M.A. Nielsen and I.L. Chuang. *Quantum computation and quantum information*. Cambridge Univ Pr, 2000.
- [41] PA Hiskett, D. Rosenberg, CG Peterson, RJ Hughes, S. Nam, AE Lita, AJ Miller, and JE Nordholt. Long-distance quantum key distribution in optical fibre. *New Journal of Physics*, 8:193, 2006.
- [42] R. Ursin, F. Tiefenbacher, T. Schmitt-Manderbach, H. Weier, T. Scheidl, M. Lindenthal, B. Blauensteiner, T. Jennewein, J. Perdigues, P. Trojek, et al. Entanglement-based quantum communication over 144 km. *Nature Physics*, 3(7):481–486, 2007.
- [43] Tobias Schmitt-Manderbach, Henning Weier, Martin Fürst, Rupert Ursin, Felix Tiefenbacher, Thomas Scheidl, Josep Perdigues, Zoran Sodnik, Christian Kurtsiefer, John G. Rarity, Anton Zeilinger, and Harald

- Weinfurter. Experimental demonstration of free-space decoy-state quantum key distribution over 144 km. *Phys. Rev. Lett.*, 98(1):010504, Jan 2007.
- [44] T. Scheidl, R. Ursin, A. Fedrizzi, S. Ramelow, X.S. Ma, T. Herbst, R. Prevedel, L. Ratschbacher, J. Kofler, T. Jennewein, et al. Feasibility of 300 km quantum key distribution with entangled states. *New Journal of Physics*, 11:085002, 2009.
- [45] Michał Horodecki, Paweł Horodecki, and Ryszard Horodecki. Separability of mixed states: necessary and sufficient conditions. *Phys. Lett. A*, 223(1-2):1 – 8, 1996.
- [46] Paweł Horodecki, Michał Horodecki, and Ryszard Horodecki. Bound entanglement can be activated. *Phys. Rev. Lett.*, 82(5):1056–1059, Feb 1999.
- [47] W. Dür, J. I. Cirac, and R. Tarrach. Separability and distillability of multiparticle quantum systems. *Phys. Rev. Lett.*, 83(17):3562–3565, Oct 1999.
- [48] W. Dür and J. I. Cirac. Classification of multiqubit mixed states: Separability and distillability properties. *Phys. Rev. A*, 61(4):042314, Mar 2000.
- [49] W. Dür and J. I. Cirac. Activating bound entanglement in multiparticle systems. *Phys. Rev. A*, 62(2):022302, Jul 2000.
- [50] Peter W. Shor, John A. Smolin, and Ashish V. Thapliyal. Superactivation of bound entanglement. *Phys. Rev. Lett.*, 90(10):107901, Mar 2003.
- [51] Somshubhro Bandyopadhyay, Indrani Chattopadhyay, Vwani Roychowdhury, and Debasis Sarkar. Bell-correlated activable bound entanglement in multiqubit systems. *Phys. Rev. A*, 71(6):062317, Jun 2005.
- [52] Lluís Masanes. All bipartite entangled states are useful for information processing. *Phys. Rev. Lett.*, 96(15):150501, Apr 2006.
- [53] Lluís Masanes. Useful entanglement can be extracted from all nonseparable states. *Journal of Mathematical Physics*, 49(2):022102, 2008.
- [54] A. Jamiolkowski. Linear transformations which preserve trace and positive semidefiniteness of operators. *Reports on Mathematical Physics*, 3(4):275 – 278, 1972.

-
- [55] Man-Duen Choi. Completely positive linear maps on complex matrices. *Linear Algebra and its Applications*, 10(3):285 – 290, 1975.
- [56] Charles H. Bennett, Sandu Popescu, Daniel Rohrlich, John A. Smolin, and Ashish V. Thapliyal. Exact and asymptotic measures of multipartite pure-state entanglement. *Phys. Rev. A*, 63(1):012307, Dec 2000.
- [57] G. Vidal. Entanglement monotones. *Journal of Modern Optics*, 47(2):355–376, 2000.
- [58] Hoi-Kwong Lo and Sandu Popescu. Concentrating entanglement by local actions: Beyond mean values. *Phys. Rev. A*, 63(2):022301, Jan 2001.
- [59] W. Dür, G. Vidal, and J. I. Cirac. Three qubits can be entangled in two inequivalent ways. *Phys. Rev. A*, 62(6):062314, Nov 2000.
- [60] Frank Verstraete, Jeroen Dehaene, and Bart De Moor. Normal forms and entanglement measures for multipartite quantum states. *Phys. Rev. A*, 68(1):012103, Jul 2003.
- [61] Maciej Lewenstein and Anna Sanpera. Separability and entanglement of composite quantum systems. *Phys. Rev. Lett.*, 80(11):2261–2264, Mar 1998.
- [62] Anna Sanpera, Rolf Tarrach, and Guifré Vidal. Local description of quantum inseparability. *Phys. Rev. A*, 58(2):826–830, Aug 1998.
- [63] B. Kraus, J. I. Cirac, S. Karnas, and M. Lewenstein. Separability in $2 \times n$ composite quantum systems. *Phys. Rev. A*, 61(6):062302, May 2000.
- [64] Paweł Horodecki, Maciej Lewenstein, Guifré Vidal, and Ignacio Cirac. Operational criterion and constructive checks for the separability of low-rank density matrices. *Phys. Rev. A*, 62(3):032310, Aug 2000.
- [65] M. Lewenstein, B. Kraus, J. I. Cirac, and P. Horodecki. Optimization of entanglement witnesses. *Phys. Rev. A*, 62(5):052310, Oct 2000.
- [66] M. Lewenstein, B. Kraus, P. Horodecki, and J. I. Cirac. Characterization of separable states and entanglement witnesses. *Phys. Rev. A*, 63(4):044304, Mar 2001.

-
- [67] Erik Alfsen and Fred Shultz. Unique decompositions, faces, and automorphisms of separable states. *Journal of Mathematical Physics*, 51(5):052201, 2010.
- [68] Charles H. Bennett, David P. DiVincenzo, Tal Mor, Peter W. Shor, John A. Smolin, and Barbara M. Terhal. Unextendible product bases and bound entanglement. *Phys. Rev. Lett.*, 82(26):5385–5388, Jun 1999.

Part II

Papers

Numerical studies of entangled positive-partial-transpose states in composite quantum systems

Jon Magne Leinaas,¹ Jan Myrheim,² and Per Øyvind Sollid¹¹*Department of Physics, University of Oslo, N-0316 Oslo, Norway*²*Department of Physics, Norwegian University of Science and Technology, N-7491 Trondheim, Norway*

(Received 19 February 2010; published 21 June 2010)

We report here on the results of numerical searches for PPT states in a series of bipartite quantum systems of low dimensions. PPT states are represented by density matrices that remain positive semidefinite under partial transposition with respect to one of the subsystems, and our searches are for such states with specified ranks for the density matrix and its partial transpose. For a series of different ranks extremal PPT states and nonextremal entangled PPT states have been found. The results are listed in tables and charted in diagrams. Comparison of the results for systems of different dimensions reveals several regularities. We discuss lower and upper bounds on the ranks of extremal PPT states.

DOI: [10.1103/PhysRevA.81.062329](https://doi.org/10.1103/PhysRevA.81.062329)

PACS number(s): 03.67.Mn, 02.40.Ft, 03.65.Ud

I. INTRODUCTION

In recent years the study of entanglement in composite quantum systems has taken several different directions. One direction is the study of entanglement from a geometrical point of view [1–5]. This has led to questions concerning the relations between different convex sets of Hermitian matrices, where the full set of density matrices is one of them. The main motivation for the interest in these convex sets is the information they give about the general question of how to identify entanglement in a composite system. Unless the system is in a *pure* quantum state, the knowledge of the corresponding density matrix does not readily disclose the state as being entangled or nonentangled, and the complexity of the corresponding problem, known as the separability problem, increases rapidly with the dimensionality of the quantum system [6].

The density operators are the normalized, positive semidefinite Hermitian operators that act on the Hilbert space of the quantum system, and in the following we shall use the notation \mathcal{D} for this set. Another convex set is the set of *nonentangled* states, usually referred to as separable states, and we use \mathcal{S} as notation for this subset of \mathcal{D} . Since the set of entangled states is the complement to the set of separable states, within the full set of density matrices, the question of identifying the entangled states can be reformulated as the question of finding the boundaries of the convex set of separable states \mathcal{S} .

For a bipartite system, there is furthermore a convex subset of the density matrices, here referred to as \mathcal{P} , which is closely related to the set of separable matrices. This is the subset of density matrices that remain positive semidefinite under the operation of partial transposition of the matrix with respect to one of the two subsystems of the composite system. In short, these states are called PPT states. A necessary condition for separability of a density matrix is that it remains positive under partial transposition, and thus the set of separable states is included in the set of PPT states, $\mathcal{S} \subset \mathcal{P}$ [7]. For bipartite systems of dimensions 2×2 and 2×3 , the two sets are in fact identical [8], but in higher dimensions the separable states form a proper subset of the set of PPT states. However, numerical studies have shown that for systems of low dimensions, such as the 3×3 system, the set \mathcal{P} is only slightly larger than \mathcal{S} [4,9].

The necessary condition that the separable density matrices remain positive under partial transposition is important since this condition is easy to check. It effectively reduces the

separability problem to a question of identifying the PPT states that are entangled, that is, that do not belong to \mathcal{S} . These states are also interesting for a separate reason, since they are known to carry *bound* entanglement, which means that the entanglement is not available through entanglement distillation, a process where entanglement of mixed states is transferred to a set of pure quantum states [10].

In the literature, there are several studies of states with bound entanglement, mostly based on the construction of specific examples. One approach has been to construct classes of PPT states with special symmetries [11–15]. Other examples have been obtained through the study of positive maps or entanglement witnesses, which on several occasions has led to constructions of classes of entangled PPT states witnessed by specific maps [16–18]. The violation of the range criterion by entangled PPT states has also given rise to several examples through the study of unextendible product bases [19] and edge states [20].

In a previous publication [9] we focused particularly on *extremal* PPT states. These are the states that define the full set \mathcal{P} of PPT states, in the sense that all other PPT states can be expressed as convex combinations of these states. The set \mathcal{P} share with the set of separable states \mathcal{S} the pure product states as extremal states, but in addition, \mathcal{P} has other extremal states that are not fully known. These extremal states are special examples of entangled PPT states. In Ref. [9] we have presented a criterion for identifying extremal PPT states, and we have there described an algorithm to systematically search for such states. By use of the method, a list of extremal PPT states was found and presented for a series of low-dimensional systems.

In the present article we follow up the study of entangled PPT states in [9] by use of numerical methods. The method described here is different from that of the publication [9] in the sense that it does not make use of direct searches for extremal PPT states, but rather of searches for PPT states with specified ranks for the density matrix and for its partial transpose. It is therefore also different from most of the other papers cited earlier in the sense that it does not aim at states with particular properties, apart from specification of the ranks. By systematically searching through matrices of different ranks, we have obtained in this way, for a series of low-dimensional systems, a list of low-rank PPT states, many of which are identified as extremal and others as nonextremal entangled

PPT states. These results supplement those of [9], where only a limited set of different types of extremal states were identified.

The results we have obtained for different low-dimensional systems show certain regularities. In particular we find extremal PPT states for essentially all ranks of the density operator and its partial transpose when these lie between an upper and a lower limit. We suggest general expressions for these limits and relate them to generic properties of the image and kernel of the density matrices. A special focus is on the properties of the extremal PPT states of *lowest* rank. In a separate publication [21] we follow up these results by a specific study of the lowest rank extremal PPT states of the 3×3 system, which are also identical to the lowest rank *entangled* PPT states in any dimension [22] (see also [23]). As discussed there, these states can be classified by a small number of parameters, and an interesting question is whether a similar classification can be given for other extremal PPT states.

II. THE METHOD

We consider a bipartite quantum system with Hilbert space $\mathcal{H} = \mathcal{H}_A \otimes \mathcal{H}_B$, where A and B label the two subsystems, and \mathcal{H}_A and \mathcal{H}_B are of dimensions N_A and N_B , respectively. The density operators ρ satisfy the normalization condition $\text{Tr} \rho = 1$, but often it is convenient to give up this condition and rather consider all density operators that differ by a normalization factor to be equivalent. The set of normalized density operators we refer to as \mathcal{D} , while $\mathcal{K}(\mathcal{D})$ is the positive cone of nonnormalized density operators. A similar notation is used for other subsets of Hermitian operators. Partial transposition is the operation on density operators that corresponds to transposition of indices of one of the subsystems, $\rho_{ij}^B \rightarrow \rho_{ji}^B$ (here chosen as subsystem B). For density operators of the full, composite system, we refer to this operation as $\rho \rightarrow \rho^P$, and it maps the convex set \mathcal{D} into another convex set denoted \mathcal{D}^P . The operation will depend on the choice of subsystem (A or B) and on the choice of basis in the corresponding Hilbert space. However, the distinction between these different choices is of no importance for our discussion. We note in particular that the mapping of sets $\mathcal{D} \rightarrow \mathcal{D}^P$ is independent of the choice. The set of PPT states is defined as the section $\mathcal{P} = \mathcal{D} \cap \mathcal{D}^P$, which means that it consists of the positive semidefinite operators that remain positive semidefinite under partial transposition.

A. Searching for density operators of given ranks

The Hermitian matrices define a real vector space, and it is convenient to introduce a complete set of matrices that are orthonormal with respect to the trace norm

$$\text{Tr}(M_i M_j) = \delta_{ij}. \quad (1)$$

A general Hermitian matrix M is then described as a vector \mathbf{x} with real components

$$x_i = \text{Tr}(M M_i). \quad (2)$$

For a composite system of Hilbert space dimension $N = N_A N_B$, the vector space of Hermitian matrices is of dimension $N^2 = N_A^2 N_B^2$.

The algorithm we use to find PPT states ρ with specified ranks (m, n) for ρ and ρ^P is the following. We expand ρ as

$$\rho = \rho(\mathbf{x}) = \sum_i x_i M_i. \quad (3)$$

The eigenvalues of ρ we write as $\lambda_i = \lambda_i(\mathbf{x})$, with $\lambda_i^P = \lambda_i^P(\mathbf{x})$ as the eigenvalues of the partially transposed matrix ρ^P . The eigenvalues of each matrix are listed in decreasing order, and for the density matrix that we are searching for, a certain number of the eigenvalues should vanish. Thus we want to have $\lambda_k = 0$ for $k = m + 1, \dots, N$ and $\lambda_k^P = 0$ for $k = n + 1, \dots, N$. The eigenvalues that should vanish we treat as components of a new vector $\boldsymbol{\mu}$ so that

$$\boldsymbol{\mu} = [\lambda_{m+1}, \lambda_{m+2}, \dots, \lambda_N, \lambda_{n+1}^P, \lambda_{n+2}^P, \dots, \lambda_N^P], \quad (4)$$

and the problem is then to find the point \mathbf{x} which solves the equation $\boldsymbol{\mu}(\mathbf{x}) = \mathbf{0}$.

We choose a starting point \mathbf{x} such that $\rho = \rho(\mathbf{x})$ as well as ρ^P are positive semidefinite matrices (it is not strictly necessary that the positivity conditions hold to begin with since they will automatically hold for the solution we obtain in the end). If the equation $\boldsymbol{\mu}(\mathbf{x}) = \mathbf{0}$ is not already solved, we search for a better approximate solution $\mathbf{x}' = \mathbf{x} + \Delta\mathbf{x}$. The linear approximation to the Taylor expansion gives an equation for $\Delta\mathbf{x}$:

$$\boldsymbol{\mu}(\mathbf{x}) + (\Delta\mathbf{x} \cdot \nabla)\boldsymbol{\mu}(\mathbf{x}) = \mathbf{0}. \quad (5)$$

In matrix form the equation can be written as

$$\mathbf{B} \Delta\mathbf{x} = -\boldsymbol{\mu}, \quad (6)$$

with $B_{ij} = \partial\mu_i / \partial x_j$. It implies another equation,

$$\mathbf{A} \Delta\mathbf{x} = \mathbf{b}, \quad (7)$$

where $\mathbf{A} = \mathbf{B}^T \mathbf{B}$ is a positive, real symmetric matrix and where $\mathbf{b} = -\mathbf{B}^T \boldsymbol{\mu}$. We use the conjugate gradient method [24] to solve the last equation for $\Delta\mathbf{x}$. The conjugate gradient method is useful because it works even if \mathbf{A} is singular. Next, we replace \mathbf{x} by $\mathbf{x}' = \mathbf{x} + \Delta\mathbf{x}$ and, if $\boldsymbol{\mu}(\mathbf{x}') \neq \mathbf{0}$, iterate in order to get successively better approximate solutions. If the method converges, we reach a value of \mathbf{x} where $\boldsymbol{\mu}(\mathbf{x}) = \mathbf{0}$ within machine precision, where the iteration is stopped.

The matrix \mathbf{B} is computed in each iteration by the first-order perturbation formula

$$\frac{\partial\lambda_k}{\partial x_j} = \psi_k^\dagger \frac{\partial\rho}{\partial x_j} \psi_k = \psi_k^\dagger M_j \psi_k, \quad k = m + 1, \dots, N_A, \quad (8)$$

where ψ_k is the eigenvector of ρ with eigenvalue λ_k . A similar formula is used for the derivatives of λ_k^P . Since these formulas are valid in first-order *nondegenerate* perturbation theory, this raises a question concerning convergence of the method at a point of degeneracy. However, in practice, we find that the method works well when the dimension of the system is not too large.

Note that, by the way the method works, all the states we find are PPT. That is the case since in the iterative search for a state with a certain number of vanishing eigenvalues for ρ and ρ^P , the eigenvalues are always ordered in such a way that the *lowest* eigenvalues are forced to be zero. This means that both the density matrix and its partial transpose will be positive semidefinite.

We have applied the method to a series of low-dimensional systems, and the results are listed in Tables I–IV and in the figures in the next section. The convergence of the method slows down with increase of the Hilbert space dimension N , and in the form we have implemented the algorithm, the practical limit of the dimension is $N \lesssim 20$. For the systems we have studied, the method has been used repeatedly with different starting points for each choice of ranks (m, n) . In most cases the iteration converges, but in some cases that does not happen, and these iterations are then simply aborted. For some values of m and n we do not find any density matrix with the given ranks, and the method will then in most cases converge to a density matrix with lower rank for either ρ or ρ^P , or both. We have not imposed any restriction to avoid that, so in practice the method searches for density matrices of ranks equal to or lower than the specified values (m, n) .

Since we have made no particular effort to optimize our code for speed, we do not discuss here details of the implementation such as convergence rates and execution times. One interesting detail, however, is the numerical accuracy of the algorithm. For $N \lesssim 20$ it is very good. In determining the ranks of the density matrices and the dimensions of the faces \mathcal{F} (see later discussion), we need to decide whether eigenvalues are equal to or different from either 0 or 1, and in general we obtain these values within machine precision of 10^{-16} . There is most of the time several orders of magnitude difference between small but nonzero eigenvalues, and eigenvalues that are zero within the machine precision.

B. Determining the dimension of the face of $\mathcal{K}(\mathcal{P})$

For each density matrix ρ found in the searches, we have evaluated and listed certain properties. Among these are the *local ranks* (r_A, r_B) of the density matrices, defined with respect to the subsystems A and B . These are the ranks of the reduced density matrices ρ_A and ρ_B . The most interesting cases are those where the density matrices have full local ranks $(r_A, r_B) = (N_A, N_B)$. If that is not the case the density matrix can be viewed as belonging to a composite system of lower dimension, which is embedded in the higher-dimensional system.

We have also evaluated and listed the dimension of the face \mathcal{F} of the convex cone $\mathcal{K}(\mathcal{P})$ to which ρ belongs. The extreme points of \mathcal{P} correspond to one-dimensional, positive rays in $\mathcal{K}(\mathcal{P})$ and are consequently characterized by $\dim \mathcal{F} = 1$. Therefore the extremal states can be identified in the tables as the density matrices with this minimal value for the dimension of the face.

The method we use to evaluate $\dim \mathcal{F}$ has earlier been described in [9]. It is based on the fact that the face \mathcal{F} to which ρ belongs can be viewed as the section between a face (or all) of $\mathcal{K}(\mathcal{D})$ and a face (or all) of $\mathcal{K}(\mathcal{D}^P)$. This means that $\rho = \rho(\mathbf{x})$ satisfies two equations:

$$\mathbf{P}\mathbf{x} = \mathbf{x}, \quad \tilde{\mathbf{Q}}\mathbf{x} = \mathbf{x}, \quad (9)$$

with \mathbf{P} as the orthogonal projection on the subspace in the vector space of Hermitian matrices defined by the face of $\mathcal{K}(\mathcal{D})$ and $\tilde{\mathbf{Q}}$ as the projection on the subspace defined by the face of $\mathcal{K}(\mathcal{D}^P)$. Note that as orthogonal projections, \mathbf{P} and $\tilde{\mathbf{Q}}$ are real and symmetric $N^2 \times N^2$ matrices. The method for

computing these matrices for a given density operator ρ is described in [9].

As follows from the preceding equations, the section between the subspaces defined by \mathbf{P} and $\tilde{\mathbf{Q}}$ is spanned by the eigenvectors of the composite, real symmetric matrix $\mathbf{P}\tilde{\mathbf{Q}}\mathbf{P}$ (or alternatively $\tilde{\mathbf{Q}}\mathbf{P}\tilde{\mathbf{Q}}$), with eigenvalues equal to 1. This implies that $\dim \mathcal{F}$ can be determined simply by diagonalizing the composite matrix and counting the number of such eigenvalues.

Since we compute the eigenvalues with machine precision, there is an unambiguous distinction between eigenvalues that are equal to or different from 1. For example, an eigenvalue of 0.999 differs from 1 by about 13 orders of magnitude.

As a consequence of the way \mathcal{F} is constructed, there is a geometrical constraint on the possible values of $\dim \mathcal{F}$ for given ranks (m, n) of ρ and ρ^P [9]. Thus, the faces of $\mathcal{K}(\mathcal{D})$ and $\mathcal{K}(\mathcal{D}^P)$ are of dimensions m^2 and n^2 , respectively, and therefore the face of $\mathcal{K}(\mathcal{D})$ is specified by $N^2 - m^2$ linear constraints, and similarly the face of $\mathcal{K}(\mathcal{D}^P)$ is specified by $N^2 - n^2$ linear constraints. If these sets of constraints are independent, they determine the dimension of the section \mathcal{F} as $\dim \mathcal{F} = m^2 + n^2 - N^2$. However, if the two sets of constraints are not fully independent, the dimension of the section is larger. Therefore the following inequality is generally valid:

$$\dim \mathcal{F} \geq m^2 + n^2 - N^2. \quad (10)$$

For extremal PPT states with $\dim \mathcal{F} = 1$, this gives an upper bound to the ranks of ρ and ρ^P :

$$m^2 + n^2 \leq N^2 + 1 \quad (\text{extremality}). \quad (11)$$

C. Counting the number of product vectors

For each density matrix ρ , we have examined the image ($\text{Im } \rho$) and kernel ($\text{Ker } \rho$) for the presence of product vectors, and the numbers of such vectors are listed. The method we use to search for product vectors in a given subspace of \mathcal{H} is described in some detail in Appendix A. To briefly outline the approach, let us assume that we search for product vectors in $\text{Im } \rho$, with \mathbf{P} as the orthogonal projection on this subspace. The vectors should satisfy the condition

$$(\mathbb{1} - \mathbf{P})(\phi \otimes \chi) = 0, \quad (12)$$

and this can be reexpressed as a minimization problem, which we in Appendix A refer to as a *double eigenvalue problem*. The solutions of Eq. (12) are the minima of the function

$$f = (\phi^\dagger \otimes \chi^\dagger)(\mathbb{1} - \mathbf{P})(\phi \otimes \chi), \quad (13)$$

with $f = 0$, and such minima can be found by the iterative approach described in Appendix A. By varying the starting point of the iteration, different minima can be identified, and by systematically searching for minima of f and of

$$1 - f = (\phi \otimes \chi)^\dagger \mathbf{P}(\phi \otimes \chi), \quad (14)$$

we have reproduced and counted the product vectors in $\text{Im } \rho$ and $\text{Ker } \rho$ for every density matrix found in the numerical searches. In the tables the number of product vectors and

the number of *linearly independent* product vectors are listed for $\text{Im } \rho$ and $\text{Ker } \rho$. The same type of iterative method for minimization over product vectors has been applied in the separability test that is described in the next section.

III. DISCUSSION OF THE RESULTS

A. Diagrammatic representation

The results of the searches are tabulated in Appendix B and are also included in condensed form in the subsequent text as Figs. 1–4. The variables of the two axes of the figures are the ranks m of ρ and n of ρ^P . The small open and filled circles in the figures indicate the ranks for states that are found in the numerical searches. As discussed earlier, all the states produced in this way are PPT. The filled (red) circles represent *extremal* PPT states with full local ranks, while the open circles represent nonextremal PPT states, either separable or entangled. Note that all diagrams are symmetric under the interchange $m \leftrightarrow n$ since in the search for PPT states there is no intrinsic difference between ρ and ρ^P .

The states we find by use of our method we refer to as *typical* for the chosen ranks (m, n) . For some ranks, there will exist states with untypical characteristics, which we do not find in the searches, presumably due to low dimensionality of the set of such states. We note, in particular, when we compare

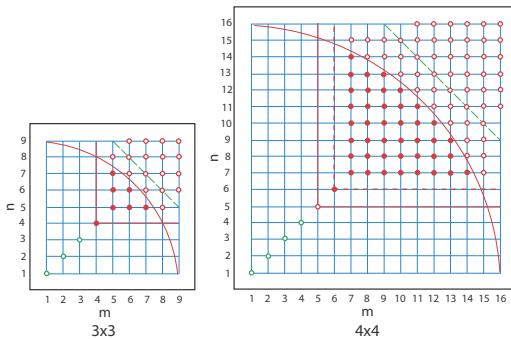


FIG. 1. (Color online) Diagrams for the ranks of PPT states in the composite systems of dimensions 3×3 and 4×4 . The coordinates m and n on the axes are the ranks of the density matrix ρ and its partial transpose ρ^P . States found by use of the numerical method discussed in the text are indicated by small circles or dots (filled circles). The green circles in the lower left corner indicate ranks for a special set of separable states, the red dots correspond to extremal PPT states, and the red circles in the upper right corner correspond to nonextremal PPT states. Ranks $(5, 5)$ in the 4×4 system is an exception; there we find both separable states and a special type of entangled, nonextremal PPT state. The unbroken, horizontal, and vertical straight red lines show the lower bound for entangled PPT states with full local ranks, the similar dashed red lines show our conjectured lower bound for extremal PPT states with full local ranks, and the red circular arcs show the upper bound for extremal PPT states. The dashed green 45° straight lines show the upper bound for the application of the separability criterion described in the text. For all ranks indicated by red circles up to and on this line (and above the circular arc), the corresponding states are always found to be entangled PPT states.

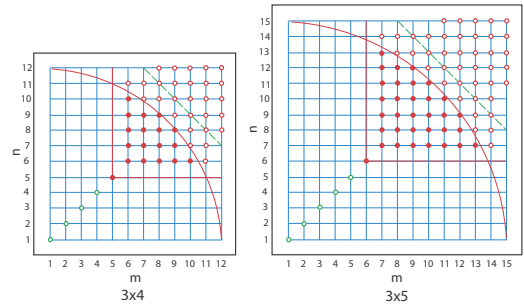


FIG. 2. (Color online) Diagrams for the ranks of PPT states in the composite systems of dimensions 3×4 and 3×5 . States found by use of the numerical method discussed in the text are indicated by the small circles or dots. Also here entangled PPT states are found for all ranks indicated by red circles up to and on the dashed green line. For further explanation of the diagrams, see Fig. 1.

the diagrams of the 3×3 and 4×4 systems, that most of the states of the 3×3 system are not seen in the diagram of the 4×4 system. However, we know that all the states of the lower-dimensional system should be present in the form of states with less than full local ranks.

For most choices of ranks (m, n) the density matrices that we find in repeated searches with different initial conditions are all found to have identical characteristics in the form of the parameters listed in the tables. There is only a small number of exceptions where density matrices with different characteristics but equal ranks (m, n) have been found. These are all listed in the tables.

B. Different groups of PPT states

There is a clear similarity between Figs. 1–4, with the states for each figure being separated into groups with different characteristics. One group consists of the low-rank states with $m = n \leq \max\{N_A, N_B\}$. These low-rank states, which are represented by the series of green circles in the figures, are all separable, with equal ranks for ρ and ρ^P . As shown in

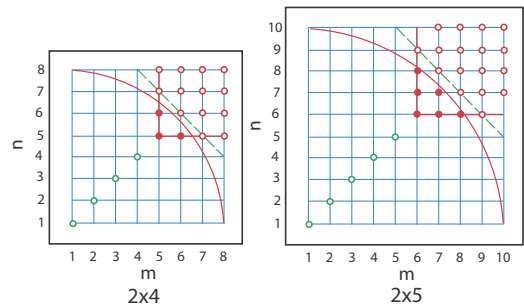


FIG. 3. (Color online) Diagrams for the ranks of PPT states in the composite systems of dimensions 2×4 and 2×5 . For explanations of the diagrams, see Figs. 1 and 2. Note that the results for the 2×4 system agree with the fact that the only possible ranks for extremal states in 2×4 are $(5, 5)$, $(6, 5)$, and $(5, 6)$ [9,25].

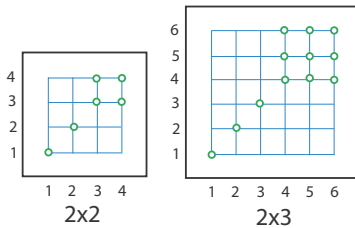


FIG. 4. (Color online) Diagrams for the ranks of PPT states in the composite systems of dimensions 2×2 and 2×3 . For these systems, all PPT states are separable, but the distinction between the special set of states with low, symmetric ranks $m = n$ and the set of states with higher, asymmetric ranks is similar to what is found in the higher-dimensional systems.

the tables, all the corresponding density matrices ρ contain a number of product vectors in their image which is equal to their rank m . In fact, it is obvious that one can construct such states by taking randomly a small number of pure product states and forming a convex combination of these. Such a sequence of separable states can be defined in all dimensions, and they are not of further interest for our discussion.

The remaining states, with ranks $m > \max\{N_A, N_B\}$ and $n > \max\{N_A, N_B\}$, are restricted to the upper right corners of the diagrams. For these values of the ranks, all states produced in our searches, with one exception, have full local ranks. [The exception is the case $(m, n) = (5, 5)$ of the 4×4 system, where in addition to full rank states, also states with less than full rank are found.] The systems of dimension 2×2 and 2×3 , represented by the diagrams in Fig. 4, are special since for these systems, all PPT states are separable. However, for the higher dimensional systems we note that the preceding restriction on the ranks of ρ and ρ^p coincides with a lower bound, found by Horodecki *et al.* [22], on the rank of *entangled* PPT states with full local ranks. (In the following we shall refer to this as the HLVC bound.) In fact, with the exception of some of the $(5, 5)$ states of the 4×4 system, we find for all ranks above and sufficiently close to this lower bound that the states are not only entangled but extremal PPT states.

As displayed by the figures, there are a few intermediate values of m , above the HLVC bound, where only symmetric ranks $m = n$ are found. We shall later discuss these states separately and focus now on the states with ranks $m \geq N_A + N_B - 1$ and $n \geq N_A + N_B - 1$. For almost all ranks that satisfy these inequalities we find PPT states. The only exceptions are some of the cases with the largest asymmetry between the values of m and n . In fact we cannot rule out that we miss these states as a consequence of the method we use. We find that with large asymmetry in m and n the numerical method seems preferably to pick up matrices with lower and more symmetric ranks. Therefore a much larger number of searches has to be performed in order to find density matrices when the ranks are highly asymmetric.

With exception for the systems 2×2 and 2×3 , all the states we find with ranks between the lower bounds $m \geq N_A + N_B - 1$ and $n \geq N_A + N_B - 1$ and the upper bound $m^2 + n^2 \leq N^2 + 1$ are *extremal* (and hence entangled) PPT states. The upper bound is the constraint [Eq. (11)] on extremality

that has already been discussed, and in the figures this bound is displayed as the red circular arc. For ranks above this bound, we have used a separability test [22] on the states, and this test shows that for all ranks that satisfy the inequality $m + n \leq 2N - N_A - N_B + 2$, we find entangled PPT states. Beyond this limit the test is not applicable.

C. Dimensions of faces and numbers of product vectors

The structure of the diagrams discussed earlier can to some extent be related to simple regularities of the parameters in the tables. We focus first on the list of the values of $\dim \mathcal{F}$. This number is constrained by the geometric bound (10), $\dim \mathcal{F} \geq m^2 + n^2 - N^2$. We note that for all states where the ranks are sufficiently large to give a positive number for this lower bound, the constraint is satisfied with equality. This means that the linear constraint equations [Eqs. (9)] that define \mathcal{F} as a section between faces of $\mathcal{K}(\mathcal{D})$ and $\mathcal{K}(\mathcal{D}^p)$ are all independent.

For all ranks $m, n \geq N_A + N_B - 1$ that give negative values for the bound, we find $\dim \mathcal{F} = 1$. This is the minimum value consistent with the fact that the density operator ρ is located on both faces. Other “accidental” relations between the two intersecting faces, therefore, seem not to be present. The fact that $\dim \mathcal{F}$ takes the minimal value consistent with this condition gives an explanation for why all the states with ranks between a lower and an upper bound are found to be extremal PPT states. For sufficiently low ranks, $m, n < N_A + N_B - 2$, we find states where $\dim \mathcal{F}$ does not take this minimum value. Therefore we see these states as corresponding to more special constructions.

The numbers of product vectors we find in $\text{Im } \rho$ and $\text{Ker } \rho$ also show a simple regularity. For a long sequence of high ranks m , all states have no product vector in $\text{Ker } \rho$ and a complete basis (in fact an overcomplete set) of product vectors in $\text{Im } \rho$. When lowering the rank, there are in some of the lists a small set of intermediate ranks where there is no product vector in neither $\text{Im } \rho$ nor $\text{Ker } \rho$, and below this there is a single extremal state at $m = n = N_A + N_B - 2$ (not present in the $2 \times N_B$ systems) with a complete set of product vectors in $\text{Ker } \rho$ and no product vector in $\text{Im } \rho$. For even lower ranks the states are also here exceptional and do not fit into this picture.

When we exclude these lowest rank states, the numbers we find in the lists are in fact identical to the numbers of product vectors expected for generic subspaces of the given dimension. To show this we consider the conditions for a product state $\phi \otimes \chi$ to be present in a randomly chosen subspace of dimension d in the Hilbert space $\mathcal{H} = \mathcal{H}_A \otimes \mathcal{H}_B$. The product state will satisfy a set of constraint equations of the form

$$\psi_k^\dagger(\phi \otimes \chi) = 0, \quad k = 1, 2, \dots, N - d, \quad (15)$$

where ψ_k is a linearly independent set of states that are all orthogonal to the chosen d -dimensional space. The solutions to the equation will generally depend on a number of continuous parameters that can be determined by parameter counting. Thus the product state will be specified by $N_A + N_B - 2$ complex parameters (when the complex normalization factors are not included), and this number is reduced by the $N - d$ complex constraint equations to give for the solution a remaining set of p complex parameters, with

$$p = N_A + N_B - 2 - N + d. \quad (16)$$

We may then distinguish between three cases: (1) $p > 0$, which means $d > N - N_A - N_B + 2$; the set of Eqs. (15) is underdetermined, and there is an infinite set of product vectors in the d -dimensional subspace, described by p complex free parameters; (2) $p = 0$, which means $d = N - N_A - N_B + 2$; the number of equations matches the number of parameters to give a finite set of solutions; and (3) $p < 0$, which means $d < N - N_A - N_B + 2$; the set of equations is overdetermined, and there is in the generic case no solution. There may, however, be solutions for specially selected subspaces.

For case 2, the number of product vectors is given by the expression

$$n_{ps} = \binom{N_A + N_B - 2}{N_A - 1} = \frac{(N_A + N_B - 2)!}{(N_A - 1)!(N_B - 1)!}. \quad (17)$$

The problem of finding this number of product vectors can be related to the problem in algebraic geometry of finding the degree of the variety defined by the Segre embedding between projective spaces $P^{N_A-1} \times P^{N_B-1} \rightarrow P^{N_A N_B - 1}$ [26]. The number given in Eq. (17) is identical to this degree.

It is straightforward to check that all the numbers in the tables are consistent with these results, except for the special low-rank states. Apart from these states, the PPT states we find in the numerical searches are therefore also in this respect typical states for the given ranks (m, n) .

D. The lowest rank extremal and entangled PPT states

For the systems with $N_A > 2$ and $N_B > 2$ the lowest rank extremal PPT states with full local ranks seem to have a special status. These states have symmetric ranks $m = n$, and for these values of m (or n) we find no states with asymmetric ranks. They are also special in the sense that they are the only ones with no product vector in $\text{Im } \rho$ and a finite, complete set of product vectors in $\text{Ker } \rho$.

For the 3×3 system these are rank (4,4) states, and the presence of product vectors in $\text{Ker } \rho$ but not in $\text{Im } \rho$ indicates that they are related to a special construction of low rank entangled PPT states for this system, with the use of unextendible product bases (UPB) [19]. The UPB is a set of orthogonal product vectors that spans a subspace ($\text{Ker } \rho$) and that cannot be extended with additional orthogonal product vectors (in $\text{Im } \rho$). The (4,4) states that we find by our method do not directly exemplify this construction since the product vectors in $\text{Ker } \rho$ are nonorthogonal, but there is a general connection to the UPB construction that we discuss in detail in a separate publication [21].

We find similar types of extremal PPT states in all the systems we have studied with dimensions of the subsystems larger than 2. This we take as an indication for the presence of such lowest rank extremal states in all higher dimensional systems. When we combine the assumption of a finite, complete set of product vectors in $\text{Ker } \rho$ and no product vector in $\text{Im } \rho$ with the expectations for the number of product vectors in generic subspaces of a given dimension, we find that these states should generally have ranks equal to $m = n = N_A + N_B - 2$. We will phrase the assumption about these states in the form of the following conjecture: The lowest rank extremal PPT state with full local ranks in an $N_A \times N_B$ system, with N_A and N_B larger than 2, is characterized by

symmetric ranks $m = n$ for the density matrix and its partial transpose, with value $m = n = N_A + N_B - 2$.

We write this as an inequality for the rank of *extremal* PPT states with full local ranks,

$$m, n \geq N_A + N_B - 2 \quad (\text{conjecture}), \quad (18)$$

and compare it to the lower bound for *entangled* PPT states with full local ranks:

$$m, n \geq \max\{N_A, N_B\} + 1 \quad (\text{HLVC}). \quad (19)$$

For systems of dimension $2 \times N_B$ we note that the HLVC bound lies above the lower bound for extremality, and therefore the bound of Eq. (18) cannot be saturated. That is in accordance with the lack of the special type of lowest-rank extremal PPT state for these systems. For systems of dimension $3 \times N_B$ (with $N_B \geq 3$) the two bounds coincide, and the lowest rank extremal states that we have found for these systems are indeed also the lowest rank entangled states. For systems of dimension $4 \times N_B$ (with $N_B \geq 4$), there is a difference of 1 between the two lower bounds, with the HLVC bound being the lowest. We have examined only one example of such systems, namely, the 4×4 system. For this system we do find entangled PPT states with lower rank than the lowest rank extremal PPT state. For general systems $N_A \times N_B$ with $N_A \leq N_B$, the difference between the two bounds is, according to our conjecture, equal to $N_A - 3$ and therefore increases linearly with the lowest dimension of the two subsystems.

The entangled PPT states with lower ranks than the lowest rank extremal PPT states with full local ranks will include only extremal PPT states with less than full local ranks, when written as convex combinations of extremal states. We have found examples of such states with ranks (5,5) in the 4×4 system. In the table such a state ρ appears with $\dim \mathcal{F} = 2$, which means that it is a convex combination of two extremal PPT states,

$$\rho = (1 - x)\rho_e + x\rho_p, \quad (20)$$

with $0 < x < 1$. One of these is a pure product state $\rho_p = ww^\dagger$, where $w = u \otimes v$ is the single product vector found in $\text{Im } \rho$. The other one is a rank (4,4) state ρ_e , which we identify as an extremal PPT state of a 3×3 subsystem. We find this state by subtracting ρ_p with the value of the coefficient x determined as discussed in [22]. To summarize, the entangled rank (5,5) PPT state ρ has full local ranks and saturates the HLVC bound but is a convex combination of two extremal PPT states that both have less than full local ranks.

A closer look at the preceding decomposition of the (5,5) state ρ motivates the following general construction of states that saturate the HLVC bound in successively higher dimensions. Assume that

$$\mathcal{H}_A = \mathcal{U}_1 \oplus \mathcal{U}_2, \quad \mathcal{H}_B = \mathcal{V}_1 \oplus \mathcal{V}_2, \quad (21)$$

where $\dim \mathcal{U}_1 = \dim \mathcal{V}_1 = 3$ and $\dim \mathcal{U}_2 = \dim \mathcal{V}_2 = 1$. We assume that \mathcal{U}_1 and \mathcal{U}_2 are complementary but not necessarily orthogonal subspaces of \mathcal{H}_A and that \mathcal{V}_1 and \mathcal{V}_2 are complementary but not necessarily orthogonal in \mathcal{H}_B .

Let ρ_e be a rank (4,4) extremal PPT state on the 3×3 dimensional subspace $\mathcal{U}_1 \otimes \mathcal{V}_1 \subset \mathcal{H}$. A property of ρ_e is that there are no product vectors in $\text{Im } \rho_e \subset \mathcal{U}_1 \otimes \mathcal{V}_1$. Let ρ_p be a pure product state $\rho_p = ww^\dagger$ with $w = u \otimes v$, $u \in \mathcal{U}_2$ and

$v \in \mathcal{V}_2$. Then define $\rho = (1-x)\rho_e + x\rho_p$ with $0 < x < 1$. The image of ρ is

$$\begin{aligned} \text{Im } \rho &= \text{Im } \rho_e \oplus \text{Im } \rho_p \\ &= \text{Im } \rho_e \oplus (\mathcal{U}_2 \otimes \mathcal{V}_2) \subset (\mathcal{U}_1 \otimes \mathcal{V}_1) \oplus (\mathcal{U}_2 \otimes \mathcal{V}_2). \end{aligned} \quad (22)$$

Since $\mathcal{U}_2 \otimes \mathcal{V}_2$ is one-dimensional, it follows that the rank of ρ is one higher than the rank of ρ_e . Similarly, the rank of ρ^P is one higher than the rank of ρ_e^P .

The only product vector in $\text{Im } \rho$ is now $w = u \otimes v$. To see this, consider the most general product vector

$$\begin{aligned} w' &= (u_1 + u_2) \otimes (v_1 + v_2) \\ &= (u_1 \otimes v_1) + (u_1 \otimes v_2) + (u_2 \otimes v_1) + (u_2 \otimes v_2), \end{aligned} \quad (23)$$

with $u_i \in \mathcal{U}_i$ and $v_j \in \mathcal{V}_j$. It is a sum of four vectors belonging to four complementary subspaces $\mathcal{U}_i \otimes \mathcal{V}_j \subset \mathcal{H}$ with $i, j = 1, 2$. In order to have $w' \in \text{Im } \rho$ we must have

$$w' \in (\mathcal{U}_1 \otimes \mathcal{V}_1) \oplus (\mathcal{U}_2 \otimes \mathcal{V}_2), \quad (24)$$

but this requires that $u_1 \otimes v_2 = u_2 \otimes v_1 = 0$. Since we want to have $w' \neq 0$, the only possibilities left are $w' = u_1 \otimes v_1$, which is not in $\text{Im } \rho$, or $w' = u_2 \otimes v_2$, which is not new.

It should be clear from this analysis that the same construction can be applied to higher dimensional systems. For example, we may reinterpret ρ_e to be the (5,5) state ρ of the 4×4 system, as constructed earlier. We reinterpret ρ_p to be a new pure product state that increases the local ranks from 4 to 5, in a similar manner as discussed, so that $\rho = (1-x)\rho_e + x\rho_p$ is a (6,6) state of the 5×5 system. The analysis of product vectors in $\text{Im } \rho$ can be done in the same way, with one exception. In this case there is already one product vector in $\text{Im } \rho_e$, and therefore there are two possible solutions for the product vector w' , namely, the newly added vector $w = u \otimes v$ and the previous product vector in $\text{Im } \rho_e$. Since the number of product vectors is lower than $\dim \text{Im } \rho$, the state is entangled, and it saturates the HLVC bound.

The construction can be continued to arbitrarily high dimension, and it will always create an entangled state that saturates the HLVC bound. The state will be a convex combination of extremal PPT states with less than full local ranks, but it will itself have full local ranks. The construction is not restricted to symmetric cases, $N_A = N_B$, since asymmetric systems can be reached by introducing product vectors which increase the dimension of only \mathcal{H}_A or \mathcal{H}_B . In this way it is possible to saturate the HLVC bound in all higher dimensional systems.

E. Checking for entanglement at higher ranks

All the states with ranks above the upper limit for extremality, that is, with

$$m^2 + n^2 > N^2 + 1, \quad (25)$$

we find to have a complete set of product vectors in their image. This means that they satisfy the necessary condition for separability given by the range criterion, which however, does not exclude the possibility that they may be entangled. To get some further information about this, we have made use of a separability criterion introduced in [22]. This condition for separability can be seen as a strengthened version of the

range criterion and is based on a relation that, for separable states, exists between product vectors in $\text{Im } \rho$ and in $\text{Im } \rho^P$. We describe subsequently the basis for this criterion and further describe the method we have applied for checking the criterion.

Assume ρ to be a separable density operator, which therefore can be written as a convex combination of product states,

$$\rho = \sum_k p_k \psi_k \psi_k^\dagger, \quad (26)$$

with $\psi_k = \phi_k \otimes \chi_k$. The partially transposed density operator can then be written as

$$\rho^P = \sum_k p_k \tilde{\psi}_k \tilde{\psi}_k^\dagger, \quad (27)$$

with $\tilde{\psi}_k = \phi_k \otimes \chi_k^*$, where χ_k^* is the complex conjugate of χ_k with respect to the same basis in \mathcal{H}_B that is used for the partial transposition. Therefore, corresponding to the set of product vectors $\{\psi_k\}$, which spans $\text{Im } \rho$, there is a set of product vectors $\{\tilde{\psi}_k\}$, which we will refer to as the conjugate set, that spans $\text{Im } \rho^P$. This implies that a necessary condition for separability of a density operator ρ is that the number of pairs of product vectors in $\text{Im } \rho$ and in $\text{Im } \rho^P$ that are conjugate is equal to or larger than the ranks of both ρ and ρ^P . We write the condition as

$$K \geq \max\{m, n\}, \quad (28)$$

with K as the number of conjugate pairs of product vectors in $\text{Im } \rho$ and $\text{Im } \rho^P$.

The preceding condition for separability is effectively restricted to cases where the ranks m and n of ρ and ρ^P are not too large. This follows since if the dimensions of $\text{Im } \rho$ and $\text{Im } \rho^P$ are sufficiently large, the number of such pairs will necessarily be infinite. The condition for the number of pairs to be finite can be determined by essentially the same method of counting parameters as used to determine the typical number of product vectors in a Hilbert space of given dimension, as discussed in Sec. III C. Thus a conjugate pair of product vectors $(\psi, \tilde{\psi})$, with $\psi = \phi \otimes \chi$ and $\tilde{\psi} = \phi \otimes \chi^*$, has to satisfy two sets of equations:

$$\theta_i^\dagger \psi = 0, \quad \xi_i^\dagger \tilde{\psi} = 0, \quad (29)$$

where $\{\theta_i\}$ is a basis of $\text{Ker } \rho$ and $\{\xi_i\}$ is a basis of $\text{Ker } \rho^P$. The number of equations that ψ has to satisfy will be equal to or will exceed the number of free parameters in this product state, provided the following condition is satisfied [22]:

$$\dim \text{Ker } \rho + \dim \text{Ker } \rho^P \geq \dim \mathcal{H}_A + \dim \mathcal{H}_B - 2. \quad (30)$$

If the condition is satisfied with proper inequality, there will typically be no solution, and if it is satisfied with equality, there will be a finite set of solutions. Expressed in terms of the ranks m and n and the Hilbert space dimensions N , N_A , and N_B , the inequality takes the form

$$m + n \leq 2N - N_A - N_B + 2, \quad (31)$$

and this sets the limit for applications of the criterion. In the diagrams this limit is indicated by the dashed green line.

For states that satisfy the preceding inequality, we have found a practical method to check the separability condition [Eq. (28)] by applying essentially the same double-eigenvalue

method as used for detecting product vectors in $\text{Im } \rho$ (and in $\text{Ker } \rho$) and which is described in Appendix A. The outline of the method is the following. Let P be the orthogonal projection on $\text{Im } \rho$ and Q the orthogonal projection on $\text{Im } \rho^P$. We consider the following bilinear function of the product state $\psi = \phi \otimes \chi$:

$$f(\psi) = \psi^\dagger(\mathbb{1} - P)\psi + \tilde{\psi}^\dagger(\mathbb{1} - Q)\tilde{\psi}, \quad (32)$$

and search for the minima of the function where $f = 0$. Since both terms in Eq. (32) are non-negative, such a solution will give zero for each term separately, and from this follow the relations $P\psi = \psi$ and $Q\tilde{\psi} = \tilde{\psi}$, which are equivalent to the two sets of Eqs. (29). The second term in Eq. (32) can be rewritten in the following way: $\tilde{\psi}^\dagger(\mathbb{1} - Q)\tilde{\psi} = \psi^\dagger(\mathbb{1} - Q^P)\psi$, with Q^P as the partial transpose of Q . This gives

$$f(\psi) = \psi^\dagger(2\mathbb{1} - P - Q^P)\psi, \quad (33)$$

and written in this way the function $f(\psi)$ has the same form as the function that is minimized in the search for product vectors in $\text{Im } \rho$ (see Sec. II C). The only difference is that the operator $\mathbb{1} - P$ is replaced by $2\mathbb{1} - P - Q^P$. The same method to search for product vectors with vanishing value for the function can therefore be used.

The result is that for all the states we have found with $m > N_A + N_B - 1$, and where Eq. (31) is satisfied as a proper inequality, there are no pairs of conjugate product vectors, and the states are therefore entangled. In the diagrams these states are located below the dashed green lines. For the states *on* the dashed green line in the diagrams the condition (31) is satisfied with equality, and for these states we find a finite number K of pairs of conjugate product vectors that is sufficiently large to satisfy the separability condition of Eq. (28). This means that just counting the number of pairs of conjugate product vectors is insufficient to determine if the states are entangled. However, with only a finite number of product vectors available it is possible to check whether the density operator can be reconstructed as a convex combination of these product states. The result is that for all ranks where Eq. (31) is satisfied with equality, we find entangled states. However, in a small number of cases, we find both separable and entangled states with the same set of ranks (m, n) . That happens for the (6, 6), (5, 7), and (7, 5) states of the 2×4 system.

IV. CONCLUDING REMARKS

The results presented in this article are based on the use of a numerical method to search for density matrices ρ of a composite, bipartite system with specified values for the ranks of ρ and its partial transpose ρ^P . The method works well for systems where the Hilbert space dimension N is not too large, in our calculations, with $N \lesssim 20$. In higher dimensions the main problem is a too-slow convergence of the iteration procedure. Additional methods to find the number of product vectors in the image and kernel of the density matrices and to determine the dimension of the corresponding face of the set of PPT states have been described. The results based on the use of these methods are listed in the tables and displayed in the figures.

The results obtained for the low-dimensional systems that we have studied reveal several regularities. For sufficiently low ranks we find only separable states of a specific form. Above a

certain value for the ranks of ρ and ρ^P the states we find are typically extremal PPT states, until the ranks reach an upper limit. In our discussion we suggest that there are in fact two lower bounds, one for entangled states with full local ranks and another, generally more restrictive, for extremal PPT states with full local ranks. The first we identify as the bound on entangled PPT states discussed in [22], and we show, by an explicit construction, how this bound can be saturated. On the basis of certain properties of the extremal states with minimal ranks that are found in our searches, we conjecture a specific value for the second, the lower bound on the ranks of extremal PPT states. The property we focus on is the number of product vectors in the image and in the kernel of this state, which makes these states different from the higher rank extremal states. Assuming this property to be present for the lowest rank extremal states in general, we draw the conclusion about the lower bound.

Above this lower bound we find in our search a large set of ranks (m, n) of ρ and ρ^P where the states are extremal. There is an upper limit to the ranks of these states, which can be understood as following from a geometrical constraint on the face of the set \mathcal{P} to which an extremal PPT state belongs. It is of interest to note that all the states we find for sufficiently low ranks are limited to the symmetric cases $m = n$, whereas for m and n above this limit we find in addition states for essentially all the asymmetric values of the ranks. However, as we have stressed, the states we find by our method should be considered as typical states for the given ranks (m, n) . This means that we cannot exclude the presence of untypical states also for ranks for which we have not identified any PPT state.

Concerning this last point, it is of interest to relate the results for the properties of the PPT states found in our searches with those of other entangled and extremal PPT states referred to in the literature [11, 12, 17–19, 27]. These states are based on special constructions which lead to certain classes of extremal PPT states. Among the states presented by these special constructions, we have found no example of states with ranks different from those referred to in our tables and figures. The main difference, however, is that these specially constructed states are not necessarily typical in the meaning used here, and in particular the number of product vectors in the image and kernel may be larger than the minimal values that we find in our searches.

In the discussion of our results we have put some emphasis on the properties of the lowest rank extremal PPT states. For all the systems we have studied they are special in the sense that they have no product state in their image but a complete, finite set of product vectors in their kernel. In a separate publication [21] we have made a detailed study of these states for the 3×3 system, where they have ranks (4, 4). We show there that these states can be related to states constructed from unextendible product bases, and the set of such states can be given an explicit parametrization. We do not know how to generalize this construction to higher dimensions, and the question of a general parametrization of extremal PPT states remains as an interesting problem for future work.

ACKNOWLEDGMENTS

Financial support from the Norwegian Research Council is gratefully acknowledged.

APPENDIX A: THE MINIMUM DOUBLE EIGENVALUE PROBLEM

Given the Hermitian matrix A , the problem considered here is to minimize the expectation value $\psi^\dagger A \psi$ over product vectors $\psi = \phi \otimes \chi$, with the normalization conditions $\phi^\dagger \phi = \chi^\dagger \chi = 1$. The problem is equivalent to a set of coupled eigenvalue problems for the two subsystems, shown in Eq. (A2), which we have previously analyzed and applied in Ref. [28]. We present here a modified iteration method, used for solving certain subproblems discussed in this article. The motivation for the new iteration method is that it may converge to different local minima, depending on the starting point for the iterations. It is important for our purposes here to be able to find all local minima.

We introduce Lagrange multipliers λ, μ and define

$$f = \sum_{i,j,k,l} \phi_i^* \chi_j^* A_{ij;kl} \phi_k \chi_l - \lambda \left(\sum_i \phi_i^* \phi_i - 1 \right) - \mu \left(\sum_j \chi_j^* \chi_j - 1 \right). \quad (\text{A1})$$

The following equations must hold at the minimum, or more generally at an extremum,

$$\begin{aligned} \frac{\partial f}{\partial \phi_i^*} &= \sum_{j,k,l} \chi_j^* A_{ij;kl} \phi_k \chi_l - \lambda \phi_i = 0, \\ \frac{\partial f}{\partial \chi_j^*} &= \sum_{i,k,l} \phi_i^* A_{ij;kl} \phi_k \chi_l - \mu \chi_j = 0, \end{aligned} \quad (\text{A2})$$

with

$$\begin{aligned} \sum_i \phi_i^* \phi_i &= \sum_j \chi_j^* \chi_j = 1, \\ \lambda &= \mu = \sum_{i,j,k,l} \phi_i^* \chi_j^* A_{ij;kl} \phi_k \chi_l. \end{aligned} \quad (\text{A3})$$

Note that $\lambda = \mu$ is the desired minimal (or extremal) value of the expectation value $\psi^\dagger A \psi$.

In each iteration, given an approximate solution $\psi = \phi \otimes \chi$, we compute the next approximation $\psi' = \phi' \otimes \chi'$ as follows. We compute $x = B\phi - \lambda\phi$, $y = C\chi - \lambda\chi$, with $\lambda = \psi^\dagger A \psi$ and

$$B_{ik} = \sum_{j,l} \chi_j^* A_{ij;kl} \chi_l, \quad C_{jl} = \sum_{i,k} \phi_i^* A_{ij;kl} \phi_k. \quad (\text{A4})$$

In practice, we compute $z = A\psi$, $u_i = \sum_j \chi_j^* z_{ij}$, $v_j = \sum_i \phi_i^* z_{ij}$, $\lambda = \phi^\dagger u = \chi^\dagger v$, $x = u - \lambda\phi$, and $y = v - \lambda\chi$. We define $\phi' = N_1(\phi + \epsilon x)$ and $\chi' = N_2(\chi + \epsilon y)$, where N_1, N_2 are normalization factors and where ϵ is determined as follows. To first order in ϵ , we have

$$(\phi + \epsilon x) \otimes (\chi + \epsilon y) = \psi + \epsilon w, \quad (\text{A5})$$

with $w = \phi \otimes y + x \otimes \chi$. Note that $\psi^\dagger w = 0$ since $\phi^\dagger x = \chi^\dagger y = 0$. The vector $s = \psi + \epsilon w$ is used as a trial vector, and the parameter ϵ is determined by minimizing $s^\dagger A s / s^\dagger s$. This is an eigenvalue problem in the two-dimensional subspace spanned by ψ and w , and it can be solved analytically.

This iteration method is based on the linear approximation in Eq. (A5), which should be good when the starting point for an iteration is close to a local minimum so that ϵ will be small. By minimizing $s^\dagger A s / s^\dagger s$, we get successively smaller values of $\psi^\dagger A \psi$, and the iterations will converge to the local minimum.

APPENDIX B: TABLES

TABLE I. Numerical results for the 2×4 and the 2×5 systems. The first column lists the ranks of ρ and ρ^P where PPT states have been found. The second column lists the lower limit for the value of the dimension of the face of $\mathcal{K}(\mathcal{P})$ for the given ranks (m, n) , while the third column lists the actual values of the dimensions for the states we have found. The fourth column lists the values of the local ranks with respect to subsystems A and B . The fifth and sixth columns give the number of product vectors in $\text{Im } \rho$ and $\text{Ker } \rho$, respectively. In each of these columns, two numbers are given, with the number to the left as the total number and the one to the right as the number of linearly independent product vectors. Symbol ∞ indicates that we find no upper limit to the number of product vectors that can be generated. In the present tables the extremal PPT states with no product state in $\text{Im } \rho$ and a complete set in $\text{Ker } \rho$, which we find in all the other tables, are missing.

(m, n)	$m^2 + n^2 - N^2$	$\dim \mathcal{F}$	(r_A, r_B)	#pv [Im ρ]	#pv [Ker ρ]
2×4					
(8,8)	64	64	(2,4)	$\infty/8$	0
(8,7)	49	49	(2,4)	$\infty/8$	0
(8,6)	36	36	(2,4)	$\infty/8$	0
(7,7)	34	34	(2,4)	$\infty/7$	0
(8,5)	25	25	(2,4)	$\infty/8$	0
(7,6)	21	21	(2,4)	$\infty/7$	0
(7,5)	10	10	(2,4)	$\infty/7$	0
(6,6)	8	8	(2,4)	$\infty/6$	0
(6,5)	-3	1	(2,4)	$\infty/6$	0
(5,5)	-14	1	(2,4)	$\infty/5$	0
(4,4)	-32	4	(2,4)	4/4	4/4
(3,3)	-46	3	(2,3)	3/3	$\infty/5$
(2,2)	-56	2	(2,2)	2/2	$\infty/6$
(1,1)	-62	1	(1,1)	1/1	$\infty/8$
2×5					
(10,10)	100	100	(2,5)	$\infty/10$	0
(10,9)	81	81	(2,5)	$\infty/10$	0
(10,8)	64	64	(2,5)	$\infty/10$	0
(9,9)	62	62	(2,5)	$\infty/9$	0
(10,7)	49	49	(2,5)	$\infty/10$	0
(9,8)	45	45	(2,5)	$\infty/9$	0
(9,7)	30	30	(2,5)	$\infty/9$	0
(8,8)	28	28	(2,5)	$\infty/8$	0
(9,6)	17	17	(2,5)	$\infty/9$	0
(8,7)	13	13	(2,5)	$\infty/8$	0
(8,6)	0	1	(2,5)	$\infty/8$	0
(7,7)	-2	1	(2,5)	$\infty/7$	0
(7,6)	-15	1	(2,5)	$\infty/7$	0
(6,6)	-28	1	(2,5)	$\infty/6$	0
(5,5)	-50	5	(2,5)	5/5	5/5
(4,4)	-68	4	(2,4)	4/4	$\infty/6$
(3,3)	-82	3	(2,3)	3/3	$\infty/7$
(2,2)	-92	2	(2,2)	2/2	$\infty/8$
(1,1)	-98	1	(1,1)	1/1	$\infty/9$

TABLE II. Numerical results for the 3×3 and the 3×4 systems. For explanations, see Table I. Except for one case in the 3×4 system, we find only one type of state, characterized by the listed properties, for each set of ranks (m, n) . The exception is the case $(4, 4)$, where we find both extremal PPT states with less than full local ranks and separable states of the same construction as those of lower ranks.

(m, n)	$m^2 + n^2 - N^2$	$\dim \mathcal{F}$	(r_A, r_B)	#pv [Im ρ]	#pv [Ker ρ]
3×3					
(9,9)	81	81	(3,3)	$\infty/9$	0
(9,8)	64	64	(3,3)	$\infty/9$	0
(9,7)	49	49	(3,3)	$\infty/9$	0
(8,8)	47	47	(3,3)	$\infty/8$	0
(9,6)	36	36	(3,3)	$\infty/9$	0
(8,7)	32	32	(3,3)	$\infty/8$	0
(8,6)	19	19	(3,3)	$\infty/8$	0
(7,7)	17	17	(3,3)	$\infty/7$	0
(8,5)	8	8	(3,3)	$\infty/8$	0
(7,6)	4	4	(3,3)	$\infty/7$	0
(7,5)	-7	1	(3,3)	$\infty/7$	0
(6,6)	-9	1	(3,3)	$\infty/6$	0
(6,5)	-20	1	(3,3)	$\infty/6$	0
(5,5)	-31	1	(3,3)	6/5	0
(4,4)	-49	1	(3,3)	0	6/5
(3,3)	-63	3	(3,3)	3/3	$\infty/6$
(2,2)	-73	2	(2,2)	2/2	$\infty/7$
(1,1)	-79	1	(1,1)	1/1	$\infty/8$
3×4					
(12,11)	121	121	(3,4)	$\infty/12$	0
(12,10)	100	100	(3,4)	$\infty/12$	0
(11,11)	98	98	(3,4)	$\infty/11$	0
(12,9)	81	81	(3,4)	$\infty/12$	0
(11,10)	77	77	(3,4)	$\infty/11$	0
(12,8)	64	64	(3,4)	$\infty/12$	0
(11,9)	58	58	(3,4)	$\infty/11$	0
(10,10)	56	56	(3,4)	$\infty/10$	0
(11,8)	41	41	(3,4)	$\infty/11$	0
(10,9)	37	37	(3,4)	$\infty/10$	0
(11,7)	26	26	(3,4)	$\infty/11$	0
(10,8)	20	20	(3,4)	$\infty/10$	0
(9,9)	18	18	(3,4)	$\infty/9$	0
(11,6)	13	13	(3,4)	$\infty/11$	0
(10,7)	5	5	(3,4)	$\infty/10$	0
(9,8)	1	1	(3,4)	$\infty/9$	0
(10,6)	-8	1	(3,4)	$\infty/10$	0
(9,7)	-14	1	(3,4)	$\infty/9$	0
(8,8)	-16	1	(3,4)	$\infty/8$	0
(9,6)	-27	1	(3,4)	$\infty/9$	0
(8,7)	-31	1	(3,4)	$\infty/8$	0
(8,6)	-44	1	(3,4)	$\infty/8$	0
(7,7)	-46	1	(3,4)	10/7	0
(7,6)	-59	1	(3,4)	10/7	0
(6,6)	-72	1	(3,4)	0	0
(5,5)	-94	1	(3,4)	0	10/7
(4,4)	-112	1	(3,3)	0	$\infty/8$
		4	(3,4)	4/4	$\infty/8$
(3,3)	-126	3	(3,3)	3/3	$\infty/9$
(2,2)	-136	2	(2,2)	2/2	$\infty/10$
(1,1)	-142	1	(1,1)	1/1	$\infty/11$

TABLE III. Numerical results for the 3×5 system. For explanations, see Table I. We here find two types of states with ranks (5,5).

(m, n)	$m^2 + n^2 - N^2$	$\dim \mathcal{F}$	(r_A, r_B)	#pv [Im ρ]	#pv [Ker ρ]
3×5					
(15,14)	196	196	(3,5)	$\infty/15$	0
(15,13)	169	169	(3,5)	$\infty/15$	0
(14,14)	167	167	(3,5)	$\infty/14$	0
(15,12)	144	144	(3,5)	$\infty/15$	0
(14,13)	140	140	(3,5)	$\infty/14$	0
(15,11)	121	121	(3,5)	$\infty/15$	0
(14,12)	115	115	(3,5)	$\infty/14$	0
(13,13)	113	113	(3,5)	$\infty/13$	0
(14,11)	92	92	(3,5)	$\infty/14$	0
(13,12)	88	88	(3,5)	$\infty/13$	0
(14,10)	71	71	(3,5)	$\infty/14$	0
(13,11)	65	65	(3,5)	$\infty/13$	0
(12,12)	63	63	(3,5)	$\infty/12$	0
(14,9)	52	52	(3,5)	$\infty/14$	0
(13,10)	44	44	(3,5)	$\infty/13$	0
(12,11)	40	40	(3,5)	$\infty/12$	0
(14,8)	35	35	(3,5)	$\infty/14$	0
(13,9)	25	25	(3,5)	$\infty/13$	0
(14,7)	20	20	(3,5)	$\infty/14$	0
(12,10)	19	19	(3,5)	$\infty/12$	0
(11,11)	17	17	(3,5)	$\infty/11$	0
(13,8)	8	8	(3,5)	$\infty/13$	0
(12,9)	0	1	(3,5)	$\infty/12$	0
(11,10)	-4	1	(3,5)	$\infty/11$	0
(13,7)	-7	1	(3,5)	$\infty/13$	0
(12,8)	-17	1	(3,5)	$\infty/12$	0
(11,9)	-23	1	(3,5)	$\infty/11$	0
(10,10)	-25	1	(3,5)	$\infty/10$	0
(12,7)	-32	1	(3,5)	$\infty/12$	0
(11,8)	-40	1	(3,5)	$\infty/11$	0
(10,9)	-44	1	(3,5)	$\infty/10$	0
(11,7)	-55	1	(3,5)	$\infty/11$	0
(10,8)	-61	1	(3,5)	$\infty/10$	0
(9,9)	-63	1	(3,5)	15/9	0
(10,7)	-76	1	(3,5)	$\infty/10$	0
(9,8)	-80	1	(3,5)	15/9	0
(9,7)	-95	1	(3,5)	15/9	0
(8,8)	-97	1	(3,5)	0	0
(8,7)	-112	1	(3,5)	0	0
(7,7)	-127	1	(3,5)	0	0
(6,6)	-153	1	(3,5)	0	15/9
(5,5)	-175	1	(3,4)	0	$\infty/10$
		5	(3,5)	5/5	$\infty/10$
(4,4)	-193	4	(3,4)	4/4	$\infty/11$
(3,3)	-207	3	(3,3)	3/3	$\infty/12$
(2,2)	-217	2	(2,2)	2/2	$\infty/13$
(1,1)	-223	1	(1,1)	1/1	$\infty/14$

TABLE IV. Numerical results for the 4×4 system. For explanations, see Table I. The pattern of the listed properties is much like that of the other tables, but here with more low-rank states below the lowest rank ($m = n = 6$) entangled PPT state with full local ranks.

(m,n)	$m^2 + n^2 - N^2$	$\dim \mathcal{F}$	(r_A, r_B)	#pv [Im ρ]	#pv [Ker ρ]
4×4					
(16,16)	256	256	(4,4)	$\infty/16$	0
(16,15)	225	225	(4,4)	$\infty/16$	0
(16,14)	196	196	(4,4)	$\infty/16$	0
(15,15)	194	194	(4,4)	$\infty/15$	0
(16,13)	169	169	(4,4)	$\infty/16$	0
(15,14)	165	165	(4,4)	$\infty/15$	0
(16,12)	144	144	(4,4)	$\infty/16$	0
(15,13)	138	138	(4,4)	$\infty/15$	0
(14,14)	136	136	(4,4)	$\infty/14$	0
(16,11)	121	121	(4,4)	$\infty/16$	0
(15,12)	113	113	(4,4)	$\infty/15$	0
(14,13)	109	109	(4,4)	$\infty/14$	0
(15,11)	90	90	(4,4)	$\infty/15$	0
(14,12)	84	84	(4,4)	$\infty/14$	0
(13,13)	82	82	(4,4)	$\infty/13$	0
(15,10)	69	69	(4,4)	$\infty/15$	0
(14,11)	61	61	(4,4)	$\infty/14$	0
(13,12)	57	57	(4,4)	$\infty/13$	0
(15,9)	50	50	(4,4)	$\infty/15$	0
(14,10)	40	40	(4,4)	$\infty/14$	0
(15,8)	33	33	(4,4)	$\infty/15$	0
(13,11)	34	34	(4,4)	$\infty/13$	0
(12,12)	32	32	(4,4)	$\infty/12$	0
(14,9)	21	21	(4,4)	$\infty/14$	0
(15,7)	18	18	(4,4)	$\infty/15$	0
(13,10)	13	13	(4,4)	$\infty/13$	0
(12,11)	9	9	(4,4)	$\infty/12$	0
(14,8)	4	4	(4,4)	$\infty/14$	0

TABLE IV. (Continued.)

(m,n)	$m^2 + n^2 - N^2$	$\dim \mathcal{F}$	(r_A, r_B)	#pv [Im ρ]	#pv [Ker ρ]
(13,9)	-6	1	(4,4)	$\infty/13$	0
(14,7)	-11	1	(4,4)	$\infty/14$	0
(12,10)	-12	1	(4,4)	$\infty/12$	0
(11,11)	-14	1	(4,4)	$\infty/11$	0
(13,8)	-23	1	(4,4)	$\infty/13$	0
(12,9)	-31	1	(4,4)	$\infty/12$	0
(11,10)	-35	1	(4,4)	$\infty/11$	0
(13,7)	-38	1	(4,4)	$\infty/13$	0
(12,8)	-48	1	(4,4)	$\infty/12$	0
(11,9)	-54	1	(4,4)	$\infty/11$	0
(10,10)	-56	1	(4,4)	20/10	0
(12,7)	-63	1	(4,4)	$\infty/12$	0
(11,8)	-71	1	(4,4)	$\infty/11$	0
(10,9)	-75	1	(4,4)	20/10	0
(11,7)	-86	1	(4,4)	$\infty/11$	0
(10,8)	-92	1	(4,4)	20/10	0
(9,9)	-94	1	(4,4)	0	0
(10,7)	-107	1	(4,4)	20/10	0
(9,8)	-111	1	(4,4)	0	0
(9,7)	-126	1	(4,4)	0	0
(8,8)	-128	1	(4,4)	0	0
(8,7)	-143	1	(4,4)	0	0
(7,7)	-158	1	(4,4)	0	0
(6,6)	-184	1	(4,4)	0	20/10
(5,5)	-206	1	(4,3)	0	$\infty/11$
		2	(4,4)	1/1	$\infty/11$
		5	(4,4)	5/5	$\infty/11$
(4,4)	-224	1	(3,3)	0	$\infty/12$
		4	(4,4)	4/4	$\infty/12$
(3,3)	-238	3	(3,3)	3/3	$\infty/13$
(2,2)	-248	2	(2,2)	2/2	$\infty/14$
(1,1)	-254	1	(1,1)	1/1	$\infty/15$

[1] M. Kus and K. Życzkowski, *Phys. Rev. A* **63**, 032307 (2001).
 [2] F. Verstraete, J. Dehaene, and B. De Moor, *J. Mod. Opt.* **49**, 1277 (2002).
 [3] A. O. Pittenger and M. H. Rubin, *Phys. Rev. A* **67**, 012327 (2003).
 [4] J. M. Leinaas, J. Myrheim, and E. Ovrum, *Phys. Rev. A* **74**, 012313 (2006).
 [5] I. Bengtsson and K. Życzkowski, *Geometry of Quantum States*, (Cambridge University Press, New York, 2006).
 [6] L. Gurvits, in *Proceedings of the 35th ACM Symposium on Theory of Computing* (ACM, New York, 2003), pp. 10–19.
 [7] A. Peres, *Phys. Rev. Lett.* **77**, 1413 (1996).
 [8] M. Horodecki, P. Horodecki, and R. Horodecki, *Phys. Lett. A* **223**, 1 (1996).
 [9] J. M. Leinaas, J. Myrheim, and E. Ovrum, *Phys. Rev. A* **76**, 034304 (2007).
 [10] M. Horodecki, P. Horodecki, and R. Horodecki, *Phys. Rev. Lett.* **80**, 5239 (1998).
 [11] D. Bruß and A. Peres, *Phys. Rev. A* **61**, 030301(R) (2000).
 [12] P. Horodecki, *Phys. Lett. A* **232**, 333 (1997).
 [13] D. Chruściński and A. Kossakowski, *Phys. Rev. A* **76**, 032308 (2007).
 [14] M. Piani, *Phys. Rev. A* **73**, 012345 (2006).
 [15] G. Tóth and O. Gühne, *Phys. Rev. Lett.* **102**, 170503 (2009).
 [16] H.-P. Breuer, *Phys. Rev. Lett.* **97**, 080501 (2006).
 [17] K. Ha, S. Kye, and Y. Park, *Phys. Lett. A* **313**, 163 (2003).
 [18] L. Clarisse, *Phys. Lett. A* **359**, 603 (2006).
 [19] C. H. Bennett, D. P. DiVincenzo, T. Mor, P. W. Shor, J. A. Smolin, and B. M. Terhal, *Phys. Rev. Lett.* **82**, 5385 (1999).
 [20] M. Lewenstein, B. Kraus, J. I. Cirac, and P. Horodecki, *Phys. Rev. A* **62**, 052310 (2000).
 [21] J. M. Leinaas, J. Myrheim, and P. Ø. Sollid, *Phys. Rev. A* **81**, 062330 (2010).
 [22] P. Horodecki, M. Lewenstein, G. Vidal, and I. Cirac, *Phys. Rev. A* **62**, 032310 (2000).

- [23] B. Kraus, J. I. Cirac, S. Karnas, and M. Lewenstein, [Phys. Rev. A](#) **61**, 062302 (2000).
- [24] G. H. Golub and C. F. Van Loan, *Matrix Computations* (North Oxford, Oxford, 1986).
- [25] R. Augusiak, J. Grabowski, M. Kus, and M. Lewenstein, [Opt. Commun.](#) **283**, 805 (2010).
- [26] R. Hartshorne, *Algebraic Geometry* (Springer, New York, 2006), p. 54.
- [27] D. P. DiVincenzo, T. Mor, P. W. Shor, J. A. Smolin, and B. M. Terhal, [Commun. Math. Phys.](#) **238**, 379 (2003).
- [28] G. Dahl, J. M. Leinaas, J. Myrheim, and E. Ovrum, [Linear Algebra Appl.](#) **420**, 711 (2007).

Low-rank extremal positive-partial-transpose states and unextendible product bases

Jon Magne Leinaas,¹ Jan Myrheim,² and Per Øyvind Sollid¹¹*Department of Physics, University of Oslo, N-0316 Oslo, Norway*²*Department of Physics, The Norwegian University of Science and Technology, N-7491 Trondheim, Norway*

(Received 15 March 2010; published 21 June 2010)

It is known how to construct, in a bipartite quantum system, a unique low-rank entangled mixed state with positive partial transpose (a PPT state) from an unextendible product basis (UPB), defined as an unextendible set of orthogonal product vectors. We point out that a state constructed in this way belongs to a continuous family of entangled PPT states of the same rank, all related by nonsingular unitary or nonunitary product transformations. The characteristic property of a state ρ in such a family is that its kernel $\text{Ker } \rho$ has a generalized UPB, a basis of product vectors, not necessarily orthogonal, with no product vector in $\text{Im } \rho$, the orthogonal complement of $\text{Ker } \rho$. The generalized UPB in $\text{Ker } \rho$ has the special property that it can be transformed to orthogonal form by a product transformation. In the case of a system of dimension 3×3 , we give a complete parametrization of orthogonal UPBs. This is then a parametrization of families of rank 4 entangled (and extremal) PPT states, and we present strong numerical evidence that it is a complete classification of such states. We speculate that the lowest rank entangled and extremal PPT states also in higher dimensions are related to generalized, nonorthogonal UPBs in similar ways.

DOI: [10.1103/PhysRevA.81.062330](https://doi.org/10.1103/PhysRevA.81.062330)

PACS number(s): 03.67.Mn, 02.40.Ft, 03.65.Ud

I. INTRODUCTION

For a composite quantum system, with two separate parts A and B , the mixed quantum states are described by density matrices that can be classified as being either entangled or separable (nonentangled). However, there is in general no easy way to classify a given density matrix as being separable or not. This problem is referred to as the separability problem, and it has been approached in the literature in different ways over the past several years [1]. As a part of this discussion there has been a focus on a subset of the density matrices which includes, but is generally larger than, the set of separable states. This is the set of the so-called positive partial transpose (PPT) states, the density matrices that remain positive under a *partial* matrix transposition, with respect to one of the subsystems, either A or B [2].

Since it is straightforward to establish whether a density matrix is a PPT state, the separability problem is reduced to identifying the subset of *entangled* PPT states. We refer here to the set of separable states as \mathcal{S} and the set of PPT states as \mathcal{P} , with $\mathcal{S} \subset \mathcal{P}$. These are both *convex* subsets of the full convex set of density matrices, which we denote as \mathcal{D} , and in principle the two sets are therefore defined by their extremal states. The extremal separable states are the pure product states, and these are also extremal states of the set \mathcal{P} . Since \mathcal{P} is in general larger than \mathcal{S} , it has additional extremal states, and these states are not fully known. The problem of finding and classifying these additional extremal states is therefore an important part of the problem to identify the PPT states that are entangled.

We have in two previous publications studied, in different ways, the problem of finding extremal PPT states in systems of low dimensions. In [3] a criterion for extremality was established and a method was described to numerically search for extremal PPT states. This method was applied to different composite systems, and several types of extremal states were found. In a recent paper [4] this study has been followed up by a systematic search for PPT states of different ranks. Series of extremal PPT states have there been identified and tabulated for different bipartite systems of low dimensions.

The study in [4] seems to show that the extremal PPT states with *lowest rank* are somehow special compared to the other extremal states. In particular we have found that these density matrices have no product vectors in their image but do have a finite, complete set of product vectors in their kernel. This was found to be a common property of the lowest rank extremal PPT states studied there, for all systems with subsystems of dimensions larger than two. This property relates these states to a particular construction, where *unextendible product bases* (UPBs) are used in a method to construct entangled PPT states [5–7].

The motivation for the present paper is to follow up this apparent link between the lowest rank extremal PPT states and the UPB construction. Our focus is particularly on the rank 4 states of the 3×3 system. The rank 4 extremal PPT states that we find numerically by the method introduced in [4] are related by product transformations to states constructed directly from UPBs. We discuss this relation and use it to give a parametrization of the rank 4 extremal PPT states.

Although a direct application of the (generalized) UPB construction to the lowest rank extremal states is restricted to the 3×3 system, the similarity between these states and the lowest rank extremal states in higher dimensions indicates that there may exist a generalization of this construction that is more generally valid. We include at the end a brief discussion of the higher dimensional cases and only suggest that a construction method, and thereby a parametrization, of such states may exist.

II. AN EXTENSION OF THE UPB CONSTRUCTION OF ENTANGLED PPT STATES

We consider in the following a bipartite quantum system with a Hilbert space $\mathcal{H} = \mathcal{H}_A \otimes \mathcal{H}_B$ of dimension $N = N_A N_B$. By definition, a separable state can be written as a density operator of the form

$$\rho = \sum_k p_k \psi_k \psi_k^\dagger, \quad (1)$$

with $p_k \geq 0$, $\sum_k p_k = 1$, and with $\psi_k = \phi_k \otimes \chi_k$ as normalized product vectors. The image of ρ , $\text{Im } \rho$, is spanned by these vectors. The fact that $\text{Im } \rho$ must be spanned by product vectors if ρ is separable is the basis for the UPB construction, which was introduced in Ref. [5] and used there to find low-rank entangled PPT states of the 3×3 system. We review here this construction and discuss a particular generalization.

Consider \mathcal{U} to be a subspace of \mathcal{H} that is spanned by a set of *orthonormal* product vectors

$$\psi_k = \phi_k \otimes \chi_k, \quad k = 1, 2, \dots, p, \quad (2)$$

which cannot be extended further in \mathcal{H} to a set of $p + 1$ orthogonal product vectors. This defines the set as an unextendible product basis. Let \mathcal{U}^\perp be the orthogonal complement to \mathcal{U} . The state proportional to the orthogonal projection onto \mathcal{U}^\perp ,

$$\rho_1 = a_1 \left(\mathbb{1} - \sum_k \psi_k \psi_k^\dagger \right), \quad (3)$$

with $a_1 = 1/(N - p)$ as a normalization factor, is then an entangled PPT state. It is nonseparable because $\text{Im } \rho_1 = \mathcal{U}^\perp$ contains no product vector, and it is a PPT state because ρ_1^p , the partial transpose of ρ_1 with respect to subsystem B , is proportional to a projection of the same form,

$$\rho_1^p = a_1 \left(\mathbb{1} - \sum_k \tilde{\psi}_k \tilde{\psi}_k^\dagger \right), \quad (4)$$

with $\tilde{\psi}_k = \phi_k \otimes \chi_k^*$. The vector χ_k^* is the complex conjugate of χ_k , in the same basis in \mathcal{H}_B as is used for the partial transposition.

The set of product vectors $\{\tilde{\psi}_k = \phi_k \otimes \chi_k^*\}$ is a new orthonormal UPB, which generally spans a different subspace than the original set $\{\psi_k = \phi_k \otimes \chi_k\}$. However, it may happen that there exists a basis for the Hilbert space \mathcal{H}_B of the second subsystem in which all the vectors χ_k have real components. In such a basis the two UPB sets are identical and the state ρ_1 is a PPT state for the simple reason that it is invariant under partial transposition, $\rho_1^p = \rho_1$. All the states given as examples in Ref. [5] are of this special kind.

An entangled PPT state ρ_1 defined by this UPB construction is a rather special density operator. $\text{Ker } \rho_1$ is spanned by product vectors, while $\text{Im } \rho_1$ contains no product vector. Since ρ_1 is proportional to the orthogonal projection onto the subspace $\text{Im } \rho_1$, it is the maximally mixed state on this subspace. There is also a symmetry between ρ_1 and ρ_1^p , such that ρ_1^p shares with ρ_1 all the properties just mentioned and has the same rank $N - p$, where $N = N_A N_B$ is the dimension of the Hilbert space and p is the number of product vectors in the UPB.

Implicitly the construction implies limits to the rank of ρ_1 . Thus, for a given Hilbert space of dimension $N = N_A N_B$ there is a lower limit to the number of product vectors in a UPB, which follows from the requirement that there should exist no product vector in the orthogonal space \mathcal{U}^\perp . The corresponding upper bound on the rank m of ρ_1 , as discussed in Ref. [4], is given by $m < N - N_A - N_B + 2$. There is also a lower bound $m > \max\{N_A, N_B\}$, which is the general lower bound on the rank of entangled PPT states with full local rank [8]. In some

special cases there exist more restrictive bounds than the ones given here [9].

For the 3×3 system these two bounds allow only one value $m = 4$ for the rank of a state ρ_1 constructed from a UPB, and for this rank explicit constructions of UPBs exist [5]. Also in higher dimensions a few examples of UPB constructions have been given [6].

The extension of the UPB construction that we shall consider here is based on a certain concept of equivalence between density operators previously discussed in [10]. The equivalence relation is defined by transformations between density operators of the form

$$\rho_2 = a_2 V \rho_1 V^\dagger, \quad (5)$$

where a_2 is a positive normalization factor, and $V = V_A \otimes V_B$, with V_A and V_B as nonsingular linear operators on \mathcal{H}_A and \mathcal{H}_B , respectively. The operators ρ_1 and ρ_2 are equivalent in the sense that they have in common several properties related to entanglement. In particular, the form of the operator V implies that separability as well as the PPT property is preserved under the transformation (5). Preservation of separability follows directly from the product form of the transformation, while preservation of PPT follows because the partially transposed matrix ρ_1^p is transformed in a similar way as ρ_1 ,

$$\rho_2^p = a_2 \tilde{V} \rho_1^p \tilde{V}^\dagger, \quad (6)$$

with $\tilde{V} = V_A \otimes V_B^*$. If ρ_1 and ρ_1^p are both positive then the transformation equations show explicitly that the same is true for ρ_2 and ρ_2^p . Furthermore, since the operators V and \tilde{V} are nonsingular, the ranks of ρ_1 and ρ_2 are the same, and so are the ranks of ρ_1^p and ρ_2^p . The same is true for the *local* ranks of the operators, which are the ranks of the reduced density operators, defined with respect to the subsystems A and B . Finally, if ρ_1 is an extremal PPT state, so is ρ_2 .

Let us again assume ρ_1 to be given by the expression (3). Since the product operator V is an invertible mapping from $\text{Im } \rho_1$ to $\text{Im } \rho_2$, and since $\text{Im } \rho_1$ contains no product vector, there is also no product vector in $\text{Im } \rho_2$, and hence ρ_2 is entangled. Similarly, the product operator $(V^\dagger)^{-1}$ is an invertible mapping from $\text{Ker } \rho_1$ to $\text{Ker } \rho_2$, and it maps the UPB in $\text{Ker } \rho_1$, Eq. (2), into a set of product vectors in $\text{Ker } \rho_2$,

$$\psi'_k = [(V_A^\dagger)^{-1} \phi_k] \otimes [(V_B^\dagger)^{-1} \chi_k], \quad k = 1, 2, \dots, p. \quad (7)$$

If the operators V_A and V_B are both unitary, then this is another UPB of orthonormal product vectors, and ρ_2 is proportional to a projection, just like ρ_1 . More generally, however, we may allow V_A and V_B to be nonunitary. Then the product vectors ψ'_k in $\text{Ker } \rho_2$ will no longer be orthogonal, but ρ_2 is nevertheless an entangled PPT state. It has the same rank as ρ_1 , but it is not proportional to a projection.

Since the normalization of the density operators ρ_1 and ρ_2 is taken care of by the normalization factors a_1 and a_2 , we may impose the normalization condition $\det V_A = \det V_B = 1$, which defines the operators as belonging to the special linear (SL) groups on \mathcal{H}_A and \mathcal{H}_B . We will say then that the two density operators ρ_1 and ρ_2 , related by a transformation of the form (5), are SL \otimes SL equivalent, or simply SL equivalent.

This construction motivates a generalization of the concept of a UPB, where we no longer require the product vectors to

be orthogonal. This generalization has also previously been proposed in the literature [7]. In the following we will refer to an unextendible product basis of orthogonal vectors as an *orthogonal UPB*. A more general UPB is then a set of product vectors that need not be orthogonal (need not even be linearly independent) but still satisfies the condition that no product vector exists in the subspace *orthogonal* to the set. The UPB defined by (7) is a special type of generalized UPB, since it is SL equivalent to an orthogonal UPB. More general types of UPBs exist, and they are in fact easy to generate, since an arbitrarily chosen set of k product vectors is typically a general UPB, when k is sufficiently large. However, if it is *not* SL equivalent to an orthogonal UPB, then we have no guarantee that there will be any entangled PPT state in the subspace \mathcal{U}^\perp orthogonal to the generalized UPB.

III. PARAMETRIZING THE UPBS OF THE 3×3 SYSTEM

We focus now on the orthogonal UPBs in the 3×3 system, which must have precisely five members. In fact, for any given set of four product vectors $\phi_k \otimes \chi_k$, there exists a product vector $\phi \otimes \chi$ orthogonal to all of them, for example with $\phi_1 \perp \phi \perp \phi_2$ and $\chi_3 \perp \chi \perp \chi_4$. And with six members in an orthogonal UPB, it would define a rank 3 entangled PPT state, which is known not to exist [8].

The general condition for five product vectors to form an orthogonal UPB in the 3×3 system was discussed in Ref. [5]. The condition implies that for any choice of *three* product vectors from the set, the first factors ϕ_k are linearly independent and so are the second factors χ_k . The orthogonality condition further implies that if the product vectors are suitably ordered, there is a cyclic set of orthogonality relations between the factors of the products of the form

$$\begin{aligned} \phi_1 \perp \phi_2 \perp \phi_3 \perp \phi_4 \perp \phi_5 \perp \phi_1, \\ \chi_1 \perp \chi_3 \perp \chi_5 \perp \chi_2 \perp \chi_4 \perp \chi_1. \end{aligned} \quad (8)$$

In Fig. 1 the situation is illustrated by a diagram composed of a pentagon and pentagram, where each corner represents a product vector. Each pair of vectors is interconnected by a line showing their orthogonality. A solid (blue) line indicates orthogonality between ϕ states (of subsystem A) and a dashed (red) line indicates orthogonality between χ states. As shown in the diagram, precisely two A lines and two B lines connect any given corner with the other corners of the diagram.

Introducing a complete set of orthonormal basis vectors α_j in \mathcal{H}_A , we write

$$\phi_k = \sum_{j=1}^3 u_{jk} \alpha_j, \quad k = 1, 2, 3, 4, 5. \quad (9)$$

We may choose, for example, α_1 proportional to ϕ_1 and α_2 proportional to ϕ_2 . If we multiply each basis vector α_j by a phase factor ω_j , and each vector ϕ_k by a normalization factor N_k , we change the 3×5 matrix u_{jk} into $\omega_j^{-1} N_k u_{jk}$. It is always possible to choose these factors so as to obtain a standard form

$$u = \begin{pmatrix} 1 & 0 & a & b & 0 \\ 0 & 1 & 0 & 1 & a \\ 0 & 0 & b & -a & 1 \end{pmatrix}, \quad (10)$$

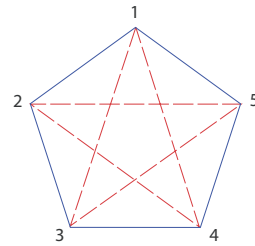


FIG. 1. (Color online) Diagrammatic representation of the orthogonality relations in a five-dimensional UPB of the 3×3 system. The corners of the diagram represent the product vectors of the UPB, and the lines represent orthogonality between pairs of states. There are two types of orthogonality, represented by the solid (blue) lines and the dashed (red) lines. The solid lines represent orthogonality between the vectors of the products that belong to subsystem A and the dashed lines represent orthogonality between the vectors belonging to subsystem B .

with a and b as real and strictly positive parameters, and with the vectors ϕ_k not normalized to length 1. A similar parametrization of the vectors of subsystem B with orthonormal basis vectors β_j gives

$$\chi_k = \sum_{j=1}^3 v_{jk} \beta_j, \quad k = 1, 2, 3, 4, 5, \quad (11)$$

and a standard form

$$v = \begin{pmatrix} 1 & d & 0 & 0 & c \\ 0 & 1 & 1 & c & 0 \\ 0 & -c & 0 & 1 & d \end{pmatrix}, \quad (12)$$

with two more positive parameters c and d . Thus, an arbitrary orthogonal UPB is defined, up to unitary transformations in \mathcal{H}_A and \mathcal{H}_B , by four continuous, positive parameters a, b, c, d .

Note that, for a given UPB, the parameter values are not uniquely determined, since this prescription does not specify a unique ordering of the five product vectors within the set. Any permutation that preserves the orthogonality relations pictured in Fig. 1 will generate a new set of values of the parameters that define the same UPB. These permutations form a discrete group with ten elements, generated by the cyclic shift $k \rightarrow k + 1$, and the reflection $k \rightarrow 6 - k$.

Given the orthonormal basis vectors α_j in \mathcal{H}_A and β_j in \mathcal{H}_B , we may think of the four positive parameters a, b, c, d as defining not only one single orthogonal UPB but a continuous family of generalized UPBs that are SL equivalent to this particular orthogonal UPB. The parameter values defining one such family may be computed from any UPB in the family via SL invariant quantities, in the following way. Given the product vectors $\phi_k \otimes \chi_k$ for $k = 1, 2, 3, 4, 5$, not necessarily orthogonal, we introduce expansion coefficients as in (9) and arrange them as column vectors

$$u_k = \begin{pmatrix} u_{1k} \\ u_{2k} \\ u_{3k} \end{pmatrix}. \quad (13)$$

Then we introduce the following quantities:

$$\begin{aligned} s_1 &= -\frac{\det(u_1 u_2 u_4) \det(u_1 u_3 u_5)}{\det(u_1 u_2 u_5) \det(u_1 u_3 u_4)} = a^2, \\ s_2 &= -\frac{\det(u_1 u_2 u_3) \det(u_2 u_4 u_5)}{\det(u_1 u_2 u_4) \det(u_2 u_3 u_5)} = \frac{b^2}{a^2}, \end{aligned} \quad (14)$$

where the values to the right are determined from the parametrization (10) of the orthogonal UPB defining the family. Similarly, we define

$$\begin{aligned} s_3 &= \frac{\det(v_1 v_2 v_3) \det(v_1 v_4 v_5)}{\det(v_1 v_2 v_5) \det(v_1 v_3 v_4)} = c^2, \\ s_4 &= \frac{\det(v_1 v_3 v_5) \det(v_2 v_3 v_4)}{\det(v_1 v_2 v_3) \det(v_3 v_4 v_5)} = \frac{d^2}{c^2}. \end{aligned} \quad (15)$$

The quantities s_1, s_2, s_3, s_4 defined in terms of 3×3 determinants are useful because they are invariant under SL transformations as in (7), and in addition they are independent of the normalization of the column vectors u_k and v_k . Obviously, many more similar invariants may be defined from five product vectors, but these four invariants are sufficient to characterize a family of UPBs that are SL equivalent to an orthogonal UPB.

There exists a less obvious further extension of the set of invariants. In fact, there are always six vectors that can be used to define invariants, since in addition to the five linearly independent product vectors of the UPB, the space spanned by these will always contain a sixth product vector. In the case of an orthogonal UPB, given by the parameters a, b, c, d , we have found (by means of a computer algebra program) explicit polynomial expressions for the components of the one extra product vector. We have checked, both analytically and numerically, that the existence of exactly six product vectors is a generic property of a five-dimensional subspace of the 3×3 dimensional Hilbert space \mathcal{H} . This number of product vectors is also consistent with the formula discussed in [4], which specifies more generally, as a function of the dimensions, the number of product vectors in a subspace of \mathcal{H} . For an orthogonal UPB in the 3×3 system the sixth vector is singled out because it is not orthogonal to the other vectors, but for a nonorthogonal UPB there is no intrinsic difference between the six vectors of the set, which should therefore be treated on an equal footing.

For a UPB that is SL equivalent to an orthogonal UPB there are strong restrictions on the values of invariants of this kind, since they are all rational functions of the four real parameters a, b, c, d . In particular, they must all take real values. A given choice of four invariants, as in (14) and (15), is sufficient to define the parameter space for the equivalence classes of these UPBs. But since the six product vectors listed in any order define the same UPB, and the same PPT state, there is a discrete set of $6! = 720$ symmetry transformations that introduce identifications between points in the corresponding parameter space. As we shall see in the following, the requirement that all four invariants s_1, s_2, s_3, s_4 should be positive allows 60 different orderings from the total of 720.

One should note that for a generalized UPB consisting of five randomly chosen product vectors the invariants will in general be complex rather than real, and it is not a priori

clear that four invariants are sufficient to parametrize the equivalence classes of random UPBs.

IV. CLASSIFYING THE RANK 4 ENTANGLED PPT STATES

We have in [4] described a method to generate PPT states ρ for given ranks (m, n) in low-dimensional systems, with $m = \text{rank } \rho$ and $n = \text{rank } \rho^P$. By repeatedly using this method with different initial data we have generated a large number of different PPT states of rank (4, 4) in the 3×3 system. They are all entangled PPT states, and as a consequence they are extremal PPT states. This follows from the fact that if they were not extremal they would have to be convex combinations involving entangled PPT states of even lower ranks, and such states do not exist.

The remarkable fact is that every one of these states has a UPB in its kernel which is SL equivalent to an *orthogonal* UPB, and the state itself is SL equivalent to the state constructed from the orthogonal UPB. We regard our numerical results as strong evidence for our belief that the four real parameters which parametrize the orthogonal UPBs give a complete parametrization of the rank 4 entangled PPT states of the 3×3 system, up to the SL (or more precisely $\text{SL} \otimes \text{SL}$) equivalence. We will describe here in more detail the numerical methods and results that lead us to this conclusion.

Assume ρ to be an entangled PPT state of rank (4, 4), found by the method described in [4]. The question to examine is whether it is SL equivalent to an entangled PPT state defined by the orthogonal UPB construction. We therefore make the *ansatz* that it can be written as $\rho \equiv \rho_2 = a_2 V \rho_1 V^\dagger$, where ρ_1 is defined by a so far unknown *orthogonal* UPB, parametrized as in (10) and (12), and where the transformation V is of product form, $V = V_A \otimes V_B$. We consider how to compute the product transformation V , assuming that it exists. The fact that we are able to find such a transformation for every (4, 4) state is a highly nontrivial result.

Given ρ , the first step is to find all the product vectors in $\text{Ker } \rho$. We solve this as a minimization problem: A normalized product vector $\psi = \phi \otimes \chi$ with $\rho \psi = 0$ is a minimum point of the expectation value $\psi^\dagger \rho \psi$. Details of the method we use are given in Ref. [4]. Empirically, we always find exactly six such product vectors $\psi_k = \phi_k \otimes \chi_k$, $k = 1, 2, \dots, 6$, any five of which are linearly independent and form a UPB, typically nonorthogonal.

Although the numbering of the six product vectors is arbitrary at this stage, we compute the invariants s_1, s_2, s_3, s_4 , substituting ϕ_k for u_k and χ_k for v_k , with $k = 1, 2, \dots, 5$. As shown by the previous discussion all four invariants have to be real, for otherwise no solution can exist. A random UPB has complex invariants, and the empirical fact that the invariants are always real for a UPB in $\text{Ker } \rho$, where ρ is a rank (4, 4) entangled PPT state, is a nontrivial test of the hypothesis that such a UPB can be transformed into orthogonal form.

It is not sufficient that the invariants are real. As shown by the expressions (14) and (15) there has to exist an ordering of the product vectors where all four invariants take positive values. The signs of the invariants will depend on the ordering of the product vectors, and most orderings produce both positive and negative invariants. For the rank (4, 4) density matrices that we have constructed, it turns out that it is always

possible to renumber the five first vectors in the set in such a way that all four invariants become positive. This is a further nontrivial test of our hypothesis.

There are in fact, in all the cases we have studied, precisely 10 of the 5! permutations of the five vectors that give positive values of the four invariants. This means that such an ordering is unique up to the symmetries noticed for the diagram in Fig. 1. However, there is a further symmetry, since the reordering which gives positive invariants works for any choice of the sixth vector of the set. The possible reorderings of all six product vectors which preserve the positivity of the invariants therefore define a discrete symmetry group with altogether $6 \times 10 = 60$ elements, which defines mappings between different, but equivalent, representations of the UPB in terms of the set of four real and positive invariants. The corresponding parameter transformations are given in the Appendix.

Assume now, for a given rank (4,4) state, that a “good” numbering has been chosen for the six product vectors $\psi_k = \phi_k \otimes \chi_k$ in the corresponding UPB, so that the four invariants defined by the first five vectors are all real and positive. The problem to be solved is then to find the transformation that brings the UPB into orthogonal form. This means finding 3×3 matrices C and D such that $\phi_k = N'_k C u_k$ and $\chi_k = N''_k D v_k$ for $k = 1, 2, \dots, 5$, with unspecified normalization constants N'_k and N''_k . Here the vectors u_k and v_k belong to an orthogonal UPB as given by the Eqs. (10) and (12), and these vectors are all known at this stage, because the invariants s_1, s_2, s_3, s_4 determine the parameters a, b, c, d . The transformation matrices C and D correspond to V_A^\dagger and V_B^\dagger in (7). The condition for two vectors ϕ_k and Cu_k to be proportional is that their antisymmetric tensor product vanishes; hence we write the following homogeneous linear equations for the matrix C :

$$\begin{aligned} \phi_k \wedge (Cu_k) &= \phi_k \otimes (Cu_k) - (Cu_k) \otimes \phi_k = 0, \\ k &= 1, 2, \dots, 5. \end{aligned} \quad (16)$$

Since the antisymmetric tensor product $\phi_k \wedge (Cu_k)$ has, for given k , three independent components, there are altogether fifteen linear equations for the nine unknown matrix elements C_{ij} . We may rearrange the 3×3 matrix C as a 9×1 matrix C and write a matrix equation

$$MC = 0, \quad (17)$$

where M is a 15×9 matrix. This equation implies that $(M^\dagger M)C = 0$. The other way around, the equation $(M^\dagger M)C = 0$ implies that $(MC)^\dagger (MC) = C^\dagger (M^\dagger M)C = 0$ and hence $MC = 0$. Thus we may compute the matrix C as an eigenvector with zero eigenvalue of the Hermitian 9×9 matrix $M^\dagger M$. The matrix D is computed in a similar way.

It is a final nontrivial empirical fact for the (4,4) states we have found that solutions always exist for the matrices C and D , whenever the ordering of the six product vectors $\psi_k = \phi_k \otimes \chi_k$ is such that the invariants s_1, s_2, s_3, s_4 are positive.

The result is that every rank (4,4) state of the 3×3 system which we have found in numerical searches [4] can be transformed into a projection operator with an orthogonal UPB in its kernel. We have also checked the published examples of entangled PPT states of rank (4,4), which are based on special

constructions [5,6,11,12], and have obtained the same result for these states. The explicit transformations have been found numerically by the method discussed here, and in all cases the four parameters a, b, c, d have been determined, with values that are unique up to arbitrary permutations of product vectors from the 60-element symmetry group.

V. SUMMARY AND OUTLOOK

The main result of this paper is a classification of the rank 4 entangled PPT states of the 3×3 system. We find empirically that every state of this kind is equivalent, by a product transformation of the form $SL \otimes SL$, to a state constructed from an orthogonal unextendible product basis. We refer to this type of equivalence as SL equivalence. We have shown how to parametrize the orthogonal UPBs by four real and positive parameters, and we have described how permutations of the vectors in the UPB give rise to identifications in the four-parameter space.

The concept of SL equivalence of states and of product vectors leads to a generalization of the concept of unextendible product bases so as to include sets of nonorthogonal product vectors, and further to the concept of equivalence classes of generalized UPBs that are SL equivalent to orthogonal UPBs. Thus, the parametrization of the orthogonal UPBs by four positive parameters is at the same time a parametrization of the corresponding equivalence classes of generalized UPBs.

We have described a method for checking whether a given rank 4 entangled PPT state in the 3×3 system is equivalent, by a product transformation, to a state constructed from an orthogonal UPB. It is a highly nontrivial result that all the rank-four entangled states that we have produced numerically, and all states of this kind that we have found in the literature, are SL equivalent to states that are generated from orthogonal UPBs. This we take as a strong indication that the parametrization of the UPBs in fact gives also a parametrization of all the equivalence classes of rank 4 entangled PPT states of the 3×3 system.

Apart from the pure product states, the rank 4 entangled PPT states are the lowest rank *extremal* PPT states among the 3×3 states that we have found in numerical searches, as reported on in [4]. The property of such a state—that it has a nonorthogonal UPB in its kernel, which means that there is a complete set of product vectors in $\text{Ker } \rho$ and no product vector in $\text{Im } \rho$ —is shared with the lowest rank extremal PPT states of the other systems that we have studied, of dimensions different from 3×3 . This has led us to conjecture that this is a general feature of the lowest rank extremal PPT states, valid also in higher dimensional systems [4], and to speculate that there may exist a generalization of the construction used for the 3×3 system in terms of orthogonal UPBs and SL transformations, which can be applied in the higher dimensional systems.

In higher dimensions the orthogonality condition is harder to satisfy, and therefore another condition may take its place as the defining characteristic of a special subset of extremal states from each SL equivalence class. This hypothetical new condition may involve the full set of product vectors in the subspace, rather than an arbitrarily selected subset as in the definition of the orthogonal UPBs. We consider examining this possibility, with the aim of parametrizing the lowest rank

extremal PPT states more generally, an interesting task for further research, and we are currently looking into the problem.

ACKNOWLEDGMENT

Financial support from the Norwegian Research Council is gratefully acknowledged.

APPENDIX: EQUIVALENT ORDERINGS OF THE SIX PRODUCT VECTORS

Assume that the sequence of product vectors $\psi_k = \phi_k \otimes \chi_k$, $k = 1, 2, 3, 4, 5$, in this order, is characterized by parameter values a, b, c, d , as computed from the invariants s_1, s_2, s_3, s_4 . It is convenient here to replace the parameters a, b, c, d by $\alpha = a^2$, $\beta = b^2$, $\gamma = c^2$, $\delta = d^2$.

Then the cyclic permutation $\psi_k \mapsto \tilde{\psi}_k$ with $\tilde{\psi}_1 = \psi_5$ and $\tilde{\psi}_k = \psi_{k-1}$ for $k = 2, 3, 4, 5$ corresponds to the following parameter transformation, which is periodic with period 5:

$$\begin{aligned} \tilde{\alpha} &= \frac{\beta}{1 + \alpha}, \\ \tilde{\beta} &= \frac{\beta}{\alpha(1 + \alpha)}, \\ \tilde{\gamma} &= \frac{1}{\gamma + \delta}, \\ \tilde{\delta} &= \frac{\gamma(1 + \gamma + \delta)}{\delta(\gamma + \delta)}. \end{aligned} \quad (\text{A1})$$

The inversion $\psi_1 \mapsto \tilde{\psi}_1 = \psi_1$, $\psi_k \mapsto \tilde{\psi}_k = \psi_{7-k}$ for $k = 2, 3, 4, 5$ corresponds to the parameter transformation $\tilde{\alpha} = \alpha$, $\tilde{\gamma} = \gamma$,

$$\begin{aligned} \tilde{\beta} &= \frac{\alpha(1 + \alpha)}{\beta}, \\ \tilde{\delta} &= \frac{\gamma(1 + \gamma)}{\delta}. \end{aligned} \quad (\text{A2})$$

Let $\psi_6 = \phi_6 \otimes \chi_6$ be the sixth product vector in the five-dimensional subspace spanned by these five product vectors. Then the sequence $\tilde{\psi}_1 = \psi_6$, $\tilde{\psi}_2 = \psi_5$, $\tilde{\psi}_3 = \psi_3$, $\tilde{\psi}_4 = \psi_4$, $\tilde{\psi}_5 = \psi_2$ corresponds to the parameter transformation $\tilde{\alpha} = \gamma$, $\tilde{\gamma} = \alpha$,

$$\begin{aligned} \tilde{\beta} &= \frac{\beta(1 + \gamma)(\alpha + \beta)(\gamma + \delta) + \delta}{\alpha(1 + \alpha + \beta)\delta + (1 + \alpha)(\alpha + \beta)(1 + \gamma)}, \\ \tilde{\delta} &= \frac{(1 + \alpha)[\beta\delta + (\alpha + \beta)\gamma(1 + \gamma + \delta)]}{[1 + \alpha + (1 + \alpha + \beta)(\gamma + \delta)]\delta}. \end{aligned} \quad (\text{A3})$$

It is not easy to see by looking at the formulas that this parameter transformation is its own inverse.

Altogether, these transformations generate a transformation group of order 60 (with 60 elements), isomorphic to the symmetry group of a regular icosahedron with opposite corners identified. Equivalently, it is the group of proper rotations of the icosahedron, excluding reflections. The icosahedron has twelve corners, and we may associate the six product vectors with the six pairs of opposite corners.

-
- [1] R. Horodecki, P. Horodecki, M. Horodecki, and K. Horodecki, *Rev. Mod. Phys.* **81**, 865 (2009).
[2] A. Peres, *Phys. Rev. Lett.* **77**, 1413 (1996).
[3] J. M. Leinaas, J. Myrheim, and E. Ovrum, *Phys. Rev. A* **76**, 034304 (2007).
[4] J. M. Leinaas, J. Myrheim, and P. Ø. Sollid, *Phys. Rev. A* **81**, 062329 (2010).
[5] C. H. Bennett, D. P. DiVincenzo, T. Mor, P. W. Shor, J. A. Smolin, and B. M. Terhal, *Phys. Rev. Lett.* **82**, 5385 (1999).
[6] D. P. DiVincenzo, T. Mor, P. W. Shor, J. A. Smolin, and B. M. Terhal, *Commun. Math. Phys.* **238**, 379 (2003).
[7] A. O. Pittenger, *Linear Algebr. Appl.* **359**, 235 (2003).
[8] P. Horodecki, M. Lewenstein, G. Vidal, and I. Cirac, *Phys. Rev. A* **62**, 032310 (2000).
[9] N. Alon and L. Lovasz, *J. Comb. Theory, Ser. A* **95**, 169 (2001).
[10] J. M. Leinaas, J. Myrheim, and E. Ovrum, *Phys. Rev. A* **74**, 012313 (2006).
[11] D. Bruß and A. Peres, *Phys. Rev. A* **61**, 030301(R) (2000).
[12] K. Ha, S. Kye, and Y. Park, *Phys. Lett. A* **313**, 163 (2003).

Unextendible product bases and extremal density matrices with positive partial transpose

Per Øyvind Sollid and Jon Magne Leinaas

Department of Physics, University of Oslo, N-0316 Oslo, Norway

(Dated: 1 November 2010)

Abstract

In bipartite quantum systems of dimension 3×3 the lowest rank entangled states that are positive under partial transposition (PPT) can be related, by product transformations, to states that are constructed by the use of unextendible product bases (UPB) in the Hilbert space of the system. Here we consider a possible generalization of the product bases, which can be related in a similar way to low-rank entangled density matrices in higher dimensions. The idea is to give up the condition of orthogonality of the product vectors, while keeping the relation between the density matrix and the projection on the associated UPB. We examine first this generalization for the 3×3 system where numerical studies indicate that one-parameter families of such generalized states can be found. Similar numerical searches in higher dimensional systems show the presence of extremal PPT states of the same form. Based on these results we indicate that the UPB construction of the lowest rank entangled states in the 3×3 system can be generalized to higher dimensions, with the use of non-orthogonal UPBs of the suggested form.

PACS numbers:

INTRODUCTION

One of the most striking features of quantum mechanics is found in the concept of entanglement. Considerable efforts have been made in understanding its properties and usefulness, with several different approaches taken [1]. One approach has been to study the geometrical structure of different convex sets of hermitian matrices that are related to subsets of quantum states with entanglement [2–7]. There are two convex subsets of the full set of density matrices, denoted \mathcal{D} , that are particularly important in this discussion. One is the set \mathcal{S} of non-entangled, or separable, states, and the other the set \mathcal{P} of density matrices that remain positive under partial transposition with respect to a subsystem. The states of \mathcal{P} are commonly referred to as PPT states. The non-entangled states are PPT by default, so we have the following set-theoretical relations $\mathcal{S} \subset \mathcal{P} \subset \mathcal{D}$.

In two previous papers we have examined the properties of entangled density matrices that are PPT, which means that they are contained in \mathcal{P} but not in \mathcal{S} [8, 9]. These states which are known to have *bound* entanglement are intrinsically interesting [10], but they are also interesting through the information they give about the full set of entangled states. In fact, the difficult part of establishing whether quantum states in general are entangled or separable is to do so for states that are PPT. This is so, since any state which is not PPT - a property that can easily be verified - is entangled.

The states studied in [8, 9] were found by performing systematic numerical searches for PPT-states with specified ranks for the density matrix ρ and for its partial transpose ρ^P . Such searches were performed for several bipartite systems of low dimensions, and in all cases, when the ranks were sufficiently low, the states were not only entangled but were typically extremal PPT states. An interesting result was that the lowest rank states of this type, with full local ranks, were found to have very similar properties, independent of their dimension. In particular they were all found to be extremal PPT states with a complete set of product states in their kernel, and no product states in their image.

For a bipartite system of dimension 3×3 there is a special subset of these lowest rank entangled PPT states that can be constructed by the use of *unextendible product bases* (UPB) [11]. The method provides a way to combine vectors in the two subsystems to form an orthogonal product basis that spans a five-dimensional subspace in the full Hilbert space, and which cannot be extended to include other product vectors orthogonal to the five states. The corresponding density matrix is constructed, up to a normalization, as the projection on the space orthogonal to the product vectors of the UPB. With the use of the numerical method described in [8] a large number of more

general entangled PPT states of rank 4 were generated, and it was shown that all of them, in a specific sense, were equivalent to density matrices that could be produced by the UPB construction. The equivalence classes were further shown to be parameterized by four real parameters, and the results were interpreted as evidence for the conclusion that all entangled PPT states of rank 4 in the 3×3 system are covered by this parametrization.

These results have motivated the present work, where we investigate a possible generalization of the UPB construction which makes it applicable to systems of dimensions higher than 3×3 . A simple copy of the UPB construction seems not possible, since in higher dimensions the orthogonality requirement is too demanding. Instead we focus on other properties of the construction. In the 3×3 system the projection on the five-dimensional subspace spanned by the orthogonal product vectors of the UPB can be written as a sum of one-dimensional projections defined by the product vectors, and the corresponding density matrix is defined as the projection on the orthogonal subspace. The partial transpose of the density matrix takes the same form, when expressed in terms of a related, conjugate UPB. In the present paper we study density matrices of the similar projection form, but without the requirement of orthogonality. Such states can be found in the 3×3 system, and we examine these states in some detail. We further focus on the question whether such generalized states can be found in systems of dimension higher than 3×3 .

The result is that we find such states in all the bipartite systems we have been able to examine. In addition to the 3×3 system this applies to systems of dimensions $3 \times n$ with n taking values up to 6, and we have further examined the 4×4 , 4×5 and 5×5 systems. The matrices we find are all of the projection form referred to above, with generalized, non-orthogonal UPBs in their kernel, and the partial transposed matrices are all found to have the same form.

The organization of the paper is as follows. We first discuss in some detail the generalized UPB construction for the lowest rank PPT states of the 3×3 system. These states have rank 4 for both for the density matrix ρ and its partial transpose ρ^P , and we thus refer to them as $(4, 4)$ states. We first illustrate the generalization by examining a special, symmetric case where the vectors of the UPB form a regular icosahedron, and find a one-parameter set of equivalent states that correspond to a linear deformation of the icosahedron. One of these states has an orthogonal UPB in its kernel, while for the general case the UPB is non-orthogonal.

We next describe a numerical method to search for more general matrices, with less symmetric UPBs. The method specifies these density matrices ρ to be projections with rank equal to 4 and to have a positive partial transpose. All matrices that we find in this way are quite remarkably not only projections, but have the form we refer to in the generalized UPB construction. Furthermore,

the partial transpose ρ^P has the same form when expressed in terms of the associated, conjugate UPB. All density matrices found in this way are extremal PPT states.

For the 3×3 system we have previously found numerically that generic extremal PPT states of rank $(4, 4)$, found by the method described in [8], can be transformed by product transformations to a projection form with orthogonal UPBs in their kernels [9]. Here we further investigate whether such states can be transformed to a projection form with more general UPBs in their kernels, dropping the orthogonality requirement on the transformed UPBs. The results show that this is the case, and furthermore strongly indicate that the projections belong to one-parameter classes of equivalent matrices, where density matrices defined by the *orthogonal* UPB construction are special cases.

For the higher-dimensional systems the method we use to generate density matrices of projection form with specified ranks also works well. When the rank is chosen to coincide with the rank of the generalized lowest rank extremal PPT states, as discussed in [8], we find matrices with the same properties as in the 3×3 system. The projection can thus be expressed in terms of a UPB in the kernel of the matrix, and the partial transpose has the same rank and structure when expressed in terms of its associated UPB. However, the method used to check equivalence under product transformations between generic extremal PPT states (of the given rank) and matrices of the correct projection form does not work so well in higher dimensions, and we have not been able to confirm that such an equivalence is present in dimensions higher than 3×3 .

We end with a summary and with a discussion of some of the questions that are left for further research.

LOWEST RANK EXTREMAL PPT STATES IN THE 3×3 SYSTEM

The construction of entangled PPT states of rank 4 in the 3×3 system, with the help of orthogonal UPBs, was originally discussed in [11]. A condition was there given for choosing a set of five vectors $\{\phi_k\}$ in subsystem A and a corresponding set of vectors $\{\chi_k\}$ in subsystem B so that the set of product vectors $\{\psi_k = \phi_k \otimes \chi_k\}$ would define an orthogonal UPB. From this set of product vectors a density operator of rank 4 could be constructed as a (normalized) projection operator in the following way

$$\rho = \frac{1}{4}(\mathbb{1} - \sum_{k=1}^5 \psi_k \psi_k^\dagger) \quad (1)$$

This form for ρ implies that the partial transpose ρ^P will have the same form when expressed in terms of a *conjugate* UPB, defined as $\{\tilde{\psi}_k = \phi_k \otimes \chi_k^*\}$, which is also a set of orthogonal product vectors. The complex conjugation of the second factor means that the partial transposition is performed with respect to subsystem B .

The important point is that the density matrix ρ , defined by the above expression, is necessarily entangled and PPT. It is entangled since there is no product state in the image of the matrix, and it is positive since it is proportional to a projection, which has only non-negative eigenvalues. For the same reason also the partial transpose is positive, and thus follows the PPT property of ρ . The density matrices defined by this construction form a proper subset of the entangled PPT states of rank 4 since the generic state of this type, according to our previous studies, will have a non-orthogonal UPB in its kernel [8].

The idea is now to relax the condition of orthogonality, but to keep other properties of the UPB construction. We examine this generalization first in the 3×3 system, but will subsequently examine the corresponding generalization for higher dimensional systems. The main condition is that the rank 4 density operator should be proportional to a projection operator, which we write as

$$\rho = \frac{1}{4}(\mathbb{1} - Q), \quad Q^2 = Q \quad (2)$$

where Q is assumed to be of the form

$$Q = 5 \sum_{k=1}^6 p_k \psi_k \psi_k^\dagger \quad (3)$$

with $\{\psi_k = \phi_k \otimes \chi_k\}$ as a set of product vectors that defines a generalized UPB. The coefficients p_k define an unspecified set of real parameters, not necessarily all positive, with $\sum_{k=1}^6 p_k = 1$.

Note that the sum over the product vectors now runs from 1 to 6. The reason for this is the following. The five dimensional subspace spanned by the UPB will always include a total of 6 product vectors [8]. When five of the product vectors are orthogonal, the 6th product state which is a linear combination of the other 5, is simply not included in the definition of ρ . We may view this as a special case of (2) and (3), with $p_6 = 0$. However, when there is no subset of the product vectors that is orthogonal it seems natural to define the generalization so that all product vectors in the five dimensional subspace are included, as we have done above.

The density matrix ρ defined by (2) and (3) is clearly entangled, since it has no product vector

in its image. Furthermore, the partial transpose ρ^P has the same form as ρ , when the product vectors ψ_k are replaced by the conjugate vectors $\tilde{\psi}_k = \phi_k \otimes \chi_k^*$, so that

$$\rho^P = \frac{1}{4}(\mathbb{1} - Q^P) \quad (4)$$

with Q^P given by

$$Q^P = 5 \sum_{k=1}^6 p_k \tilde{\psi}_k \tilde{\psi}_k^\dagger \quad (5)$$

Also in this case the vectors $\tilde{\psi}_k$ form a generalized UPB, however, the rank of Q^P is not necessarily the same as the rank of Q and neither is positivity of ρ^P obvious from the above expressions.

If all the coefficients p_k are positive and the operator Q thus is separable, this will imply that ρ^P is positive and of the same rank as ρ . However, since studies of higher dimensional systems seem to show that this is a too restrictive requirement, we instead make the assumption that Q^P , like Q , is a projection operator, so that $(Q^P)^2 = Q^P$. This also secures that ρ^P is positive and of the same rank as ρ , and consequently that ρ is an entangled PPT state.

For the generalization of the UPB construction we thus assume both the density matrix ρ and its partial transpose ρ^P to satisfy conditions of the form given by (2) and (3). At this point we lack a prescription for choosing vectors ϕ_k and χ_k of the subsystems so that the product vectors $\psi_k = \phi_k \otimes \chi_k$ define density matrices ρ and ρ^P that satisfy these conditions. For this reason we have instead focussed on the question if we can find, by numerical searches, states that satisfy these criteria, first in the 3×3 system and then in higher dimensional systems. In the 3×3 system we can, however, make an explicit construction of such states as a special case, and we shall discuss that case in the next section.

A SPECIAL CASE: THE ICOSAHEDRON

An especially symmetric case, with non-orthogonal product states, is formed by the icosahedron construction described here. The vectors ϕ_k and χ_k of the subsystems that combine into the product vectors of the generalized UPB are in this case all chosen to be real. The six vectors ϕ_k define the six symmetry axes of a regular icosahedron that pass through its twelve corners. A particular choice of (non-normalized) vectors is specified by the following sets of Cartesian coordinates

$$\phi_1 = (-\phi, 0, 1), \quad \phi_2 = (-1, \phi, 0), \quad \phi_3 = (1, \phi, 0),$$

$$\phi_4 = (\phi, 0, 1), \quad \phi_5 = (0, -1, \phi), \quad \phi_6 = (0, 1, \phi) \quad (6)$$

with $\phi = (\sqrt{5} + 1)/2$ as the golden ratio. These are also the coordinates of six of the corners of the icosahedron, when the center is located at the origin.

The second set of vectors, $\{\chi_k\}$, is chosen as the same set (6), but in order to form the correct combinations $\psi_k = \phi_k \otimes \chi_k$, the ϕ_k and χ_k vectors have to be differently ordered. A particular choice is $\chi_k = \phi_{(2k+4) \bmod 5}$ for $k = 1, \dots, 5$ and $\chi_6 = -\phi_6$, but in total there are 60 acceptable orderings, related to the 60 rotational symmetries of the icosahedron. With all these orderings the six product vectors span a five-dimensional subspace of the Hilbert space.

The vectors (6) define six equiangular lines, which means that the scalar product between all pairs of vectors are equal up to a sign. With normalized vectors the scalar products are

$$g_{kl}^A \equiv \phi_k^\dagger \phi_l = \pm \frac{1}{\sqrt{5}}, \quad g_{kl}^B \equiv \chi_k^\dagger \chi_l = \pm \frac{1}{\sqrt{5}}, \quad k \neq l \quad (7)$$

For the product vectors $\psi_k = \phi_k \otimes \chi_k$ the scalar products are also equal up to a sign, and by choosing the particular ordering of the χ_k , referred to above, we obtain

$$g_{kl} = g_{kl}^A g_{kl}^B = -\frac{1}{5} \quad \forall k \neq l, \quad k, l = 1, \dots, 6 \quad (8)$$

We now consider the following operator

$$Q = \frac{5}{6} \sum_{k=1}^6 \psi_k \psi_k^\dagger \quad (9)$$

which is of the form (3) with all six coefficients equal, $p_k = 1/6$. The condition that it should define a projection, $Q^2 = Q$, can be written as

$$\psi_k = 5 \sum_{l \neq k} g_{lk} \psi_l, \quad g_{lk} = \psi_l^\dagger \psi_k \quad (10)$$

and this should be satisfied for all k . When g_{kl} is chosen as in (8) it gives the symmetric condition

$$\sum_{k=1}^6 \psi_k = 0 \quad (11)$$

and it is straight forward to check that this is equation is satisfied for the product vectors of the regular icosahedron.

The product vectors $\{\psi_k\}$ define a generalized UPB. Thus, there is no product vector orthogonal to the set, as can easily be checked, and the vectors are non-orthogonal. The set defines an entangled PPT state in the form of the density operator

$$\rho = \frac{1}{4}(\mathbb{1} - \frac{5}{6} \sum_{k=1}^6 \psi_k \psi_k^\dagger) \quad (12)$$

It is entangled since there is no product vector in its image, and it is PPT since the vectors are all real, and the partial transposition thus leaves the density operator invariant, $\rho^P = \rho$.

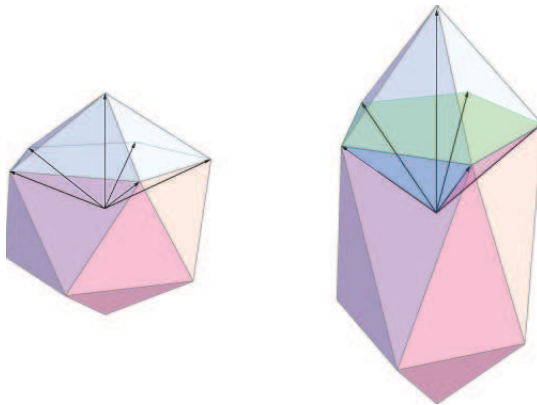


FIG. 1: The icosahedron construction. A regular icosahedron, shown to the left, defines a set of six equiangular lines through the twelve corners. A corresponding set of six vectors along these lines are shown in the figure. Tensor products of six pairs of such vectors define the vectors of the UPB, as explained in the text, and all of these appear with equal weight in the construction of the corresponding entangled PPT state. To the right a stretched icosahedron is shown where five of the vectors are used to define an orthogonal UPB. These vectors point along edges of a regular pyramid with a pentagon as base, which appears upside down in the figure. This construction has previously been referred to as the Pyramid [11]. The corresponding UPB defines an entangled PPT state where the five product states appear with equal weight, and where the sixth vector does not appear.

States that are related by non-singular product transformations

$$\rho' = S\rho S^\dagger, \quad S = S_A \otimes S_B \quad (13)$$

where A and B refer to the two subsystems, all have the same characteristics as being separable or entangled. They also share the property of being positive or not under partial transposition and they have the same rank. This is trivially the case for unitary product transformations, but it is also true for non-unitary transformations, in which case the transformed matrix ρ' should further

be normalized to unity. The operators S_A and S_B can be restricted, without loss of generality, to be unimodular, and for this reason we refer to the relation as $SL \otimes SL$ -equivalence (or simply SL -equivalence) [9]. For the density operator (12) there is a subset of such SL -equivalent states that can be written in the form of projections (3). Clearly unitary product transformations will leave this form invariant, but it is of interest to note that there is a one-parameter set of non-unitary transformations that also leaves the projection form invariant. As opposed to the unitary transformations these transformations will change the coefficients p_k in the expansion (3).

The non-unitary SL -transformations are of the symmetric form $S = S_A \otimes S_B$ with $S_A = S_B$, where S_A rescales the length in the direction of one of the symmetry axes of the icosahedron. In the following we choose this to be the direction of ϕ_6 , so that the transformation squeezes or elongates the icosahedron along this axis. This can be described in terms of a stretching parameter λ , so that the unit vectors pointing towards the corners of the deformed icosahedron are

$$\phi_k(\lambda) = N(\lambda) \left(\phi_k + (\lambda - 1)(\phi_6^\dagger \phi_k) \phi_6 \right), \quad k \neq 6; \quad \phi_6(\lambda) = \phi_6 \quad (14)$$

with $N(\lambda)$ as a normalization constant. For symmetry reasons, the coefficients $p_k(\lambda)$ are all equal for $k \neq 6$. It is straight forward to show that

$$p_6(\lambda) = \frac{4 + 2\lambda^2 - \lambda^4}{20 + 10\lambda^2}; \quad p_k(\lambda) = \frac{(1 - p_6(\lambda))}{5} \quad \forall \quad k \neq 6 \quad (15)$$

The stretching parameter is chosen with $\lambda = 1$ for the regular icosahedron with $p_k = 1/6$ for $k = 1, \dots, 6$, in which case all product vectors contribute equally. When $\lambda = 0$ the squeezed icosahedron collapses to a plane, at which point the set of product vectors cease to be a UPB since the vectors ϕ_k for $k = 1, \dots, 5$ all lie in the two-dimensional plane orthogonal to ϕ_6 . For the particular value $\lambda = \sqrt{2\phi}$ the five product vectors, with $k = 1, 2, \dots, 5$, become orthogonal, and thereby define an orthogonal UPB. This is the Pyramid construction discussed as a particular case of a UPB construction in [11]. In this case the coefficients are $p_k = 1/5$ for $k \neq 6$ and $p_6 = 0$. The relation between this set and the stretched icosahedron is illustrated in Fig.1.

THE GENERAL CASE OF RANK (4, 4) ENTANGLED PPT STATES

We focus now on general entangled PPT states of rank (4, 4) in the 3×3 system, which are necessarily also extremal PPT states. In a previous study [8] we have numerically produced a large number of such states, and we have found that they all can be transformed, by product

transformations, to states of the special form given by (1), with an *orthogonal* UPB in the kernel of the density matrix [9]. The question that we now discuss is whether these are only special cases, and that more general states on the projection form given by (2) and (3) can be found. In order to examine this we have applied two different numerical methods to search for density matrices of the desired form.

The first method applies search criteria which do not directly refer to the conditions (2) and (3). Instead the search is for density matrices ρ with the correct rank 4, which are PPT and of projection form. This means that all the non-vanishing eigenvalues should be equal. The method is essentially the same as used in [8] to search for PPT states of rank (4, 4). Here however, we impose no restriction on the rank of ρ^P , only that $\det \rho^P \geq 0$. It is a linearized, iterative method which specifies a certain number of the eigenvalues of ρ to vanish, and in this case also the remaining eigenvalues to be equal. We refer to [8] for details concerning the iterative method. A similar approach is also used in the second method, to be discussed below.

The result is that the numerical method works well, and a large number of states which satisfy the search criteria have been found. Even if we do not introduce any explicit constraint on ρ^P , only the conditions that ρ is PPT and is proportional to a projection, we find always ρ^P also to be proportional to a projection. Thus, both ρ and ρ^P satisfy the conditions (2) and (3).

To gain some more information about the type of density matrices we want to obtain, we have applied a second numerical method. It introduces a search for a product transformation which maps, if possible, a chosen rank (4, 4) extremal PPT state into the form of a projection. We do not, in this search either, impose any condition on how this projection is expressed in terms of product vectors. Also this method applies a linearized, iterative approach to determine the product transformation, which we now outline.

Let us denote the initial density matrix by ρ_0 and the final density matrix by ρ . Their relation should then be of the form

$$\rho = S\rho_0S^\dagger, \quad S = S_A \otimes S_B \tag{16}$$

and the condition that the transformed density matrix is a projection gives

$$S\rho_0S^\dagger S\rho_0S^\dagger = S\rho_0S^\dagger \tag{17}$$

(Note that the density matrix ρ is then not normalized to unity.) The transformation S is assumed

to be non-singular, and the condition can then be simplified to

$$\rho_0 S^\dagger S \rho_0 = \rho_0 \quad (18)$$

The unknown transformation matrix S we parametrize by expressing S_A and S_B as linear combinations of a complete set of 3×3 hermitian matrices. The corresponding product transformations are parametrized by 17 real parameters μ_k , which we interpret as components of a vector $\boldsymbol{\mu}$. Furthermore we express the rank 4 matrices as 16-component vectors in the space of hermitian operators within the image of ρ_0 . Written as a vector equation, Eq. (18) has the form

$$\mathbf{F}(\boldsymbol{\mu}) = \rho_0 \quad (19)$$

Assume now that $\boldsymbol{\mu}'$ is a trial vector that gives an approximate solution to Eq. (19). We write the deviation from the true solution as $\Delta\boldsymbol{\mu} = \boldsymbol{\mu} - \boldsymbol{\mu}'$, and treat this as a perturbation. To first order in $\Delta\boldsymbol{\mu}$ the equation reads in matrix form

$$\mathbf{B}\Delta\boldsymbol{\mu} = \rho_0 - \mathbf{F} \quad (20)$$

with \mathbf{B} as a real, non-quadratic 16×17 matrix with elements $B_{kn} = \partial F_k / \partial \mu_n$, and where both \mathbf{F} and \mathbf{B} are evaluated with the trial vector $\boldsymbol{\mu}'$. By multiplying with the transposed matrix \mathbf{B}^T and introducing the positive, real symmetric matrix $\mathbf{A} = \mathbf{B}^T \mathbf{B}$, as well as $\mathbf{a} = \mathbf{B}^T(\rho_0 - \mathbf{F})$, the equation can be written in the form

$$\mathbf{A}\Delta\boldsymbol{\mu} = \mathbf{a} \quad (21)$$

where \mathbf{a} and \mathbf{A} are determined by the trial vector $\boldsymbol{\mu}'$ and $\Delta\boldsymbol{\mu}$ is the unknown to be determined by the equation. Written in the form (21) the equation is well suited to be solved numerically by the conjugate gradient method [12].

An iterative approach is used to find a solution of the original problem. A starting point $\boldsymbol{\mu}_1$ is chosen for the trial vector, and this determines the initial versions of \mathbf{a} and \mathbf{A} . Eq. (21) is then solved numerically to give a first solution $\Delta\boldsymbol{\mu}_1$. The trial vector is then updated with $\boldsymbol{\mu}_2 = \boldsymbol{\mu}_1 + \Delta\boldsymbol{\mu}_1$, this vector is used to improve \mathbf{a} and \mathbf{A} , and a new improved solution $\Delta\boldsymbol{\mu}_2$ of (21) is found. If repeated iterations of this procedure leads to convergence, in the sense $\Delta\boldsymbol{\mu} \rightarrow 0$, the limit value of $\boldsymbol{\mu}$ gives a solution to the original problem (19) and (18).

A possible problem with this method is that the solution we find may correspond to a singular transformation matrix S , which will not give a density matrix ρ with correct properties. However, for the 3×3 system, by repeatedly applying the method with different starting points, we have found that usually the convergence of the method is quite rapid, and the solution that we find corresponds to a non-singular product transformation.

The result from applying the above method to the rank $(4, 4)$ states of the 3×3 system is that for a large number of initial density matrices that we have used, we can in all cases transform the density matrix by a non-singular product transformation to a matrix with the form of a projection. Also, in all cases, we find density matrices ρ that have the form specified by (2) and (3), when expressed in terms of the (non-orthogonal) UPB in the kernel of the density matrix. Furthermore, the partially transposed density matrices ρ^P are, in all cases, proportional to projections, and can be written in the form given by (2) and (3). This happens even if only ρ is required to have the form of a projection in the numerical search.

By keeping ρ_0 in (18) fixed and choosing repeatedly different starting points μ_1 in (19) for the first iteration, we get different results for the the density matrix ρ determined by the above method. This indicates that there is a large number of different states on projection form within a given set of SL -equivalent $(4, 4)$ states. In fact there are several indications that there is a one parameter set of such states, which can be related by non-unitary product transformations, within any given equivalence class of extremal PPT states with this rank. The first indication is simply based on parameter counting. As already discussed the number of equations that determine a product transformation that transforms a state of rank 4 to the projection form is 16 while the number of parameters to be determined by the equations is 17.

The second indication is found by listing the parameter sets $\{p_k, k = 1, 2, \dots, 6\}$ for SL -equivalent states on projection form that we generate by our method. As shown in Fig.2a a large set of different distribution is found, consistent with the assumption that there is a continuum of equivalent states. If one of the parameters is restricted to a very limited interval, the corresponding sets $\{p_k\}$ seem either to be identical (up to the limitation set by the fixed parameter), or to divide into a small number of distinct groups, each of which are essentially identical. This is illustrated in Fig.2b. This is consistent with the assumption that the full set is specified, up to a discrete set of possibilities, by a single continuous parameter.

All this seems to show that the picture is similar to that of the icosahedron case, so that any extremal PPT state of rank $(4, 4)$ is SL -equivalent to a one parameter set of states on the projection form given by (2) and (3). And for each of these the partial transposed density matrices has the

same projection form. (Note that the trivial equivalence under unitary product transformations is not included in this parameter counting.)

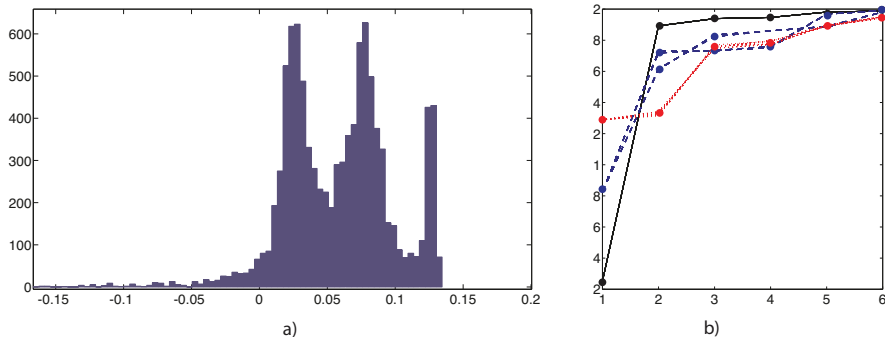


FIG. 2: **a)** The figure shows the distribution of the smallest coefficient in the set $\{p_k\}$ for approximately 9500 SL -equivalent states on projection form, all of which are SL -equivalent to a generic rank $(4,4)$ extremal state. We observe that we find a large distribution that seems to cover all possible values from 0 up to an upper limit which is smaller than $1/6$, which is the upper limit of the icosahedron states. This implies that such generic rank $(4,4)$ extremal states are less symmetric than the icosahedron-class of states. The continuous nature of the distribution also supports the one-parameter family theory, while we do not have an explanation for the particular profile of the distribution. **b)** These plots show some of the sets $\{p_k\}$ where the smallest parameter is specified within a very limited interval. With this limitation the rest of the set is found to be uniquely defined within essentially the same limitation. In one case, however (the dashed blue curve), there are two distinct groups of parameter sets with the same smallest coefficient. These observations support the claim that the SL -equivalent states on projection form defines a continuous one-parameter set of states.

HIGHER DIMENSIONS

The lowest rank extremal PPT states in the 3×3 system have their counterparts in higher dimensional systems. Thus, in previous numerical studies of PPT states in several systems of dimension $N_A \times N_B$, with N_A and N_B larger than 2, we have found such states with rank given by

$$r = N_A + N_B - 2 \quad (22)$$

for both ρ and ρ^P [8]. These PPT states are typically extremal, all with a UPB with a finite number of (non-orthogonal) product vectors in their kernel. This is a situation which is different from what we find for entangled PPT states with other values of the rank. Based on these results

we have conjectured that, quite generally for higher dimensional systems, the number (22) gives the lowest rank of extremal PPT states *with full local ranks* for a bipartite system of dimension $N_A \times N_B$. The number of product states for a UPB associated with any of these states is [8]

$$p = \frac{(N_A + N_B - 2)!}{(N_A - 1)!(N_B - 1)!} \quad (23)$$

and the number of linearly independent product states is

$$d = N_A N_B - N_A - N_B + 2 \quad (24)$$

In Table 1 we have listed the relevant number of product states for the systems which we have studied numerically in this work. The table also includes a list of dimensions for the sets of PPT states with the relevant ranks in these systems, as well as the number of parameters needed to specify the classes of *SL*-equivalent matrices of this type. These numbers are based on numerical studies that we have now performed, and which are described below.

system	ranks	p/d	dimensions
3×3	(4, 4)	6/5	36/4
3×4	(5, 5)	10/7	55/9
3×5	(6, 6)	15/9	77/13
3×6	(7, 7)	21/11	102/16
4×4	(6, 6)	20/10	75/15
4×5	(7, 7)	35/13	96/18
5×5	(8, 8)	70/17	119/23

TABLE I: Ranks and numbers of product states in the kernel of lowest rank extremal PPT states (with full local rank) in a series of bipartite systems of low dimensions. The first column gives the dimensions of the two subsystems, the second column the ranks of the density matrices and their partial transpose (which are equal for all these states), the third column gives the total number of product states in the kernel of the density matrices as well as the number of linearly independent product vectors, and the fourth column gives the dimension of the set of the density matrices and the number of parameters needed to parameterize the classes of *SL*-equivalent density matrices.

The method used to determine the dimensions of the sets of PPT states is based on the counting of different ways to make small perturbations away from a density matrix ρ of a given rank (m, n) , in such a way that the ranks of the matrix and its partial transpose are preserved. Consider then ρ_0 to be an extremal PPT state, and (m, m) to be the (symmetric) ranks of the density matrix and its transpose. A perturbation of this state we write as

$$\rho = \rho_0 + \epsilon\sigma, \quad \epsilon \ll 1 \quad (25)$$

Further, let P be the projector onto the image of ρ_0 and Q the projector onto the image of ρ_0^P . The following conditions, $(I - P)\sigma(I - P) = 0$ and $(I - Q)\sigma^P(I - Q) = 0$, secures that the ranks (m, m) , to first order in ϵ , do not change under the perturbation. We rewrite the conditions as

$$\sigma = P\sigma + \sigma P - P\sigma P \equiv \phi_P(\sigma), \quad \sigma^P = Q\sigma^P + \sigma^P Q - Q\sigma^P Q \equiv \phi_Q(\sigma^P) \quad (26)$$

The maps ϕ_P and ϕ_Q define linear operators \mathbf{P} and \mathbf{Q} that act as projectors on the real vector space of hermitian matrices. The previous equations can therefore be written as

$$\mathbf{P}\sigma = \sigma, \quad \mathbf{Q}\sigma^P = \sigma^P \quad (27)$$

with σ and σ^P viewed as vectors. The partial transpose can further be expressed as a linear operator $\mathbf{\Pi}$ in this space, so that $\mathbf{\Pi}\sigma = \sigma^P$ [13]. With the definition $\bar{\mathbf{Q}} \equiv \mathbf{\Pi}\mathbf{Q}\mathbf{\Pi}$, the two equations in (27) can be combined in the single equation

$$\mathbf{P}\bar{\mathbf{Q}}\mathbf{P}\sigma = \sigma \quad (28)$$

and the number of linearly independent matrices σ that obey this equation will then be precisely the dimension of the set of matrices with rank (m, m) in which ρ_0 sits.

The number of linearly independent matrices σ can be found by calculating the matrix $\mathbf{P}\bar{\mathbf{Q}}\mathbf{P}$ and counting the number of its eigenvalues that are equal to 1. As we are interested in the dimension of the set of *extremal* density matrices, with the specified rank, we have also checked whether the states close to ρ_0 are typically extremal. This has been done by repeatedly perturbing ρ_0 in different directions and checking the perturbed states for extremality. Since the rank, for a finite perturbation, will generally increase as a higher order effect in ϵ , we have in each perturbation corrected for this by including a second search, if necessary, for a closely density matrix with correct rank, before checking for extremality.

The result is that for all the states listed in Table 1, we find that the density matrices with the correct ranks (m, m) in the neighborhood of a chosen extremal density matrix are typically also extremal. This we take as a clear indication that the dimension we calculate is also the dimension of the set of *extremal* states with the given rank.

To determine from this dimension the number of parameters that is needed to parametrize the classes of SL -equivalent states, we have subtracted the number of parameters that specify a product transformation of the form $SL(N_A, \mathbb{C}) \times SL(N_B, \mathbb{C})$. Each factor is specified by $2N^2 - 2$

real parameters, and the total number of parameters is therefore $2(N_A^2 + N_B^2) - 4$. The numbers given in Table 1 are obtained by such subtractions. In particular the number of parameters found in this way for the $(4, 4)$ states of the 3×3 system is 4. This agrees with the conclusion reached in [9].

PROJECTION OPERATORS IN HIGHER DIMENSIONS

The same numerical methods that have been used to study the $(4, 4)$ states of the 3×3 system we have also applied to the extremal PPT states in higher dimensional systems. A specific case is the 4×4 system, where the relevant states are of rank $(6, 6)$. These density matrices have a UPB with 20 product vectors in their kernel, 10 of these being linearly independent. As shown in Table 1 we find that these states form a 75-parameter subset within the 255-parameter set of density matrices of the 4×4 system. The number of parameters determining a product transformation in the 4×4 system is 60, which leaves us with 15 parameters with which to parameterize the equivalence classes.

The method we use to search for PPT states of the correct rank and on projection form, works well also for this system, and we have by use of the method generated a large number of density matrices with these characteristics. We find, precisely as in the 3×3 system, that the density matrices always have a diagonal form, similar to (3), when expressed in terms of the product vectors of the UPB. In the 4×4 system the correct expressions for the density matrix ρ and the corresponding projection Q is

$$\rho = \frac{1}{6}(\mathbb{1} - Q), \quad Q = 10 \sum_{k=1}^{20} p_k \psi_k \psi_k^\dagger, \quad Q^2 = Q \quad (29)$$

with $\psi_k = \phi_k \otimes \chi_k$ as the product states of the UPB. Precisely as in the 3×3 system we also here find that the partially transposed operator Q^P is a projection with the same rank as Q , so for the density matrices that we find there is complete symmetry between ρ and ρ^P ,

$$\rho^P = \frac{1}{6}(\mathbb{1} - Q^P), \quad Q^P = 10 \sum_{k=1}^{20} p_k \tilde{\psi}_k \tilde{\psi}_k^\dagger, \quad (Q^P)^2 = Q^P \quad (30)$$

where $\tilde{\psi}_k = \phi_k \otimes \chi_k^*$ are the product vectors of the conjugate UPB.

The states we find have generally $p_k \neq 0$ for all $k = 1, 2, \dots, 20$. However, while most of these coefficients are positive, a small number of them will usually be negative. This is different from

what we find in the 3×3 system, where the typical situation is that all p_k are positive, but where we occasionally find one of them to be negative.

Also for the 4×4 system we have investigated the possibility of transforming a generic extremal PPT state of rank $(6, 6)$ to the projection form. The method we use is the same as for the 3×3 system, where we search for solutions to Eq. (18), with ρ_0 as a density matrix with the correct rank, which is generated by the method described in [8]. However, as opposed to the case with the $(4, 4)$ states of the 3×3 system, we have only for special choices of matrices ρ_0 been able to find product transformations that transform ρ_0 to the projection form. In the general case the iterative method that we use does not converge to an acceptable solution. Instead it shows a slow convergence towards a singular transformation matrix.

The lack of convergence in this case may be a consequence of the increase in the number of variables in the problem, and therefore to a decrease in the efficiency of the iterative procedure. But a clear possibility is that in the 4×4 system a generic extremal PPT state of rank $(6, 6)$ cannot be transformed by a product transformation to the form of a projection. In fact, the form of the equation (18) that we seek solutions for may indicate that this is the case. By counting the variables of the equation we find that the set of equations is underdetermined in the 3×3 system, but it is overdetermined in the 4×4 system as well as in other higher dimensional systems. (That does not, however, exclude the possibility that for the special density matrices that we consider there should exist solutions to the equation.)

The other higher-dimensional systems that are listed in Table 1 have been studied by the same methods as the 3×3 and 4×4 systems, and the results are essentially the same as for the 4×4 system. This means that the searches for PPT states ρ with rank m as specified in Table 1, which are proportional to projection operators, are in most cases successful. By varying the initial value in the search we have therefore been able, for most of the listed systems, to generate a large number of different solutions. For systems of dimension $N = N_A N_B \geq 20$ the iterative methods become rather slow, so the number of solutions we have found for them is somewhat smaller, though we find solutions also there. In all cases we find density matrices of the same form as shown in (29). We also find in all cases that the partially transposed matrix ρ^P is of the same rank as ρ . It is also a projection, and therefore we have a complete symmetry between ρ and ρ^P , similar the one given by (29) and (30) for the 4×4 system.

For comparison we have also made searches for PPT states that are proportional to projections with ranks higher than those indicated in Table 1, in which case there is typically no UPB in the kernel of the matrix. The result is that we are able to find also such density matrices, but now the

situation is different. In these cases the typical solution ρ has a partial transpose ρ^P with a higher rank and which is not proportional to a projection.

We have for all the listed higher dimensional systems also performed searches for product transformations that transform a generic extremal PPT state, with the specified rank, to projection form. For these systems the result is the same as for the 4×4 system, that the searches in most cases are unsuccessful. Thus, only for the 3×3 system do we find that we are able to transform the generic extremal PPT states of the given rank into the projection form.

CONCLUSIONS

The motivation for the present work has been to examine the possibility of generalizing the method of constructing entangled PPT states with the use of unextendible product bases (UPB). The established form of this construction is to use a set of orthogonal product states, with no product states in the orthogonal subspace, and to define the corresponding density matrix as a projection operator with the UPB in its kernel. The method applies particularly to rank $(4, 4)$ states in bipartite quantum systems of dimension 3×3 , and as previously shown in numerical studies all entangled PPT states with this rank seem to be equivalent under product transformations to the states constructed in this way [9].

In higher dimensional bipartite systems there are states that share many of the properties with the $(4, 4)$ states of the 3×3 system. They have all a complete set of product states in their kernel and no product state in their image, and they all seem also to share the property of being the lowest rank extremal PPT states in the system under consideration. The idea is to extend the UPB construction to these states. It seems not to be possible to extend the construction with *orthogonal* product states to higher dimensions, and we have focussed on the possibility of using non-orthogonal UPBs which keep some of the other properties of the original construction. Our assumption is that we can define these density matrices more generally as projections which can be expressed in a particular way in terms of product vectors of the non-orthogonal UPB.

We have first examined this generalization for rank $(4, 4)$ extremal PPT states of the 3×3 system. In this case an explicit example can be found, with the vectors of the generalized UPB defined by the symmetry axes of an icosahedron. All the six product vectors of this UPB appear with equal weight in the definition of the corresponding extremal PPT state. We can further show, by a linear deformation of the icosahedron, that a one-parameter set of different density matrices on projection form exists, where the matrices are equivalent under product transformations.

To study more general states we have applied numerical methods. The first method is to search for PPT states which have rank 4 and which are proportional to projections. The searches have been used to generate a large set of such states and these states have been found always to be on the form suggested by the generalized UPB construction, where ρ and ρ^P have equal ranks, are both proportional to projections and have the same form when expressed in terms of the product vectors of the UPBs associated with the two matrices.

A second method has been used to check whether generic extremal PPT states of rank $(4, 4)$ are equivalent under product transformations to density matrices of the form suggested for the generalized UPB construction. This has been demonstrated numerically and the numerical studies suggest that each state is equivalent to a one-parameter set of density matrices of this form where the matrices associated with an orthogonal UPB constitute a discrete subset.

To examine the relevance of the generalized UPB construction in bipartite systems of higher dimensions, we have first studied numerically the dimensions of the sets of extremal PPT states of the corresponding ranks. We have then applied the same numerical methods as used for the 3×3 system to search for density matrices of the suggested form. The search is thus for PPT states on projection form, with the specified rank, and the result are similar to those found in the 3×3 system. For all the systems a large number of states which satisfy the search criteria have been found, and they all show a complete symmetry between the density matrix and its partial transpose. They have the same rank, are both projections and can be expressed in terms of the product vectors of the associated UPBs in the same way. This demonstrates that the requirements suggested for a generalized UPB construction are satisfied for a large set of states in all these systems.

We have however observed a difference between the 3×3 system and higher-dimensional systems when performing searches for states of projection form that are equivalent under product transformations to a randomly generated extremal PPT state of the correct rank. As we mentioned, in the 3×3 system the results indicate that any extremal PPT state with the specified rank is equivalent to a one-parameter set of states on projection form, where the states associated with *orthogonal* UPBs form a discrete subset. In higher dimensions similar searches have been unsuccessful in most cases. This may suggest that the density matrices in higher dimensions that are of the form specified in the searches form a proper subset of the full set of extremal PPT states with the given rank. However, we do not exclude that the search method itself may be responsible for the result, due to a slower convergence for systems of higher dimensions.

Based on these results we suggest that the generalized UPB construction may be relevant for

construction of low-rank extremal PPT states in higher dimensions. Our study thus shows that extremal PPT states of the suggested form exist in all the higher-dimensional systems we have been able to examine. However, we still lack a concrete prescription for constructing generalized UPBs which define density matrices with the right properties. This problem, to find such a prescription, and also the question about how general the density matrices of this form are, we shall therefore have to leave as interesting questions for further studies.

-
- [1] Horodecki, Ryszard and Horodecki, Paweł and Horodecki, Michał and Horodecki, Karol, *Rev. Mod. Phys.* **81**, 865 (2009).
 - [2] M. Kus and K. Życzkowski, *Phys. Rev. A* **63**, 032307 (2001).
 - [3] F. Verstraete, J. Dehaene and B. De Moor, *Jour. Mod. Opt.* **49**, 1277 (2002).
 - [4] M. Lewenstein, B. Kraus, P. Horodecki and J. I. Cirac, *Phys. Rev. A* **63**, 044304 (2001).
 - [5] A.O. Pittenger and M.H. Rubin, *Phys. Rev. A* **67**, 012327 (2003).
 - [6] J. M. Leinaas, J. Myrheim and E. Ovrum, *Phys. Rev. A* **74**, 012313 (2006).
 - [7] I. Bengtsson and K. Życzkowski, Cambridge University Press (2006).
 - [8] J. M. Leinaas, J. Myrheim and P.Ø. Sollid, *Phys. Rev. A*, **81**, 062329 (2010)
 - [9] J. M. Leinaas, J. Myrheim and P.Ø. Sollid, *Phys. Rev. A*, **81**, 062330 (2010)
 - [10] M. Horodecki, P. Horodecki and R. Horodecki, *Phys. Rev. Lett.* **80**, 5239 (1998).
 - [11] C.H. Bennett, D.P. DiVincenzo, T. Mor, P.W. Shor, J.A. Smolin, and B.M. Terhal, *Phys. Rev. Lett.* **82**, 5385 (1999).
 - [12] G. H. Golub and C. F. Van Loan, *Matrix Computations* (North Oxford Academic Publishing, 1986)
 - [13] J. M. Leinaas, J. Myrheim and E. Ovrum, *Phys. Rev. A* **76**, 034304 (2007).

Low rank positive partial transpose states and their relation to product vectors

Leif Ove Hansen^a, Andreas Hauge^a, Jan Myrheim^a, and Per Øyvind Sollid^b
(a) Department of Physics, Norwegian University of Science and Technology,

N-7491 Trondheim, Norway

(b) Department of Physics, University of Oslo,
N-0316 Oslo, Norway

December 13, 2010

Abstract

It is known that entangled mixed states that are positive under partial transposition (PPT states) must have rank at least four. In a previous paper we presented a classification of rank four entangled PPT states which we believe to be complete. In the present paper we continue our investigations of the low rank entangled PPT states. We use perturbation theory in order to construct rank five entangled PPT states close to the known rank four states, and in order to compute dimensions and study the geometry of surfaces of low rank PPT states. We exploit the close connection between low rank PPT states and product vectors. In particular, we show how to reconstruct a PPT state from a sufficient number of product vectors in its kernel. It may seem surprising that the number of product vectors needed may be smaller than the dimension of the kernel.

1 Introduction

Quantum entanglement between subsystems of a composite physical system is a phenomenon which clearly distinguishes quantum physics from classical physics [1]. Entangled quantum states show correlations between measurements on the subsystems which can not be modelled within classical physics with local interactions. A classical model would have to be a joint probability distribution of quantities that are incompatible in the quantum theory, and the existence of such a joint probability distribution, consistent with locality, implies so called Bell inequalities [2], or even equalities as in the three particle states known as GHZ states, introduced by Mermin, Greenberger, Horne, and Zeilinger [3, 4]. The correlations in entangled quantum states violate Bell inequalities and GHZ equalities.

A pure classical state of a composite system has no correlations between measurements on subsystems, since classical measurements are deterministic. A statistical ensemble of pure classical states, what we may call a mixed classical state, can have correlations, but these correlations can not violate Bell inequalities, by definition.

The only pure quantum states that are not entangled are the pure product states, which resemble pure classical states in that they have no correlations at all. By definition, a mixed quantum state is a statistical ensemble of pure quantum states, and it is said to be separable if it can be mixed entirely from pure product states. The separable mixed states are not entangled, since they can not violate Bell inequalities. The entangled mixed states are precisely those that are non-separable. For this reason,

the mathematical distinction between separable and non-separable mixed states is important from the physical point of view.

The separability problem, how to characterize the set \mathcal{S} of separable mixed states and decide whether a given mixed state is separable or not, is known to be a difficult mathematical problem [5]. It motivates our work presented here and in previous papers, although we have not studied so much the separable states directly as the larger class of mixed states called PPT states [6, 7, 8, 9].

The separable mixed states have the property that they remain positive after partial transposition, they are PPT states, for short. The set \mathcal{P} of PPT states is in general larger than the set \mathcal{S} of separable states, but the difference between the two sets is surprisingly small in low dimensions, and in the very lowest dimensions, 2×2 , 2×3 , and 3×2 , there is no difference [10].

The condition of positive partial transpose is known as the Peres separability criterion [11]. It is a powerful separability test, especially in low dimensions where the difference between the two sets \mathcal{P} and \mathcal{S} is small. It can be used for example to prove that any pure quantum state is either entangled or a pure product state.

We study especially the lowest rank entangled PPT states, on the assumption that they are the easiest ones to understand. In the present paper we discuss in particular how to construct PPT states of rank 4 and 5 in 3×3 dimensions, and rank 6 in 4×4 dimensions. A central theme is how the states are constrained by the existence of product vectors in the kernel. Another central theme is perturbation theory, which we use to construct rank 5 PPT states close to rank 4 states, and to study surfaces of PPT states of fixed low rank. We compute numerically the dimensions of such surfaces, and we show how to follow a surface by numerical integration of an equation of motion.

The relation between PPT states and product vectors

The close connection between PPT states and product vectors has been used earlier, for example to prove the separability of sufficiently low rank PPT states [12].

Bennett et al. [13, 14] introduced a method for constructing low rank mixed states that are obviously entangled PPT states, using what they called Unextendible Product Bases (UPBs). From a UPB, defined as a maximal set of orthogonal product vectors which is not a complete basis of the Hilbert space, one constructs an orthogonal projection Q and the complementary projection $P = \mathbb{1} - Q$. Then $\rho = P/(\text{Tr } P)$ is an entangled PPT state.

The UPB construction is most successful in the special case of rank 4 PPT states in 3×3 dimensions. In Ref. [9] we argued, partly based on evidence from numerical studies, that an extended version of the UPB construction, including nonunitary but nonsingular product transformations on the states, is general enough to produce all rank 4 entangled PPT states in 3×3 dimensions.

Unfortunately, attempts to apply the UPB method directly in higher dimensions fail, even when the kernel contains product vectors, because there can not exist a sufficient number of orthogonal product vectors. The orthogonality is essential in the construction by Bennett et al. of the PPT state as a projection operator. We would like to generalize the construction in such a way that it works without the orthogonality condition.

One possible generalization is to construct projection operators as more general convex combinations, or even as non-convex linear combinations, of pure product states. This idea is explored in a separate paper [15].

In the present paper we discuss in general the constraints imposed on a PPT state ρ by the existence of product vectors in its kernel, and we show that these constraints are so strong that they actually determine the state uniquely. A surprising discovery is that in cases where the kernel contains a finite overcomplete set of product vectors, the state ρ can be reconstructed from only a subset of the product

vectors, and the number of product vectors needed may even be smaller than the dimension of the kernel.

From this point of view, the important question is exactly what conditions the product vectors must satisfy in order for the constraint equations to have a solution for ρ . We can answer this question in the familiar special case of rank 4 PPT states in 3×3 dimensions, but not in other cases. We consider this an interesting problem for future research.

Outline of the paper

The contents of the present paper are organized as follows. First we review some linear algebra, in particular degenerate perturbation theory, in Sections 2, 3, and 4. The main purpose is to introduce notation and collect formulas for later reference.

In Section 5 we discuss the rank 4 PPT states in 3×3 dimensions. We review the UPB construction, based on orthogonal product vectors in the kernel, before we describe an approach which is different in that the product vectors need not be orthogonal. The new approach also throws some new light on a set of reality conditions that limit the selection of product vectors to be used for constructing rank 4 PPT states.

In Section 6 we discuss the rank 5 PPT states in 3×3 dimensions. We find an 8 dimensional surface of rank 5 PPT states in every generic 5 dimensional subspace, but we have not found any general method to construct such states. However, we show how to construct rank 5 PPT states by perturbing rank 4 PPT states. Again, the product vectors in the kernel of the rank 4 state play an important role in our construction of the rank 5 states.

In Section 7 we discuss rank 6 PPT states in 4×4 dimensions. The kernel of such a state has dimension 10, and contains 20 product vectors. The remarkable result we find is that the state can be constructed from only 7 product vectors in the kernel. An arbitrary set of 7 product vectors does not produce a rank 6 PPT state, but we do not know how to select sets of product vectors that can be used in such a construction.

In Section 8 we discuss briefly how to determine numerically the dimensions of surfaces of PPT states of fixed rank. We find that the dimensions are given by a simple counting of independent constraints, except for the very lowest rank states, for which the constraints are not independent.

Finally, we discuss in Section 9 how to study a surface of PPT states by numerical integration of equations of motion for curves on the surface. In this way one may study for example the curvature of the surface, or how a curve on the surface approaches the boundary of the surface.

2 Some basic linear algebra

2.1 Density matrices

Let H_N be the set of Hermitean $N \times N$ matrices. It has a natural structure as a real Hilbert space of dimension N^2 with the scalar product

$$(X, Y) = \text{Tr}(XY) . \tag{1}$$

A mixed state, or density matrix, is a positive Hermitean matrix of unit trace. We define

$$\mathcal{D} = \mathcal{D}_N = \{ \rho \in H_N \mid \rho \geq 0, \text{Tr} \rho = 1 \} . \tag{2}$$

Because it is Hermitian, a density matrix ρ has a spectral representation in terms of a complete set of orthonormal eigenvectors $\psi_i \in \mathbb{C}^N$ with real eigenvalues λ_i ,

$$\rho = \sum_{i=1}^N \lambda_i \psi_i \psi_i^\dagger \quad \text{with} \quad \psi_i^\dagger \psi_j = \delta_{ij}, \quad \mathbb{1} = \sum_{i=1}^N \psi_i \psi_i^\dagger. \quad (3)$$

The rank of ρ is the number of eigenvalues $\lambda_i \neq 0$. The pseudoinverse of ρ is defined as

$$\rho^+ = \sum_{i, \lambda_i \neq 0} \lambda_i^{-1} \psi_i \psi_i^\dagger, \quad (4)$$

it is equal to the inverse ρ^{-1} if ρ is invertible. The matrices

$$P = \rho^+ \rho = \rho \rho^+ = \sum_{i, \lambda_i \neq 0} \psi_i \psi_i^\dagger, \quad Q = \mathbb{1} - P = \sum_{i, \lambda_i = 0} \psi_i \psi_i^\dagger \quad (5)$$

are Hermitian and project orthogonally onto two complementary orthogonal subspaces of \mathbb{C}^N , P onto $\text{Im} \rho$, the image of ρ , and Q onto $\text{Ker} \rho$, the kernel of ρ . The relations $P\rho = \rho P = P\rho P = \rho$ and $Q\rho = \rho Q = Q\rho Q = 0$ will be used in the following.

We say that ρ is positive, or positive semidefinite, and we write $\rho \geq 0$, when $\lambda_i \geq 0$ for $i = 1, 2, \dots, N$. An equivalent condition is that $\psi^\dagger \rho \psi \geq 0$ for all $\psi \in \mathbb{C}^N$. It follows from the last inequality and the spectral representation of ρ that $\psi^\dagger \rho \psi = 0$ if and only if $\rho \psi = 0$.

The definition of positive Hermitian matrices by inequalities of the form $\psi^\dagger \rho \psi \geq 0$ implies that \mathcal{D} is a convex set. That is, if ρ is a convex combination of $\rho_1, \rho_2 \in \mathcal{D}$,

$$\rho = \lambda \rho_1 + (1 - \lambda) \rho_2 \quad \text{with} \quad 0 < \lambda < 1, \quad (6)$$

then $\rho \in \mathcal{D}$. Furthermore, since $\text{Ker} \rho = \{\psi \mid \psi^\dagger \rho \psi = 0\}$ when $\rho \geq 0$, it follows that

$$\text{Ker} \rho = \text{Ker} \rho_1 \cap \text{Ker} \rho_2, \quad (7)$$

independent of λ , when ρ is a convex combination as above. Since $\text{Ker} \rho$ is independent of λ , so is $\text{Im} \rho = (\text{Ker} \rho)^\perp$.

A convex set is defined by its extremal points: those points that are not convex combinations of other points. The extremal points of \mathcal{D} are the pure states of the form $\rho = \psi \psi^\dagger$ with $\psi \in \mathbb{C}^N$. Thus, the spectral representation in eq. (3) is an expansion of ρ as a convex combination of N or fewer extremal points of \mathcal{D} .

Finite perturbations

In the following, let ρ be a density matrix and define the projections P and $Q = \mathbb{1} - P$ as in eq. (5). Consider a perturbation

$$\rho' = \rho + \epsilon A, \quad (8)$$

where $A \neq 0$ is Hermitian, and $\text{Tr} A = 0$ so that $\text{Tr} \rho' = \text{Tr} \rho$. The real parameter ϵ may be finite or infinitesimal, we will first consider the case when ϵ is finite.

We observe that if $\text{Im} A \subset \text{Im} \rho$, or equivalently if $PAP = A$, then there will be a finite range of values of ϵ , say $\epsilon_1 \leq \epsilon \leq \epsilon_2$ with $\epsilon_1 < 0 < \epsilon_2$, such that $\rho' \in \mathcal{D}$ and $\text{Im} \rho' = \text{Im} \rho$. This is so because the eigenvectors of ρ with zero eigenvalue will remain eigenvectors of ρ' with zero

eigenvalue, and all the positive eigenvalues of ρ will change continuously with ϵ into eigenvalues of ρ' .

The other way around, if $\rho' \in \mathcal{D}$ for $\epsilon_1 \leq \epsilon \leq \epsilon_2$ with $\epsilon_1 < 0 < \epsilon_2$, then ρ' is a convex combination of $\rho + \epsilon_1 A$ and $\rho + \epsilon_2 A$ for every ϵ in the open interval $\epsilon_1 < \epsilon < \epsilon_2$. Hence $\text{Img } \rho'$ is independent of ϵ in this interval, implying that $\text{Img } A \subset \text{Img } \rho$ and $PAP = A$.

This shows that ρ is extremal in \mathcal{D} if and only if there exists no $A \neq 0$ with $\text{Tr } A = 0$ and $PAP = A$. Another formulation of the condition is that there exists no $\rho' \in \mathcal{D}$ with $\rho' \neq \rho$ and $\text{Img } \rho' = \text{Img } \rho$. A third equivalent formulation of the extremality condition is that the equation

$$PAP = A \quad (9)$$

for the Hermitean matrix A has $A = \rho$ as its only solution (up to proportionality). In fact, if $PBP = B$ and $\text{Tr } B \neq 0$, then we have $PAP = A$ and $\text{Tr } A = 0$ when we take

$$A = B - (\text{Tr } B) \rho . \quad (10)$$

Infinitesimal perturbations

Assume now that $\text{Img } A \not\subset \text{Img } \rho$. The question is how an infinitesimal perturbation affects the zero eigenvalues of ρ . When ρ is of low rank we need degenerate perturbation theory, which is well known from any textbook on quantum mechanics.

To first order in ϵ , the zero eigenvalues of ρ are perturbed into eigenvalues of ρ' that are ϵ times the eigenvalues of QAQ on the subspace $\text{Ker } \rho$. Similarly, to first order in ϵ , the positive eigenvalues of ρ are perturbed into positive eigenvalues of ρ' , in a way which is determined by how ρ and PAP act on $\text{Img } \rho$.

It is clear from this that, to first order in ϵ , the condition

$$QAQ = 0 \quad (11)$$

is necessary and sufficient to ensure that the rank of ρ' equals the rank of ρ , and that $\rho' \geq 0$ both for $\epsilon > 0$ and for $\epsilon < 0$.

More generally, to first order in ϵ , the rank of ρ' equals the rank of ρ plus the rank of QAQ . For example, if we want to perturb ρ in such a way that the rank increases by one, then we have to choose A such that

$$QAQ = \alpha \phi \phi^\dagger , \quad (12)$$

where $\phi \in \text{Ker } \rho$ is a normalized eigenvector of QAQ with $\alpha \neq 0$ as eigenvalue. Since QAQ is Hermitean, α must be real. If $\alpha > 0$, then $\rho' \geq 0$ for $\epsilon > 0$ but not for $\epsilon < 0$.

Projection operators on H_N

Using the projections P and Q defined above we define projection operators on H_N , the real Hilbert space of Hermitean $N \times N$ matrices, as follows,

$$\begin{aligned} \mathbf{P}X &= PXP , \\ \mathbf{Q}X &= QXQ = X - PX - XP + PXP , \\ \mathbf{R}X &= (\mathbf{I} - \mathbf{P} - \mathbf{Q})X = PX + XP - 2PXP . \end{aligned} \quad (13)$$

Here \mathbf{I} is the identity on H_N . It is straightforward to verify that these are complementary projections, with $\mathbf{P}^2 = \mathbf{P}$, $\mathbf{Q}^2 = \mathbf{Q}$, $\mathbf{PQ} = \mathbf{QP} = \mathbf{0}$, and so on. They are symmetric with respect to the natural scalar product on H_N , for example,

$$(X, \mathbf{PY}) = \text{Tr}(XPYP) = \text{Tr}(PXPY) = (\mathbf{PX}, Y). \quad (14)$$

Hence they project orthogonally, and relative to an orthonormal basis of H_N they are represented by symmetric matrices.

Relative to an orthonormal basis of \mathbb{C}^N with the first basis vectors in $\text{Im} \rho$ and the last basis vectors in $\text{Ker } \rho$, a Hermitean matrix X takes the block form

$$X = \begin{pmatrix} U & V \\ V^\dagger & W \end{pmatrix}, \quad (15)$$

with $U^\dagger = U$ and $W^\dagger = W$. In this basis we have

$$P = \begin{pmatrix} I & 0 \\ 0 & 0 \end{pmatrix}, \quad Q = \begin{pmatrix} 0 & 0 \\ 0 & I \end{pmatrix}, \quad (16)$$

and hence,

$$\mathbf{P}X = \begin{pmatrix} U & 0 \\ 0 & 0 \end{pmatrix}, \quad \mathbf{Q}X = \begin{pmatrix} 0 & 0 \\ 0 & W \end{pmatrix}, \quad \mathbf{R}X = \begin{pmatrix} 0 & V \\ V^\dagger & 0 \end{pmatrix}. \quad (17)$$

2.2 Composite systems

Product vectors

If $N = N_A N_B$ then the tensor product spaces $\mathbb{C}^N = \mathbb{C}^{N_A} \otimes \mathbb{C}^{N_B}$ (a complex tensor product) and $H_N = H_{N_A} \otimes H_{N_B}$ (a real tensor product) may describe a composite quantum system with two subsystems A and B of Hilbert space dimensions N_A and N_B .

A vector $\psi \in \mathbb{C}^N$ then has components $\psi_I = \psi_{ij}$, where

$$I = 1, 2, \dots, N \quad \leftrightarrow \quad ij = 11, 12, \dots, 1N_B, 21, 22, \dots, N_A N_B. \quad (18)$$

A product vector $\psi = \phi \otimes \chi$ has components $\psi_{ij} = \phi_i \chi_j$. We see that ψ is a product vector if and only if its components satisfy the quadratic equations

$$\psi_{ij} \psi_{kl} - \psi_{il} \psi_{kj} = 0. \quad (19)$$

These equations are not all independent, the number of independent complex equations is

$$K = (N_A - 1)(N_B - 1) = N - N_A - N_B + 1. \quad (20)$$

For example, if $\psi_{11} \neq 0$ we get a complete set of independent equations by taking $i = j = 1$ and $k = 2, 3, \dots, N_A$, $l = 2, 3, \dots, N_B$.

Since the equations are homogeneous, any solution $\psi \neq 0$ gives rise to a one parameter family of solutions $c\psi$ with $c \in \mathbb{C}$. A vector ψ in a subspace of dimension n has n independent complex components. Since the most general nonzero solution must contain at least one free complex parameter, we conclude that a generic subspace of dimension n will contain nonzero product vectors if and only if

$$n \geq K + 1 = N - N_A - N_B + 2. \quad (21)$$

The limiting dimension

$$n = N - N_A - N_B + 2 \quad (22)$$

is particularly interesting. In this special case a nonzero solution will contain exactly one free parameter, which has to be a complex normalization constant.

Thus, up to proportionality there will exist a finite set of product vectors in a generic subspace of dimension $n = N - N_A - N_B + 2$. The number of product vectors is [8]

$$p = \binom{N_A + N_B - 2}{N_A - 1} = \frac{(N_A + N_B - 2)!}{(N_A - 1)! (N_B - 1)!} . \quad (23)$$

A generic subspace of lower dimension will contain no nonzero product vector, whereas any subspace of higher dimension will contain a continuous infinity of different product vectors (different in the sense that they are not proportional).

Partial transposition

The following relation between matrix elements,

$$(X^P)_{ij;kl} = X_{il;kj} , \quad (24)$$

defines X^P , the partial transpose of the Hermitian matrix X with respect to the second subsystem.

A density matrix ρ is called separable if it is a convex combination of tensor product matrices,

$$\rho = \sum_k p_k \sigma_k \otimes \tau_k , \quad (25)$$

with $\sigma_k \in \mathcal{D}_{N_A}$, $\tau_k \in \mathcal{D}_{N_B}$, $p_k > 0$, $\sum_k p_k = 1$. We denote by \mathcal{S} the set of separable matrices.

The partial transpose of the above separable matrix is

$$\rho^P = \sum_k p_k \sigma_k \otimes (\tau_k)^T \geq 0 . \quad (26)$$

The positivity of ρ^P is known as the Peres criterion, it is an easily testable necessary condition for separability. For this reason it is of interest to study the set of PPT (Positive Partial Transpose) matrices, defined as

$$\mathcal{P} = \{ \rho \in \mathcal{D} \mid \rho^P \geq 0 \} = \mathcal{D} \cap \mathcal{D}^P . \quad (27)$$

We may call it the Peres set. A well known result is that $\mathcal{P} = \mathcal{S}$ for $N = N_A N_B \leq 6$, whereas \mathcal{P} is strictly larger than \mathcal{S} in higher dimensions [10].

We will classify low rank PPT states by the ranks (m, n) of ρ and ρ^P , respectively. Note that ranks (m, n) and (n, m) are equivalent for the purpose of classification, because of the symmetric roles of ρ and ρ^P .

Product transformations

A product transformation of the form

$$\rho \mapsto \rho' = aV\rho V^\dagger \quad \text{with} \quad V = V_A \otimes V_B, \quad (28)$$

where a is a normalization factor and $V_A \in \text{SL}(N_A, \mathbb{C})$, $V_B \in \text{SL}(N_B, \mathbb{C})$, preserves positivity, rank, separability, and other interesting properties that the density matrix ρ may have. For example, it preserves positivity of the partial transpose, because

$$(\rho')^P = a\tilde{V}\rho^P\tilde{V}^\dagger \quad \text{with} \quad \tilde{V} = V_A \otimes V_B^*. \quad (29)$$

The image and kernel of ρ and ρ^P transform in the following ways,

$$\text{Img } \rho' = V \text{Img } \rho, \quad \text{Ker } \rho' = (V^\dagger)^{-1} \text{Ker } \rho, \quad (30)$$

and

$$\text{Img } (\rho')^P = \tilde{V} \text{Img } \rho^P, \quad \text{Ker } (\rho')^P = (\tilde{V}^\dagger)^{-1} \text{Ker } \rho^P. \quad (31)$$

All these transformations are of product form and hence preserve the number of product vectors in a subspace.

We say that two density matrices ρ and ρ' related in this way are $\text{SL} \otimes \text{SL}$ equivalent, or simply SL equivalent. The concept of SL equivalence is important to us here because it simplifies very much our efforts to classify the low rank PPT states.

3 Restricted perturbations

We have seen that eq. (9) ensures that the perturbation $\rho' = \rho + \epsilon A$ preserves the image of ρ , so that $\text{Img } \rho' = \text{Img } \rho$ for infinitesimal values of the perturbation parameter ϵ , and $\text{Img } \rho' \subset \text{Img } \rho$ even for finite values of ϵ . The weaker condition in eq. (11) ensures only that the rank of ρ' equals the rank of ρ for infinitesimal values of ϵ .

We want to discuss how to use perturbations with similar restrictions in order to study, for example, the extremal points of the convex set \mathcal{P} . In particular, we are interested in perturbations that either preserve the ranks (m, n) of ρ , or else change these ranks in controlled ways.

In a similar way as we did for ρ , we define \tilde{P} and $\tilde{Q} = \mathbb{1} - \tilde{P}$ as the orthogonal projections onto $\text{Img } \rho^P$ and $\text{Ker } \rho^P$. Then we define

$$\begin{aligned} \tilde{\mathbf{P}}X &= (\tilde{P}X^P\tilde{P})^P, \\ \tilde{\mathbf{Q}}X &= (\tilde{Q}X^P\tilde{Q})^P = X - (\tilde{P}X^P)^P - (X^P\tilde{P})^P + (\tilde{P}X^P\tilde{P})^P, \\ \tilde{\mathbf{R}}X &= (\mathbf{I} - \tilde{\mathbf{P}} - \tilde{\mathbf{Q}})X = (\tilde{P}X^P)^P + (X^P\tilde{P})^P - 2(\tilde{P}X^P\tilde{P})^P. \end{aligned} \quad (32)$$

These are again projections on the real Hilbert space H_N , like \mathbf{P} , \mathbf{Q} and \mathbf{R} , again symmetric with respect to the natural scalar product on H_N .

We may now use the projection operators on H_N to impose various restrictions on the perturbation matrix A .

Testing for extremality in \mathcal{P}

The extremality condition for \mathcal{P} is derived in a similar way as the extremality condition for \mathcal{D} based on eq. (9). Clearly ρ is extremal in \mathcal{P} if and only if there exists no $\rho' \in \mathcal{P}$, $\rho' \neq \rho$, with both $\text{Img } \rho' = \text{Img } \rho$ and $\text{Img}(\rho')^P = \text{Img } \rho^P$. Another way to formulate this condition is that $A = \rho$ is the only solution of the two equations $\mathbf{P}A = A$ and $\tilde{\mathbf{P}}A = A$.

Since \mathbf{P} and $\tilde{\mathbf{P}}$ are projections, the equations $\mathbf{P}A = A$ and $\tilde{\mathbf{P}}A = A$ together are equivalent to the single eigenvalue equation

$$(\mathbf{P} + \tilde{\mathbf{P}})A = 2A. \quad (33)$$

They are also equivalent to either one of the eigenvalue equations

$$\mathbf{P}\tilde{\mathbf{P}}\mathbf{P}A = A, \quad \tilde{\mathbf{P}}\mathbf{P}\tilde{\mathbf{P}}A = A. \quad (34)$$

Note that the operators $\mathbf{P} + \tilde{\mathbf{P}}$, $\mathbf{P}\tilde{\mathbf{P}}\mathbf{P}$, and $\tilde{\mathbf{P}}\mathbf{P}\tilde{\mathbf{P}}$ are all real symmetric and therefore have complete sets of real eigenvalues and eigenvectors. In fact, the eigenvalues are all non-negative, because the operators are positive semidefinite.

When we diagonalize $\mathbf{P} + \tilde{\mathbf{P}}$ we will always find $A = \rho$ as an eigenvector with eigenvalue 2. If it is the only solution of eq. (33), this proves that ρ is extremal in \mathcal{P} . If A is a solution not proportional to ρ , then we may impose the condition $\text{Tr } A = 0$ (replace A by $A - (\text{Tr } A)\rho$ if necessary), and we know that there exists a finite range of both positive and negative values of ϵ such that $\rho' = \rho + \epsilon A \in \mathcal{P}$, hence ρ is not extremal.

It should be noted that in our numerical calculations we may find eigenvalues of $\mathbf{P} + \tilde{\mathbf{P}}$ that differ from 2 by less than one per cent. However, since eigenvalues are calculated with a precision close to the internal precision of the computer, which is of order 10^{-16} , there is never any ambiguity as to whether an eigenvalue is equal to 2 or strictly smaller than 2.

Perturbations preserving the PPT property and ranks

The rank and positivity of ρ is preserved by the perturbation, to first order in ϵ , both for $\epsilon > 0$ and $\epsilon < 0$, if and only if $\mathbf{Q}A = 0$. Similarly, the rank and positivity of ρ^P is preserved if and only if $\tilde{\mathbf{Q}}A = 0$. These two equations together are equivalent to the single eigenvalue equation

$$(\mathbf{Q} + \tilde{\mathbf{Q}})A = 0. \quad (35)$$

Again $\mathbf{Q} + \tilde{\mathbf{Q}}$ is real symmetric and has a complete set of real eigenvalues and eigenvectors.

In conclusion, the perturbations that preserve the PPT property, as well as the ranks (m, n) of ρ and ρ^P , to first order in ϵ , are the solutions of eq. (35).

We may want to perturb in different ways, for example such that $\text{Img } \rho' = \text{Img } \rho$, but not necessarily $\text{Img}(\rho')^P = \text{Img } \rho^P$, we only require $(\rho')^P$ and ρ^P to have the same rank. Then the conditions on A are that $\mathbf{P}A = A$ and $\tilde{\mathbf{Q}}A = 0$, or equivalently,

$$(\mathbf{I} - \mathbf{P} + \tilde{\mathbf{Q}})A = 0. \quad (36)$$

4 Product vectors in the kernel

Assume that $\rho \in \mathcal{P}$. Recall that the equations $w^\dagger \rho w = 0$ and $\rho w = 0$ for $w \in \mathbb{C}^N$ are equivalent, and so are the equations $w^\dagger \rho^P w = 0$ and $\rho^P w = 0$, because $\rho \geq 0$ and $\rho^P \geq 0$. Taken together with the

identity

$$(x \otimes y)^\dagger \rho (u \otimes v) = (x \otimes v^*)^\dagger \rho^P (u \otimes y^*) \quad (37)$$

this puts strong restrictions on ρ when we know a number of product vectors in $\text{Ker } \rho$.

Assume from now on that w is a product vector, $w = u \otimes v$. Defining $\tilde{w} = u \otimes v^*$ we have the general relation

$$w^\dagger \rho w = \tilde{w}^\dagger \rho^P \tilde{w}. \quad (38)$$

Assume furthermore that $w \in \text{Ker } \rho$, this is equivalent to the condition that $\tilde{w} \in \text{Ker } \rho^P$. For any $z \in \mathbb{C}^N$ we have the condition on ρ that $z^\dagger \rho w = 0$. In particular, when z is an arbitrary product vector, $z = x \otimes y$, we have the two conditions on ρ that

$$(x \otimes y)^\dagger \rho (u \otimes v) = 0 \quad (39)$$

and

$$(x \otimes v)^\dagger \rho (u \otimes y) = (x \otimes y^*)^\dagger \rho^P (u \otimes v^*) = 0. \quad (40)$$

Assume that $w_i = u_i \otimes v_i \in \text{Ker } \rho$ for $i = 1, 2, \dots, n$. Then for arbitrary values of the indices i, j, k we have the following constraints on ρ ,

$$(u_i \otimes v_j)^\dagger \rho (u_k \otimes v_k) = (u_i \otimes v_k)^\dagger \rho (u_k \otimes v_j) = 0. \quad (41)$$

Let us introduce matrices

$$A_{klij} = (u_k \otimes v_l)(u_i \otimes v_j)^\dagger, \quad (42)$$

and Hermitean matrices

$$B_{klij} = A_{klij} + (A_{klij})^\dagger, \quad C_{klij} = i(A_{klij} - (A_{klij})^\dagger), \quad (43)$$

then the constraints on ρ are of the form

$$\text{Tr}(\rho B_{kkij}) = \text{Tr}(\rho C_{kkij}) = \text{Tr}(\rho B_{kjik}) = \text{Tr}(\rho C_{kjik}) = 0. \quad (44)$$

Each equation $\text{Tr}(\rho B) = 0$ with $B \neq 0$ or $\text{Tr}(\rho C) = 0$ with $C \neq 0$ is one real valued constraint. Of course, the constraints in eq. (44) are not all independent, we have for example that $C_{kkkk} = 0$.

5 Rank (4, 4) PPT states in 3×3 dimensions

5.1 The UPB construction of entangled PPT states

We will review briefly the construction of a rank (4, 4) entangled and extremal PPT state ρ in 3×3 dimensions from an unextendible orthonormal product basis (a UPB) of $\text{Ker } \rho$ [13]. The UPB consists of five orthonormal product vectors $w_i = N_i u_i \otimes v_i$ with the property that there exists no product vector orthogonal to all of them. We include real normalization factors N_i here because we want to normalize such that $w_i^\dagger w_j = \delta_{ij}$ without necessarily normalizing the vectors u_i and v_i .

The orthogonality of the product vectors w_i follows from the orthogonality relations $u_1 \perp u_2 \perp u_3 \perp u_4 \perp u_5 \perp u_1$ and $v_1 \perp v_3 \perp v_5 \perp v_2 \perp v_4 \perp v_1$. There is the further condition that any three

vectors u_i and any three v_i are linearly independent. The five dimensional subspace spanned by these product vectors is the kernel of the density matrix

$$\rho = \frac{1}{4} \left(\mathbb{1} - \sum_{i=1}^5 w_i w_i^\dagger \right), \quad (45)$$

which is proportional to a projection operator. The partial transpose of ρ is

$$\rho^P = \frac{1}{4} \left(\mathbb{1} - \sum_{i=1}^5 \tilde{w}_i \tilde{w}_i^\dagger \right), \quad (46)$$

with $\tilde{w}_i = N_i u_i \otimes v_i^*$. Thus we have both $\rho \geq 0$ and $\rho^P \geq 0$ by construction. Note that if all the vectors v_i are real, $v_i^* = v_i$, then ρ is symmetric under partial transposition, $\rho^P = \rho$.

By a unitary product transformation as in eq. (30) we may transform the above orthogonal UPB into the standard unnormalized form [9]

$$u = \begin{pmatrix} 1 & 0 & a & b & 0 \\ 0 & 1 & 0 & 1 & a \\ 0 & 0 & b & -a & 1 \end{pmatrix}, \quad v = \begin{pmatrix} 1 & d & 0 & 0 & c \\ 0 & 1 & 1 & c & 0 \\ 0 & -c & 0 & 1 & d \end{pmatrix}, \quad (47)$$

with a, b, c, d as positive real parameters. The following quantities determine these parameters,

$$\begin{aligned} s_1 &= -\frac{\det(u_1 u_2 u_4) \det(u_1 u_3 u_5)}{\det(u_1 u_2 u_5) \det(u_1 u_3 u_4)} = a^2, \\ s_2 &= -\frac{\det(u_1 u_2 u_3) \det(u_2 u_4 u_5)}{\det(u_1 u_2 u_4) \det(u_2 u_3 u_5)} = \frac{b^2}{a^2}, \end{aligned} \quad (48)$$

and

$$\begin{aligned} s_3 &= \frac{\det(v_1 v_2 v_3) \det(v_1 v_4 v_5)}{\det(v_1 v_2 v_5) \det(v_1 v_3 v_4)} = c^2, \\ s_4 &= \frac{\det(v_1 v_3 v_5) \det(v_2 v_3 v_4)}{\det(v_1 v_2 v_3) \det(v_3 v_4 v_5)} = \frac{d^2}{c^2}. \end{aligned} \quad (49)$$

These ratios of determinants are invariant under general $\text{SL} \otimes \text{SL}$ transformations, as well as independent of the normalization of the vectors.

In Ref. [9] we presented numerical evidence that every entangled rank (4, 4) PPT state is $\text{SL} \otimes \text{SL}$ equivalent to some state of the form of eq. (45) with real product vectors as given in eq. (47).

This means that the surface of all rank (4, 4) entangled PPT states has dimension 36. We count 32 degrees of freedom due to the $\text{SL}(3, \mathbb{C}) \otimes \text{SL}(3, \mathbb{C})$ transformations, plus the 4 real $\text{SL} \otimes \text{SL}$ invariant parameters a, b, c, d in eq. (47).

5.2 A different point of view

We will present here the construction of an entangled PPT state ρ of rank (4, 4) as seen from a different point of view. When ρ has rank 4 it means that $\text{Ker } \rho$ has dimension 5. A generic 5 dimensional subspace in $\mathbb{C}^9 = \mathbb{C}^3 \otimes \mathbb{C}^3$ has a basis of product vectors. In fact, it contains exactly 6 product vectors, any 5 of which are linearly independent. By eq. (22), 5 is the limiting dimension for which the number of product vectors is nonzero and finite, and the number 6 is consistent with eq. (23).

Any set of 5 product vectors $w_i = u_i \otimes v_i$, orthogonal or not, may be transformed by an $SL \otimes SL$ transformation to the standard unnormalized form

$$u = \begin{pmatrix} 1 & 0 & 0 & 1 & 1 \\ 0 & 1 & 0 & 1 & p \\ 0 & 0 & 1 & 1 & q \end{pmatrix}, \quad v = \begin{pmatrix} 1 & 0 & 0 & 1 & 1 \\ 0 & 1 & 0 & 1 & r \\ 0 & 0 & 1 & 1 & s \end{pmatrix}, \quad (50)$$

with p, q, r, s as real or complex parameters. We impose here again the condition that any three u_i and any three v_i should be linearly independent. There is always a 6th product vector which is a linear combination of the above 5,

$$u_6 = \begin{pmatrix} \frac{s-r}{ps-qr} \\ \frac{1-s}{q-s} \\ \frac{r-1}{r-p} \end{pmatrix}, \quad v_6 = \begin{pmatrix} \frac{p-q}{ps-qr} \\ \frac{q-1}{q-s} \\ \frac{1-p}{r-p} \end{pmatrix}. \quad (51)$$

The values of the above invariants as functions of the new parameters are

$$s_1 = -\frac{p}{q}, \quad s_2 = q - 1, \quad s_3 = \frac{r-s}{s}, \quad s_4 = \frac{r}{1-r}. \quad (52)$$

The parameters p, q, r, s are actually new invariants, they can not be changed by $SL \otimes SL$ transformations.

If the values of p, q, r, s are such that the invariants s_1, s_2, s_3, s_4 are all real and strictly positive, then we may use eq. (48) and eq. (49) to find corresponding values of a, b, c, d , and we may transform from the non-orthogonal standard form in eq. (50) to the orthogonal standard form in eq. (47), which in turn defines the rank (4, 4) state in eq. (45).

We see from eq. (52) that the invariants are all strictly positive if and only if p, q, r, s are all real, and $p < 0, q > 1, 0 < r < 1, 0 < s < r$. These inequalities define the regions marked 1 in the (p, q) and (r, s) planes as plotted in Fig. 1.

As discussed in ref. [9] there are 10 permutations of the product vectors w_i for $i = 1, 2, \dots, 5$ which preserve the positivity of the invariants. These permutations form a group G which is the symmetry group of a regular pentagon, exemplified by the rotation, or cyclic permutation, $w_i \mapsto \tilde{w}_i$ with

$$\tilde{w}_1 = w_5, \quad \tilde{w}_2 = w_1, \quad \tilde{w}_3 = w_2, \quad \tilde{w}_4 = w_3, \quad \tilde{w}_5 = w_4, \quad (53)$$

and the reflection

$$\tilde{w}_1 = w_4, \quad \tilde{w}_2 = w_3, \quad \tilde{w}_3 = w_2, \quad \tilde{w}_4 = w_1, \quad \tilde{w}_5 = w_5. \quad (54)$$

For short, we write the rotation as 51234 and the reflection as 43215.

There are altogether $5! = 120$ permutations of the 5 product vectors w_i , and they fall into 12 classes (left cosets of the group G as a subgroup of the permutation group S_5) which are not transformed into each other by G . We number the classes from 1 to 12, and pick one representative from each class as follows,

$$\begin{array}{llllll} 1 : 12345 & 2 : 13245 & 3 : 21345 & 4 : 23145 & 5 : 31245 & 6 : 32145 \\ 7 : 12435 & 8 : 14235 & 9 : 21435 & 10 : 24135 & 11 : 13425 & 12 : 14325 \end{array} \quad (55)$$

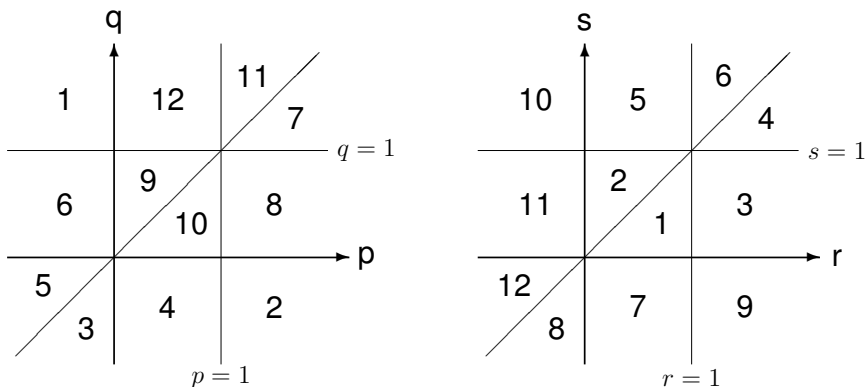


Figure 1: Regions for the parameters p, q, r, s defined in eq. (50) such that the product vectors $u_i \otimes v_i$ for $i = 1, 2, \dots, 5$ are in the kernel of a rank $(4, 4)$ extremal PPT state. The (p, q) plane is divided into 12 regions, with 12 corresponding regions in the (r, s) plane. The numbers 1 to 12 refer to the permutations of product vectors given in eq. (55). For example, if (p, q) is in region 7, (r, s) must also be in region 7.

Each of these 12 classes defines a positivity region in each of the two parameter planes, where all 4 invariants $\tilde{s}_1, \tilde{s}_2, \tilde{s}_3, \tilde{s}_4$ computed from the permuted product vectors are positive. The 12 regions are disjoint and fill the planes completely, as shown in Fig. 1. On the border lines between the regions the condition of linear independence between any three u vectors and any three v vectors is violated.

To summarize, we have learned how to test whether a set of 5 product vectors $w_i = u_i \otimes v_i$, which is generic in the sense that any three u vectors are linearly independent and any three v vectors are also linearly independent, span the kernel of a rank $(4, 4)$ PPT state. We transform to the standard form defined in eq. (50), by a product transformation and normalization. Then the necessary and sufficient condition is that the parameters p, q, r, s are all real, and that the parameter pairs (p, q) and (r, s) lie in corresponding regions in the parameter planes, as shown in Figure 1.

It should be stressed that these conclusions are based in part on numerical evidence, and we have no analytical proof which is complete in every detail.

We will discuss next how to reconstruct a PPT state from the product vectors in its kernel.

5.3 Matrix representation relative to a non-orthonormal basis

Consider a basis $\{e_i\}$ consisting of vectors that need not be orthonormal. The scalar products

$$g_{ij} = e_i^\dagger e_j \quad (56)$$

define the metric tensor g as a Hermitean matrix. In the usual way, we write the inverse matrix g^{-1} with upper indices, so that

$$\sum_j g^{ij} g_{jk} = \delta_k^i. \quad (57)$$

We define the dual vectors e^j such that

$$e^i = \sum_j g^{ji} e_j, \quad (e^i)^\dagger = \sum_j g^{ij} e_j^\dagger. \quad (58)$$

They satisfy the orthogonality relations

$$(e^i)^\dagger e_j = e_j^\dagger e^i = \delta_j^i, \quad (59)$$

and the completeness relation

$$\mathbb{1} = \sum_{i,j} e_i g^{ij} e_j^\dagger = \sum_j e^j e_j^\dagger = \sum_i e_i (e^i)^\dagger. \quad (60)$$

Using the dual basis vectors and the completeness relation we may write any matrix A as

$$A = \sum_{i,j} e^i \tilde{A}_{ij} (e^j)^\dagger \quad \text{with} \quad \tilde{A}_{ij} = e_i^\dagger A e_j. \quad (61)$$

5.4 Conditions on ρ from product vectors in $\text{Ker } \rho$

It is possible to construct the rank $(4, 4)$ PPT state ρ directly from 5 product vectors in $\text{Ker } \rho$ without transforming first the product vectors to the orthogonal form. We now describe this construction.

Given three product vectors $w_i = u_i \otimes v_i$ in $\text{Ker } \rho$, with the restriction that all three u_i and all three v_i are linearly independent. Then we have the following product basis of \mathbb{C}^9 , not necessarily orthonormal,

$$e_{ij} = u_i \otimes v_j, \quad ij = 11, 12, 13, 21, 22, 23, 31, 32, 33. \quad (62)$$

With respect to this basis we may define matrix elements of ρ like in eq. (61),

$$\tilde{\rho}_{ij;kl} = e_{ij}^\dagger \rho e_{kl}. \quad (63)$$

In order to count the independent constraints, it is convenient use the standard form of the product vectors defined in eq. (50). Now all the constraints from eq. (44) imply that

$$\tilde{\rho} = \begin{pmatrix} 0 & 0 & 0 & 0 & 0 & 0 & 0 & 0 & 0 \\ 0 & a_1 & b_1 & 0 & 0 & 0 & 0 & b_2 & 0 \\ 0 & b_1^* & a_2 & 0 & 0 & b_3 & 0 & 0 & 0 \\ 0 & 0 & 0 & a_3 & 0 & b_4 & b_5 & 0 & 0 \\ 0 & 0 & 0 & 0 & 0 & 0 & 0 & 0 & 0 \\ 0 & 0 & b_3^* & b_4^* & a_4 & 0 & 0 & 0 & 0 \\ 0 & 0 & 0 & b_5^* & 0 & 0 & a_5 & b_6 & 0 \\ 0 & b_2^* & 0 & 0 & 0 & 0 & b_6^* & a_6 & 0 \\ 0 & 0 & 0 & 0 & 0 & 0 & 0 & 0 & 0 \end{pmatrix}, \quad (64)$$

with real diagonal elements a_1, a_2, \dots, a_6 and complex off-diagonal elements b_1, b_2, \dots, b_6 . This Hermitean 9×9 matrix contains 18 real parameters, which means that there are altogether $81 - 18 = 63$ independent real constraints.

Including the fourth product vector from eq. (50) gives additional constraints $\tilde{\rho}w_4 = 0$, or explicitly written out,

$$\begin{aligned}
a_1 + b_1 + b_2 &= 0, \\
b_1^* + a_2 + b_3 &= 0, \\
a_3 + b_4 + b_5 &= 0, \\
b_3 + b_4 + a_4 &= 0, \\
b_5^* + a_5 + b_6 &= 0, \\
b_2 + b_6 + a_6 &= 0.
\end{aligned} \tag{65}$$

Here we have simplified slightly by complex conjugating the 4th and the 6th equation. These are complex equations, to be split into real and imaginary parts. The real parts are 6 independent equations, whereas the complex parts are only 5 independent equations. However, we get another independent equation as the imaginary part of, for example, the complex equation

$$(u_1 \otimes v_4)^\dagger \rho (u_4 \otimes v_2) = a_1 + b_1^* + b_2 = 0. \tag{66}$$

The end result is that all the off-diagonal matrix elements b_i have to be real. Altogether, we get 12 independent real constraints, 6 from the real parts and 6 from the imaginary parts of the equations.

Thus, including the 4th product vector in $\text{Ker } \rho$ increases the number of independent real constraints from 63 to 75, and reduces the number of real parameters in ρ from 18 to 6.

The generic case with 5 product vectors is that there are 81 independent constraints, leaving only the trivial solution $\rho = 0$. In order to end up with one possible solution for ρ we have to choose the parameters p, q, r, s to be real.

When we choose real values for p, q, r, s , there is always (generically) exactly one solution for ρ , that is, there are 80 independent constraints. The problem is that this uniquely determined matrix ρ , or its partial transpose, has in general both positive and negative eigenvalues.

The condition to ensure that both $\rho \geq 0$ and $\rho^P \geq 0$ (with the proper choice of sign for ρ), when the parameters p, q, r, s are real, is that the pair (p, q) and the pair (r, s) must lie in corresponding parameter regions, as shown in Fig. 1.

5.5 Separable states of rank (4, 4)

A separable state of rank 4 has the form

$$\rho = \sum_{i=1}^4 \lambda_i \psi_i \psi_i^\dagger, \tag{67}$$

with $\lambda_i > 0$, $\sum_{i=1}^4 \lambda_i = 1$, $\psi_i^\dagger \psi_i = 1$, and $\psi_i = C_i \phi_i \otimes \chi_i$ with C_i as a normalization constant. In the generic case when any three vectors ϕ_i and any three χ_i are linearly independent, we may perform an $\text{SL} \otimes \text{SL}$ transformation and obtain the standard form

$$\phi = \begin{pmatrix} 1 & 0 & 0 & 1 \\ 0 & 1 & 0 & 1 \\ 0 & 0 & 1 & 1 \end{pmatrix}, \quad \chi = \begin{pmatrix} 1 & 0 & 0 & 1 \\ 0 & 1 & 0 & 1 \\ 0 & 0 & 1 & 1 \end{pmatrix}. \tag{68}$$

In this standard form the χ vectors are real, and hence $\rho^P = \rho$.

The kernel $\text{Ker } \rho$ consists of the vectors that are orthogonal to all 4 product vectors ψ_i , and it contains exactly 6 product vectors $w_i = N_i u_i \otimes v_i$, as follows,

$$u = \begin{pmatrix} 0 & 0 & 0 & 1 & 1 & 1 \\ 0 & 1 & -1 & 0 & 0 & -1 \\ 1 & 0 & 1 & 0 & -1 & 0 \end{pmatrix}, \quad v = \begin{pmatrix} 1 & 1 & 1 & 0 & 0 & 0 \\ -1 & 0 & 0 & 1 & 1 & 0 \\ 0 & -1 & 0 & -1 & 0 & 1 \end{pmatrix}. \quad (69)$$

Note that the product vectors in the kernel of a separable rank $(4, 4)$ PPT state are not generic, in that there are subsets of three linearly dependent vectors both among the u vectors and among the v vectors.

The surface of separable states of rank 4 has dimension $35 = 32 + 3$, where 32 is the number of parameters of the group $\text{SL}(3, \mathbb{C}) \otimes \text{SL}(3, \mathbb{C})$ and 3 is the number of independent coefficients λ_i in eq. (67).

6 Rank $(5, 5)$ PPT states in 3×3 dimensions

6.1 The surface of rank $(5, 5)$ PPT states

Since we believe that we understand completely the rank $(4, 4)$ entangled states in dimension 3×3 , a natural next step is to try to understand the $(5, 5)$ states in the same dimension.

As discussed in the previous section, a generic 5 dimensional subspace in 3×3 dimensions contains exactly 6 product vectors, which can be transformed by $\text{SL} \otimes \text{SL}$ transformations, as in eqs. (30) and (31), into the standard form given in eqs. (50) and (51), with $\text{SL} \otimes \text{SL}$ invariant complex parameters p, q, r, s . Thus, each such subspace belongs to an equivalence class under $\text{SL} \otimes \text{SL}$ transformations, and the equivalence classes are parametrized by 8 real parameters. There is a discrete ambiguity in the parametrization, since it depends on the ordering of the 6 product vectors.

In one given generic 5 dimensional subspace we may construct a 5 dimensional set of rank $(5, 5)$ separable states as convex combinations of the 6 product vectors in the subspace. However, we find numerically that the dimension of the surface of rank $(5, 5)$ PPT states with the given subspace as image is not 5 but 8. We compute this dimension in the following way.

We search numerically for one rank $(5, 5)$ state ρ , for example by the methods described in [8]. The state we find will typically be entangled and extremal in \mathcal{P} . From this state ρ we compute the projections $P, Q, \tilde{P}, \tilde{Q}$ as described in Sections 2 and 3, and we look for perturbations $\rho' = \rho + \epsilon A$, with $\text{Tr } A = 0$, where A satisfies both equations $\mathbf{P}A = PAP = A$ and $\mathbf{Q}A = (\tilde{Q}A^P\tilde{Q})^P = 0$, or equivalently eq. (36),

$$(\mathbf{I} - \mathbf{P} + \tilde{\mathbf{Q}})A = 0. \quad (70)$$

The number of linearly independent solutions for A is the dimension of the surface of rank $(5, 5)$ PPT states at the point ρ .

We believe that the dimension 8 can be understood as follows. We may fix both subspaces $\text{Im } \rho$ and $\text{Im } \rho^P$, this means that we fix the projections P and \tilde{P} and determine ρ as a solution of the equation

$$(2\mathbf{I} - \mathbf{P} - \tilde{\mathbf{P}})\rho = 0, \quad (71)$$

with $\text{Tr } \rho = 1$. Then there is typically no solution at all for ρ , solutions exist only for special pairs of subspaces. If now the two 5 dimensional subspaces are chosen in such a way that a solution exists, then the solution is (typically) unique, and the uniqueness means that ρ is an extremal point of \mathcal{P} .

We may fix instead $\text{Im} \rho$ but not $\text{Im} \rho^P$, only the rank of ρ^P . Then there is a set of solutions for ρ described by 8 real parameters. It is a natural guess that the role of these 8 parameters is to specify the $\text{SL} \otimes \text{SL}$ equivalence class to which the 5 dimensional subspace $\text{Im} \rho^P$ belongs.

In fact, when we fix $\text{Im} \rho$ there is no degree of freedom left corresponding to $\text{SL} \otimes \text{SL}$ transformations. This is so because the set of product vectors in $\text{Im} \rho$ is discrete and can not be transformed continuously within the fixed subspace $\text{Im} \rho$. Hence, the only way to vary the subspace $\text{Im} \rho^P$ without varying $\text{Im} \rho$ is to vary the equivalence class of $\text{Im} \rho^P$.

Figure 2 shows a two dimensional section through the set of density matrices. The section is defined by the maximally mixed state, by a randomly selected rank $(5, 5)$ entangled and extremal PPT state ρ , and by a direction A through ρ such that the perturbed state $\rho' = \rho + \epsilon A$ is a rank $(5, 5)$ PPT state for infinitesimal positive and negative ϵ , and has $\text{Im} \rho' = \text{Im} \rho$ even for finite ϵ . The figure illustrates the fact that the difference between the sets \mathcal{P} and \mathcal{S} is small. It also illustrates that the difference between \mathcal{P} and \mathcal{S} is largest close to extremal entangled PPT states.

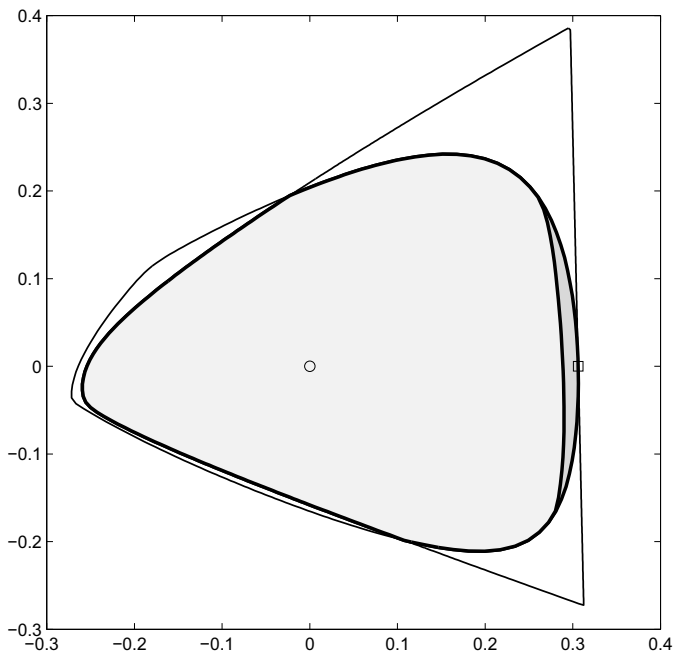


Figure 2: Two dimensional section through \mathcal{D} , the set of density matrices in 3×3 dimensions. The boundaries of \mathcal{S} , the set of separable states, and of \mathcal{P} , the set of PPT states, are both drawn as thick lines. The boundaries of \mathcal{D} and of \mathcal{D}^P , the set of partially transposed density matrices, cross at two points, they are drawn as thin lines where they do not coincide with the boundary of \mathcal{P} . The origin, marked by a small circle, is the maximally mixed state. The point marked by a small square is an extremal rank $(5, 5)$ PPT state. The boundary of \mathcal{D} is drawn through this point as a thin straight line. The boundary of \mathcal{D}^P is drawn thick at this point, because it is also the boundary of \mathcal{P} . The lightly shaded region around the origin is \mathcal{S} . The small and more darkly shaded region close to the $(5, 5)$ state is the difference between \mathcal{P} and \mathcal{S} . Away from this small region, the boundaries of \mathcal{P} and \mathcal{S} are indistinguishable in the plot.

If we want to allow both $\text{Img } \rho$ and $\text{Img } \rho^P$ to vary, but still require the ranks of ρ and ρ^P to be 5, the equation to be solved for the perturbation A is

$$(\mathbf{Q} + \tilde{\mathbf{Q}})A = 0. \quad (72)$$

In this case the number of linearly independent solutions for A is 48, and this is the dimension of the surface of all rank $(5, 5)$ PPT states.

We understand the dimension 48 as follows. There are $8 + 8 = 16$ parameters for the $\text{SL} \otimes \text{SL}$ equivalence classes of the subspaces $\text{Img } \rho$ and $\text{Img } \rho^P$. And there are 32 parameters for the $\text{SL}(3, \mathbb{C}) \otimes \text{SL}(3, \mathbb{C})$ transformations.

To summarize, an extremal (and hence entangled) rank $(5, 5)$ PPT state ρ is uniquely determined by eq. (71), as soon as we specify the 5 dimensional subspaces $\text{Img } \rho$ and $\text{Img } \rho^P$. Each subspace $\text{Img } \rho$ and $\text{Img } \rho^P$ is determined by 8 real $\text{SL} \otimes \text{SL}$ invariant parameters and an $\text{SL} \otimes \text{SL}$ transformation.

According to our understanding, based on numerical studies, which is so far only a plausible hypothesis, the 8 invariant parameters can be chosen independently for $\text{Img } \rho$ and $\text{Img } \rho^P$, but the $\text{SL} \otimes \text{SL}$ transformations can not be chosen independently. However, we do not know the relation that clearly exists between $\text{Img } \rho$ and $\text{Img } \rho^P$.

In other words, we do not know any explicit procedure for constructing the most general rank $(5, 5)$ PPT states. Therefore we turn next to a more restricted problem.

6.2 Perturbing from rank $(4, 4)$ to rank $(5, 5)$

We will see now how to construct $(5, 5)$ states that are infinitesimally close to $(4, 4)$ states.

Consider once more an infinitesimal perturbation $\rho' = \rho + \epsilon A$, this time with ρ as the rank $(4, 4)$ state defined in eq. (45), involving the standard real product vectors defined in eq. (47). The most general case is equivalent to this special case by some $\text{SL} \otimes \text{SL}$ transformation.

An extra bonus of this special choice of ρ is that $\rho^P = \rho$. In the notation we have used above, we have projections $P = \tilde{P}$ on $\text{Img } \rho = \text{Img } \rho^P$ and $Q = \tilde{Q}$ on $\text{Ker } \rho = \text{Ker } \rho^P$.

Conditions on the perturbation matrix A

By eq. (12), the condition for ρ' to have rank 5 is that

$$QAQ = \alpha ww^\dagger, \quad (73)$$

where α is a real number, $\alpha \neq 0$, and

$$w = \sum_{i=1}^5 c_i w_i, \quad (74)$$

with complex coefficients c_i such that

$$w^\dagger w = \sum_{i=1}^5 |c_i|^2 = 1. \quad (75)$$

Similarly, the condition for $(\rho')^P$ to have rank 5 is that

$$\tilde{Q}A^P\tilde{Q} = QA^PQ = \beta zz^\dagger, \quad (76)$$

where β is real, $\beta \neq 0$, and

$$z = \sum_{i=1}^5 d_i w_i \quad \text{with} \quad z^\dagger z = \sum_{i=1}^5 |d_i|^2 = 1. \quad (77)$$

Note that the possibilities that ρ' has rank either (4, 5) or (5, 4) are included if we allow either α or β to be zero.

By eq. (23), there is one extra product vector in $\text{Ker } \rho = \text{Ker } \rho^P$, it may be written as

$$w_6 = \sum_{i=1}^5 a_i w_i, \quad (78)$$

this time with real coefficients a_i . Since $w_i = N_i u_i \otimes v_i$ with N_i real and v_i real for $i = 1, 2, \dots, 6$, we have for any Hermitean matrix A that

$$w_i^\dagger A w_i = w_i^\dagger A^P w_i. \quad (79)$$

By the definition of the projection Q we have that $Q w_i = w_i$ for $i = 1, 2, \dots, 6$. It follows then from eq. (73) that

$$w_i^\dagger A w_i = w_i^\dagger Q A Q w_i = \alpha |w_i^\dagger w|^2, \quad (80)$$

and from eq. (76) that

$$w_i^\dagger A^P w_i = w_i^\dagger Q A^P Q w_i = \beta |w_i^\dagger z|^2. \quad (81)$$

Together with eq. (79) this gives the equations

$$\alpha |c_i|^2 = \beta |d_i|^2 \quad (82)$$

for $i = 1, 2, \dots = 5$, and the 6th equation

$$\alpha \left| \sum_{i=1}^5 a_i c_i \right|^2 = \beta \left| \sum_{i=1}^5 a_i d_i \right|^2. \quad (83)$$

It follows further that

$$\alpha = \sum_{i=1}^5 \alpha |c_i|^2 = \sum_{i=1}^5 \beta |d_i|^2 = \beta, \quad (84)$$

and that

$$|c_i| = |d_i| \quad \text{for} \quad i = 1, 2, \dots, 5. \quad (85)$$

Thus, the coefficient d_i can differ from c_i only by a phase factor. The total of 5 phase factors are reduced to 4 independent phase factors by the extra equation

$$\left| \sum_{i=1}^5 a_i c_i \right| = \left| \sum_{i=1}^5 a_i d_i \right|. \quad (86)$$

For infinitesimal values of ϵ , both ρ' and $(\rho')^P$ will have four eigenvalues infinitesimally close to $1/4$ and one eigenvalue close to zero, which is $\epsilon\alpha$ for ρ' and $\epsilon\beta$ for $(\rho')^P$. This eigenvalue is the same for ρ' and $(\rho')^P$, since $\alpha = \beta$. With $\alpha > 0$ this means that both $\rho' \geq 0$ and $(\rho')^P \geq 0$ for $\epsilon > 0$, but not for $\epsilon < 0$. Thus, we get automatically a PPT state of rank $(5, 5)$, we never get rank $(5, 4)$ or $(4, 5)$. Also it never happens that ρ' is not a PPT state for the reason that one of ρ' or $(\rho')^P$ has a negative eigenvalue.

For a more general rank $(4, 4)$ state ρ , which is obtained by some $\text{SL} \otimes \text{SL}$ transformation from a state of the special type discussed here, the smallest positive eigenvalues of ρ' and $(\rho')^P$ are no longer equal. But they are still tied together in such a way that they go to zero simultaneously when we move along the surface of $(5, 5)$ states and approach its boundary. The boundary must therefore consist of $(4, 4)$ states.

Computing A

Define $W = ww^\dagger$ and $Z = zz^\dagger$, in the same notation as above. These are both projections, $W^2 = W$ and $Z^2 = Z$, with $QW = WQ = W$ and $QZ = ZQ = Z$. It follows from eq. (73) and eq. (76) that

$$\begin{aligned} WAW &= WQAQW = \alpha W^3 = \alpha W = QAQ, \\ ZA^P Z &= ZQA^P QZ = \beta Z^3 = \beta Z = QA^P Q. \end{aligned} \quad (87)$$

Like in eq. (13) and eq. (32) we define

$$\mathbf{P}X = PXP, \quad \mathbf{Q}X = QXQ, \quad \tilde{\mathbf{P}}X = (PX^P P)^P, \quad \tilde{\mathbf{Q}}X = (QX^P Q)^P, \quad (88)$$

and furthermore,

$$\mathbf{W}X = WXW, \quad \tilde{\mathbf{Z}}X = (ZX^P Z)^P. \quad (89)$$

We may also define $\mathbf{S} = \mathbf{Q} - \mathbf{W}$ and $\tilde{\mathbf{S}} = \tilde{\mathbf{Q}} - \tilde{\mathbf{Z}}$, these are again orthogonal projections on H_N .

The least restrictive conditions we may impose on A are now that both $\mathbf{S}A = 0$ and $\tilde{\mathbf{S}}A = 0$, or equivalently,

$$(\mathbf{S} + \tilde{\mathbf{S}})A = 0. \quad (90)$$

To compute A from this equation we introduce an orthonormal basis in the real Hilbert space H_N . Relative to this basis, the operator $\mathbf{S} + \tilde{\mathbf{S}}$ is represented by a real symmetric positive semidefinite matrix, which has a complete set of real eigenvectors with real eigenvalues. We choose A as an eigenvector of $\mathbf{S} + \tilde{\mathbf{S}}$ with eigenvalue zero.

Apart from the trivial solution $A = \rho$, we find 37 linearly independent solutions of eq. (90). 36 out of these 37 are perturbations that do not depend on either vector w or z , and that give $\rho' = \rho + \epsilon A$ as a rank $(4, 4)$ state both for $\epsilon > 0$ and $\epsilon < 0$. They satisfy the conditions $\mathbf{Q}A = 0$ and $\tilde{\mathbf{Q}}A = 0$, but because $\mathbf{W} = \mathbf{W}Q$ and $\tilde{\mathbf{Z}} = \tilde{\mathbf{Z}}Q$ they also satisfy the conditions

$$\mathbf{W}A = \mathbf{W}Q A = 0, \quad \tilde{\mathbf{Z}}A = \tilde{\mathbf{Z}}Q A = 0, \quad (91)$$

and hence eq. (90). The number 36 is the dimension of the surface of rank $(4, 4)$ extremal PPT states, as noted in Subsection 5.1. The 37th independent solution is the one giving a rank $(5, 5)$ extremal PPT state.

A more restricted class of perturbations consists of those where we fix the 5 dimensional subspace $\text{Img } \rho'$ to be the direct sum of the 4 dimensional subspace $\text{Img } \rho$ and the one dimensional subspace of the vector w . The projection on $\text{Img } \rho'$ is then

$$P_5 = P + W , \quad (92)$$

and the partial condition on A is that $\mathbf{P}_5 A = A$, when we define

$$\mathbf{P}_5 X = P_5 X P_5 . \quad (93)$$

The full condition on A is that

$$(\mathbf{P}_5 - \tilde{\mathbf{S}})A = A . \quad (94)$$

Again apart from the trivial solution $A = \rho$, we find 5 linearly independent solutions of eq. (94), of which 4 give ρ' as a rank $(4, 4)$ state both for $\epsilon > 0$ and $\epsilon < 0$. The 5th independent solution is the one giving ρ' as a rank $(5, 5)$ extremal PPT state.

The 4 directions that only give new $(4, 4)$ states are easily identified, since they do not depend on the vector z . To find them we simply repeat the calculation with a “wrong” z , violating the conditions (85) and (86). In this way we find no $(5, 5)$ state, but we find the same set of perturbations into $(4, 4)$ states. The number 4 is the dimension of the surface of $(4, 4)$ states with image within the fixed 5 dimensional subspace projected out by the projector P_5 .

There is a natural explanation of why this surface has dimension 4. In fact, when we fix P_5 and look for $(4, 4)$ states with image within this fixed 5 dimensional subspace, we eliminate all degrees of freedom corresponding to $\text{SL} \otimes \text{SL}$ transformations. But we still allow variations of the 4 real $\text{SL} \otimes \text{SL}$ invariant parameters that are needed to define a rank $(4, 4)$ state.

We conclude that for fixed vectors w and z there is one direction away from the surface of rank $(4, 4)$ extremal PPT states and into the surface of rank $(5, 5)$ extremal PPT states.

For a fixed vector w there is a 4 parameter family of acceptable vectors z . Recall that these 4 parameters determine the 5 relative phases between the coefficients c_i in eq. (74) and the corresponding coefficients d_i in eq. (77).

The vector w is an arbitrary vector in the 5 dimensional kernel of the unperturbed state ρ , hence it contains 4 complex parameters, or 8 real parameters, after we take out an uninteresting complex normalization factor. Altogether, there are $8 + 4 = 12$ independent directions away from the 36 dimensional surface of rank $(4, 4)$ PPT states and into the surface of rank $(5, 5)$ PPT states.

When we perturb an arbitrary rank $(5, 5)$ PPT state in such a way that we preserve the ranks of the state and its partial transpose, we find numerically that the surface of rank $(5, 5)$ PPT states has dimension 48. The fact that $48 = 36 + 12$ is consistent with the hypothesis that we can reach every rank $(5, 5)$ PPT state if we start from a rank $(4, 4)$ PPT state and move continuously along the surface of rank $(5, 5)$ PPT states.

7 Rank $(6, 6)$ entangled PPT states in 4×4 dimensions

We will discuss in some detail one more example of the relation between PPT states and product vectors. According to eq. (22), the rank $(6, 6)$ PPT states in 4×4 dimensions represent just the limiting case with a finite number of product vectors in the kernel, in this respect they are similar to the rank $(4, 4)$ states in 3×3 dimensions.

The kernel of a rank 6 state in 16 dimensions has dimension 10, and the generic case, according to eq. (23), is that it contains exactly 20 product vectors, any 10 of which are linearly independent. We will see here that the product vectors in the kernel put such strong restrictions on the state that the rank (6, 6) PPT state may be reconstructed uniquely from only 7 product vectors in its kernel.

To see how it works, take a set of product vectors in 4×4 dimensions. We may take random product vectors, or else a set of product vectors with the special property that they belong to $\text{Ker } \rho$ where ρ is a rank (6, 6) PPT state. We find numerically that the number of constraints generated by fewer than 7 product vectors is the same in both cases. We find the following numbers.

From 4 product vectors assumed to lie in $\text{Ker } \rho$ for an unknown ρ , or actually lying in $\text{Ker } \rho$ for a known ρ , we get 172 independent constraints on ρ of the form given in eq. (44). These constraints leave 84 free real parameters in ρ , before we normalize and set $\text{Tr } \rho = 1$.

From 5 product vectors in $\text{Ker } \rho$ we get 205 independent constraints, leaving 51 parameters in ρ .

From 6 product vectors in $\text{Ker } \rho$ we get 234 independent constraints, and 22 parameters in ρ .

Finally, 7 product vectors in $\text{Ker } \rho$ give either 255 or 256 independent constraints, and either 1 or 0 real parameters in ρ . If there is one parameter left, it is a proportionality constant, to be fixed by the normalization condition $\text{Tr } \rho = 1$.

The standard form of 7 product vectors in 4×4 dimensions, generalizing eq. (50), is the following,

$$u = \begin{pmatrix} 1 & 0 & 0 & 0 & 1 & 1 & 1 \\ 0 & 1 & 0 & 0 & 1 & p_1 & p_4 \\ 0 & 0 & 1 & 0 & 1 & p_2 & p_5 \\ 0 & 0 & 0 & 1 & 1 & p_3 & p_6 \end{pmatrix}, \quad v = \begin{pmatrix} 1 & 0 & 0 & 0 & 1 & 1 & 1 \\ 0 & 1 & 0 & 0 & 1 & p_7 & p_{10} \\ 0 & 0 & 1 & 0 & 1 & p_8 & p_{11} \\ 0 & 0 & 0 & 1 & 1 & p_9 & p_{12} \end{pmatrix}. \quad (95)$$

There are 12 complex parameters p_1, p_2, \dots, p_{12} , that is, 24 real parameters. These are invariant in the sense that we can not change them by $\text{SL}(4, \mathbb{C}) \otimes \text{SL}(4, \mathbb{C})$ transformations.

Not just any arbitrary set of 7 product vectors defines a rank (6, 6) PPT state. We arrive at this conclusion not only because we find numerically that 7 generic product vectors allow only $\rho = 0$ as solution of all the constraint equations, but also because a dimension counting shows that we need less than 24 invariant parameters in order to parametrize the rank (6, 6) PPT states.

Take one known rank (6, 6) PPT state ρ and perturb it into another rank (6, 6) PPT state $\rho' = \rho + \epsilon A$ with ϵ infinitesimal. Here A must be a solution of eq. (35), with operators \mathbf{Q} and $\tilde{\mathbf{Q}}$ defined relative to ρ as explained. The number of linearly independent solutions for A , found numerically, is 76, including the trivial solution $A = \rho$. This shows that the surface of rank (6, 6) PPT states has 75 real dimensions.

Of these 75 dimensions, 60 dimensions result from product transformations $\rho \mapsto V\rho V^\dagger$ with $V = V_A \otimes V_B$ and $V_A, V_B \in \text{SL}(4, \mathbb{C})$. The remaining 15 dimensions must correspond to 15 $\text{SL} \otimes \text{SL}$ invariant parameters of the 7 product vectors.

It is also worth noting that, by the counting explained in the next section, the set of 6 dimensional subspaces of \mathbb{C}^{16} has real dimension $16^2 - 6^2 - 10^2 = 120$, much larger than the dimension 75 of the surface of (6, 6) states. Thus, not every 6 dimensional subspace of \mathbb{C}^{16} is the host of a rank (6, 6) PPT state, as one would expect from the analogy to the case of the rank (4, 4) PPT states in \mathbb{C}^9 .

8 Dimension counting

We will describe in this section how to compute numerically the dimensions of surfaces of PPT states of given ranks. We list some numerical results, and discuss how they may be understood in most cases by a simple counting of constraints, assuming the constraints to be independent.

We start with a useful exercise. We want to compute the real (as opposed to complex) dimension of the set of all r dimensional subspaces of an N dimensional complex Hilbert space.

First note that the unitary group $U(k)$ has k^2 real dimensions. Take an orthonormal basis of the Hilbert space. The first r basis vectors define an r dimensional subspace, the orthogonal complement of which is defined by the last $s = N - r$ basis vectors. A $U(N)$ transformation transforms this basis into another orthonormal basis, but the $U(r)$ transformations within the first r basis vectors, and the $U(s)$ transformations within the last s basis vectors, do not change either subspace. It follows that the dimension of the set of r dimensional subspaces, equal to the dimension of the set of s dimensional subspaces, is

$$d = N^2 - r^2 - s^2 = 2rs . \quad (96)$$

Assuming that we have found a PPT state ρ of rank (m, n) , it lies on a surface of rank (m, n) PPT states. We compute the dimension of the surface at this point by counting the number of independent solutions A of eq. (35),

$$(\mathbf{Q} + \tilde{\mathbf{Q}})A = 0 , \quad (97)$$

equivalent to the two equations

$$\mathbf{Q}A = QAQ = 0 , \quad \tilde{\mathbf{Q}}A = (\tilde{Q}A^P\tilde{Q})^P = 0 . \quad (98)$$

We have to throw away the trivial solution $A = \rho$. We get a lower bound for the dimension if we assume that the constraints on A from the two equations in eq. (98) are independent. The equation $QAQ = 0$ represents $(N - m)^2$ real constraints, since Q is the orthogonal projection on the $N - m$ dimensional subspace $\text{Ker } \rho$. Similarly, the equation $\tilde{Q}A^P\tilde{Q} = 0$ represents $(N - n)^2$ real constraints, since \tilde{Q} is the orthogonal projection on the $N - n$ dimensional subspace $\text{Ker } \rho^P$. Because the constraints are not necessarily independent, we get the following lower bound for the dimension,

$$d \geq N^2 - (N - m)^2 - (N - n)^2 - 1 . \quad (99)$$

Take $N = 3 \times 3 = 9$ as an example. We find numerically that eq. (99) holds with equality for all ranks from the full rank $(m, n) = (9, 9)$ down to $(m, n) = (5, 5)$. In particular, for rank $(5, 5)$ the dimension of the surface is

$$d = 9^2 - 4^2 - 4^2 - 1 = 48 . \quad (100)$$

By eq. (96) the set of 5 dimensional subspaces has dimension 40, hence we should expect to find an 8 dimensional surface of rank $(5, 5)$ PPT states in every 5 dimensional subspace. And that is actually what we find.

For rank $(4, 4)$ the constraints are not all independent, and we have the strict inequality

$$d = 36 > 9^2 - 5^2 - 5^2 - 1 = 30 . \quad (101)$$

The set of 4 dimensional subspaces has again dimension 40, hence there can not exist rank $(4, 4)$ PPT states in every 4 dimensional subspace. There are $40 - 36 = 4$ constraints restricting the 4 dimensional subspaces supporting rank $(4, 4)$ PPT states, and in each 4 dimensional subspace there can exist at most one unique such state. The 4 constraints are the conditions that the 4 parameters a, b, c, d in eq. (47), or p, q, r, s in eq. (50), have to be real.

If we want to compute the dimension of the surface of rank (m, n) PPT states with fixed image space, we have to count the independent solutions of eq. (36),

$$(\mathbf{I} - \mathbf{P} + \tilde{\mathbf{Q}})A = 0 , \quad (102)$$

equivalent to the two equations

$$\mathbf{P}A = PAP = A , \quad \tilde{\mathbf{Q}}A = (\tilde{Q}A^P\tilde{Q})^P = 0 . \quad (103)$$

The equation $\mathbf{P}A = A$ leaves m^2 real parameters in A and represents $N^2 - m^2$ real constraints, as is visualized in eq. (17). The lower bound on the dimension is therefore

$$d \geq N^2 - (N^2 - m^2) - (N - n)^2 - 1 = m^2 - (N - n)^2 - 1 . \quad (104)$$

In the above example with $N = 9$ and $(m, n) = (5, 5)$ we find numerically $d = 8$, as already mentioned, so that the inequality in eq. (104) holds as an equality. With $(m, n) = (4, 4)$, on the other hand, we get

$$d = 0 \geq 4^2 - 5^2 - 1 = -10 . \quad (105)$$

9 Numerical integration

In this section we will describe a numerical method for tracing curves on a surface of PPT states of fixed ranks (m, n) . This is a tool for studying the geometry of the surface, for example by tracing geodesics to see how they curve, or studying how the surface approaches a boundary consisting of states of lower ranks.

9.1 Equations of motion

The perturbation expansion $\rho(t + \epsilon) = \rho(t) + \epsilon A$ for $\rho = \rho(t)$ is equivalent to the differential equation

$$\dot{\rho} = A . \quad (106)$$

We use the notation

$$\dot{\rho} = \frac{d\rho}{dt} , \quad \dot{\rho}^+ = \frac{d\rho^+}{dt} . \quad (107)$$

We defined the pseudoinverse ρ^+ in eq. (4), in order to define $P = \rho^+\rho = \rho\rho^+$ and $Q = \mathbb{1} - P$, the orthogonal projections on $\text{Img } \rho$ and $\text{Ker } \rho$, respectively. There are similar relations for \tilde{P} , the projection on $\text{Img } \rho^P$, and $\tilde{Q} = \mathbb{1} - \tilde{P}$, the projection on $\text{Ker } \rho^P$. We defined orthogonal projections on H_N , the space of Hermitean matrices, in eq. (13) and eq. (32).

If X is a Hermitean matrix with $\text{Img } X \subset \text{Img } \rho$ then $X = PX = XP$, or equivalently, $QX = XQ = 0$. Assuming that these relations hold at any ‘‘time’’ t we may differentiate and get that

$$\dot{X} = \dot{P}X + P\dot{X} = \dot{X}P + X\dot{P} . \quad (108)$$

Equivalently,

$$Q\dot{X} = \dot{P}X , \quad \dot{X}Q = X\dot{P} . \quad (109)$$

Multiplication by Q from the left and from the right gives that

$$Q\dot{X}Q = 0. \quad (110)$$

It follows further that

$$\dot{X} = (P + Q)\dot{X}(P + Q) = P\dot{X}P + X\dot{P} + \dot{P}X. \quad (111)$$

The special case $X = \rho$ gives the equation

$$QAQ = 0 \quad (112)$$

as a consistency condition for eq. (106) with the relations $\rho = P\rho = \rho P$. Eq. (112) is the same as eq. (11), the condition for the rank of ρ to be constant. We may want to replace it with the stronger condition that $\text{Img } \rho$ should be constant, eq. (9),

$$PAP = A. \quad (113)$$

Setting $X = \rho$ in eq. (109) gives the equations

$$QA = \dot{P}\rho, \quad AQ = \rho\dot{P}, \quad (114)$$

and multiplication by ρ^+ gives that

$$QA\rho^+ = \dot{P}P, \quad \rho^+AQ = P\dot{P}. \quad (115)$$

Differentiating the equation $P = P^2$ gives that $\dot{P} = \dot{P}P + P\dot{P}$, hence

$$\dot{P} = QA\rho^+ + \rho^+AQ. \quad (116)$$

Differentiating the relation $\rho^+ = \rho^+\rho\rho^+$ we get that

$$\dot{\rho}^+ = \dot{\rho}^+P + \rho^+A\rho^+ + P\dot{\rho}^+. \quad (117)$$

When we left and right multiply here by P we obtain the relation

$$P\dot{\rho}^+P = -\rho^+A\rho^+. \quad (118)$$

Hence, using eq. (111) with $X = \rho^+$, together with eq. (116), we get that

$$\dot{\rho}^+ = QA(\rho^+)^2 + (\rho^+)^2AQ - \rho^+A\rho^+. \quad (119)$$

The equations (106), (116), and (119) may be integrated together, as soon as we specify how to calculate A as a function of ρ . There are, of course, equations similar to (116) and (119) that hold for the projection \tilde{P} related to the partial transpose ρ^P , and for the pseudoinverse $(\rho^P)^+$.

As a specific example, consider how to generate a curve $\rho = \rho(t)$ lying on the 48 dimensional surface in H_N of rank (5, 5) PPT states in 3×3 dimensions passing through a given state $\rho(0)$. We then have to satisfy the two conditions on A that

$$\mathbf{Q}A = QAQ = 0, \quad \tilde{\mathbf{Q}}A = (\tilde{Q}A^P\tilde{Q})^P = 0. \quad (120)$$

Or equivalently eq. (35),

$$(\mathbf{Q} + \tilde{\mathbf{Q}})A = 0. \quad (121)$$

Alternatively, we may want to generate a curve that follows the 8 dimensional surface in H_N of rank (5, 5) PPT states such that the 5 dimensional subspace $\text{Img } \rho$ is kept fixed, but the 5 dimensional subspace $\text{Img } \rho^P$ is allowed to change. This means that we replace the condition $QAQ = 0$ by the condition $PAP = A$. The single condition to be satisfied is then eq. (36),

$$(\mathbf{I} - \mathbf{P} + \tilde{\mathbf{Q}})A = 0. \quad (122)$$

In this case P is constant but $\tilde{Q} = \tilde{Q}(t)$ may vary as a function of t .

9.2 Geodesic equations

Both conditions (121) and (122) are of the form

$$\mathbf{T}A = 0. \quad (123)$$

Differentiating this equation gives that

$$\mathbf{T}\dot{A} + \dot{\mathbf{T}}A = 0. \quad (124)$$

It follows that

$$\dot{A} = B - \mathbf{T}^+\dot{\mathbf{T}}A, \quad (125)$$

where \mathbf{T}^+ is the pseudoinverse of \mathbf{T} , and B is an arbitrary Hermitean matrix with $\mathbf{T}B = 0$.

By definition, a geodesic on an embedded surface (think of a great circle on the surface of a sphere as an example) is a curve which does not change its direction on the surface. Hence, it changes direction in the embedding space only as much as it has to in order to stay on the surface. This would mean that we choose $B = 0$ in eq. (125). Or if we normalize A to unit length, fixing $\text{Tr} A^2 = 1$, we set $B = \alpha A$ and choose α such that $\text{Tr}(\dot{A}A) = 0$.

9.3 Numerical results

We have done numerical integrations by a standard fourth order Runge–Kutta method. With ρ and A of order one and time steps of order 10^{-4} this gives a precision of order 10^{-16} , which is the machine precision.

Figure 3 shows a geodesic curve $\rho(t)$ on the 8 dimensional curved surface of rank $(5, 5)$ PPT states with $\text{Im}g \rho(t)$ constant. Figure 4 shows the 5 nonzero eigenvalues of ρ and ρ^P . The condition that one eigenvalue of either ρ or ρ^P goes to zero defines the boundary of the surface. We see that the curve approaches the boundary twice, but turns around each time and continues in the interior. The eigenvalue spectra of ρ and ρ^P are remarkably similar, yet they are not identical. When both ρ and ρ^P simultaneously get one dominant eigenvalue, we interpret it as an indication that ρ approaches a pure product state.

It is quite natural that a geodesic chosen at random will not hit the boundary, since the boundary consists of rank $(4, 4)$ PPT states and has dimension 4, while the surface itself has dimension 8. In order to hit the boundary we can not follow a geodesic, we have to integrate the equation $\dot{\rho} = A$ and choose the direction A in such a way that the smallest positive eigenvalue of ρ goes to zero. When we do so, the smallest eigenvalue of ρ^P goes to zero simultaneously with the eigenvalue of ρ , although the ratio between the two eigenvalues goes to a value different from one. Hence the curve ends at a $(4, 4)$ state on the boundary. The explanation for this coupling of eigenvalues of ρ and ρ^P was given in Subsection 6.2.

10 Summary

The work presented here is part of an ongoing programme to study quantum entanglement in mixed states. We have studied here low rank entangled PPT states using perturbation theory and the close relation between PPT states and product vectors.

One result obtained is an understanding of how to construct rank $(5, 5)$ PPT states in 3×3 dimensions by perturbing rank $(4, 4)$ states. We use perturbation theory to study surfaces of PPT states

of given ranks, and in particular to compute dimensions of such surfaces, for example the surface of $(5, 5)$ states. However, it is still an unsolved problem how to construct general rank $(5, 5)$ PPT states that are not close to rank $(4, 4)$ states. We are even farther from a full understanding of higher rank PPT states in 3×3 dimensions, or in higher dimensions.

A special class of PPT states are those of special ranks so that their kernel is spanned by product vectors and contains a finite number of product vectors. We have shown that these states may be reconstructed uniquely from a subset of the product vectors in the kernel, and the number of product vectors needed may be smaller than the dimension of the kernel. This result raises new interesting questions to be answered by future research, for example, how to identify finite sets of product vectors that define PPT states with these product vectors in their kernel.

Acknowledgments

We acknowledge gratefully research grants from The Norwegian University of Science and Technology (Leif Ove Hansen) and from The Norwegian Research Council (Per Øyvind Sollid). Leif Ove Hansen, Jan Myrheim, and Per Øyvind Sollid also want to thank NORDITA for hospitality during the workshop and conference on quantum information in Stockholm in September and October 2010.

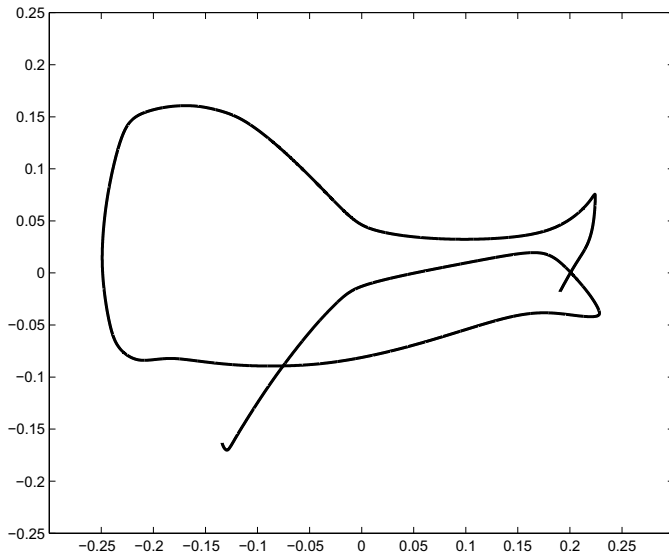


Figure 3: A projection of a geodesic curve on the 8 dimensional surface of rank $(5, 5)$ PPT states with a fixed image space. We have made a principal component analysis and plotted the two largest principal components. The curve starts middle right and ends lower left.

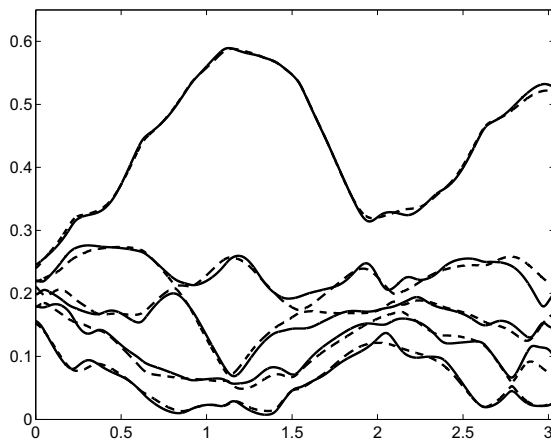


Figure 4: Variation along the curve in Fig. 3 of the 5 nonzero eigenvalues of the density matrix (full drawn lines) and its partial transpose (broken lines). The abscissa is the arc length along the curve.

References

- [1] R. Horodecki, P. Horodecki, M. Horodecki, and K. Horodecki, *Quantum entanglement*, Rev. Mod. Phys. **81**, 865–942 (2009).
- [2] J.S. Bell, *On the Einstein Podolsky Rosen paradox*, Physics **1**, 195 (1964).
- [3] D.M. Greenberger, M.A. Horne, and A. Zeilinger, *Going beyond Bell's theorem*. P. 69 in *Bell's Theorem, Quantum Theory, and Conceptions of the Universe*, M. Kafatos, ed., Kluwer, Dordrecht, The Netherlands (1989). Reproduced as arXiv:0712.0921 (2007).
- [4] N.D. Mermin, *What's wrong with these elements of reality?* Phys. Today **43**, 9 (June 1990).
- [5] L. Gurvits, *Classical deterministic complexity of Edmonds' problem and quantum entanglement*. In Proceedings of the Thirty-Fifth ACM Symposium on Theory of Computing (ACM, New York, 2003), pp. 10-19.
- [6] J.M. Leinaas, J. Myrheim and E. Ovrum, *Geometrical aspects of entanglement*, Phys. Rev. A **74**, 012313 (2006).
- [7] J.M. Leinaas, J. Myrheim and E. Ovrum, *Extreme points of the set of density matrices with positive partial transpose*, Phys. Rev. A **76**, 034304 (2007).
- [8] J.M. Leinaas, J. Myrheim and P.Ø. Sollid, *Numerical studies of entangled PPT states in composite quantum systems*, Phys. Rev. A **81**, 0062329 (2010).
- [9] J.M. Leinaas, J. Myrheim and P.Ø. Sollid, *Low-rank extremal positive-partial-transpose states and unextendible product bases*, Phys. Rev. A **81**, 0062330 (2010).
- [10] M. Horodecki, P. Horodecki and R. Horodecki, *Separability of mixed states: necessary and sufficient conditions*, Phys. Lett. A **223**, 1 (1996).
- [11] A. Peres, *Separability Criterion for Density Matrices*, Phys. Rev. Lett. **77**, 1413 (1996).
- [12] P. Horodecki, M. Lewenstein, G. Vidal, and I. Cirac, *Operational criterion and constructive checks for the separability of low-rank density matrices*, Phys. Rev. A, **62**, 032310 (2000).
- [13] C.H. Bennett, D.P. DiVincenzo, T. Mor, P.W. Shor, J.A. Smolin, and B.M. Terhal, *Unextendible Product Bases and Bound Entanglement*, Phys. Rev. Lett. **82**, 5385 (1999).
- [14] D.P. DiVincenzo, T. Mor, P.W. Shor, J.A. Smolin, and B.M. Terhal, *Unextendible Product Bases, Uncompletable Product Bases and Bound Entanglement*, Commun. Math. Phys. **238**, 379 (2003).
- [15] P.Ø. Sollid and J.M. Leinaas, *Unextendible product bases and extremal density matrices with positive partial transpose*. In preparation.

